

NSL 64-360
DECEMBER 1964

NASA-CR-65014

GPO PRICE \$ _____

OTS PRICE(S) \$ _____

FINAL REPORT

CONTRACT NAS-9-3717

Hard copy (HC) 6.00

Microfiche (MF) 1.25

PREPARED FOR:

MANNED SPACECRAFT CENTER
NATIONAL AERONAUTICS AND SPACE ADMINISTRATION
HOUSTON, TEXAS

**APOLLO DOCKING TEST DEVICE
DESIGN STUDY**

FACILITY FORM 802	N65-24718	(FHRU)
	(ACCESSION NUMBER)	1
	2011	(CODE)
	CR 65014	11
(NASA CR OR TMX OR AD NUMBER)	(CATEGORY)	

NORTHROP SPACE LABORATORIES
3401 WEST BROADWAY, HAWTHORNE, CALIFORNIA 90250

NORTHROP CORPORATION

NSL 64--360
DECEMBER 1964

FINAL REPORT

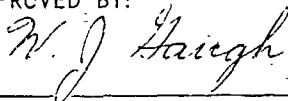
CONTRACT NAS-9-3717

PREPARED FOR:

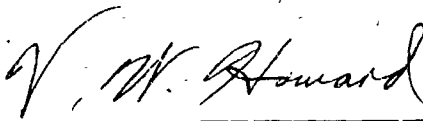
MANNED SPACECRAFT CENTER
NATIONAL AERONAUTICS AND SPACE ADMINISTRATION
HOUSTON, TEXAS

**APOLLO DOCKING TEST DEVICE
DESIGN STUDY**

APPROVED BY:



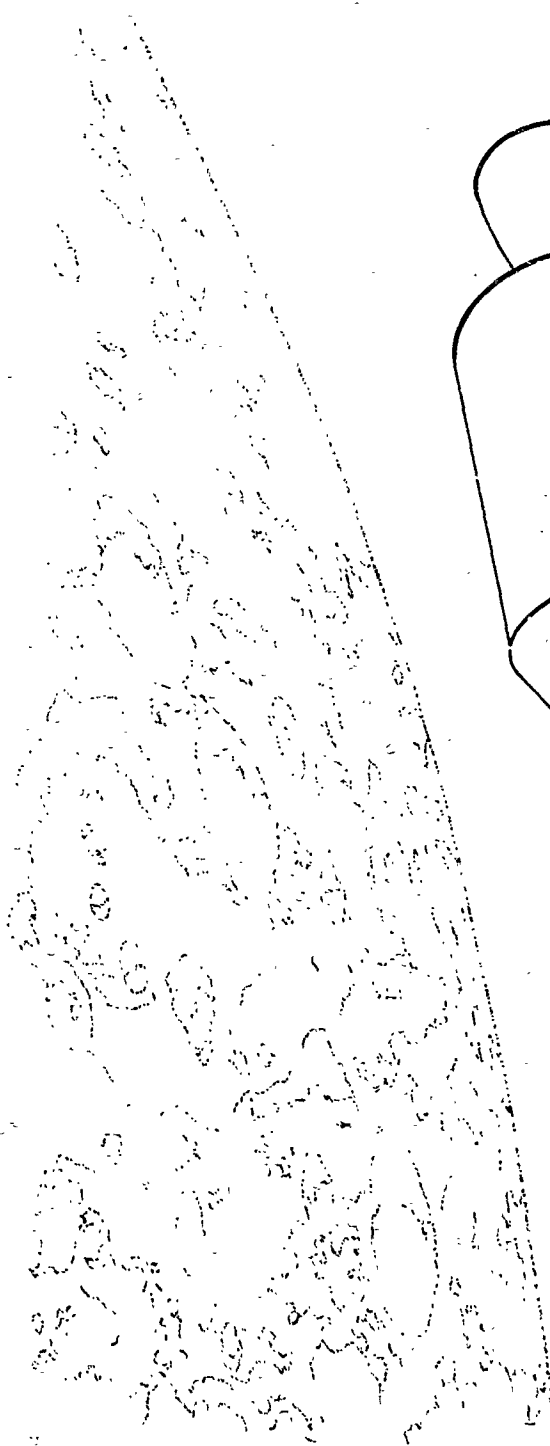
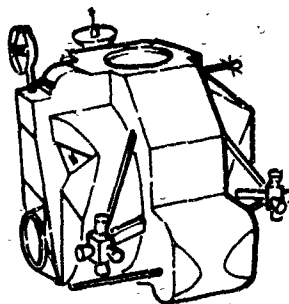
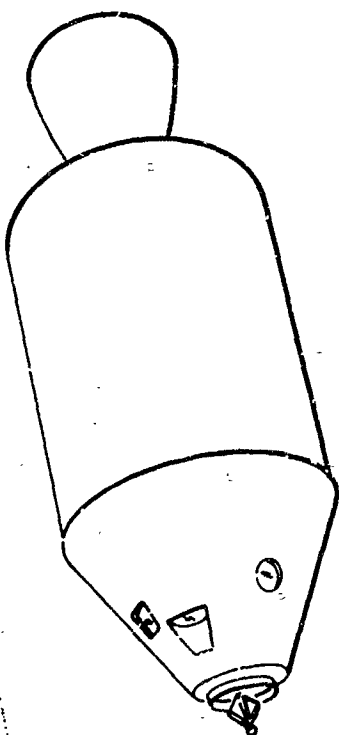
WILLIAM J. GAUGH
PROGRAM MANAGER



DR. V. W. HOWARD
VICE PRESIDENT
AND MANAGER
SYSTEMS DEPARTMENT

NORTHROP SPACE LABORATORIES
3401 WEST BROADWAY, HAWTHORNE, CALIFORNIA 90250

NORTHROP CORPORATION



NORTHROP SPACE LABORATORIES

TABLE OF CONTENTS

<u>SECTION</u>	<u>PAGE</u>
1.0 SUMMARY.....	1-1
2.0 INTRODUCTION.....	2-1
3.0 SIMULATION SYSTEM DESCRIPTION.....	3-1
3.1 General.....	3-2
System Development.....	3-2
System Description.....	3-4
System Operation, Performance and Requirements.....	3-5
3.2 Mounting Structure.....	3-9
Mechanical Design.....	3-9
Structural Dynamics.....	3-30
3.3 Servo Control System.....	3-35
Requirements.....	3-36
Summary of Results.....	3-41
Hydraulic Fluid Selection.....	3-64
Servo Control Console.....	3-69
Measurement Subsystem.....	3-69
Transmission Line.....	3-72
Analog Computer.....	3-74
3.4 Chamber Interfaces.....	3-90
Vibration Isolation.....	3-90
Chamber Penetration.....	3-94
Installation And Removal.....	3-96
Safety.....	3-96
3.5 Specifications, Ancillary Equipment and Requirements.....	3-100
4.0 CONCLUSIONS	4-1

NORTHROP SPACE LABORATORIES

TABLE OF CONTENTS (Continued)

<u>SECTION</u>		<u>PAGE</u>
5.0	RECOMMENDATIONS.....	5-1
6.0	APPENDICES -	
	APPENDIX A - ELASTIC STRUCTURAL DYNAMICS DEVELOPMENT.....	A-1
	APPENDIX B - SERVO CONTROL SYSTEM DEVELOPMENT....	B-1
	APPENDIX C - OPERATIONAL CONDITIONS AFFECTING HYDRAULIC FLUID SELECTION.....	C-1
	APPENDIX D - BULK MODULUS DEFINITIONS AND FACTORS INVOLVED.....	D-1
	APPENDIX E - CLASSES OF HYDRAULIC FLUIDS AND THEIR CHARACTERISTICS.....	E-1
	APPENDIX F - COMPARISON CHART, SPECIFIC PROPERTIES OF FLUIDS FOR SELECTION..	F-1
	APPENDIX G - SIMULATION OF TWO RIGID BODIES.....	G-1
	APPENDIX H - FUEL SLOSHING.....	H-1
	APPENDIX I - ELASTIC CORRECTIONS TO EQUATIONS OF MOTIONS.....	I-1
	APPENDIX J - EFFECTS OF GRAVITY ON EQUATION OF MOTION.....	J-1
	APPENDIX K - PROBE - DROGUE RELATIONSHIP.....	K-1
	APPENDIX L - ANALOG COMPUTER PROGRAM.....	L-1
7.0	REFERENCES.....	7-1

NORTHROP SPACE LABORATORIES

LIST OF ILLUSTRATIONS

<u>FIGURE/TABLE</u>	<u>TITLE</u>	<u>PAGE</u>
3-1	NAA PROBE & DROGUE DOCKING MECHANISM.....	3-3
3-2	FUNCTIONAL DIAGRAM - SIMULATOR SYSTEM.....	3-8
TABLE 3-1	OF CONCEPT TRADEOFFS.....	3-14
3-3	SKELETON FRAMING OF MOUNTING STRUCTURE.....	3-16
3-4	TENTH SCALE MODEL WHICH ILLUSTRATES OUR SIX DEGREE OF FREEDOM MOTION CONCEPT.....	3-17
3-5	PERSPECTIVE SKETCH OF THE INTERIM SIMULATOR DESIGN.....	3-20
3-5A	PROPOSED DROGUE MOUNTING STRUCTURE FROM WHICH OUR FINAL DESIGN EVOLVED.....	3-21
3-6	PERSPECTIVE SKETCH OF THE FINAL SIMULATOR DESIGN.....	3-22
3-7	APOLLO DOCKING SIMULATOR INSTALLATION IN CHAMBER E.....	3-23
3-8	PROBE MECHANISM LAYOUT.....	3-25
3-9	DROGUE MECHANISM LAYOUT.....	3-27
3-10	FUNCTIONAL DIAGRAM - CONTROL SYSTEM INTERFACE	3-37
TABLE 3-2	DESIGN VALUE SUMMARY.....	3-39
3-11	FUNCTIONAL BLOCK DIAGRAM - SINGLE AXIS SERVO CONTROL.....	3-43
TABLE 3-3	INITIAL ESTIMATE OF CONTROL SYSTEM HYDRAULIC PARAMETERS.....	3-44
3-12	DISPLACEMENT, VELOCITY AND ACCELERATION DESIGN LIMIT LINES FOR THE AXIAL, VERTICAL AND LATERAL CARRIAGE MOTION.....	3-45
3-13	SERVO MECHANIZATION DIAGRAM - Z AXIS CONTROL.	3-49
3-14	SERVO BLOCK DIAGRAM - Z AXIS SYSTEM.....	3-50
3-15	VERTICAL CARRIAGE CONTROL SYSTEM (.01 x REAL TIME SCALE).....	3-51
3-16	TIME RESPONSE OF Z-AXIS SERVO TO STEP INPUT COMMAND.....	3-54

NORTHROP SPACE LABORATORIES

LIST OF ILLUSTRATIONS (Continued)

<u>FIGURE/TABLE</u>	<u>TITLE</u>	<u>PAGE</u>
3-17	FREQUENCY RESPONSE PLOT OF Z-AXIS SERVO.....	3-55
3-18	Z-AXIS SERVO RESPONSE TO CRITICAL-CASE DYNAMICS.....	3-58
3-19	Z-AXIS SERVO COMPLEX STIFFNESS CHARACTERISTICS..	3-61
TABLE 3-4	FINAL CONTROL SYSTEM PARAMETERS INCLUDING CONSIDERATION OF SYSTEM DYNAMIC RESPONSE REQUIREMENTS.....	3-65
TABLE 3-5	SUMMARY OF HYDRAULIC FLUID PROPERTIES.....	3-68
3-20	CONTROL CONSOLE.....	3-70
3-21	SIX COMPONENT INTERNAL STRAIN GAGE BALANCE.....	3-71
3-22	TYPICAL TRANSMISSION LINE.....	3-75
3-23	DOCKING SIMULATION COMPUTER BLOCK DIAGRAM.....	3-78
3-24	SIMULATOR AXES AND ALIGNMENTS.....	3-80
3-25	EULER ANGLE NOMENCLATURE.....	3-81
3-26	AXIS NOMENCLATURE.....	3-32
3-27	TYPICAL COMPUTER RUN SHOWING OUTPUTS TO SIMULATOR SERVO SYSTEM.....	3-87
3-28	NORTHROP AD-256 ANALOG COMPUTER.....	3-88
3-29	TRANSLATIONAL FORCES PRODUCED IN SIMULATOR.....	3-91
3-30	FORCE TRANSMITTED TO LUNAR PLANE THROUGH ISOLATION SYSTEM (Z-Axis Forces Assuming In- finite Impedance for Lunar Plane).....	3-93
3-31	CHAMBER PORT PENETRATION FLANGE.....	3-95
A-1	MATHEMATICAL MODEL OF PROBE STRUCTURE.....	A-3
A-2	IBM PROGRAM RESONANT FREQUENCIES RESULTS.....	A-6
B-1	GENERALIZED BLOCK DIAGRAM FOR THE Z-AXIS SERVO..	B-2
B-3	MECHANICAL MODEL FOR THE Z CARRIAGE.....	B-5
b-4	GENERAL BLOCK DIAGRAM.....	B-6
B-5	GENERALIZED COMBINED BLOCK DIAGRAM.....	B-7

NORTHROP SPACE LABORATORIES

LIST OF ILLUSTRATIONS (Continued)

<u>FIGURE/TABLE</u>	<u>TITLE</u>	<u>PAGE</u>
B-6	TYPICAL CHARACTERISTICS OF FLOW CONTROL VALVES....	B-9
B-7	TYPICAL CHARACTERISTICS OF FLOW CONTROL VALVES....	B-10
B-8	BLOCK DIAGRAM WITH SYSTEM PARAMETER.....	B-12
B-9	RATE LOOP ROOT-LOCUS.....	B-14
B-10	PRESSURE LOOP ROOT-LOCUS.....	B-16
B-11	POSITION LOOP ROOT-LOCUS	B-18
TABLE B-1	NOISE SENSIVITY ABOVE 60 cps.....	B-22
L-1	KEY TO ANALOG SYMBOLS.....	L-2
L-2	PROBE VEHICLE MOTION - ROTATIONAL MOTION.....	L-3
L-3	PROBE VEHICLE MOTION - TRANSLATIONAL MOTION.....	L-4
L-4	PROBE VEHICLE MOTION- ROTATIONAL RATE PRODUCTS....	L-5
L-5	DROGUE VEHICLE MOTION - ROTATIONAL MOTION.....	L-5
L-6	DROGUE VEHICLE MOTION - TRANSLATIONAL MOTION.....	L-6
L-7	DROGUE VEHICLE MOTION - ROTATIONAL RATE PRODUCTS..	L-7
L-8	SIMULATOR MOTION - ANGLE DEVELOPMENT.....	L-9
L-9	SIMULATOR MOTION - TRANSLATIONAL MOTION.....	L-10
L-10	SIMULATOR MOTION - VEHICLE RESOLUTIONS.....	L-11
L-11	ATTITUDE CONTROL.....	L-11
L-12	PROBE-DROGUE INTERACTION - POSITION RELATIONSHIP..	L-12
L-13	PROBE-DROGUE INTERACTION - FORCE AND MOMENTS.....	L-13
L-14	COMPUTER OPERATION CONTROL.....	L-14
TABLE B-1	SUMMARY OF ESTIMATED COMPUTER REQUIREMENTS.....	L-14
L-15	FORCE AND MOMENT RESOLUTION.....	L-15

SECTION 1.0

SUMMARY

SECTION 1.0

SUMMARY

The docking simulator system described in this report is intended for use in confirming the design of the Apollo probe and drogue docking mechanisms under simulated space conditions. These tests will investigate the transient dynamics which occur during docking impact and latch-up. This simulator system was designed as a result of National Aeronautics and Space Administration Manned Spacecraft Center study contract NAS-9-3717. This contract specifies as its objective that the test facility components shall be designed such that:

- (1) Component compatibility with the rest of the facility is assured,
- (2) Sufficient detail is specified to allow fabrication and assembly of the components with minimum design modifications, and
- (3) Maximum accuracy is obtained during facility operations.

A comprehensive study was conducted and the design object was fulfilled. The concept developed was determined to be feasible and within the current state of the art. Significant characteristics of this design include the following:

The probe-drogue relative degrees of freedom have been divided such that the desired dynamic performance is obtained.

NORTHROP SPACE LABORATORIES

The structure has adequate strength for the purpose of mounting the docking system mechanisms, drive systems, and instrumentation. It will allow for ready installation and removal from the space chamber. It has been stiffened locally such that no servo control loop compensations are necessary to nullify the effect of structural resonances. This framework is mounted in a manner such that minimum vibrational energy is transmitted to NASA's Chamber B. In fact, all known Chamber B constraints, including safety and penetration, have been investigated and satisfied.

The drive system also has adequate strength, frequency response, and motion envelope to provide six relative degrees of freedom and necessary displacement between the probe and drogue.

The measurement system senses and transmits both relative probe-drogue position and load-moment signals compatible with other system components. The position measurement system and the drive system form a positive servo system.

The servo control system is unique in that the closed (multi) loop over-all transfer function will provide linear performance. The servo drive system will receive motion commands from an analog computer. The computer yields solutions to the rigid body equations of motion, bending mode equations, and fuel slosh equations that describe the docking vehicles. These solutions are virtually instantaneous responses to measured forces and moments which are generated by the impact of the docking mechanisms.

The analog computer equations contain all the required degrees of freedom, wherein the rigid body dynamic equations have been simplified considerably. A unique approach used to develop these equations resulted in a program which requires the minimum number of computer components.

NORTHROP SPACE LABORATORIES

Several methods of satisfactorily transmitting signals to and from the remotely located analog computer were investigated; a 24 circuit high level analog transmission line was selected for a tunnel installation.

Ancillary equipment requirements were determined. All design criteria can be met by use of standard equipment items or by current engineering state of the art.

Drawings and specifications were prepared and are included along with comprehensive analyses and supporting data which are presented as appendices to this report.

Conclusions and recommendations have been provided to facilitate fabrication and assembly of the docking simulator system and to enhance complete achievement of all program objectives.

SECTION 2.0

INTRODUCTION

SECTION 2.0

INTRODUCTION

The National Aeronautics and Space Administration's Apollo manned lunar landing program requires the performance of various rendezvous and docking maneuvers in space by the Command/Service Module and the Lunar Excursion Module space vehicles. The mission requires the successful execution of three docking maneuvers, one in earth-orbit, one after insertion into a trans-lunar trajectory, and one in lunar orbit. These maneuvers will involve several different vehicle configurations each exhibiting different dynamic characteristics. The docking system, designed by North American Aviation (NAA), must perform the following functions while exposed to the thermal-vacuum environment of space:

1. Non-destructively dissipate energy due to the relative motion between the docking spacecraft for all contact conditions specified in the docking envelope,
2. Control the relative translatory and rotational motions between the docking spacecraft within acceptable limits during the contact phase of the docking maneuver,
3. Provide adequate structural integrity at the interface between the spacecraft so that final latching may be achieved by the appropriate crewman,
4. Permit satisfactory separation of the spacecraft, and
5. Possess a reusable capability.

NORTHROP SPACE LABORATORIES

To verify the docking capability of the probe and drogue mechanisms in the space environment prior to actual manned space flight tests, they are to be installed and tested under various dynamic and environmental conditions on a docking simulator inside NASA/MSC's Space Simulation Chamber B, in Houston, Texas.

These mechanisms and the simulator device will be subjected to a near-space environment inside the chamber at ambient pressures and temperatures and under 10^{-5} Torr vacuum and solar radiation conditions.

Two series of tests are proposed. The first testing will provide development data for possible improvement in the design of the two pieces involved. The subsequent testing will provide qualification data to substantiate the estimated reliability of this hardware.

Two large vehicles impacting in space requires that large changes in momentum and kinetic energy be considered. Because the two pieces being tested are relatively small, the inertia characteristics of the large vehicles must be simulated. This requires that the kinetics involved be described and a method of obtaining instantaneous solutions be provided. These solutions must be fed into a power system which is capable of duplicating the momentum and kinetic energy required for simulation of the large vehicles. When this power system drives the bodies into impact, some means of measuring the forces and moments reacting on the two test pieces must be devised so that the effect of the impact can be reflected instantaneously in the kinematic solution and driving power system. Although several impacts may result before the vehicles latch up, the simulation test can be continued until one of the resulting motions exceed some specified limit. The latches are then remotely released and the two test pieces are driven to their initial positions before starting the next test run.

NORTHROP SPACE LABORATORIES

The pertinent data from each run is recorded for analysis later. Although each run will require less than ten seconds, the elapsed time per run will be three minutes, approximately. Assuming the testing proceeds satisfactorily, it might continue for a twenty-four hour cycle before the simulation system is deactivated. After deactivation, a man can safely enter the vacuumized chamber, conduct a detailed inspection of the test pieces and other equipment, and possibly aid in recalibration of the equipment.

Considerable background data are required before such a simulator system can be designed. If the three space flight conditions are to be investigated during the development and/or qualification testing, then complete inertia, elastic mode and fuel slosh data is necessary for correct simulation of these flight conditions. Pertinent data on the static and dynamic characteristics of the vacuum chamber should be obtained. Procurement, installation and checkout of a large, quality analog computer and associated equipment are required. The environment of the transmission line which connects this computer with the test chamber is necessary. Responsible and experienced personnel should be assigned and trained. The detailed test program, including objectives, variables to be recorded, and methods of analysis, should be made known.

The sections which follow in this report reflect the effort, understanding and experience which Northrop has applied to develop solutions to these problems during the study phase of this project.

The report discusses the design concept and the system elements, operation and performance characteristics. Problem areas are discussed. The mounting structure, servo control system, transmission line, and analog computer network configurations are described. Chamber interface considerations including wall penetration, contamination, and mechanical mounting are presented. Installation, removal, and operational safety procedures and considerations are included. Ancillary equipment, maintenance requirements, and shipping plans are described. Specifications and drawings, study conclusions, and recommendations have been prepared. Technical appendices support the design analysis and the computer program model.

SECTION 3.0

SIMULATION SYSTEM DESCRIPTION

SECTION 3.0

SIMULATION SYSTEM DESCRIPTION

This section presents the description of the simulation system and includes the discussions pertaining to the overall system development concept, operation, performance, and other ancillary requirements. The mounting structure is discussed and the design evolution and characteristics are presented along with sketches, drawings, and a photograph of a tenth scale model. Structural dynamics, thermal effects, and mounting probe-drogue mechanisms are discussed.

For the purposes of logical discussion, the servo control system is defined to include the actuator drive system, dynamic force balance system, the transmission line, and the analog computer.

The relationships of the system with regard to the space simulation chamber are discussed in terms of vibration isolation, chamber penetration, safety, and equipment installation and removal requirements. The last portion of this section presents preliminary specifications for the purpose of describing all major elements and general requirements pertaining to the simulation system description.

3.1 General

SYSTEM DEVELOPMENT

The overall system analysis involved the study of a docking simulator system which would provide the capability to test the Apollo probe and drogue mechanisms under simulated space environmental conditions. Problems associated with this study and the development of a suitable design required analysis of data provided by MSC regarding the space simulation chamber B and the associated analog computer at the Houston Facility. This equipment will be utilized in the testing of the probe-drogue mechanisms provided by NAA (See Figure 3-1). Other information and data from GAEC regarding the LEM and state of the art techniques, processes, and components also were evaluated.

These analyses indicated the requirement for a relatively large servo system and associated supporting structure and the development of mathematical models and computer networks to allow inclusion of the analog computer as a part of the servo system.

Structural support, chamber isolation and penetration considerations, along with safety, installation and removal requirements influenced the development of the basic frame structure, the probe-drogue mounting structure and the servo actuated carriages. In the course of development of the servo actuating system the servo performance requirements also introduced a predominate influence on the system design. The force measuring system, essential to provide the analog computer with the transient force inputs necessary to simulate the inertial characteristics of the Apollo LEM and C/SM, necessitated integration with the force balances and mounting structures for the probe and the drogue.

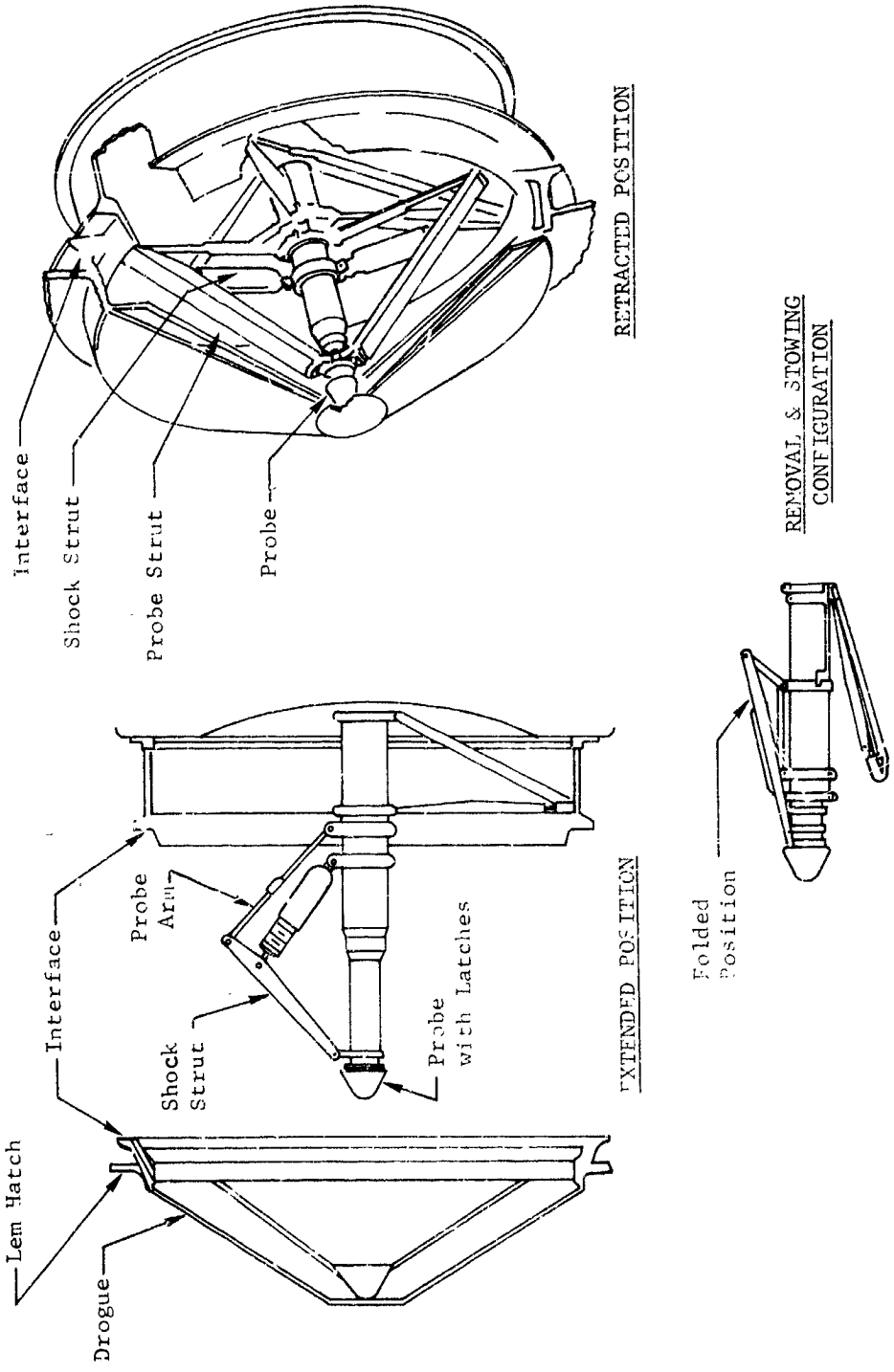


FIGURE 3-1 NAA PROBE & DROGUE DOCKING MECHANISM

NORTHROP SPACE LABORATORIES

The utilization of the analog computer required development of mathematical models and corresponding analog computer programs. These provided the necessary signals to operate the servo system actuators following impact of the probe and drogue. Additionally, the requirement that the analog computer be located remotely from the chamber necessitated the analyses and design of compatible transmission lines. These problems and the resulting constraints defined the overall system concept and design.

SYSTEM DESCRIPTION

The Docking Simulation System is composed of the following elements:

Basic Mounting Structure, consisting of the structural framework, probe and drogue mounting blocks, hydraulic actuators, force measurement balances and other feedback sensing devices, hydraulic lines, and electrical wiring.

Seismic Mass, and vibration isolators, by which the mounting structure is supported and dynamically isolated from the chamber "lunar plane" support base.

Chamber Penetration Seal, through which three hydraulic lines and three electrical cables pass to connect to power and control equipment located outside the chamber.

Actuator Oil Conditioning Unit, located directly outside the chamber and consisting of electrical motors, hydraulic pumps, temperature and pressure regulators, accumulators, heat exchangers, filters, and controls to supply oil to and from the servo valves.

Vacuum System, located directly outside the chamber and providing vacuum for the hydraulic actuator gravity-feed oil sump drains; consists of electrical motors, pumps, regulators, and associated lines.

Control Console, to be operated by personnel viewing the simulator by closed circuit television, and consisting of the servo control amplifiers, remote manual controls, hydraulic system controls, voice communication equipment, and electronic safety system; contains power supplies,

NORTHROP SPACE LABORATORIES

amplifiers, detectors, and signal conditioning equipment associated with the force measurement system; interconnects the servo control amplifiers with the chamber cabling and differential driving and receiving amplifiers of the transmission line.

Transmission Line, consisting of 24 lines approximately 5000 feet in length and interconnecting the control console at the chamber with the remotely located analog computer.

Transmission Line Termination Rack, interconnecting the transmission line with the analog computer, and containing differential driving and receiving amplifiers, power and control switches.

Analog Computer and Recorders, provided by NASA/MSL, to simulate mathematically the characteristics of the Apollo C/S and LEM Modules and to control movement of the simulator mechanisms. The computer receives forces and moments in the form of d.c. voltage signals supplied through the transmission line termination rack, and transmits translation and rotational rate, displacement, and angular information by d.c. voltage to the control console at the chamber for application to the actuator servo. Also, time correlated outputs and inputs are recorded graphically.

SYSTEM OPERATION, PERFORMANCE, AND REQUIREMENTS

System Operation

Upon completion of system installation and initial checkout, the probe-drogue test operations are relatively simple to accomplish. Essentially, all that is required is the activation of the electrical power to the various subsystems by operation of the appropriate power switches at the control console, performance of the calibration and self check process, setting the analog computer potentiometers and the initial conditions to be simulated. The control console operator, remotely observing the simulator in the chamber by means of closed circuit television, ascertains that the system is in a "go" condition by voice telecommunication with the computer personnel and control console indications. Upon authorization by the test conductor the console operator transfers control to the computer personnel who initiate "test start."

NORTHROP SPACE LABORATORIES

Duration of the test nominally requires less than ten seconds. Simulation data is recorded automatically at the analog computer facility. The console operator will continually monitor the chamber television while power is applied to the simulation system to effect immediate shut-down of hydraulic and electrical power in the event of an emergency, not otherwise handled automatically. Upon completion of a test run the console operator resumes control and remotely releases the probe latchup mechanism. He resets the simulator to reference conditions, allows reset of the computer and either shuts down or initiates the next test run.

System Performance

The subject simulator system is capable of impacting two bodies together in a prescribed manner by controlling the translational and angular relative accelerations of the two bodies. It also simulates the individual inertia and structural elastic response characteristics assigned to these two bodies prior to and following their impact. The values of such characteristics are dependent upon the simulated and actual momentum together with the kinetic energy absorption capacity of the object being impacted. Typical values which can be simulated are indicated by the following example. The two impacting Apollo spacecraft vehicles weigh on the order of 32 (Earth) tons each and impact at 2 fps. The impact limit capacity exceeds 10,000 pounds. The simulator accepts bodies up to 30 inches in diameter and weighing up to 500 pounds.

The actuator mechanisms provide for six relative degrees of freedom and allow relative displacements as follows; full axial stroke of 36 inches with lateral and vertical displacements of ± 14 inches. The relative angular displacement capability are ± 35 degrees in pitch and yaw, and ± 180 degrees in roll. The axial, vertical and lateral velocities which can be developed range from zero to two fps. Roll, pitch and yaw angular velocities are limited to two degrees per second. The simulator has an acceleration capability greater than 64 feet per second squared with a frequency response extending from zero through 20 cps with essentially flat response (± 3 db, with less than 45 degrees of phase lag at 20 cps) and down less than 12 db at 60 cps.

NORTHROP SPACE LABORATORIES

A functional block diagram depicting the relationships and functional flow is presented in Figure 3-2. Locations of functional elements are indicated.

System Requirements

After initial installation and checkout, during normal operational use, the system requires electrical power in the following categories and capacities;

440 V	60 cps	3 phase at 500 amperes
115 V	400 cps	3 phase at 30 amperes

The 440 volt power is required at the chamber facility to power the hydraulic actuator conditioning unit. The 115 volt, 400 cps power is required to power the control console in the chamber building and the transmission line termination rack at the analog computer. Approximately 20 amperes are required by the console. No 115 volt, 60 cps power is required; it is desirable to avoid its use in the console, transmission line, and analog computer equipment to minimize stray pickup of 60 cycles.

Approximately 80 square feet of floor space adjacent to the chamber is required for the hydraulic actuator conditioning unit and the vacuum system. The 440 volt power source is required in this area. Approximately 50 square feet of floor space, accessible to a television monitor, and in an area suitable for personnel during test runs, is necessary. This console can be located on the second floor at the rear of the control room. This equipment requires 400 cycle power.

At the analog computer facility, rack space for two standard panels will be needed. These panels will connect to the transmission line and the analog computer and require 400 cycle power.

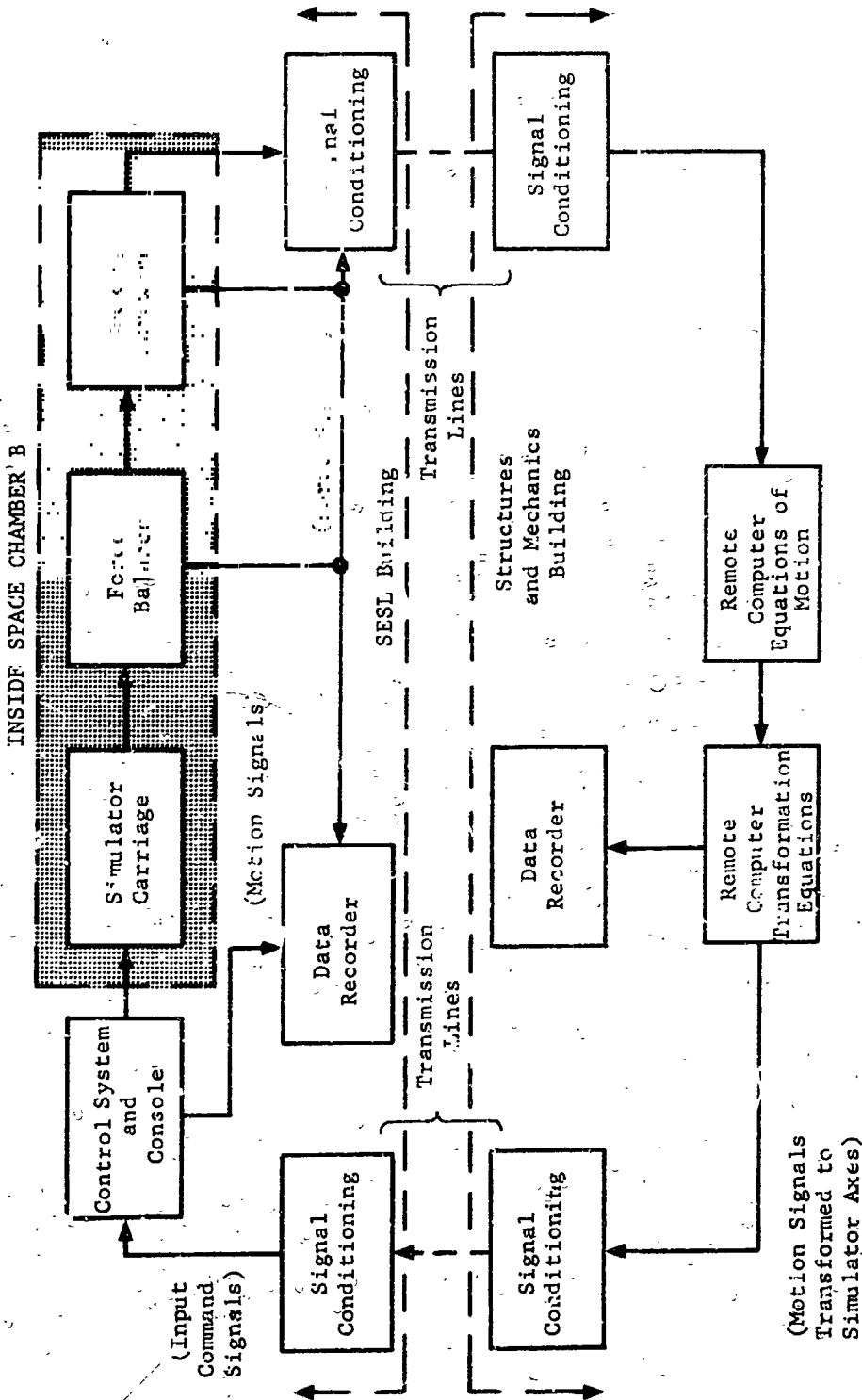


FIGURE 3-2 FUNCTIONAL DIAGRAM - SIMULATOR SYSTEM

3.2 Mounting Structure

MECHANICAL DESIGN

The basic mechanical design objective was to develop a structure of adequate strength and stiffness to support and drive the docking system throughout the performance range requested without violating chamber B constraints.

Evolution of Concept

The problem was to obtain the optimum distribution of the minimum number of degrees of freedom between the probe and drogue actuation systems. After many trade-offs were investigated, a final design evolved. It incorporates vertical and lateral linear translation plus roll angular motion on the probe mechanism, whereas the drogue has axial translation plus yaw and pitch angular motions.

There are two primary considerations which dictated the evolution of our concept. First, the probe and drogue motions must stay within the 5.6 foot diameter solar radiation pattern. Second, they must satisfy various performance specifications. The specifications for the three translational degrees of freedom are essentially the same, whereas the roll angular degree of freedom requirement is much less than those for the pitch and yaw motions.

Any rigid body can be considered as having six degrees of freedom relative to inertial space. Thus, two docking bodies would have an absolute total of twelve degrees of freedom relative to inertial space, and six degrees of freedom relative to each other. Therefore, only six degrees of freedom are needed to define completely the motion of one rigid body relative to another. Therefore, only six degrees of freedom are needed to simulate the motion of the probe vehicle relative to the motion of the drogue vehicle.

NORTHROP SPACE LABORATORIES

The following subsections consider the various combinations and distributions of these six degrees of freedom and indicate the evolution of our concept. Each subsection heading refers to a possible distribution of the six degrees of freedom between the probe and drogue vehicles. Each subsection then discusses the effects of various combinations and their order of mounting on the actuation system.

Three and Three. This distribution is the one from which our final design evolved. That is, we selected three degrees of freedom for the probe actuation and three for the drogue. It is interesting to consider the reasoning used to determine which three were applied to the probe actuation system and the order in which they are mounted. Putting the roll motion on the probe required that only the relatively smaller mass of the roll control actuator had to be accelerated by the remaining two degrees of freedom. (One might infer that because the probe roll moment of inertia is much smaller than that of the drogue that this was a consideration -- actually, it was not because the roll actuation system inertia predominates.) The remaining two degrees of freedom were selected so as to minimize cross-coupling of inertia loads. (Here again one might infer that the relative weights of the 80 pound probe or 20 pound drogue were important -- but the actuation system weight is several thousand pounds.) Hence, the vertical and lateral translation were selected as the remaining probe degrees of freedom. However, there are many more trade-offs to be discussed and evaluated before the optimization of our concept is fully explained and justified.

The optimum separation of the vertical and lateral system involved their relative inertias because these inertias cannot be uncoupled. That is, whether the vertical motion should also carry the inertia of the lateral actuation system or should the lateral actuator be required to carry the vertical actuation system. Either choice would require that the roll mechanism be moved because it must be mounted on these translation systems. The question is resolved because Negators are

NORTHROP SPACE LABORATORIES

to be used. Negators are springs that exert a constant vertical force regardless of their displacement and are used on the vertical translation system to nullify the static weight of the total probe actuator system. The Negator selected has a relatively low inertia and a natural frequency above 60 cps. If the vertical plus Negator mechanism is mounted on the lateral actuation system, then the inertia of the Negator must be added to the lateral system and the static weight of the whole system must be carried by the lateral rod bearings. A better design concept results from mounting the roll on the lateral and this combination on the vertical system and by using a slightly larger Negator to nullify the static weight of the whole system.

The drogue system must provide the remaining three degrees of freedom which are pitch, yaw, and axial translation. We have selected the pitch system to be carried by the yaw system. This combination is moved by the axial actuation system.

The trade-off considerations involved here were the determinations as to which of these three actuator systems should carry the other two systems. Because the required translation performance is relatively lower than the angular, the axial actuator system was selected to carry the other two. The pitch and yaw performance requirements are identical so the determining factor in the design of this gimbal arrangement is that the drogue cone and pressure seal be kept within the 5.6 foot diameter solar radiation pattern. That is, if the yaw system were carried by the pitch actuation system, a simple pitch gimbal ring design would indicate that the pitch ring would cast a shadow at large negative pitch angles. This shadowing can be prevented by designing a more complicated pitch support, but this results in an increase in the inertia of the system. Many types of pitch-yaw gimbaling mechanisms were considered. Our design mounts the drogue face in the plane of the pitch and yaw gimbals so that only a minimum of vertical and lateral probe motion is required to transverse the face of the drogue, regardless of the pitch

NORTHROP SPACE LABORATORIES

and yaw angles of the drogue. Note then, that the center of the drogue disk is a fixed point which can be used as the origin of an orthogonal, triad set of simulator reference axes.

Before discussing another interesting combination of the three degrees of freedom, another constraint must be mentioned. Consider that although the simulator moves both the probe and drogue, the governing equations (being solved instantaneously in the analog computer) specify the location of one point only on the probe and one point only on the drogue. This reference point on the probe has been selected as the base attach point of the probe centerline rather than the probe tip. This is because the actual probe is to be tested and the full scale flight dynamic response of the probe is inherent. That is, the actuation system behind the probe is essentially rigid because the actuator structure elasticity will be compensated for in the equations. Similar statements apply to the drogue mounting reference point.

Now consider the probe system having pitch and/or yaw degree(s) of freedom. If the base of the probe were pitched and/or yawed, then the drogue system would have to possess vertical and/or lateral motion. The required translation motion would be much greater than that used with our final concept. That is, pitching the base of the probe would translate the probe tip through an arc which must be followed by a translational displacement of the drogue. A logical modification would be to keep the probe tip centered on a point in space, but this would require that the probe system also have paired degrees of freedom. For example, if pitch were on the probe, then it would also have to have the vertical translation degree of freedom. Similarly, yaw would require lateral motion on the probe. Therefore, pitch and/or yaw on the probe increases the translation requirements for the drogue or probe. This increase in translation requirements eventually will reflect itself in a more expensive system. One more consideration involved the case where the drogue has vertical and/or lateral translation and the probe has the

NORTHROP SPACE LABORATORIES

pitch and/or yaw motion. Additional translation of the drogue is required because of the compression of the probe tip. This compression results from the probe shock absorbing recoil mechanism.

Six and Zero. This is an obvious, first choice; i.e., to consider all of the degrees of freedom on either the probe or drogue mechanisms. An immediate consideration here might be the relative mass, moments of inertia and products of inertia of the probe and drogue. However, one soon realizes that the inertia of the actuation system predominates, so that the inertia of the probe and drogue is an insignificant consideration.

Putting all of the six degrees of freedom on the probe (or drogue) would require a complicated actuation system which would have needlessly high inertia, and hence, relatively poor frequency response. There would be considerable cross-coupling of the elastic dynamics for some of the motions. However, such a system would warrant more consideration if the relative inertia of the probe (or drogue) predominated over that of the six degree of freedom actuator system. Accordingly, this configuration is not considered to be applicable to the present design.

Five and One. This configuration possibility would use five of the degrees of freedom on one mechanism and the remaining degree of freedom on the other mechanism. This configuration might have merit if one of the degrees of freedom required extremely high performance relative to the others. However, the present design requirements are just the opposite. The three translation requirements are identical, two of the three angular requirements are the same and the remaining (roll) motion requirements are low. Therefore, this configuration possibility is not considered to be applicable to the present design.

Four and Two. This configuration was a likely possibility for detail consideration if two of the degrees of freedom required extremely high response performance. However, this was not the case for the present design requirements so this configuration was not considered in detail.

A summary of these trade-offs is presented in Table 3-1.

NORTHROP SPACE LABORATORIES

TABLE 3-1 OF CONCEPT TRADEOFFS

Degrees of Freedoms	Sequence of Coupling		Remarks
	Probe	Drogue	
Note: Asterisk denotes final design concept.			
(3 and 3)*	<u>Vertical</u> system carries <u>Lateral</u> system which carries <u>Roll</u> actuator.		Minimizes inertia coupling and mass.
(3 and 3)	<u>Lateral</u> system carries <u>Vertical</u> system which carries <u>Roll</u> actuator.		Lateral rod bearings must carry more load.
(3 and 3)*		<u>Axial</u> system carries <u>Yaw</u> system which carries <u>Pitch</u> actuator.	Minimizes inertia coupling and mass.
(3 and 3)		<u>Axial</u> system carries <u>Pitch</u> system which carries <u>Yaw</u> actuator.	Possible shadow on drogue and/or excessive inertia.
(3 and 3)	<u>Pitch</u> and/or <u>Yaw</u> systems.		Drogue must then have excessive lateral and vertical motions.
(3 and 3)	Probe tip fixed during Probe Pitch and Yaw.		Probe supporting structure must translate and rotate.
(6 and 0)	Probe	or Drogue	Excessive inertias.
(5 and 1)	Probe	or Drogue	No one motion needs high performance.
(4 and 2)	Probe	or Drogue	No two motions need high performance.

Description of Structure

After having decided upon a design concept, the next step was to lay out (i.e., "frame") the mounting structure. Figure 3-3 presents a perspective sketch of the mounting structural skeleton. Because of the obvious simplicity of this illustration, it will be used in the introductory discussion of the various system components. A tenth scale model was also constructed as a visual aid, see Figure 3-4. Both the interim and final configuration are identical in concept to this skeleton. Note that the probe and its seal are mounted on a cylindrical structure which simulates the forward portion of the tunnel in the command module. (At this period in time, MSC was considering pressurizing the tunnel and actuating the seal latches. Later, this consideration was omitted from the test design requirements.) The cylindrical structure then tapers down into a small shaft which enters into the large hydraulic actuator housing. The shaft attaches to the outer case of the force balance. This balance, which is inside the actuator housing, is then connected to the roll angle actuation mechanism. Note that this actuator housing is suspended on two horizontal bars which provide the probe with the lateral degree of freedom. The hydraulic actuator cylinders are (hypothetically) inside the suspension mountings. Next, notice that the ends of these horizontal rods (i.e., piston rods) are supported by an attachment to vertical rods. The vertical degree of freedom is provided by the hydraulic actuators which are inside these attachment fittings.

Again, referring to Figure 3-3, note that the drogue was tentatively enclosed in a tapered structure to facilitate pressurizing the back side of the drogue cone. MSC has subsequently deleted this constraint. The tapered structure attaches to a shaft which is joined to the outer case of the force balance in the same manner used for the probe system. This balance is mounted inside the same cylindrical housing which is attached to the pitch gimbal ring. This ring is driven by the pitch angle actuators which are hypothetically housed inside the pitch gimbal ring

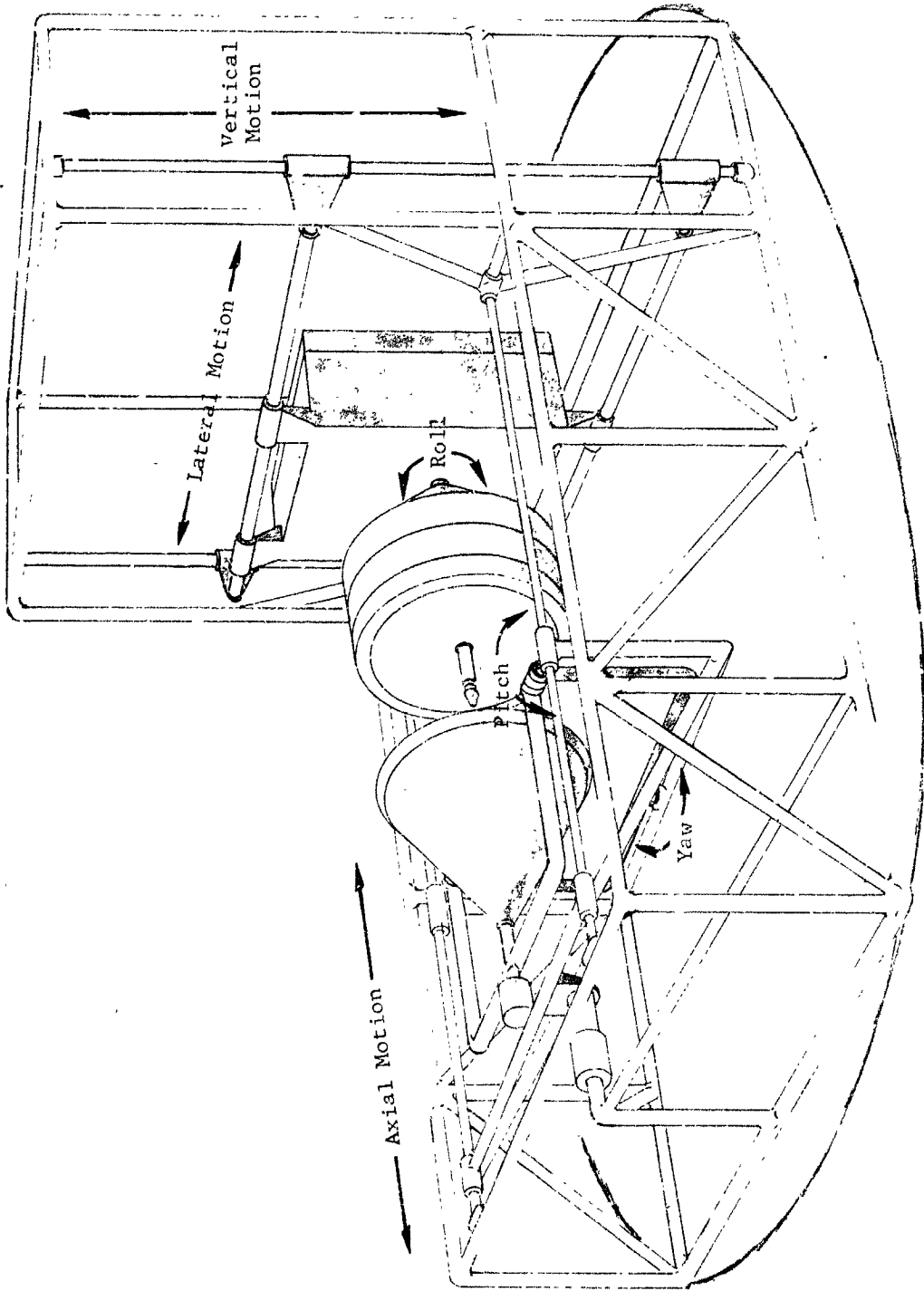


FIGURE 3-3 SKELETON FRAMING OF MOUNTING STRUCTURE



FIGURE 3-4 TENTH SCALE MODEL WHICH ILLUSTRATES OUR SIX DEGREE OF FREEDOM MOTION CONCEPT.

NORTHROP SPACE LABORATORIES

attachment to the yaw gimbal ring. (External, linear actuators are used in the actual design). The base of the yaw gimbal is attached to the yaw actuator, which in turn, is supported by a horizontal bar. This U-shaped horizontal bar is supported by bearings which slide on horizontal side rods. This U-shaped bar is actually part of a trusswork which slides axially on the two horizontal side rods. The axial motion is obtained from a hydraulic actuator that is cantilevered from a tripod support at the end of the simulator support truss frame.

The effect of cross-coupling in the probe and drogue actuation system is similar. The probe system will be discussed as it is typical. In our design, the probe can be rolled relative to the drogue without introducing any system cross-coupling. If the probe is accelerated vertically, then the roll degree of freedom actuator system is also accelerated vertically. The key point here, from a kinematics point of view, is that the roll motion remains uncoupled from the vertical motion. From a structural loads viewpoint, the roll actuation system should have its center of gravity in or near the plane of the vertical motion actuators in order to minimize bending moment stresses due to the roll system "overhang."

From a structural dynamics viewpoint, all of the actuation systems will have natural frequencies. For example, consider moving the probe up and down sinusoidally throughout a two inch amplitude and slowly increasing the frequency of oscillation. At some frequency, the actuator power requirements to produce the oscillations would diminish rapidly and this would indicate experimentally the lowest natural frequency of the vertical degree of freedom. Because we have postulated a constant amplitude oscillation, nothing unexpected happens to the structure or probe motion at or near this first natural frequency of the vertical degree of freedom. However, the power versus frequency requirements must be considered (i.e. transfer functions) in the design and control of the actuation system. In summary then, each

NORTHROP SPACE LABORATORIES

of the six degrees of motion freedom have (natural) frequencies which the respective actuation system must control. In general, the systems were designed with as much stiffness as practical and with minimum inertia so that the lowest natural frequency would have a high value. Hence, there are a minimum number of natural frequencies at which the actuation servos must be compensated.

The simulator framework shown in Figure 3-3 appears to sit on a disc which typifies the lunar plane of Chamber B. As discussed in Section 3.4, the simulator framework is bolted to a large steel plate which acts as a seismic mass. This plate is supported on large damped springs which isolate the Chamber B lunar plane from the transient motions of the seismic mass.

The pattern of solar simulation can be enhanced by tilting the structural mounting if this is desired.

Our interim simulator design is presented as Figure 3-5. Note that the probe and drogue seals are backed up by cylindrical structures which were to have the same elastic characteristics as the flight vehicles. Although the various actuator mechanisms are basically the same as those which were discussed for the skeleton framing configuration, they are much more massive. Similarly, the framing structure appears quite rigid because the frame tube sizes were selected for deflection characteristics rather than stress levels. Also, many types and variations of drogue gimbal ring mounting were investigated. For example, Figure 3-5A presents one such proposed design whose X-frame bracing was incorporated in the final configuration. The overall size of this frame is 19 feet long, ten feet wide and ten feet high. The estimated weight was 10,000 pounds. However, subsequent investigation of the servo system necessitated an optimization of translation requirements which permitted use of an actuator having shorter length and higher natural frequency. This also permitted a more compact and rigid structure which became our final simulator design as shown in Figure 3-6 and the pullout Figure 3-7. The details and structural dynamics of this structure are discussed in a following section of the report.

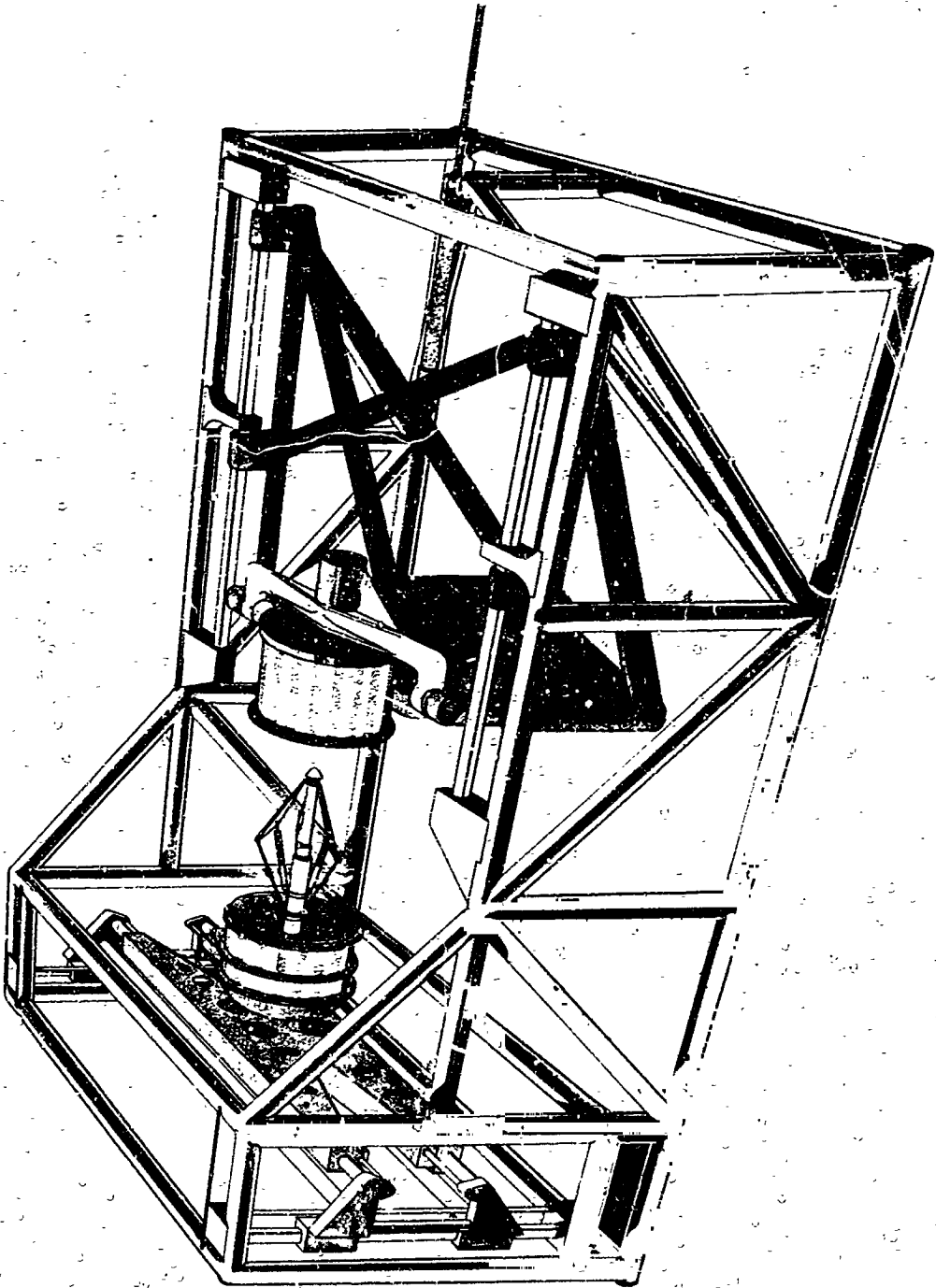


FIGURE 3-5 PERSPECTIVE SKETCH OF THE INTERIM SIMULATOR DESIGN

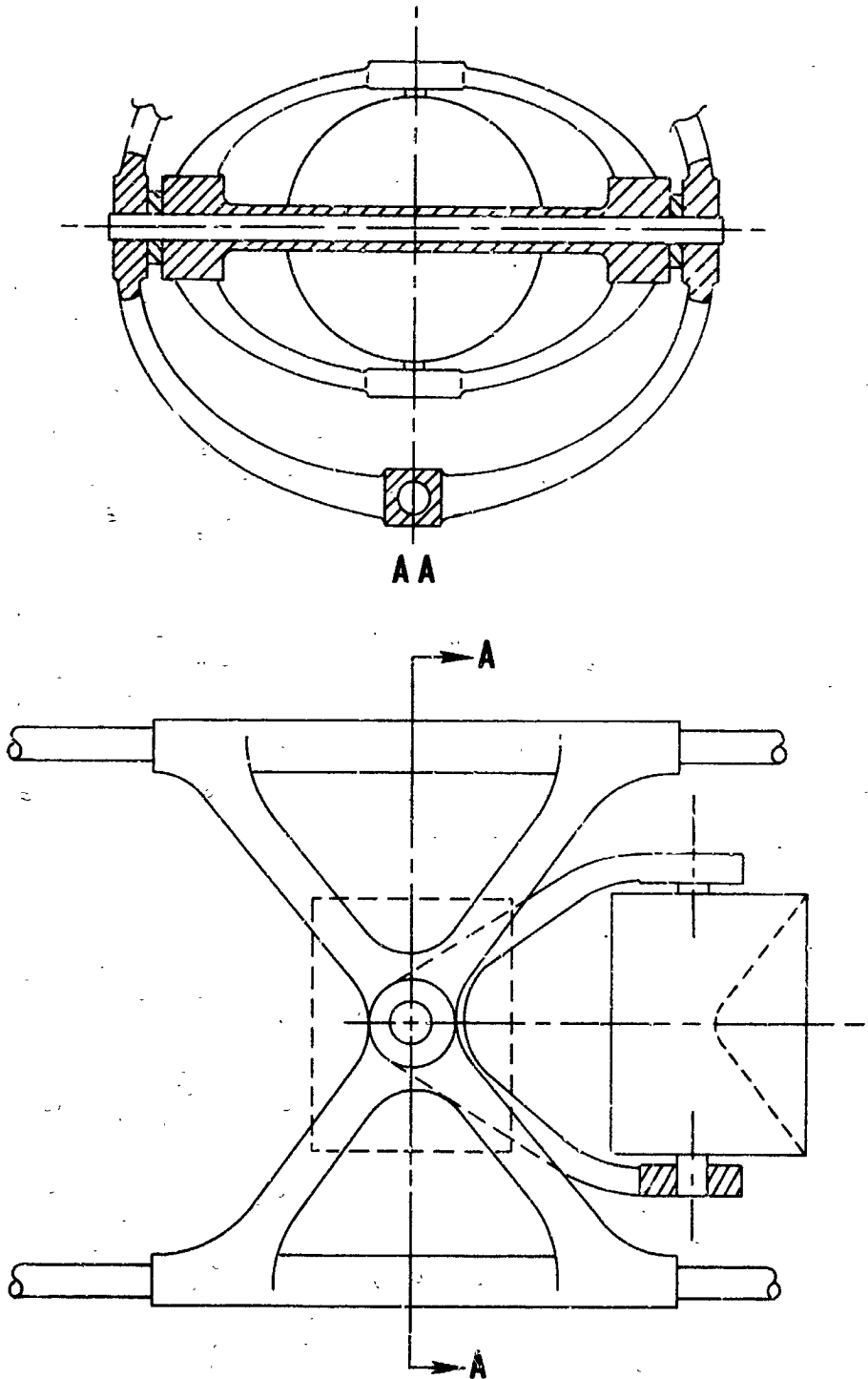


FIGURE 3-5A PROPOSED DROGUE MOUNTING STRUCTURE
FROM WHICH OUR FINAL DESIGN EVOLVED

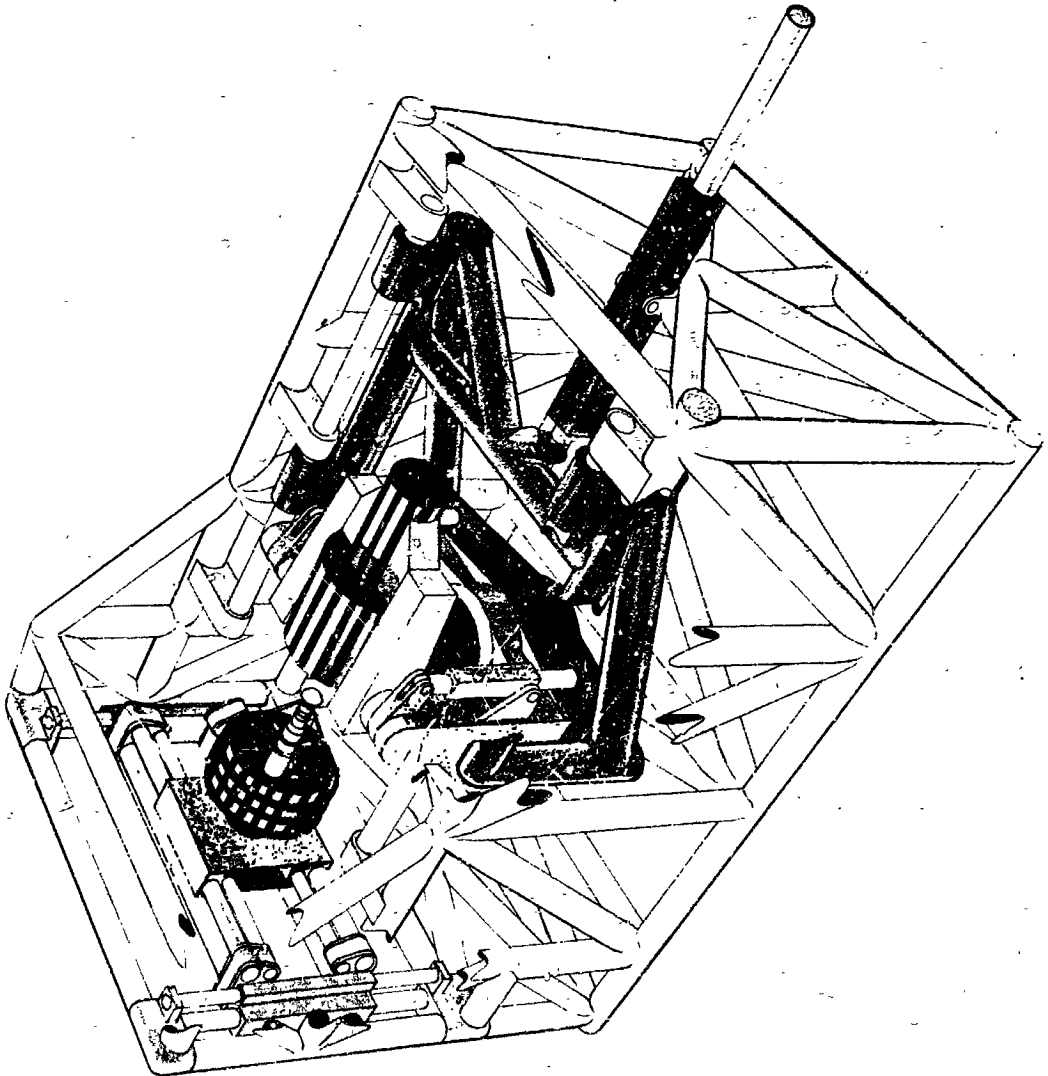
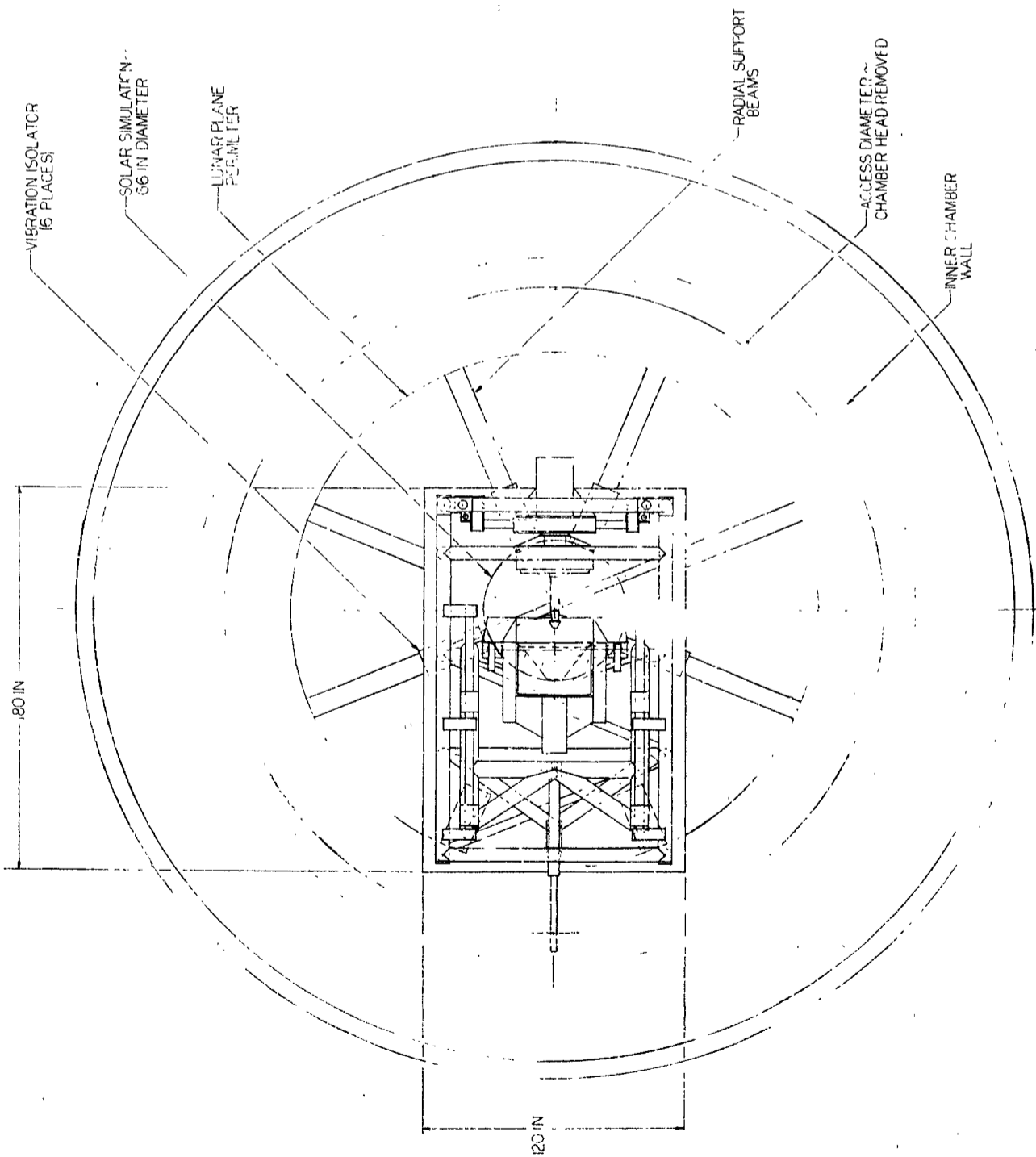
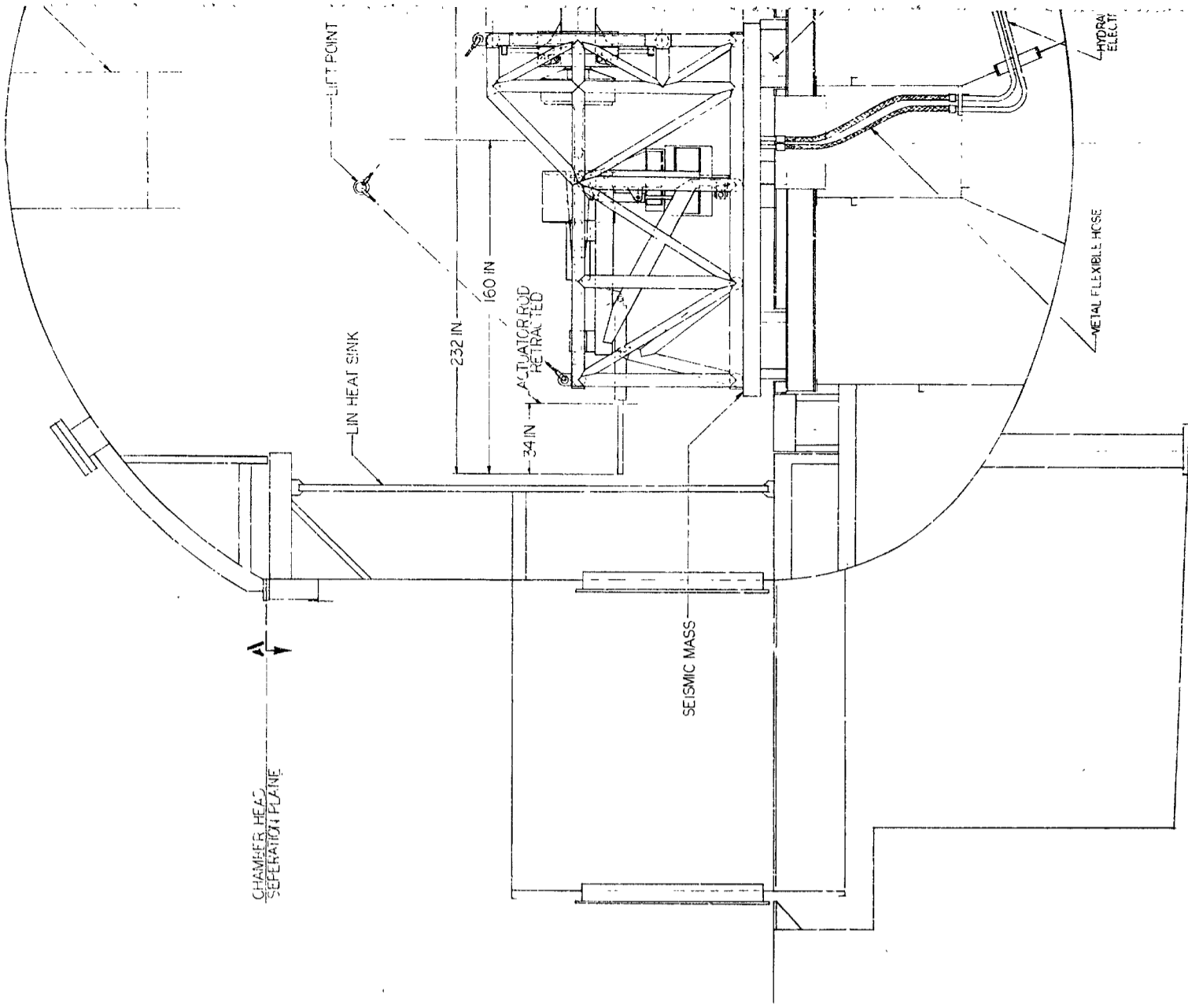
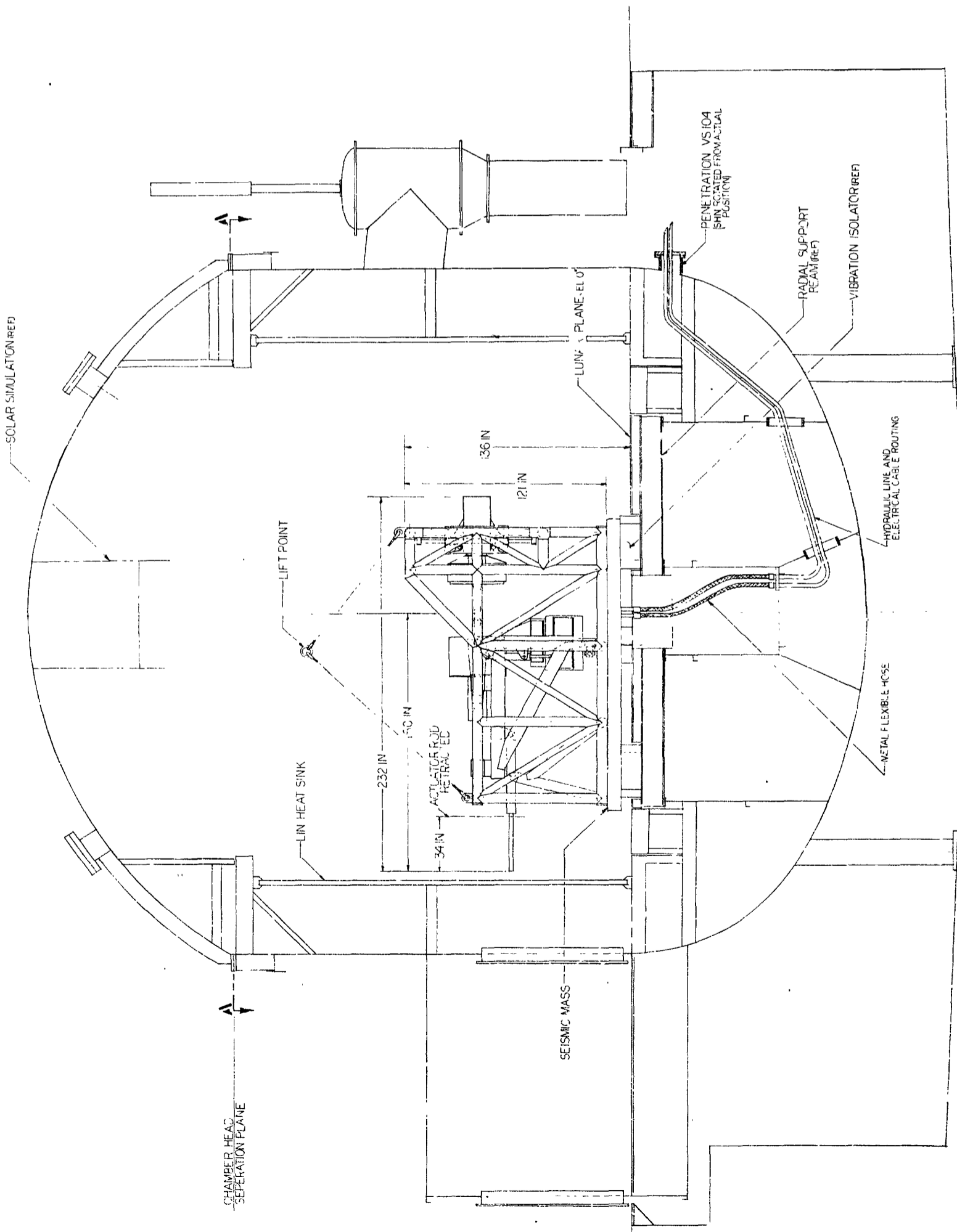


FIGURE 3-6 PERSPECTIVE SKETCH OF THE FINAL SIMULATOR DESIGN



SECTION A-A

FIGURE 3-7 APOLLO DOCKING SIMULATOR INSTALLATION IN CHAMBER B.



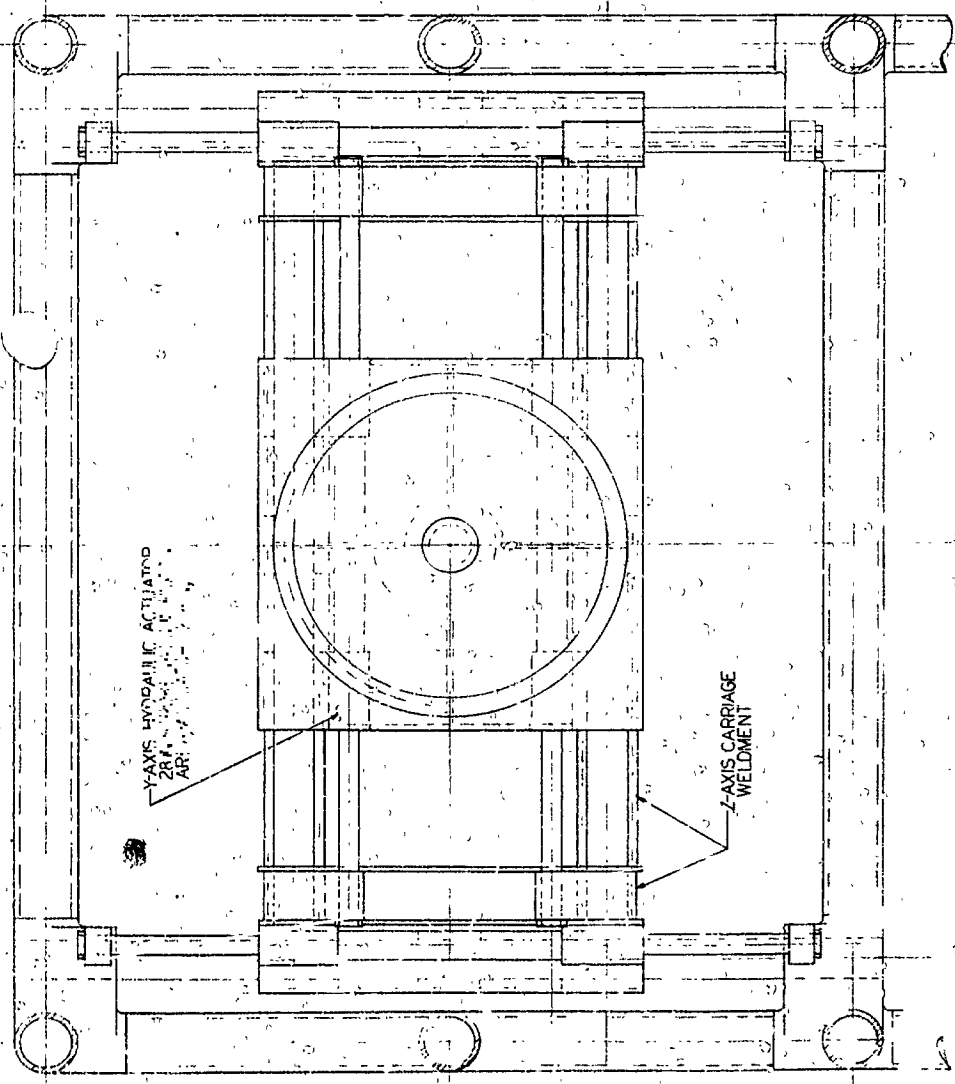
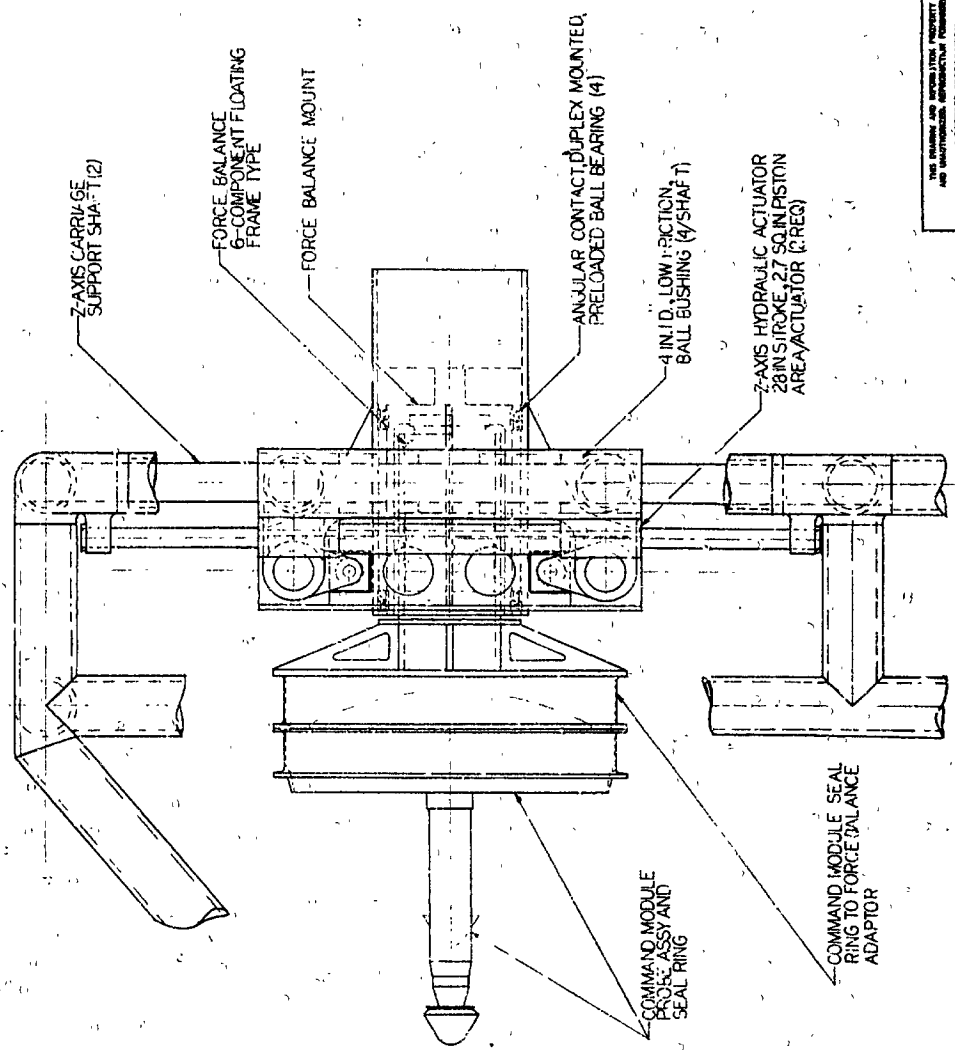
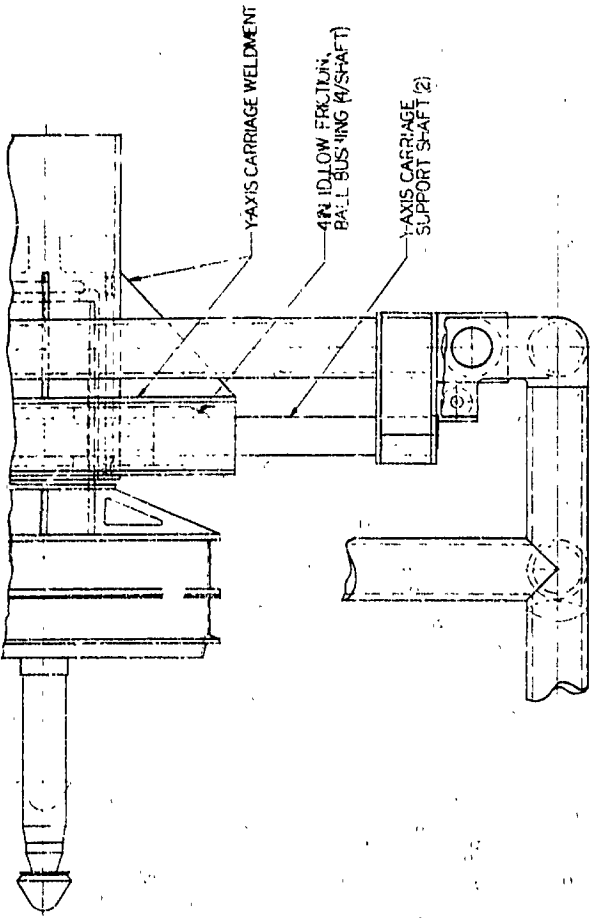
THE DATA AND INFORMATION CONTAINED HEREIN IS UNCLASSIFIED EXCEPT WHERE SHOWN OTHERWISE BY THE MARKING		SCALE 1/20 MODEL 2	APPROVED DATE BY WJ STA-MAN/1/63
NORTHROP CORPORATION NORTHROP SPACE LABORATORIES		APOLLO DOCKING SIMULATOR CHAMBER B INSTALLATION	

Probe Mounting

The probe assembly is supported by the seal ring as in the actual vehicle (See Figure 3-8). Either the actual Command Module Structure or a simulated structure will be used for the seal ring. This ring is attached to the balance adaptor fitting, which is a light weight stainless steel weldment with a journal type attachment to the balance outer case. The force measurement balance is discussed in section 3.3 of this report. The inner rod of the balance is attached to a circular housing which is carried by angular contact anti-friction bearings supported by the lateral translation carriage. These bearings have sufficient preload to eliminate unwanted backlash. The circular housing which supports the balance inner rod is driven by the roll servo motor through a total angular displacement of 360 degrees.

The lateral translation carriage is a minimum weight stainless steel weldment which is supported on anti-friction adjustable bore bushings rolling on hardened and ground stainless steel shafts attached to the vertical translation carriage. Motion is provided by two linear hydraulic actuators whose resultant force acts essentially through the center of gravity in two planes and are in the same vertical plane as the support shafts. The bodies of these actuators are mounted rigidly to the lateral translation carriage. The piston rods are connected to the vertical translation carriage thus allowing for a minimum width of the vertical carriage. Hydraulic fluid will be fed into these actuators through the center of the piston rods to minimize the number of flexible hydraulic lines required. Lateral travel of the carriage will be stopped at the ends of its travel by fluid metering type shock absorber devices to prevent balance damage by excessive decelerative forces.

The vertical translation carriage is a stainless steel weldment of the "picture frame" type which surrounds the lateral translation carriage. It is guided by anti-friction adjustable bore bushings rolling on hardened and ground stainless steel shafts which are attached to the external frame.



APPROVED	DATE	BY	THE ENGINEERING AND RESEARCH CENTER OF THE UNIVERSITY OF MICHIGAN
REVISIONS	NO. 2	DATE	WORKSHOP CORRECTIONS
DRAWN BY			W. J. STANNARD
APOLLO DOCKING SIMULATOR PROBE MECHANISM LAYOUT			

FIGURE 3-8 PROBE MECHANISM LAYOUT

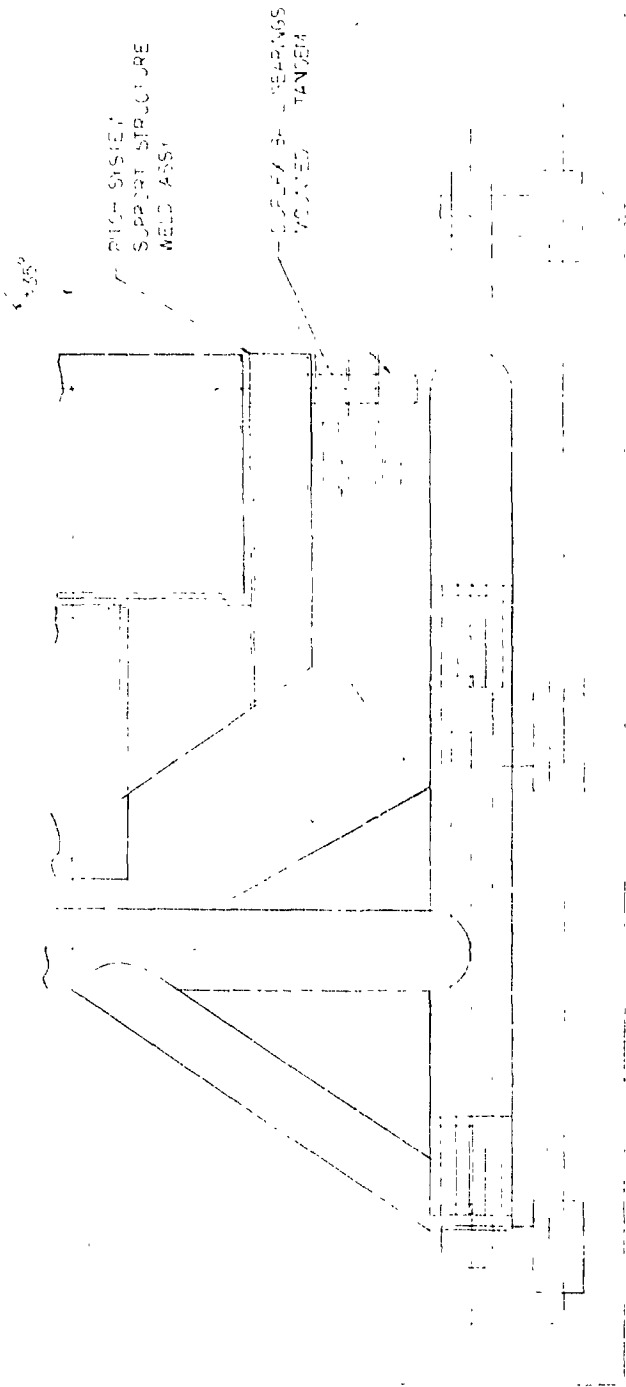
NORTHROP SPACE LABORATORIES

Motion is provided by two linear hydraulic actuators which are equally spaced on either side of the center of gravity of the vertically translating mass when the lateral carriage is in the center of its travel. The wide spacing of the actuators minimizes the percentage of mass shifted from one actuator to the other as the lateral carriage translates off of center position. The bodies of these actuators are mounted rigidly to the vertical carriage and the piston rods are connected to the support frame thus allowing a minimum frame height. Hydraulic fluid will be fed into these actuators through the center of the piston rods enabling the servo control valves for the vertical carriage to be mounted to the support frame, thus reducing the mass of the vertically translating carriage. The dead weight of the vertical carriage and all parts attached to it will be offset by Negator springs, a constant force low inertia device, which reduces the size of the vertical actuators required and provides equal acceleration of the carriage in both directions. Vertical travel of the carriage will be stopped at the ends of its travel by fluid metering type shock absorber devices to prevent balance damage by excessive decelerative forces.

Drogue Mounting

The drogue assembly is supported by a seal ring as in the actual vehicle (See Figure 3-9). Either the Lunar Excursion Module structure or a simulated structure may be used. This seal ring structure is in turn mounted to one end of a force measurement balance discussed in section 3.3.

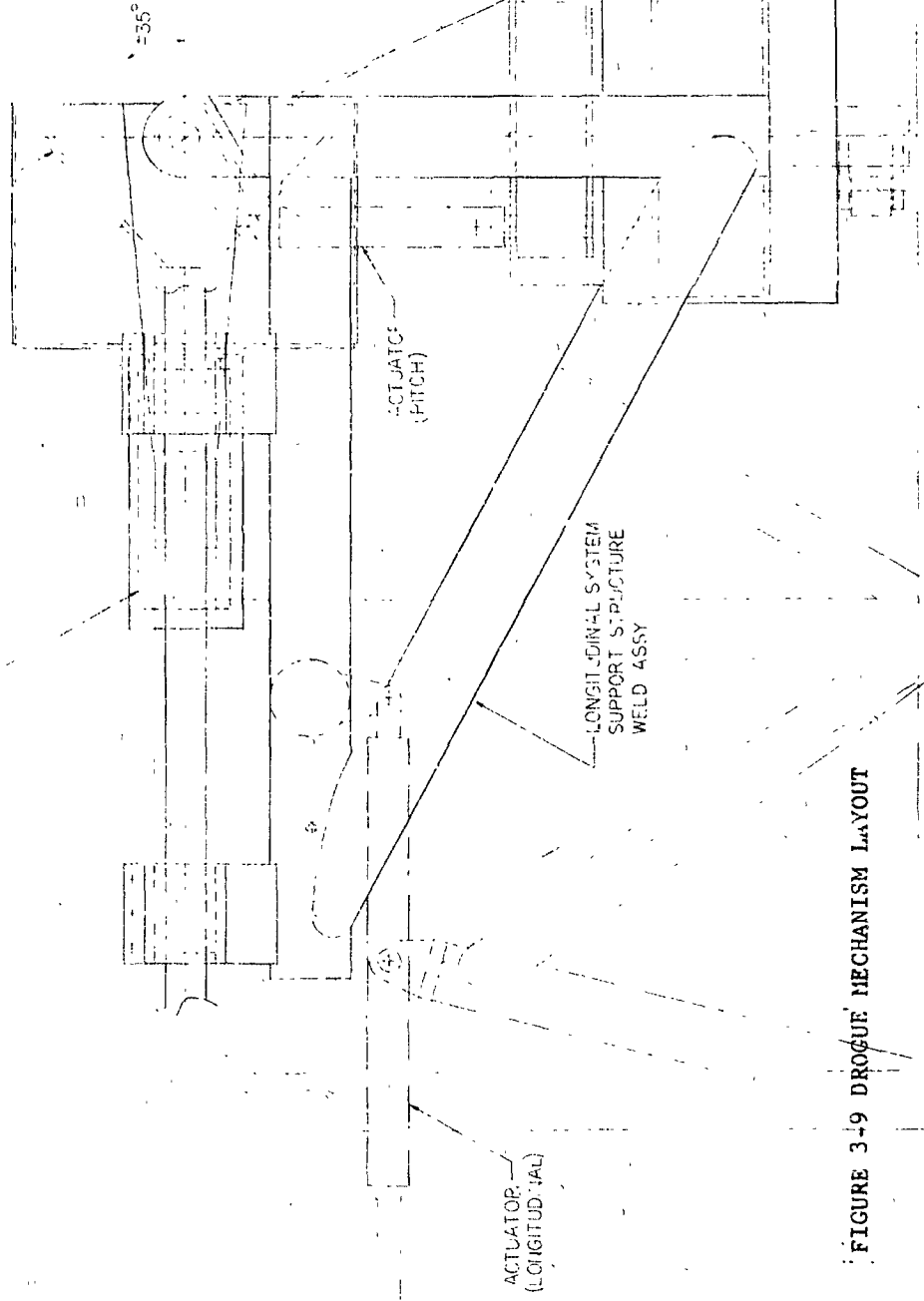
The opposite end of the force balance is supported by a rigid welded stainless steel pitch support structure. The pitch structure is gimbal-mounted where two hydraulic cylinders each actuating a bell crank drive it ± 35 degrees in the vertical plane. The pitch structure is supported by a system of tandem mounted duplex bearings. These bearings will be preloaded to remove any undesirable backlash.



SCD.

—IMPROVE ASSY
3 ATTACH PTS

—PITCH BALANCE
SIX COMPLETE



—BALL BUSHING
GROUND SHEET

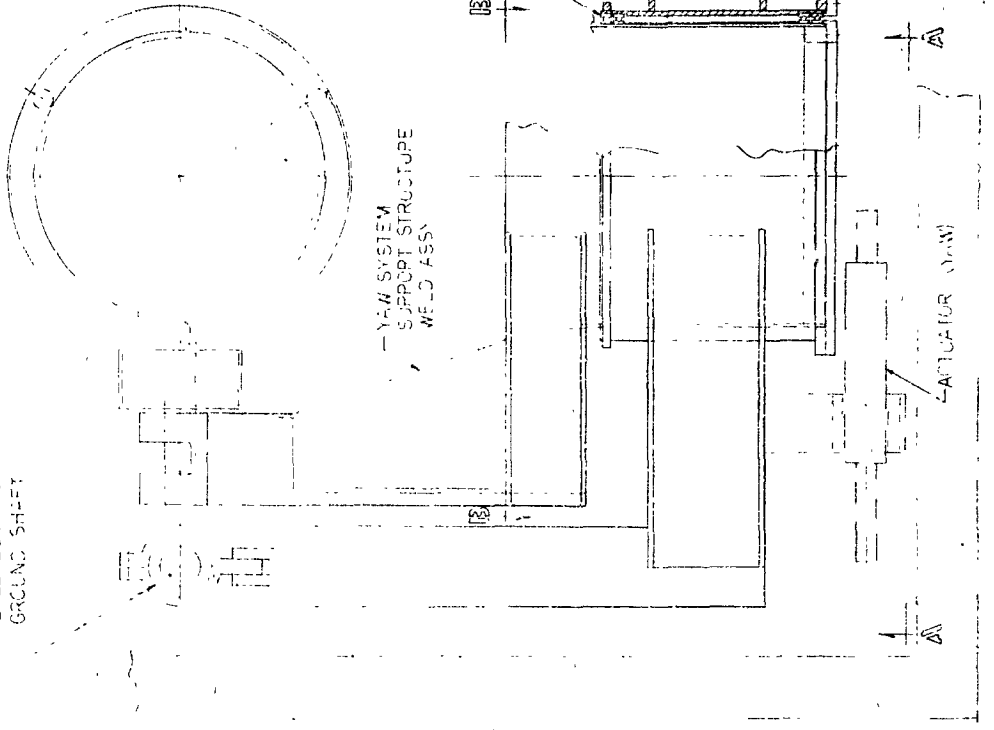
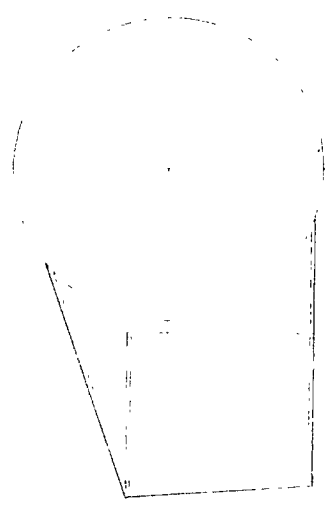
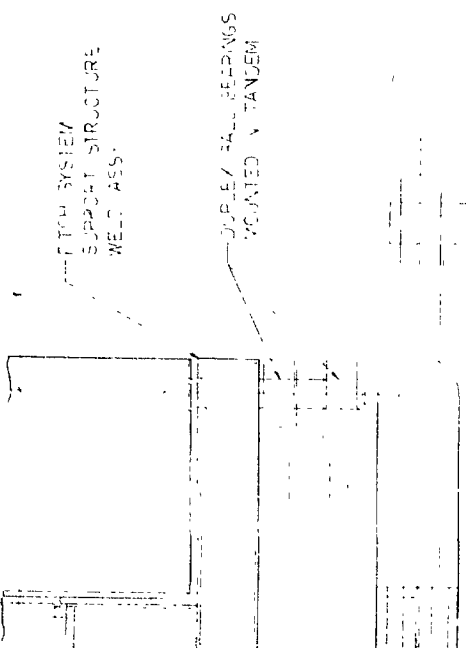


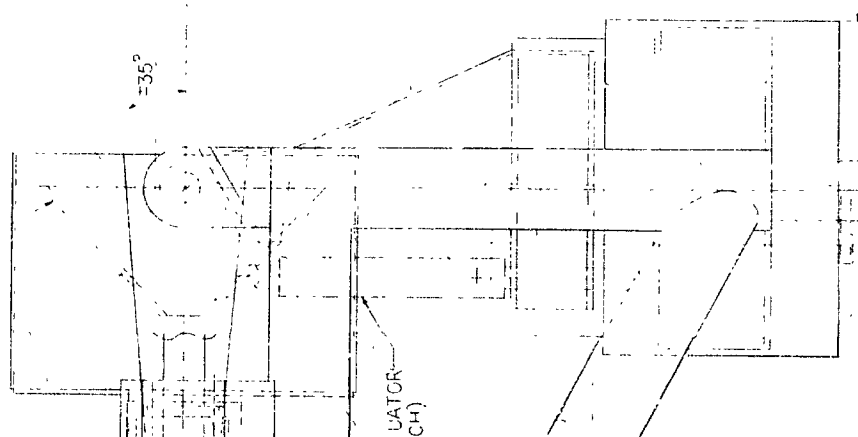
FIGURE 3-9 DROGUE MECHANISM LAYOUT



6. A

13. B

EM. SPOGGE ASSY
3 ATTACH PTS



BALL BEARING
ANGULAR CONTACT
30° TAPER
DUPLEX MOUNTING
(TTP)

YAW SYSTEM
SUPPORT STRUCTURE
WELD ASSY

36.00
STROKE

DESIGNED AND DEVELOPED BY	SCALE	APPROVED
NO UNAUTHORIZED REPRODUCTION PERMITTED BY	1/8"	DATE
INSTRUMENT CORPORATION	2	APPROVED
INSTRUMENT FACILITIES		DATE
APPROVED BY		DATE
APPROVED BY		DATE
APOLLO GUIDING MECHANISM LAYOUT		
ROSCOE MECHANISM		

NORTHROP SPACE LABORATORIES

The entire above mentioned pitch assembly structure is in turn supported by a welded stainless steel yaw structure. The yaw structure is supported by a system of angular contact duplex bearings mounted in tandem. These bearings are preloaded to remove backlash and will allow for structural thermal expansion or contraction. The yaw structure is moved through its angular motion ± 35 degrees in the lateral plane by a bell crank driven with a hydraulic cylinder.

The above pitch and yaw mounting assemblies are supported by a welded stainless steel carriage structure. This carriage structure is suspended from a pair of rails by preloaded ball bushing assemblies. The carriage structure translates 34 inches axially. A hydraulic cylinder supplies the driving force to the carriage.

All structural components of the drogue mounting assembly are designed for minimum deflections, compact size, and ease of fabrication. Support ball bearings in the system will realize medium working loads and be lubricated with silicone base grease.

Thermal Effects

The problems of temperature induced stress in the structure and base plate was investigated and found to be negligible. In addition, the effect of the structure and base plate thermal radiation upon the simulation of the docking environment is discussed.

Preliminary studies of the temperature response of the structure and base plate were performed in order to determine whether or not any temperature related problem areas exist. The simplifying assumption used in the studies was that the temperature gradient across the thicknesses are negligible. This assumption closely approximates what is actually occurring due to the relatively large thermal conductances in relation to the rates of heat transfer involved. Using this assumption, it was found that no large temperature gradients will occur in the base plate and support structure when subjected to a sudden change from room environment to simulated space environment.

NORTHROP SPACE LABORATORIES

Starting from an initial temperature of 70 degrees F., it was estimated that the major support structure will cool down to -85 degrees F., in 24 hours, while the base plate will cool down to -30 degrees F. in the same time period. The effect of the solar simulation beam upon the temperature gradients in the base plate was found to be negligible. It is estimated that these temperature gradients at any instant in time will be less than 30 degrees F.

The three environments in which docking will be simulated are earth orbit, translunar and lunar orbit. Infrared and reflected simulated solar radiation will impinge upon the docking simulator from the relatively warm base plate and support structure thereby degrading the simulation of these environments unless steps are taken to reduce these effects. The steps to be taken to improve the simulation of the desired environments are dependent upon the degree of simulation desired. For example, in order to simulate deep space, a liquid nitrogen curtain shield coated with a non-reflective coating should be placed between the docking simulator and the base plate. A close approximation to this can be obtained by shielding the base plate with a thin shield coated on the base side with a polished surface to reflect the infrared radiation of the base plate. On the side facing the docking simulator, a black coating would be used to absorb the solar radiation and emit to the cold walls of the vacuum chamber.

Shields with appropriate coatings can partially simulate the albedo and infrared radiation from Earth and the lunar surfaces. The design of the structure and base plate and possible modifications to more nearly simulate the desired environments should be accounted for in the NAA design of the probe and drogue.

STRUCTURAL DYNAMICS

General Design Approach

The philosophy of the design of the structure of the dynamic docking simulator relative to its structural dynamic characteristics is to maintain all natural frequencies above 60 cycles/second. This relatively high frequency criteria will eliminate, or at least alleviate, many problems which would be incurred if lower resonant frequencies were allowed to exist:

1. This frequency is above the natural frequencies of interest in the docking bodies and above the fuel sloshing frequencies so that compensation for simulator frequencies will not be required in the computer program.
2. The control system response is down about ten db at 60 cycles/second so the control system analysis which was based on rigid mass assumptions is valid (See Section 3.3).
3. Since control system response is attenuated above 60 cycles/second, the vibratory exciting force at the structural resonant frequencies will be relatively small and material damping will be sufficient to attenuate the vibration response. No special structural damping devices will be necessary.

The resonance corresponding to the mass of the probe or drogue and their supporting structure on the force balance will probably be the most critical response in the simulator. The force balance will measure accelerations imposed by the motion of the simulator as well as the forces incurred during docking. In the low frequency range of interest these accelerations will simply be those accelerations which the docking vehicles would actually experience. However, near the resonant frequency of the force balance itself, these acceleration readings will be vastly in error. Since the measurements at the force balance are fed through the computer to the control system of the

simulator, the high forces at resonance could cause the system to become unstable. Therefore considerable care will be taken to assure that the force balance resonant frequency is high enough so that the control system characteristics will attenuate the response sufficiently to maintain stability.

Every precaution will be taken during the final design of the simulator to assure that the required dynamic characteristics are achieved. This will include a careful analysis in which the characteristics of the structure and the control system will be combined to ascertain system response. However, it is recognized that in a system of this complexity, unforeseen structural characteristics may appear when the simulator is tested. Therefore provision is made to place accelerometers at critical points on the structure to provide stabilizing feed back signals to the control system. This approach has been utilized with complete success in the Northrop six-degree-of-freedom dynamic flight simulator (Reference 1).

In a preliminary analysis of the dynamic characteristics of the simulator the drogue and probe systems were considered separately. Simplified dynamic models were studied in order to determine the major resonant frequencies. The general methods of analysis are described in References 2 and 3. An example of the analysis is shown in Appendix A.

The dynamic modes considered, included motion of the probe system in the Z-axis coupled with pitch; vibration of the drogue system in the X-axis coupled with vibration in the Z-axis and pitch; lateral and yaw vibration of the probe system; and lateral yaw, and roll vibration of the drogue system.

Typical of the results obtained are the resonant frequencies of the probe system in the coupled vertical and pitch vibration mode. These frequencies were computed to be 60 cps, 170 cps, 216 cps, and 524 cps. With the exception of the 60 cps frequency, which is due to vibration of the probe on the force balance, all of these frequencies are well above the 60 cps criterion established for this system.

Drogue System Dynamics

The drogue system (Figure 3-9) consists of a carriage which moves along support bars in the x-direction, a yaw structure which mounts on the carriage and rotates about the z-axis, and the pitch structure which supports the drogue and is pivoted on the yaw structure to give pitch motion about the y-axis. A feature of the design is its symmetry about a vertical plane, which effectively uncouples vibration in the x-axis and in pitch from vibration in the y-axis and yaw.

Each of the two large diameter support bars on which the carriage rides are supported at three points to the simulator frame. The center support results in high rigidity in the lateral and vertical directions. If a more detailed dynamic analysis to be performed in the lateral direction shows that more rigidity in the present design is necessary, then, cross members will be added to the top of the frame structure which supports these bars.

Maximum rigidity is obtained in the carriage structure through the use of large diameter tubing arranged to take advantage of the fundamentally rigid triangular configuration. Again additional stiffness can be obtained in the lateral direction by the addition of cross tie members if analysis shows this to be necessary. The large cross section of the box sections supporting the yaw axis bearing housing provides the maximum resistance to twisting and bending deflections from yaw structure loading.

The yaw structure of the drogue system poses a particularly difficult design problem since it is necessary to have a highly rigid structure to reduce inertia coupling and to support the pitch system and still avoid any structural members passing over the drogue which would interfere with simulated sunlight. In addition it is desirable to reduce the yaw inertia

loading on the axial and pitch servos. These goals are achieved through the use of a yoke type of structure with maximum stiffness designed into its members. The yaw structure is supported in large diameter bearings (on the order of 30 inches) in the carriage structure. This large diameter provides the rigidity required at this critical point in the design. A short coupled box structure joins the yaw axis shaft to the yoke arms resulting in minimum twisting and bending deflections. The yoke arms are tapered box beams which provide high rigidity in both torsion and bending.

The pitch structure of the drogue system again is basically a yoke shaped configuration and is built up of boxed beam structure to give rigidity in bending and torsion. This structure furnishes a rigid support for the force balance to which the drogue is attached.

Probe System Dynamics

The probe system (Figure 3-8) consists of a vertical carriage supported by two vertical guide bars secured to the simulator frame, and a lateral carriage supported by two horizontal guide bars secured to the vertical carriage. The roll axis system consisting of a rotary actuator, the probe and its support structure, and the force balance, is carried by the lateral carriage.

The fixed guide bars supporting the vertical carriage are mounted in massive structures in the frame so that for analysis purposes they are considered to be built-in. The portion of these bars passing within the carriage structure is guided for almost the whole length of the carriage by ball bearing bushings. Since the motion of the carriage is limited to approximately plus or minus 13-1/2 inches, there is only 27 inches of length where bending can take place. Therefore with the large diameter guide bars which are used, deflections will be very small resulting in high response frequencies in the direction of the x and y axis and in pitch. The large distance between these bars also assures high resonant frequencies in yaw.

NORTHROP SPACE LABORATORIES

The lateral carriage is supported on horizontal bars which are essentially identical to the vertical carriage guide bars. Therefore, since the rigidities are the same, the resonant frequencies will be even higher since the mass carried is approximately one half of that carried by the vertical guide bars. The principal difference in the two portions of the system is that the guide bars for the lateral carriage are much closer together than for the vertical carriage. This distance between the bars affects the rigidity in pitch. However, the overhanging load, which causes pitching moments, is quite small since the center of gravity of the lateral carriage assembly falls within a few inches of the plane of the guide bars. Therefore, a high resonant frequency in pitch will exist.

The roll axis portion of the probe due to the low inertias involved and the close coupled construction will have relatively high frequencies with the exception of the force balance deflections as were previously discussed.

Simulator Frame and Support Structure Dynamics

The simulator frame must withstand all reactive forces imposed by the simulator actuators. Therefore, its dynamic characteristics are equal in importance to the dynamics involved in the moving portions of the system. High rigidity is obtained in this design through the use of heavy wall stainless steel tubing joined by fusion welding into a single integral frame. The frame members are efficiently arranged in a truss type of structure to provide the maximum stiffness.

The reactive loads of the actuators which are transmitted to the frame structure must then be reacted on the support structure of the simulator frame. Since the environmental simulation chamber in which this dynamic simulator is to be mounted could not be expected to withstand the applied loads, a seismic block supported on vibration isolators will be utilized for mounting the simulator. Details of the design for this mounting system are described in section 3.4, Chamber Interfaces.

3.3 Servo Control System

The Servo Control System, which includes the analog computer as an element, performs the necessary control and recording functions for the docking simulation tests. This system positions and moves the probe and drogue mechanisms in a controlled manner to verify their docking capability under various conditions. At the start of a test these movements are programmed to the actuator servo system to cause the probe and drogue to come together in a prescribed manner. After initial contact, these movements are controlled, but are unprogrammed, and are dependent upon the effects of the actual mechanical contact and the pre-set inertial characteristics which were assigned to the mechanisms by means of the computer. The computer simulates mathematically the characteristics of both the Apollo Command/Service Module to which the probe is attached, and the Lunar Excursion Module to which the mating drogue is attached. This substitution for vehicle dynamics results in separate but appropriate and representative application of forces and movements by the actuators to both the probe and drogue, respectively. Strain gage transducers sense forces of the impact between the probe and drogue and provide the computer with force and moment data to close the servo force loop. Additionally, recorders associated with the servo control system provide a graphic record of all operations and movements of the probe and drogue. This data is time correlated to the analog computer computations and outputs, and denotes forces, moments, accelerations, velocities, and positions of the probe-drogue mechanisms for each docking maneuver.

The six-axis servo control system provides the controlled power necessary to reproduce the six degree-of-freedom simulator carriage motions in direct response to the transformed voltage commands of the

D.D.S. computer. This response must be accurately maintained with respect to both time and magnitude over a range of motion amplitudes and frequencies which duplicate the real dynamic inputs at the base of the docking structures. Figure 3-10 illustrates the interfaces which exist between the control system, the simulator carriages, the transformed input signal commands received from the computer, and the output motion signals provided to the data recorder.

The information presented in this section includes: the preliminary control system performance requirements, a description of the preliminary system design mechanization, a discussion of the system synthesis and analysis, and a summary of the performance achieved.

3.3.1. REQUIREMENTS

Design values based on information supplied by MSC/SID, representing critical-case requirements for relative forces and motions between the probe and drogue, in the probe/drogue axis system, are summarized below.

Accelerations are:

$$\begin{aligned}\ddot{X} &= 0 \text{ to } 13.7 \text{ ft/sec}^2 \\ \ddot{Z}, \ddot{Y} &= 0 \text{ to } 42 \text{ ft/sec}^2 \\ \ddot{\theta}, \ddot{\psi} &= 0 \text{ to } 3.1 \text{ rad/sec}^2 \\ \ddot{\phi} &\text{ not specified by MSC/SID}\end{aligned}$$

The above values must be met while simultaneously furnishing the following loads:

Longitudinal probe force: 2050 lb

Lateral probe force: 1150 lb

Maximum velocity ranges are:

$$\begin{aligned}\dot{X}, \dot{Z}, \dot{Y} &= 0 \text{ to } 2 \text{ ft/sec} \\ \dot{\theta}, \dot{\psi} &= 0 \text{ to } 0.11 \text{ rad/sec} \\ \dot{\phi} &= 0 \text{ to } 0.018 \text{ rad/sec}\end{aligned}$$

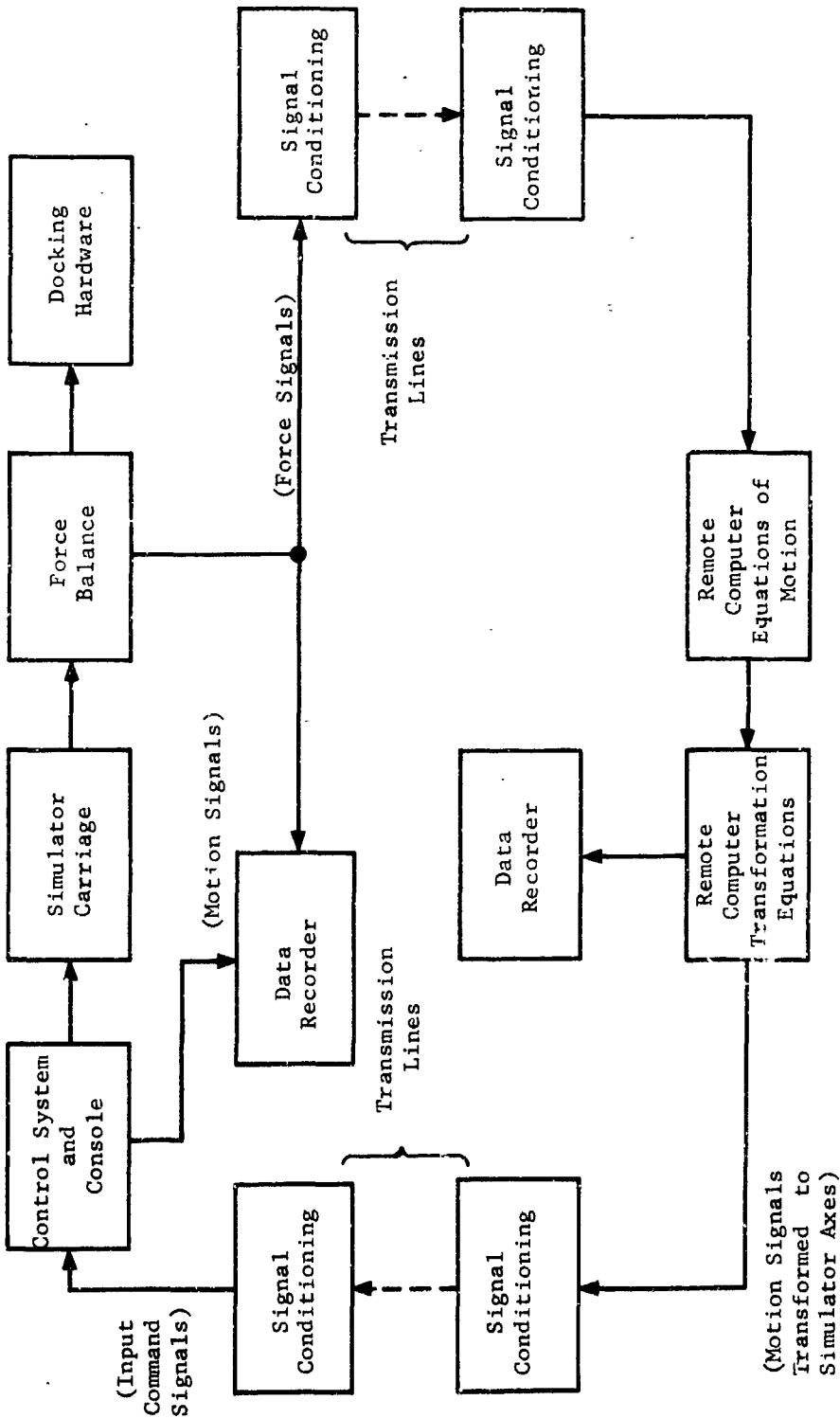


FIGURE 3-10 FUNCTIONAL DIAGRAM - CONTROL SYSTEM INTERFACE

NORTHROP SPACE LABORATORIES

The following loads at the probe tip approximate maximum loading conditions:

Longitudinal: 3000 lb

Lateral: 3200 lb

Limit loads for the roll axis are expected to occur during engagement of the tunnel seal interface. Estimates of this maximum loading, based on a friction coefficient of 0.5 between the tunnel sealing surfaces and with a probe retracting force of 1000 lb., yields a roll moment for preliminary design purposes of 10,000 inch-lb.

Required response times associated with the rigid body motions are defined on the basis of the steady rise time for the output accelerations to change from zero to the maximum values stated above. This rise time supplied by MSC/SID for preliminary design purposes for all translational and rotational axes (except roll) is 0.02 seconds.

The control system dynamic response requirements must also include consideration of higher frequency elastic modes of the docking vehicle structures superimposed on the lower frequency fuel slosh and rigid body equations of motion.

Estimated upper limits for the structural bending frequencies are given as:

First bending mode = 27 cps

Second bending mode = 49 cps

The envelope of permissible relative positions between the docking vehicles, just prior to collision, defines the design range of total displacements required.

A summary of control system output design values established for each D.D.S. carriage servo-drive system is given in Table 3-2. Values shown encompass the range of rigid body motions defined above; the 2g acceleration capability assigned to the three translational axes includes

NORTHROP SPACE LABORATORIES

TABLE 3-2 DESIGN VALUE SUMMARY

AXIS	DISPLACEMENT	VELOCITY	ACCELERATION	LIMIT LOAD DUE TO DOCKING COLLISION
X	± 17 inches	24 in/sec	772 in/sec ²	3000 lb
Y	± 13.5 inches	24 in/sec	772 in/sec ²	3200 lb
Z	± 13.5 inches	24 in/sec	772 in/sec ²	3200 lb
θ	± 0.61 rad	0.11 rad/sec	3.5 rad/sec ²	40,500 in-lb
ψ	± 0.61 rad	0.11 rad/sec	3.5 rad/sec ²	40,500 in-lb
ϕ	± 3.14 rad	0.018 rad/sec	Not Specified By MSC/SID	10,000 in-lb

NORTHROP SPACE LABORATORIES

a limited margin for simultaneous simulation of vehicle structural bending modes. Displacements and forces shown agree with the mechanical arrangement of the D.D.S. simulator carriages.

An exact statement of the minimum acceptable dynamic response requirements is not possible on the basis of existing data supplied by MSC/SID. Therefore, it is estimated for preliminary design purposes that an acceptable control system response, appraised in terms of response to a sinusoidal input, is defined by the following characteristics:

Amplitude: Flat within ± 3 db to 20 cps;
down not more than 12 db at 60 cps.

Phase: Not greater than 45 degrees at 20 cps.

It is assumed that the above criteria apply to all control axes.

In order to establish specifications on the control system design, in terms of the above performance requirements, it is necessary to examine the control system interfaces, i.e. the servo output load imposed by the simulator carriages and the input command signals received from the computer.

Input Command Signals

The signal conditioning amplifiers will be designed to match the D.C. command signals to the requirements of the servo control systems; the maximum voltage level will be ± 5 V.D.C. In order to avoid ground reference problems, both sides of each input signal circuit will be isolated from all ground references.

Simulator Carriages

Referring to Figure 3-10, it is seen that the output motions produced by the control system must be transmitted by the simulator carriage structure to the base of the docking hardware. For the precise transmission of the control system output motions, it is a necessary

requirement on the mechanical design of the carriages that the transmissibility of these structures be essentially 1 over the design range of control forces and frequencies. Therefore, for purposes of the preliminary control system design, rigid carriage structures are assumed within the servo frequency range of interest. This assumption leads also to a servo output load which may be approximated by a single lumped mass structure. The validity of this assumption may be examined by reference to the discussions of the transmissibilities and higher order elastic equations of motion of the carriage structures presented in Section 3.2 of this report.

Calculations based on the preliminary D.D.S. layout design give the following total masses and moments of inertia (including docking hardware) as seen by the output of each servo-drive system:

$$m_x = 3673 \text{ lbs.}$$

$$m_y = 2270 \text{ lbs.}$$

$$m_z = 4028 \text{ lbs.}$$

$$I_\theta = 2706 \text{ in-lb-sec}^2$$

$$I_\psi = 4440 \text{ in-lb-sec}^2$$

$$I_\phi = 114 \text{ in-lb-sec}^2$$

In concluding the statement of control system design requirements, the additional assumption regarding interfaces is made that the servo actuator on each control axis is backed up by an infinite mass. The structural implications of this assumption are also discussed in Section 3.4.

SUMMARY OF RESULTS

This section gives a summary of the results of the Phase I control system design and a statement of the performance achieved. Justifications supporting the technical approach have been principally established through design development and operation of existing Northrop two-degree and six-

NORTHROP SPACE LABORATORIES

degree of freedom flight dynamics simulators. The analytical basis for the results are mathematically derived in Appendix B of this report.

The selected design approach uses similar electro-hydraulic servo mechanizations on each of the six control axes, differing only in the magnitude of the control power required. Figure 3-11 shows a functional block diagram which represents any single control axis. The control power is from a 3000 psi common source hydraulic supply. Table 3-3 summarizes the actuator sizes and the hydraulic flow requirements for each control axis based only on the magnitude of the output motions and load requirements established in the preceding section. (It will be shown later that adjustments to these initial actuator sizes are required due to dynamic response requirements.) In order to minimize the inherent open-loop, non-linear characteristics of valve controlled servos, the actuator sizes and valve flow rates are computed on the basis of one-half the total system supply pressure, i.e. the maximum forces required are available with one-half system pressure drop across the actuator and the maximum velocities required are available with one-half system pressure drop across the valve. An examination of the required output forces shows that the forces for the 2g acceleration of the carriages are the dominant factor in determining the actuator sizes in the three translational axes while the design force due to the docking collision (or engagement of the tunnel seal) predominates in the three rotational axes.

For sinusoidal output motions, Figure 3-12 shows the motion envelope defined by Table 3-3, for the three translational axes, with respect to available output displacement amplitudes versus frequency. The three rotational axes encounter only velocity limitations up to a much higher frequency because the force available in these axes is based on the collision forces required.

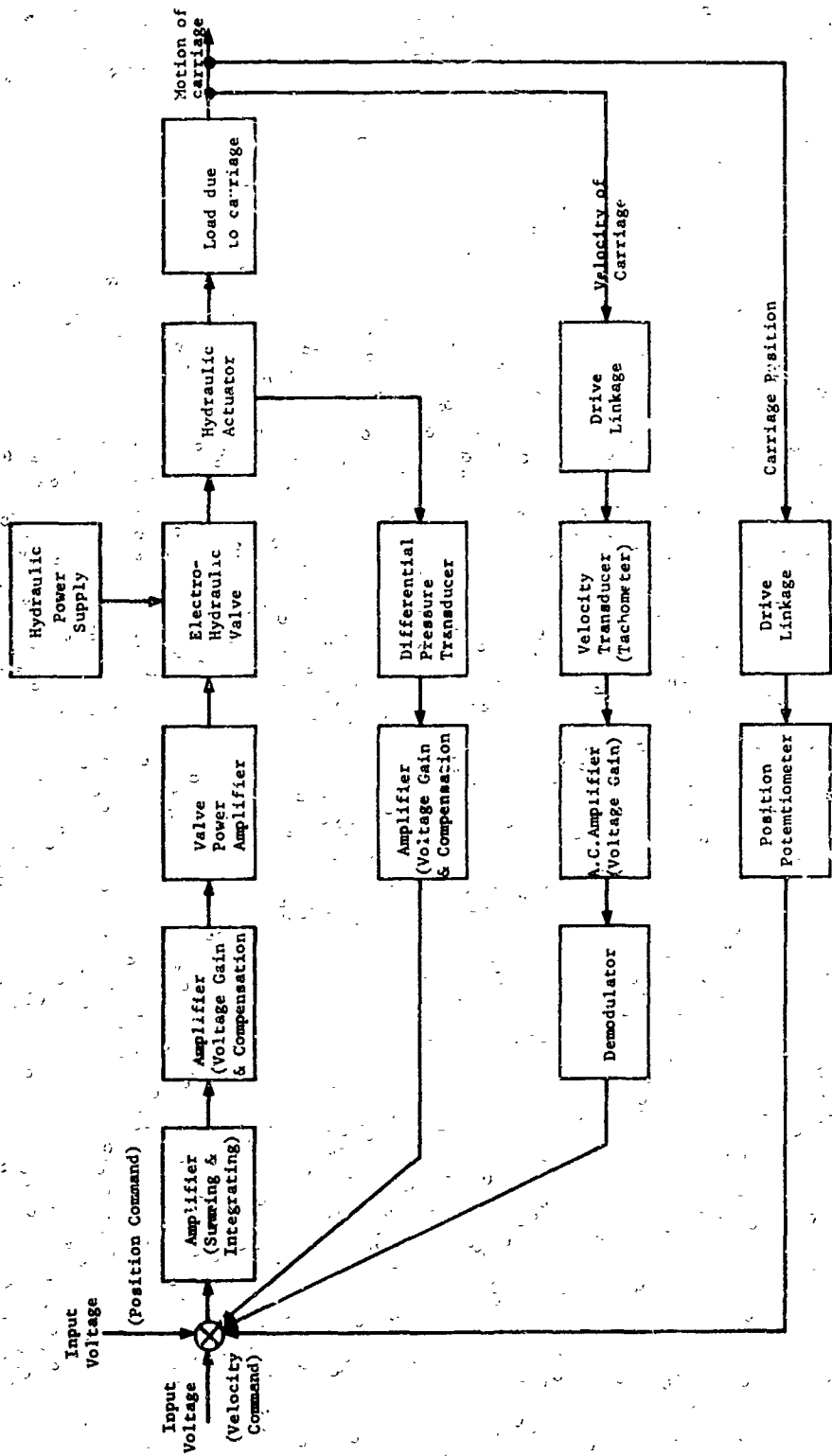


FIGURE 3-11 FUNCTIONAL BLOCK DIAGRAM - SINGLE AXIS SERVO CONTROL

TABLE 3-3 INITIAL ESTIMATE OF CONTROL SYSTEM HYDRAULIC PARAMETERS

	X	Y	Z	Θ	Ψ	Φ
Load Inertia	9.5 lb-sec ² /in	5.9 lb-sec ² /in	10.4 lb-sec ² /in	2706 in-lb-sec ²	4440 in-lb-sec ²	11 1/4 in-lb-sec ²
Max. Force Due to Collision	3000 lb	3200 lb	3200 lb	40500 in-lb	40500 in-lb	10000 in-lb
Total Displacement	± 17 in	± 13.5 in	± 13.5 in	± 0.61 rad (± 35°)	± 0.61 rad (± 35°)	± 3.14 rad (± 180°)
Max. Load Velocity	24 in/sec	24 in/sec	24 in/sec	0.11 rad/sec	0.11 rad/sec	0.018 rad/sec
Max. Load Acceleration	772 in/sec ²	772 in/sec ²	772 in/sec ²	3.5 rad/sec ²	3.5 rad/sec ²	Not Specified by MSC/SID
** Volumetric						
* Displacement of Actuator	4.9 in ³ /in	3.03 in ³ /in	5.37 in ³ /in	27.0 in ³ /rad	27.0 in ³ /rad	6.7 in ³ /rad
* Flow Rate	118 in ³ /sec (30.7 gpm)	72.7 in ³ /sec (18.2 gpm)	129 in ³ /sec (33.5 gpm)	2.97 in ³ /sec (0.77 gpm)	2.97 in ³ /sec (0.77 gpm)	0.12 in ³ /sec (0.03 gpm)

* Specified at 1500 psi.

** Dual Actuators, all entries are total for both actuators.

- NOTES: 1. Volumetric displacements and flow rates shown. Consider only requirements due to magnitudes of control motions and forces.
2. See Table III for final estimates which also consider requirements due to dynamic response.

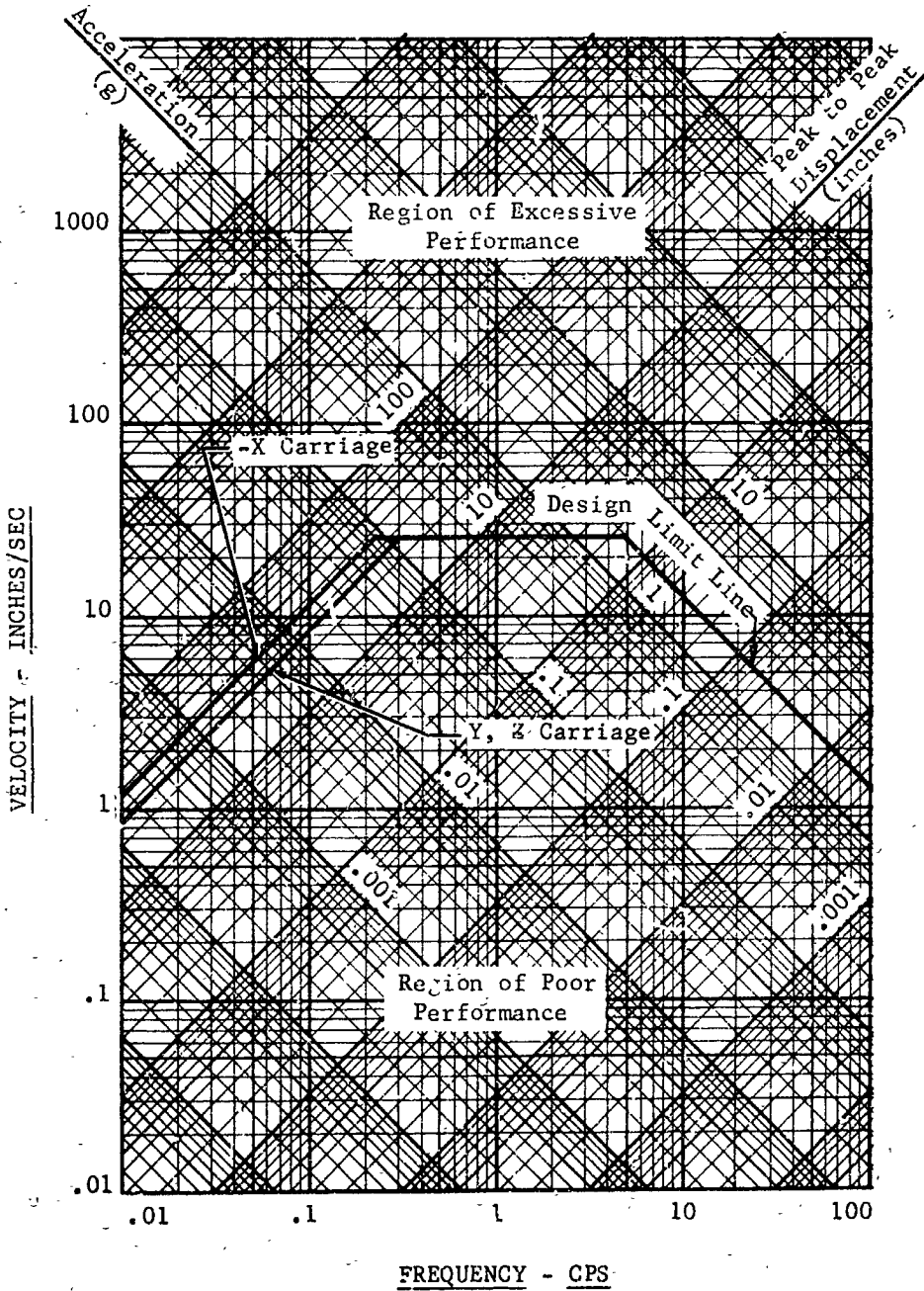


FIGURE 3-12 DISPLACEMENT, VELOCITY AND ACCELERATION DESIGN LIMIT LINES FOR THE AXIAL, VERTICAL AND LATERAL CARRIAGE MOTION

NORTHROP SPACE LABORATORIES

For hydraulic servo systems, with output loads which are principally due to inertia forces, the ultimate limit on obtainable dynamic response is related to the natural frequency of the hydraulic actuator and its load inertia. This frequency is given by:

$$\omega_n = \sqrt{\frac{K_o}{m}}$$

where

ω_n = undamped natural frequency (rad/sec)

K_o = hydraulic spring rate due to the compliance of the hydraulic fluid trapped in the actuator with the valve ports closed (lbs/inch)

m = mass of the load (lb-sec²/inch)

The type of servo actuators selected to supply the control power for each control axis (except roll) are double-acting hydraulic cylinders; the pitch and yaw axes use bell-crank connected cylinders to obtain the limited angular displacements (± 35 degrees) required. Therefore, the actuator hydraulic spring rate of each servo drive axis, except roll, may be computed with the actuator sizes (volumetric displacements and total displacements) given in Table 3-3 because the total trapped fluid volume is approximately equal to the total internal volume of the actuator. The fluid spring rate is then given by

$$K_o = \frac{2DN}{l}$$

where

D = volumetric displacement of the actuator (in³/in)
for translation; (in³/rad) for rotations

N = adiabatic bulk modulus of the hydraulic fluid (lbs/in²)

l = 1/2 the peak to peak displacement of the actuator (inches
for translation; radians for rotations).

NORTHROP SPACE LABORATORIES

Using a design value of 200,000 lbs/in² for the fluid bulk modulus and using the load inertia and actuator parameters of Table 3-3, the following tabulation gives the characteristic frequency of each servo axis (except roll).

	X	Y	Z	θ	Ψ
K _o	1.12 x 10 ⁵ lbs/in	8.99 x 10 ⁴ lbs/in	1.59 x 10 ⁵ lbs/in	1.77 x 10 ⁷ in-lb/rad	1.77 x 10 ⁷ in-lb/rad
ω _n	109 rad/sec	123 rad/sec	123 rad/sec	81.0 rad/sec	63.2 rad/sec

Because of the larger angular displacement required in the roll axis (± 180 degrees), the type of rotary hydraulic actuator selected to drive this axis operates in the manner of a hydraulic motor. Therefore the total trapped fluid volume in the roll actuator is much smaller than the volume of fluid displaced over the total travel. This factor when combined with the low load inertia of the roll axis is expected to produce a characteristic frequency which is higher than those of the other servo-drive systems. Also, the rotating actuator has a low moment of inertia.

An examination of the characteristic actuator and load frequencies tabulated above, reveals that only the Z or Y axis, with servo actuator sizes based only on considerations of the required magnitudes of output forces and motions, present a possibility for also satisfying the dynamic response requirements established in Section 3.3, i.e. a system amplitude response which is approximately flat to 20 cps. Therefore, attention has been concentrated on the design synthesis of the Z-axis control system. This approach was selected with the intent that if satisfactory results were possible with the 123 rad/sec, Z-axis characteristic actuator-load frequency then an appropriate increase in the size of the other axis actuators would produce equivalent characteristic frequencies and therefore equivalent dynamic performance.

NORTHROP SPACE LABORATORIES

One of the principal results of the Phase I servo design study is the successful analytical mechanization of this Z-axis servo with an assigned actuator-load frequency of 123 rad/sec. The final system mechanization is shown in Figure 3-13. Analytical evaluation of the performance achieved agrees well with all requirements established in Section 3.3. The valve and actuator sizes used in this Z-axis mechanization agree with those tabulated for the Z-axis in Table 3-3. Values assigned to other loop components are typical of available commercial hardware. It should be noted that the Z-axis carriage design requires matched, tandem hydraulic cylinders in order that the resultant total actuating force pass through the c.g. of the carriage. Therefore, the mechanization shown represents either of the matched pair of Z-axis servo drives. In each, the total Z-axis load inertia, hydraulic flow requirement, hydraulic spring rate, and cylinder size are halved. The ultimate performance available, as limited by the restrictive 123 rad/sec actuator-load frequency, however, is unaffected.

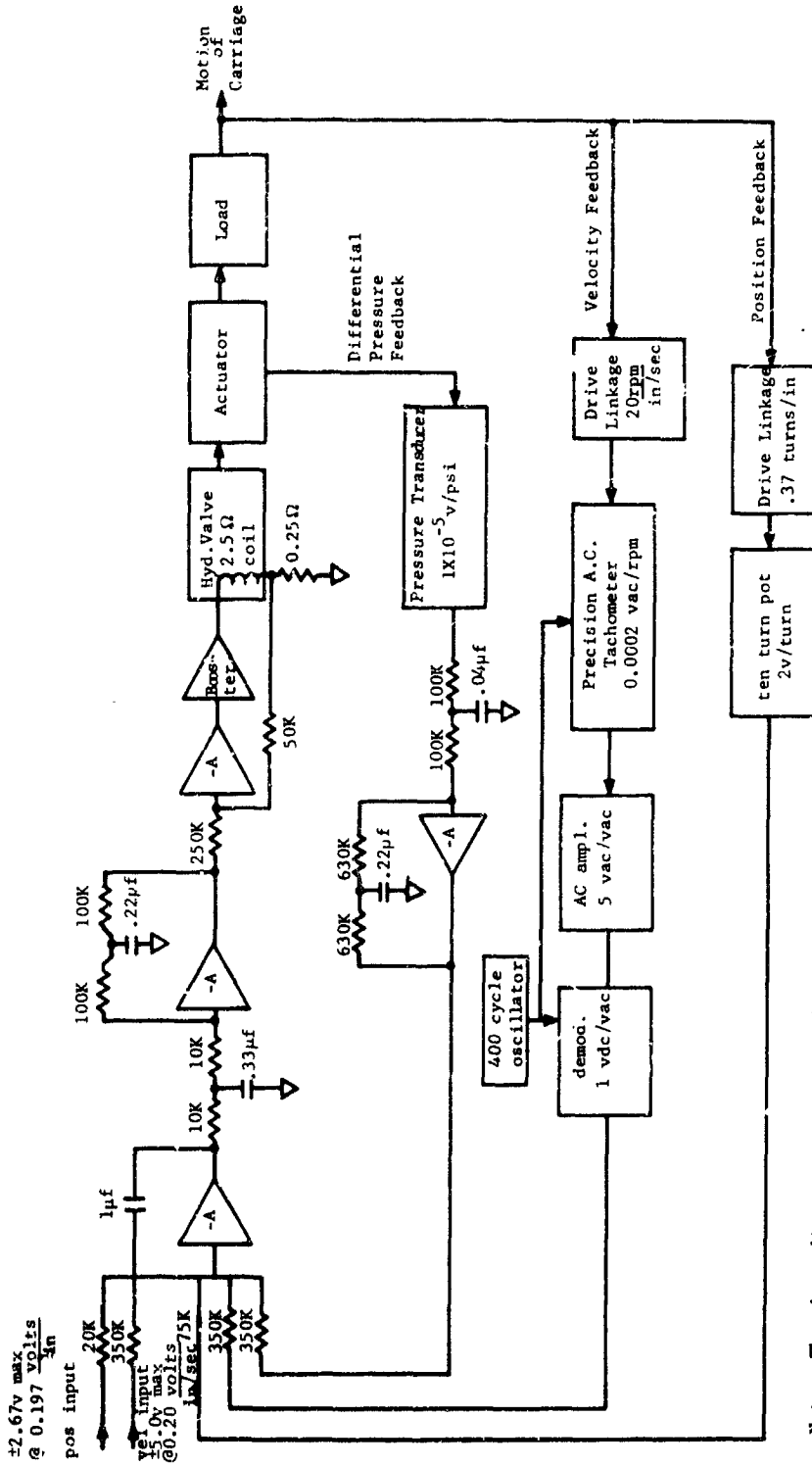
A servo block diagram representation of the Z-axis servo is shown in Figure 3-14. Much of the work in establishing optimum loop compensations and gains was performed using an analog computer simulation of this multi-loop system. A diagram showing the equivalent computer mechanization is given in Figure 3-15.

The following comments will serve to describe the essential operating characteristics of the servo:

Overall Servo Transfer Functions

The closed-loop transfer function relating the input voltage v_{V_i} to the output velocity, V_o , is given by

$$\frac{V_o}{v_{V_i}} = \frac{0.27 s \left(\frac{s+100}{100} \right) \left(\frac{s+250}{250} \right) \frac{\text{in/sec}}{\text{volt}}}{\left(\frac{s^2 + 64s + 160^2}{150^2} \right) \left(\frac{s^2 + 420s + 440^2}{440^2} \right) (s+980) (s+18) (s+78)}$$



Note: The above diagram represents either of two tandem z-axis servo drive systems.

FIGURE 3-13 - SERVO MECHANIZATION DIAGRAM - Z-AXIS CONTROL

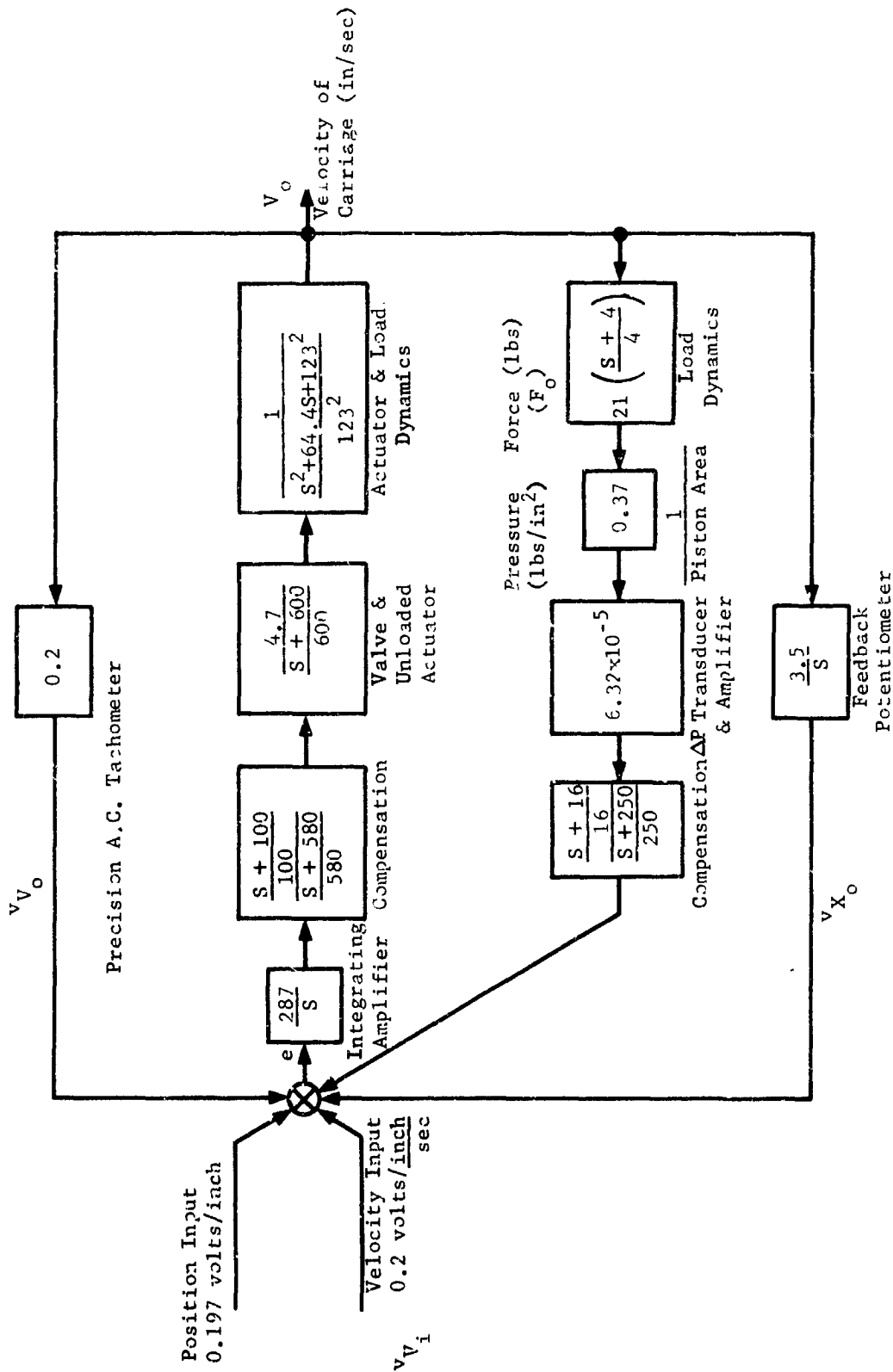


FIGURE 3-14 SERVO BLOCK DIAGRAM - Z-AXIS SYSTEM

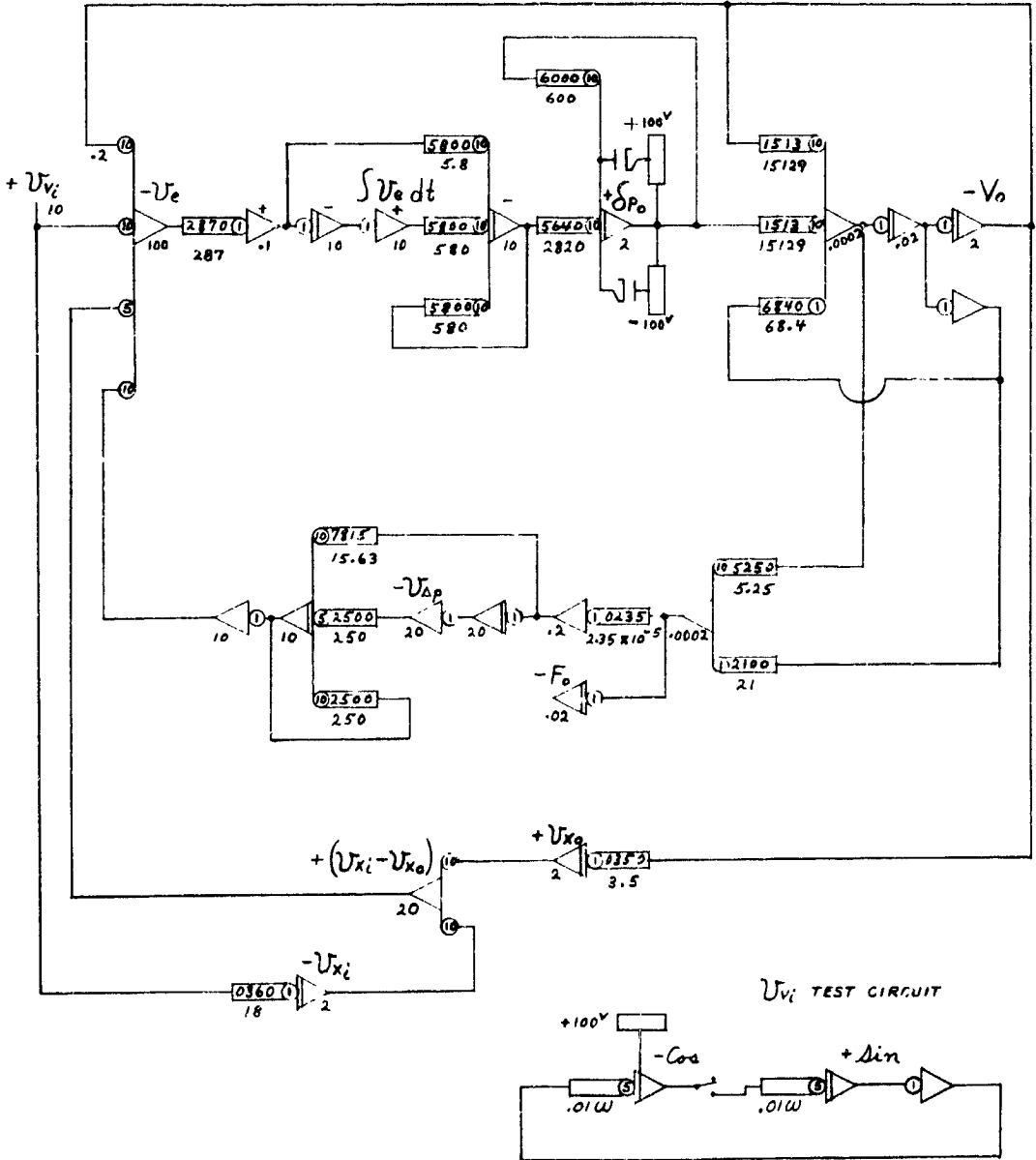
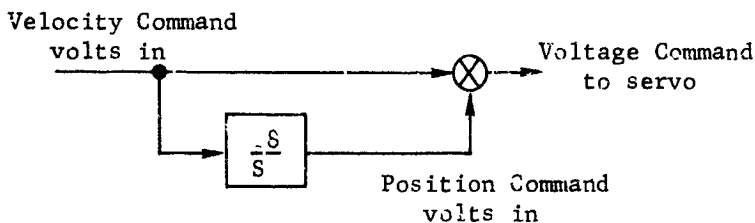


FIGURE 3-15 VERTICAL CARRIAGE CONTROL SYSTEM
(.01 x REAL TIME SCALE)

NORTHROP SPACE LABORATORIES

The complete analytical derivation of this system transfer function is presented in Appendix B of this report.

An examination of this transfer function, in terms of response to sinusoidal input voltage commands, shows that below 18 rad/sec the servo behaves as a positional servo; above 18 rad/sec and up to the second order lag at 160 rad/sec, the behavior closely approximates an ideal velocity servo. The necessary input command voltage, generated by the D.D.S. computer amplifiers, therefore, must be of the form:



An input of this form provides input compensation which may be expressed as

$$\frac{\text{Voltage supplied to servo}}{\text{Computer Velocity Command (volts)}} = \frac{(S + 18)}{(S)}$$

The overall servo velocity response including the above specified form of the input, therefore becomes

$$\frac{V_o}{V_i} = \frac{5 \frac{(S + 100)}{(100)} \frac{(S + 250)}{(250)} \frac{\text{in/sec}}{\text{volt}}}{\left(\frac{S^2 + 64S + 160^2}{160^2} \right) \left(\frac{S^2 + 420S + 440^2}{440^2} \right) \left(\frac{S + 180}{580} \right) \left(\frac{S + 78}{78} \right)}$$

and a constant closed loop gain with respect to output velocity is maintained from zero frequency up to the second order lag at 160 rad/sec.

The specified form of the input voltage may be interpreted as a requirement for both velocity and position command voltages where the position command voltage level, expressed in $\frac{\text{volts}}{\text{inch}}$, is 18 times the velocity command voltage level

expressed in $\frac{\text{volts}}{\text{inch/sec}}$. In the mechanization shown on Figure 3-13, this voltage level adjustment has been provided by the choice of the input resistors at the servo summing junction such that the voltage level of both the command velocity and position signals required from the D.D.S. computer are approximately $0.2 \frac{\text{volts}}{\text{in/sec}}$ and $0.2 \frac{\text{volt}}{\text{inch}}$.

The time response of the servo to a step input voltage command, with both velocity and position voltage components as specified above, is shown in Figure 3-16. This response trace was obtained from the analog computer simulation of the final Z-axis servo mechanization.

Performance Characteristics

A frequency plot of the amplitude and phase response of the overall Z-axis servo is given in Figure 3-17. The close agreement as shown by Figure 3-17, between the analytically derived phase and amplitude frequency characteristics and the frequency response characteristics measured from the analog computer simulation, serves as a check on the validity of both the simulation setup and the mathematical computations of the servo analysis.

The system dynamic response shown by Figure 3-17, is considered to represent the best compromise between stability and dynamic response. An adjustment of loop gains could provide a decrease in the magnitude of the resonant peak at a sacrifice in dynamic response. The principal damping of the actuator-load resonance is provided by the action of the pressure feedback control loop. The significant effect of this loop closure may be seen by reference to the root locus plot of Figure B-10 in Appendix B.

Listed below is a summary of the Z-axis servo performance. The analytical derivation of all performance characteristics is presented in Appendix B.

NORTHROP SPACE LABORATORIES

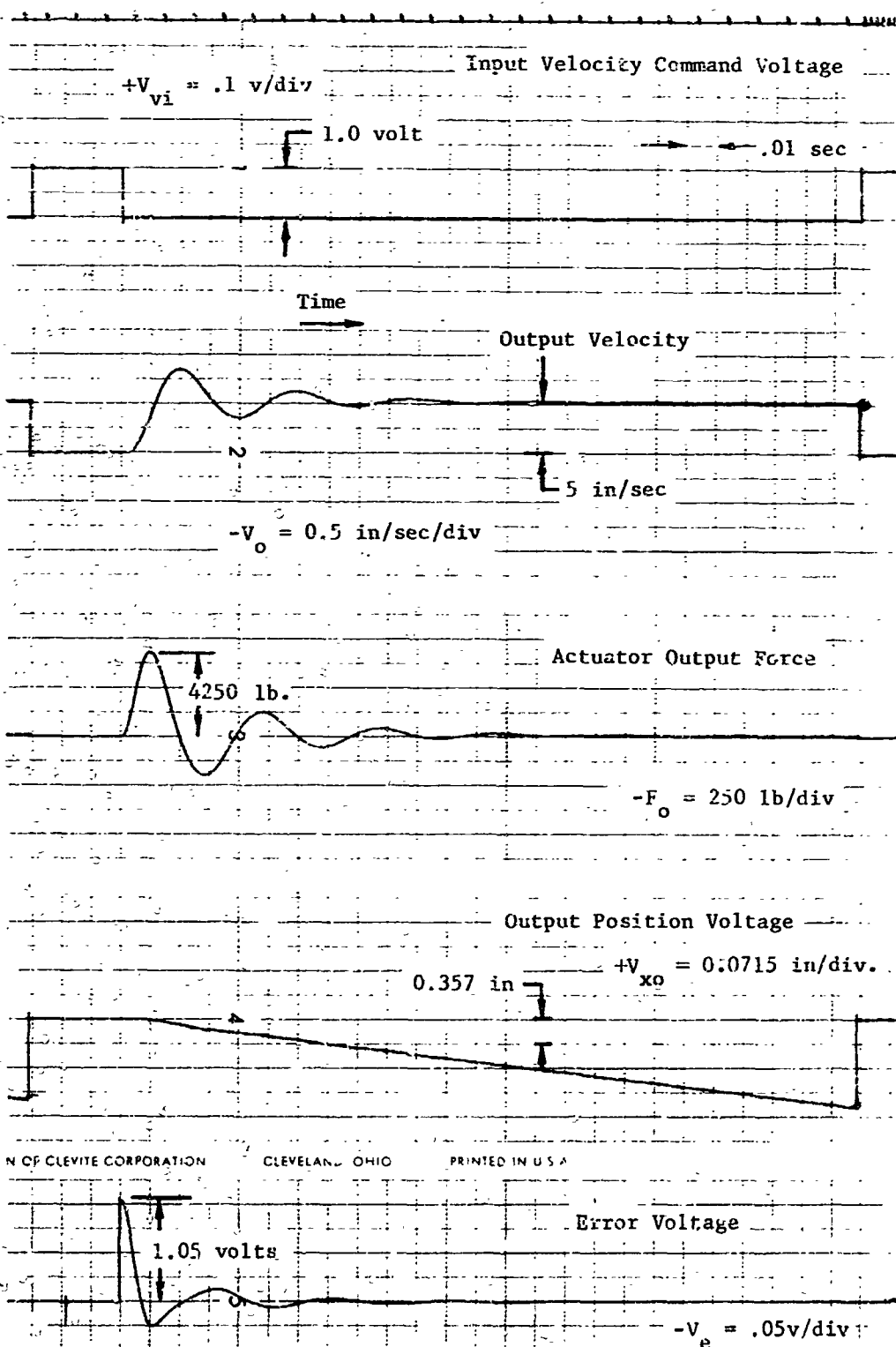


FIGURE 3-16 TIME RESPONSE OF Z-AXIS SERVO TO STEP INPUT COMMAND

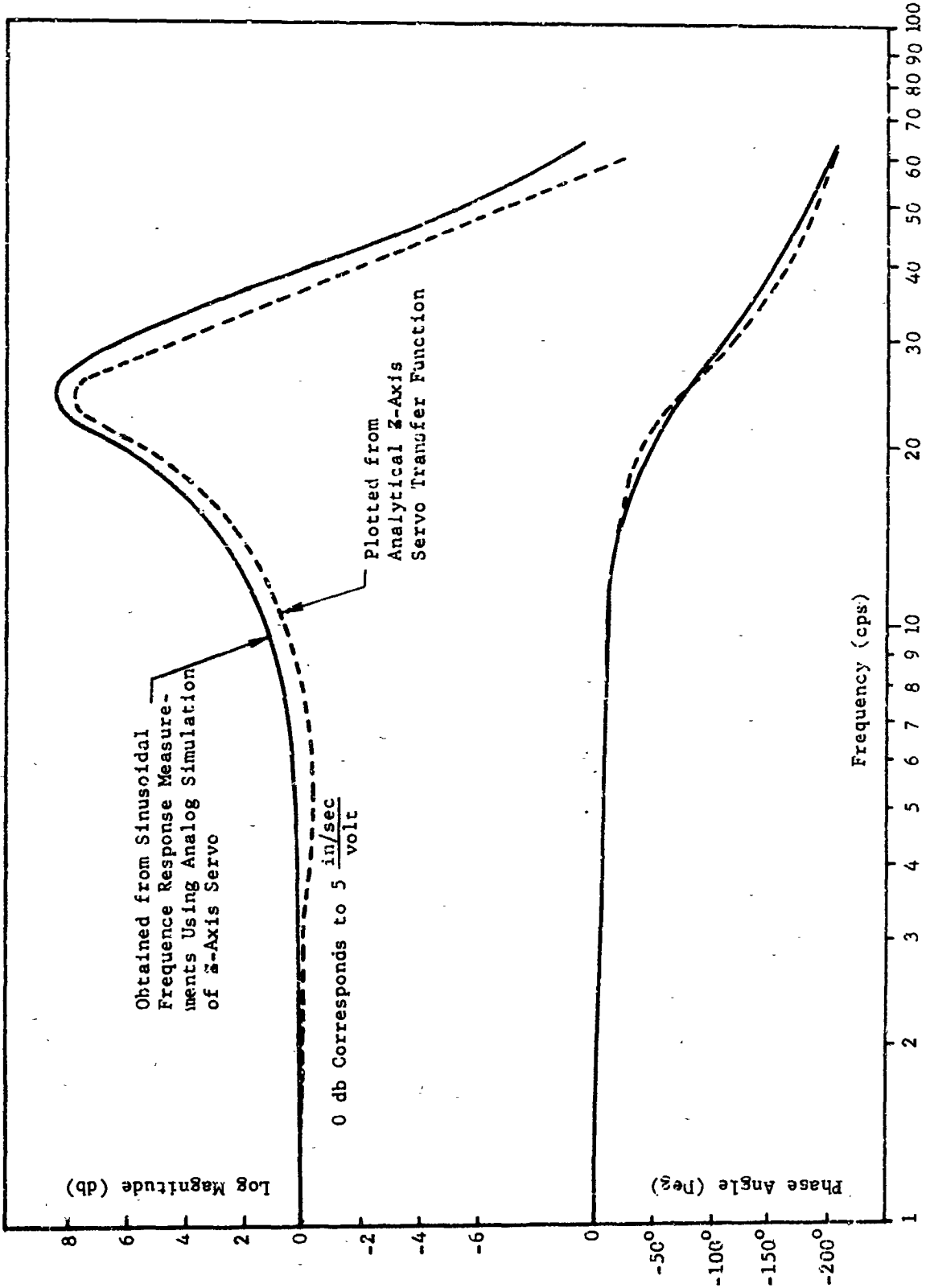


FIGURE 3-17 FREQUENCY RESPONSE PLOT OF Z-AXIS SERVO

NORTHROP SPACE LABORATORIES

$\zeta = 0.2$ (ratio of actual damping to critical damping of the dominant system resonance)

$\omega_n = 25.5$ cps (undamped natural frequency of the dominant resonance of the system)

$T_s = 0.125$ sec. (settling time required for the error response to a unit step function to arrive at and stay within two percent of the final value)

$(e_{ss})_{\text{step}} = 0 \frac{\text{in/sec}}{\text{in/sec}}$ (Steady state velocity error due to a unit velocity input)

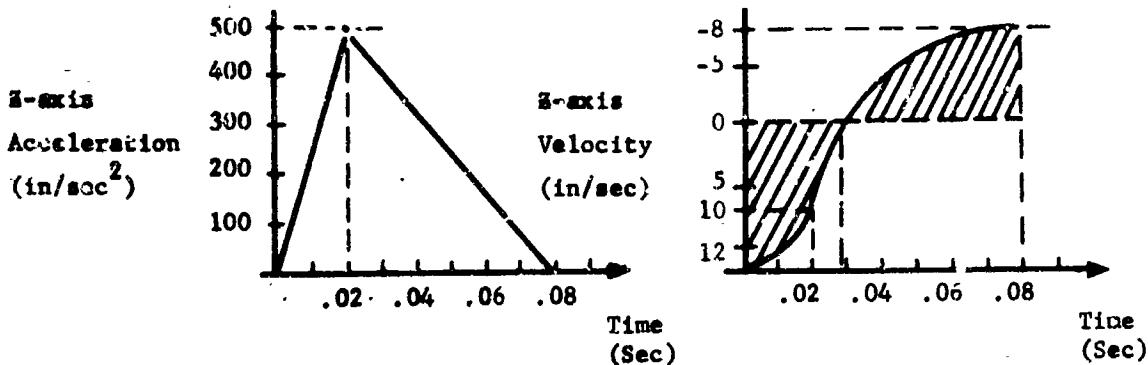
$(e_{ss})_{\text{ramp}} = 0.0225 \frac{\text{in/sec}}{\text{in/sec}^2}$ (Steady state velocity error due to a unit acceleration input)

Phase lag = 40 degrees at 20 cps.

Gain margin = 5

The above steady state error coefficients show that the system responds to steady velocity inputs with a zero output velocity error. This characteristic results from the integrating operational amplifier which is mechanized in the forward loop of the servo.

Information furnished by MSC/SID gives expected critical-case servo drive dynamic requirements based on rigid-body motions which occur due to docking dynamics in lunar orbit. The approximate character of these dynamics referenced to relative motions between the probe and drogue, in the probe/drogue axis system is sketched below for the Z-axis motions.



Note: Areas A and B must be equal because probe penetration must equal zero when acceleration returns to zero.

NORTHROP SPACE LABORATORIES

The accuracy with which the Z-axis servo can reproduce the critical-case dynamics defined above, represents an ultimate basis for appraising the performance achieved. The output response of the Z-axis servo, to the specific input command sketched above, has been measured using the Z-axis servo analog computer simulation described previously. A plot of the time response recorded from this test is presented in Figure 3-18

The total collision force between the probe and drogue structures are related to the values of spring compliance and damping which have been designed into the probe assembly. This total force may be expressed by the following relationship.

$$F_T \approx bV_o + KX_o$$

where

F_T = total force on collision

b = probe damping coefficient (not a constant)

V_o = relative velocity between probe and drogue

K = probe spring rate (not a constant)

X_o = relative position between drogue and probe, i.e., penetration

Referring to Figure 3-18, it may be seen that integration of the error between the commanded and actual velocities (difference of the areas under the velocity curves) defines the time history of the error on position. The combined errors then, on position and velocity, according to the above expression, define the overall accuracy achieved in the reproduction of the actual collision over the time interval of contact between the probe and drogue. These errors in the reproduction of the true (ideal) motions of V_o and X_o when combined with the probe hardware design values of b and K would yield a solution for the accuracy in the reproduction of the true (ideal) time history of the total collision force.

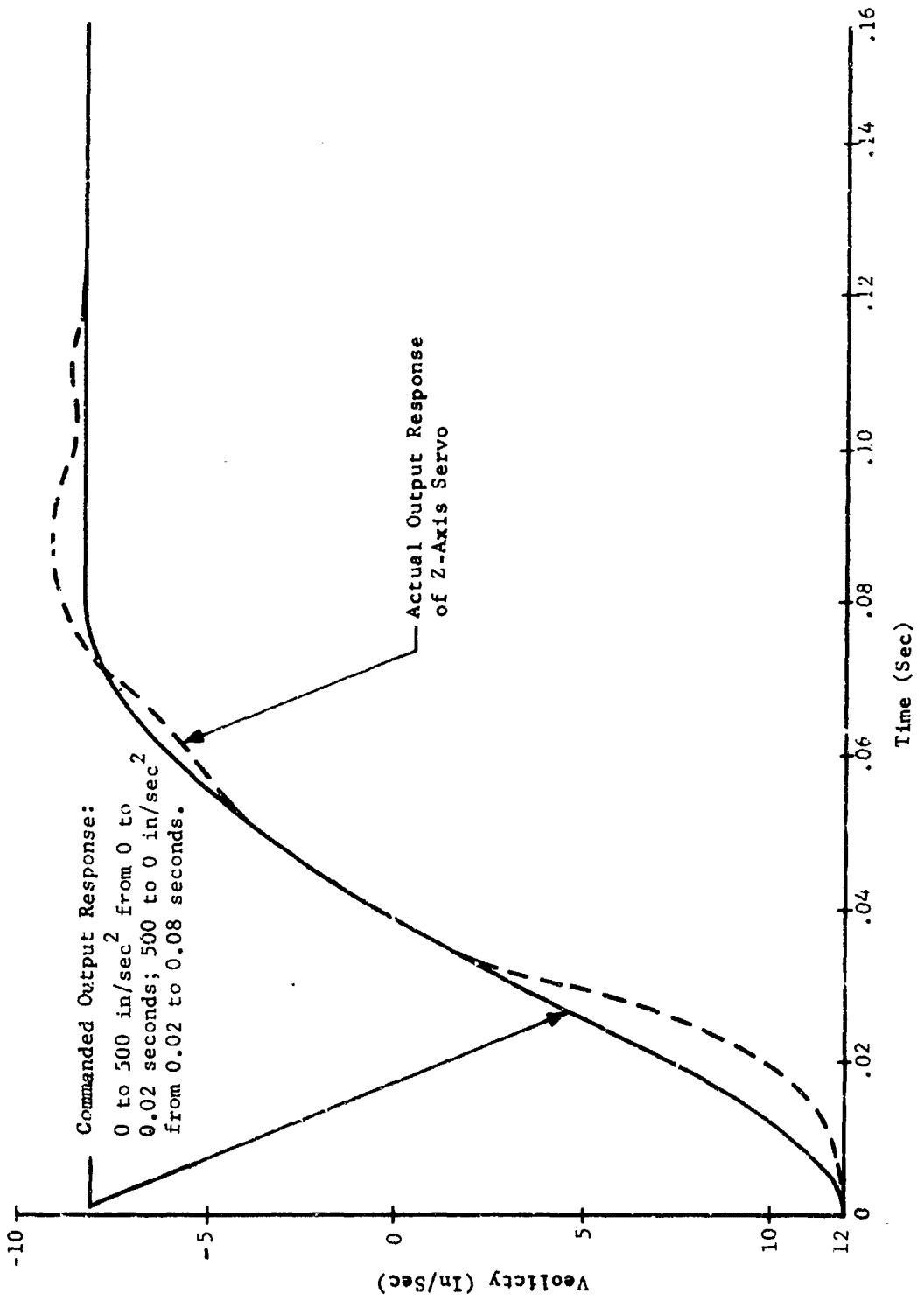


FIGURE 3-18 Z-AXIS SERVO RESPONSE TO CRITICAL-CASE DYNAMICS

NORTHROP SPACE LABORATORIES

Servo Noise Sensitivity

The noise sensitivity to unwanted signals in the control system are tabulated in Table B-1 of Appendix B. This table indicates that the control system will be sensitive to 60 cps noise but will be insensitive to noise much above 60 cps. The sensitivity to 60 cps signals justifies the requirement that all D.C. power, which is applied to the control system, will be obtained from 400 cps power supplies. Any 800 cps ripple on the D.C. would be attenuated to a point where it would not affect the control system.

Table B-1 of the appendix also indicates that noise frequencies below 60 cps will also affect the servo. This noise will be reduced to a minimum by employing transducer cables which are twisted shielded pairs feeding into both active inputs of an operational amplifier at the servo summing junction such that all common mode pickup will be rejected. Since, in a differential amplifier, both inputs and the output are isolated from one another, this arrangement will also avoid ground reference problems between the servo system components located on the simulator carriages within the vacuum chamber, and the servo electronic components located in the control console. It is expected that signal wires connecting the servo components within the chamber and the components within the console will require approximately 75 feet of electrical cable.

Servo Stiffness

The sensitivity of the Z-axis servo position (or velocity) to forces applied to the output has been analyzed in Appendix B. High servo stiffness is essential not only with regard to the ability of the servo to duplicate velocity commands received from the D.D.S. computer but also in regard to the ability of the servo to resist load disturbances caused by forces generated in the other servo-drive axes.

NORTHROP SPACE LABORATORIES

Flow control valves will be used in all servo-drive axes because the extremely high pressure gain of this type of control valve provides a high level of inherent stiffness in the servo. The dynamic behavior of both the position and velocity feedback loops also contribute to the stiffness of the overall system. Because of the dynamic behavior of the feedback, the overall system exhibits a complex stiffness characteristic, i.e. the stiffness is frequency dependent. Figure 3-19 is a frequency plot showing the overall system compliance, expressed in inches/lb. to sinusoidal loads applied to the servo output. This plot is expressed by equation #25 of the appendix.

Discussion of Servo Mechanization

The accuracy of the servo system in reproducing precise output motion commands is essentially dependent only upon the accuracy of the position and velocity feedback signals. Sufficient open loop gain has been provided to make the servo behavior independent of small nonlinearities in the forward loop. The ultimate accuracy of the feedback signals are in turn determined by the velocity and position feedback sensors (tachometer and potentiometer).

The type of velocity sensor selected is a precision A.C. computing tachometer equipped with a thermal sensing bridge and integral heaters which virtually eliminate errors introduced as a result of temperature variations. The heater is excited by a magnetic or equivalent amplifier. The tachometer excitation is 400 cps. The A.C. output signal is amplified before demodulation. It is expected that sufficient filtering of the 800 cps ripple will be provided by the forward loop integrating amplifier. Drive linkages on the translational axes will be designed to provide dynamically accurate conversion from linear to rotary motion.

The position signal is obtained from a 10-turn precision potentiometer. The type selected provides infinite resolution ideally suited for a high resolution servo. Therefore, problems due to small discontinuities common to conventional wire wound potentiometers are

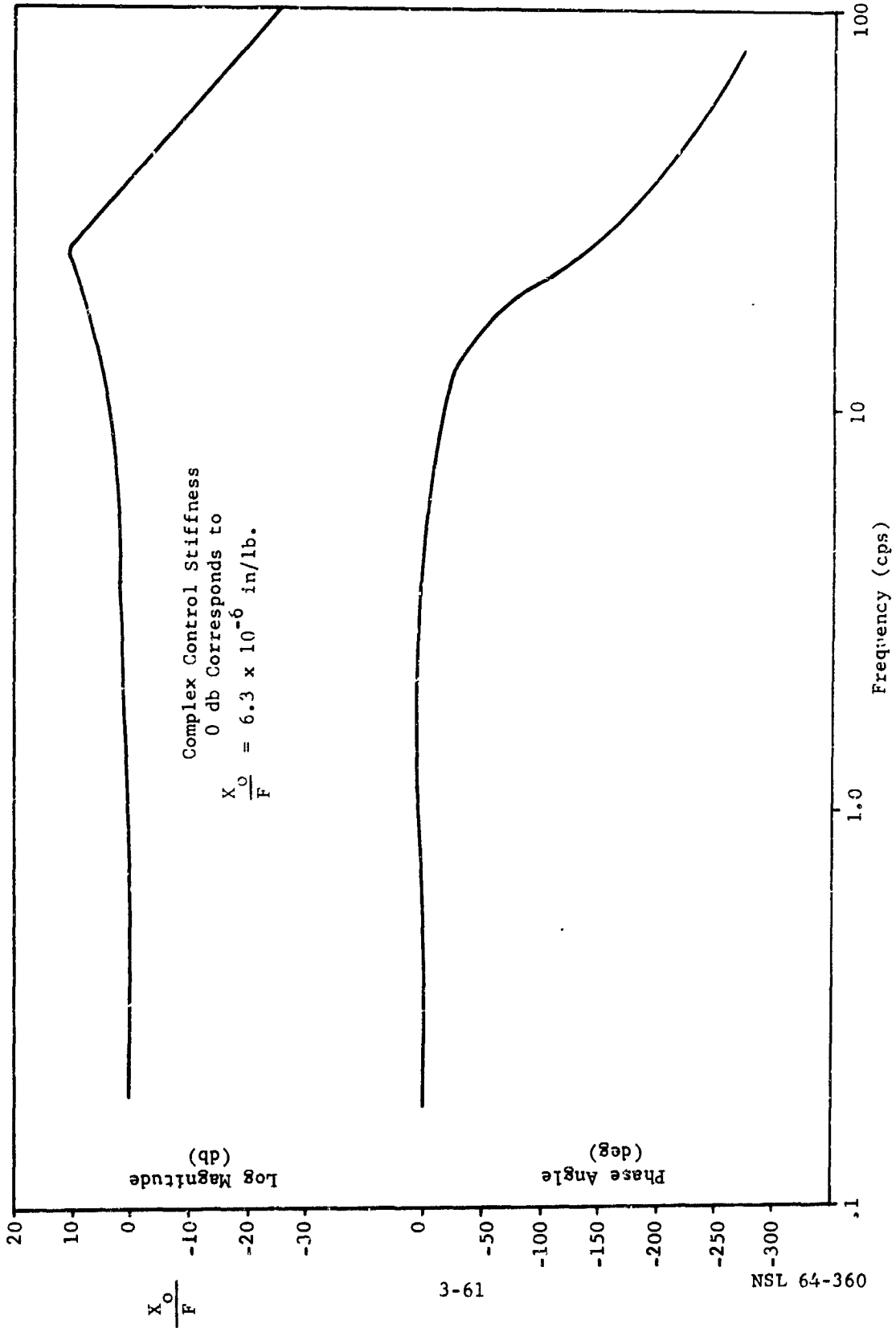


FIGURE 3-19 Z-AXIS SERVO COMPLEX STIFFNESS CHARACTERISTICS

NORTHROP SPACE LABORATORIES

eliminated. Temperature control will be provided by integral heaters and compensation.

The hydraulic valves are proportional, single-stage, electro-hydraulic flow control valves. The type of valve selected was developed specifically for use in high-flow, high performance hydraulic dynamic simulators. The valve spool is driven directly by an electromagnetic driver. A motion feedback loop, closed around the valve spool, provides the high dynamic performance required. The overall valve and driver will be designed to provide a response, equivalent to the 600 rad/sec time constant used in the Z-axis servo analysis. The valve amplifier will supply approximately 40 watts of control power. As illustrated on the mechanization diagram, Figure 3-13, a current feedback loop closed around the valve amplifier and driver, will eliminate changes in the valve gain due to temperature induced resistance variations in the drive coil. This current feedback loop also eliminates the electrical time constant which would otherwise result from the valve coil impedance. Provisions for integral heaters will also be provided for temperature control of the valve. The valve design will handle flow rates of up to 40 G.P.M. at 1500 psi pressure drop.

Since the design response range of the servo extends above 60 cps, it is essential that all D.C. electrical power for servo operation be derived from 400 cps A.C. power sources. This requirement as discussed previously is necessary in order to avoid 60 cps noise.

Servo control loops, equivalent to the mechanization diagram shown on Figure 3-13, will be closed around each hydraulic actuator in those axes (Y, Z, θ) using dual actuators. This approach insures dynamic synchronization between the tandem cylinders.

NORTHROP SPACE LABORATORIES

Hydraulic Servo Actuators

All of the servo-drive axes, except roll, use hydraulic actuating cylinders of tie-rod construction fabricated from 300 series stainless steel. Instead of piston seals the piston is lapped to the cylinder bore with sufficient clearance to provide a hydraulic bearing to virtually eliminate breakaway friction. The cylinder ends are constructed to provide similar hydraulic bearing supporting the rod and also providing a labyrinth seal. A method of scavenging the hydraulic bearing discharge and preventing excessive leakage into the vacuum chamber will be provided.

The rotary servo actuator for the roll axis drive has been developed for high performance servo applications with large inertia loads. The actuator is a servo adaptation of the hydraulic gear-motor principle and will incorporate features to minimize starting friction. The angular shaft travel will be ± 180 degrees.

Servo System Electronics

The mechanization diagram of Figure 3-13 shows several DC amplifiers. The amplifiers used for lead compensation will be of standard solid-state operational differential design. The forward loop of Figure 3-13 shows a summing integrator. The amplifier for this integration will be an extremely low drift and low noise all-silicon solid-state plug-in chopper stabilized device.

The hydraulic servo controller, for the valve control, will consist of a 50 watt DC transistorized power amplifier with built-in power supplies.

Other Servo-Drive Axes

In concluding a statement of design requirements for the other servo-drive axes, it is necessary to correct the design parameter tabulation of Table 3-3 in order to bring the characteristic frequency of the load-actuator resonance of the other servo-drive systems up to

NORTHROP SPACE LABORATORIES

the 123 rad/sec frequency used in the mechanization of the Z-axis system. This final tabulation is given in Table 3-4. Corresponding adjustments are included with respect to the flow required in each axis in order to satisfy the original output velocity requirements. Actuator and valve sizes shown are again based on the condition that a pressure drop of not more than one-half of the system supply pressure, across either the valve or the actuator, is necessary to produce the required output motions specified.

HYDRAULIC FLUID SELECTION

Statement of Problem

Selection is required for a hydraulic fluid to function in a high performance hydraulic servo system designed to operate the docking simulator mechanism. The simulator will be located within the NASA Manned Spacecraft Center Space Chamber B, pumped down to a chamber pressure as low as 10^{-5} to 10^{-6} torr. The hydraulic control equipment is primarily a closed loop system, environmentally external to the vacuum chamber. A significant aspect which will influence the selection of fluid is the direct exposure of some quantity of the fluid to the space chamber. This is expected to occur on actuator rod surfaces, exposing a viscous fluid film layer, since fluid is constantly pumped into the system within the vacuum chamber. To keep the simulator and Chamber B clean, the effects of limited fluid exposure are to be minimized to an acceptable condition by selecting a fluid with a vapor pressure lower than 10^{-5} torr at the ambient chamber temperature. The very low vapor pressure of the selected hydraulic oil is maintained through the removal of unwanted gases and contaminants by imposing a vacuum on the low pressure side of the hydraulic system including the hydraulic reservoir. For this purpose, a separate vacuum system is included in the ancillary equipment. To provide the maximum system safety with respect to toxicity, fire and explosive hazard, fluid characteristics of low vapor pressure, fire resistance and nontoxicity will be prime considerations.

TABLE 3-4 FINAL CONTROL SYSTEM PARAMETERS INCLUDING CONSIDERATION OF SYSTEM DYNAMIC RESPONSE REQUIREMENTS

	X	** Y	** Z	** Θ	Ψ	Φ
Load Inertia	9.5 lb-sec ² /in	5.9 lb-sec ² /in	10.4 lb-sec ² /in	2706 in-lb-sec ²	4440 in-lb-sec ²	114 in-lb-sec ²
Total Displacement	+ 17 in	+ 13.5 in	+ 13.5 in	+ 0.61 rad ($\pm 35^\circ$)	+ 0.61 rad ($\pm 35^\circ$)	+ 3.14 rad ($\pm 180^\circ$)
Max. Load Velocity	24 in/sec	24 in/sec	24 in/sec	0.11 rad/sec	0.11 rad/sec	0.018 rad/sec
Volumetric Displacement of Actuator	6.11 in ³ /in	3.03 in ³ /in	5.37 in ³ /in	63 in ³ /rad	103 in ³ /rad	6.7 in ³ /rad
Flow Rate	147 in ³ /sec (36.7 gpm)	72.7 in ³ /sec (18.2 gpm)	129 in ³ /sec (53.5 gpm)	6.94 in ³ /sec (1.73 gpm)	11.3 in ³ /sec (2.83 gpm)	0.12 in ³ /sec (0.03 gpm)
Natural Frequency (ω_n)	123 rad/sec	123 rad/sec	123 rad/sec	123 rad/sec	123 rad/sec	Not * Determined
Hydraulic Spring Rate (K_o)	1.44x10 ⁵ lbs/in	8.99x10 ⁴ lbs/in	1.59x10 ⁵ lbs/in	4.13x10 ⁷ in-lb/rad	6.75x10 ⁷ in-lb/rad	Not * Determined

* * Dual actuators, all entries are total for both actuators.
 * Not expected to be critical. see discussion in text.

NORTHROP SPACE LABORATORIES

Operational procedures will include techniques for minimizing pressure unbalances between the hydraulic system low pressure side and the ambient pressure external to the servo system.

To achieve the desired velocities and frequency response in the servo system, a high spring constant is required for the system including the fluid and system lines and components. System performance requires operation at frequencies up to 60 cycles per second with large masses involved. Accordingly, to achieve a rapid response, liquids with high bulk modulus (low compressibility) must be used.^{4,5} A bulk modulus requirement for hydraulic fluid, to be used at 1500 to 3000 psi and a nominal ambient temperature ($70^{\circ} \pm 10^{\circ} F$), has been determined to be 300,000 psi minimum in order to provide an effective system bulk modulus in excess of 200,000 psi. System modulus derating is based on expected latitude in operating conditions and reflects experience with working systems based on analysis of a given system to determine expected values and experimental measurement of an actual system behavior.

The operational requirements (Appendix C) of the servomechanism system are such as to require a hydraulic fluid with a low vapor pressure and low evaporation rate, a high bulk modulus, viscosity which satisfies lubricity and response characteristics, and which is fire resistant and non-toxic. Further requirements are a low particulate contamination level in the fluid and minimum air, nitrogen, or water vapor entrainment to minimize viscosity and modulus changes in the fluid.

Fluid Selection

The basis for the selection of the servohydraulic fluid depends on the characteristics needed for functional requirements and compatibility with the environmental and operational conditions in chamber B. A stable, room temperature, fire-resistant servo fluid will operate in a slightly warm loop external to the vacuum and will provide an interface

NORTHROP SPACE LABORATORIES

with the surroundings within the chamber. Examination of the properties of all chemical types of useful hydraulic fluids leads to the selection of a phosphate ester as a most likely candidate because of the combination of high bulk modulus (Appendix D) and high spontaneous ignition temperature, and low vapor pressure. A discussion on the significance of fire-resistant tests for phosphate esters appears in Appendix E.

Specific phosphate ester fluids with excellent overall properties are Pydraul 60 (Monsanto Chemical Co.) and Cellubes 90 and 150 (Celanese Chemical Co.). These fluids possess excellent lubricity, fire resistance, and fluid stability. A summary of the properties of these fluids appears in Table 3-5. On the basis of fire resistance, low vapor pressure, and viscosity-temperature relationships, Cellulube 90 appears to be superior to the others and will be utilized subject to confirming tests.

Cleanliness of the simulator and space chamber will be favored by the use of a functional fluid with a minimal evaporation rate under the vacuum conditions. Cellulube 90 is an excellent fluid in this respect. Extrapolation of vapor pressure data gives an estimated vapor pressure of 5×10^{-7} mm Hg. at 80° F. Calculation, using the Langmuir equation ($u =$ evaporation rate, gram/cm²/sec = $5.833 \times 10^{-2} P_{\text{mm}} (M/T)$ gives the low evaporation rate of 3.143×10^{-9} gram/cm²/sec. at 80° F.

The vapor pressure of the fluid controls the mass transfer rate; therefore, the contribution to chamber pressure is expected to be negligible. The limited absorption, which may occur on chamber walls, especially at cryogenic panels, should be acceptable, and can be further reduced by use of cooling shields.

The survey of chemical classes included phosphate, silicate and dibasic acid esters, disiloxanes, silicones, fluorosilicones, polyphenyl ethers and superrefined hydrocarbons. A discussion of the characteristics of these chemical types appears in Appendix E. Fluids of particular interest, but possessing some property limitations, are Oronite HTHF 70 (disiloxane), used in the B-70, Oronite HTHF 7277B (disiloxane), developed for Dyna-Soar, and OS-124 (polyphenyl ether). These fluids are compared with Pydraul 60 and the Cellulubes in Appendix F.

TABLE 3-5 SUMMARY OF HYDRAULIC FLUID PROPERTIES

ITEM	PROPERTY	FORMULA 60 328,000	CELLULUBE 90 350,000	CELLULUBE 150 350,000	PREFERRED REQUIREMENT
1.	Bulk Modulus 1000 - 3000 psi				300,000 psi (min.) for fluid 207,000 psi (min.) for system
2.	Viscosity (Kinematic, centistokes (CS))	11.7 at 100°F	10.2 at 100°F	J2.1 at 100°F	200 CS, maximum for worst case condition; range of about 70-90 sau or 10-20 cs preferred. * 40 SUS for pump lubricity
	Saybolt (SUS)	62 at 100°F 43 at 140°F	96 at 100°F 49 at 150°F	151 at 100°F 29.5 at 150°F	
3.A	Vapor pressure, torr (mm.Hg.)	2×10^{-5} at 70°F *	5×10^{-7} at 80°F *	5×10^{-7} at 80°F *	(1) on order of 10^{-5} to 10^{-6} torr (mm. Hg.) at 70°F
3.B	Evaporation rate, gram/cm ² sec. (calc'd) **	12.84×10^{-7} (70°F)	3.413×10^{-9} (80°F)	3.413×10^{-9} (80°F)	(2) negligible evaporation rate in chamber vacuum
4.	Fire Resistance Auto Ignition (Temp.) High Pressure Spray Test Low Pressure Spray Test	Self-extinguishing 1200°F Passes Barely Passes	Self-extinguishing 1200°F Passes Passes	Self-extinguishing 1200°F Passes Passes	Fire resistant No auto ignition in 5 parts oxygen atmosphere. No detonation in vacuum pump operation.
5.	Toxicity Skin exposure vapor phase	Toxicity low (used near food areas). Minimal hazard Inhalation low at V.P. No MAC values	No toxic cases reported Minimal hazard Inhalation low at V.P. No Mac values	No toxic cases reported. Minimal hazard Inhalation low at V.P. No MAC values	Physiologically inert. No adverse dermal or respiratory effects.
6.	Stability Hydrolytic Oxidation Thermal Corrosion Electrical (dielectric strength) Foaming	Stable at boiling point Stable Excellent to 250°F. Noncorrosive -- "Nonfoaming"	Stable at boiling point Stable Excellent to 250°F. Noncorrosive 410 volts/mil "Nonfoaming"	Stable at boiling point Stable Excellent to 250°F Noncorrosive 330 volts/mil "Nonfoaming"	Stable to hydrolysis by water, oxidation, thermal exposure, and noncorrosive to metals and alloys in the system. Non-conductor - good dielectric Nonfoaming or low foaming with unstable foam.

* By extrapolation of vapor pressure data for a plot of $\log P_{\text{mm}}$ vs. $1/T^{\circ}K$
** Calculated from Langmuir equation."

SERVO CONTROL CONSOLE

All control and monitoring functions during operation of the simulator will be performed from a single location within the Space Environment Simulation Laboratory. The general concept and arrangement of the control console is illustrated in Figure 3-20. The control console will house all equipment related to control, programming, monitoring and communications. A separate equipment rack adjacent to the control console will house all stationary control system electronic components and all signal conditioning amplifiers which resolve the transmission line interface

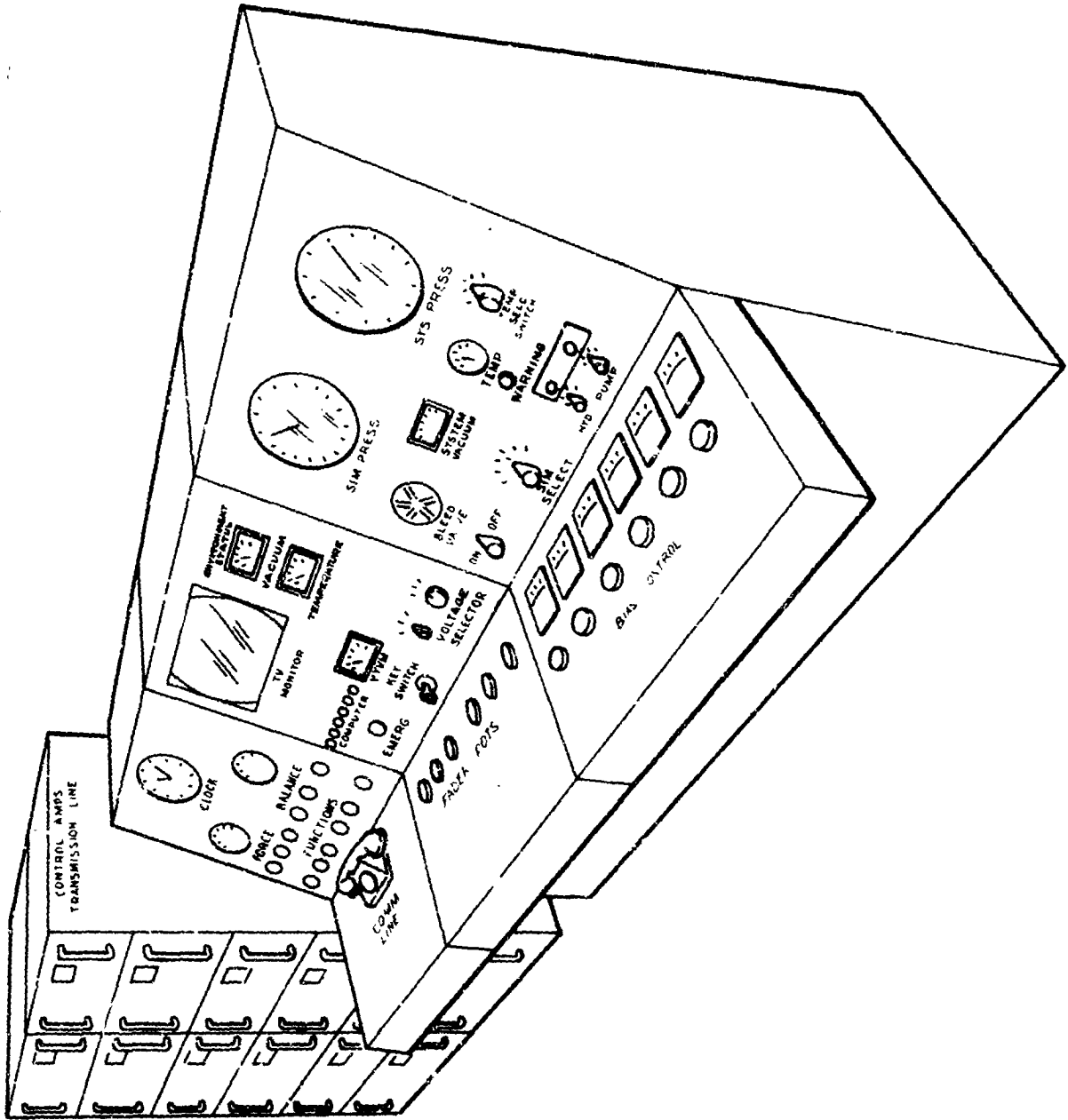
MEASUREMENT SUBSYSTEM

Dynamic Force Measurement

The collision forces between the probe and drogue assembly will be measured by six component internal strain gage balances of the floating-frame type. See Figure 3-21. The floating-frame balance was selected as the dynamic force measurement transducers for the simulator. This type of balance is a well-proven device which has been in use for many years in both static and dynamic force measurement. The most favorable advantage is its exceptionally low deflections which result in the high natural frequencies required of the docking simulator.

The primary frame consists of an inner rod, which fastens to the roll servo actuator for the probe and the pitch gimbal structure for the drogue, and a cylindrical outer case, which is inserted into and attaches to the adaptor structure supporting either the probe or drogue. Forces and moments are resisted by individually removable elements, employing flexure pivots, connected between the inner rod and outer case of the balance.

The six force and moment sensing components of the balance consist of two normal force elements for determination of normal force and pitching moment, two side force elements for determination of side force and yawing moment, a dual axial force element, and a dual roll



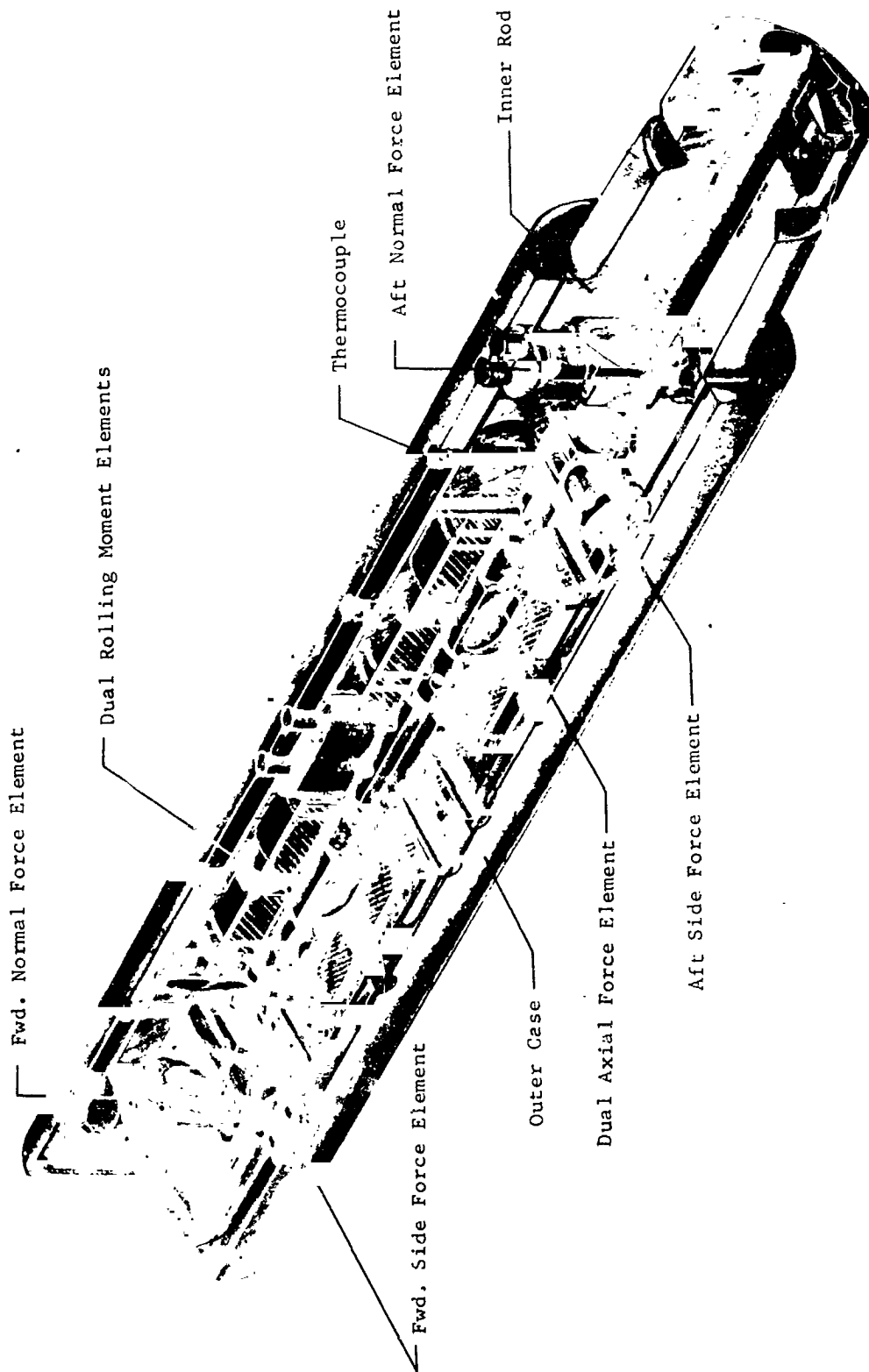


FIGURE 3-21 SIX COMPONENT INTERNAL STRAIN GAGE BALANCE

element. All of the force elements are designed so as to produce natural frequencies of the support system above the frequencies of interest in the docking simulation.

The normal and side force elements are equipped with relaxation members at either end and are arranged to act in roll as a set of crossed ribbon flexures. Similar relaxation members provide compliance in the axial force direction. The rolling moment elements are provided with flexure pivots at either end which are designed to transmit pure roll moment to the gage section. The dual axial force element is located inside the dual roll element and transmits axial force from the outer case to the inner rod.

The balances will be provided with thermal conditioning jackets or sleeves to maintain operating temperature between 60° F and 180° F.

An alternating-current bridge excitation is employed. The strain gage bridge output is first augmented in an a-c amplifier, demodulated, and fed to the differential driving amplifier of the transmission line.

TRANSMISSION LINE

The accuracy and response of computer controlled systems are critically dependent on the method used to connect remote sensors with their computer. The system employed in the docking simulator application requires that the control system be connected to an analog computer by 24 transmission lines, 5000 feet long, which must transmit analog signals in the frequency range of 0 to 600 cps.

Several methods are available to transmit this information. These include: phase modulation, frequency modulation, and direct analog. Modulation transmission is ideal and can be leased from local telephone service organizations, but is not necessary for transmission lines of this length. The direct analog method provides an adequate and reliable means to connect the servo to the computer, and because of its economic and other advantages will be utilized.

NORTHROP SPACE LABORATORIES

Problems of interest include: phase lag, attenuation, ground problems, electrostatic pickup, electromagnetic pickup, and cross-talk.

In direct analog transmission, the phase lag due to the distributed shunt capacitance and series resistance is found to be insignificant for a frequency range up through 600 cps⁶. Also, for this frequency range, the attenuation due to leakage, copper, and dielectric losses is constant.

Interference due to electrostatic, electromagnetic, cross-talk, and ground problems require signal conditioning at both the receiver and transmitter. Pickup and cross-coupling are reduced to a minimum by transmitting high level (5 volts) signals and employing driving amplifiers with a very low output impedance (1 Ω or less). The low output impedance of the driving amplifier will shunt any high impedance interference to ground. To further reduce the effect of pickup and coupling, the driving and receiving amplifiers are of the difference type such that any common mode coupling will be rejected at the receiver. To further reduce pickup, all transmission lines will be twisted pairs.

In a differential amplifier, both inputs and output are isolated from one another, accordingly, ground problems will not exist between the two ends of the transmission line.

All transmission lines for this system will be loaded at their receiving end with the characteristic impedance of the line such that current traveling along the line will not be reflected at the load, resulting in current traveling back towards the transmitter. Temperature effects on this impedance are negligible.

NORTHROP SPACE LABORATORIES

A typical transmission line from the computer to the control system will contain the equipment shown in Figure 3-22. The differential driving and receiving amplifiers at the chamber end of the line are off-the-shelf solid state devices having excellent reliability and high stability characteristics. The driving amplifiers are wideband differential DC types featuring high input impedance over wide gain ranges. The receiving amplifiers are standard operational units exhibiting low noise, drift-free, service proven capabilities. The signals at the simulator end of the line are at the 5 volt level. All signals on the transmission line will be at this level. The receiving amplifiers at the analog computer end of the line are located in the transmission line termination rack and convert the 5 volt level signals from the simulator up to the 100 volt level. These 100 volt receiving amplifiers utilize standard vacuum tube circuitry. The driving amplifiers returning computer commands to the simulator servo system transform the 100 volt computer output to the 5 volt level accepted by the transmission line.

ANALOG COMPUTER

Computer Program

The analog computer must substitute for the vehicle dynamics and command the motions of the simulator elements accordingly. Basically, the computer accepts as inputs the three forces and three moments developed by the simulator force balance for each vehicle for a total of twelve inputs.

The dc voltage levels at which these variables come from the transmission line converters are first adjusted to the levels required for computation. These signals as forcing functions, are used by the computer to solve the equations of motion for some point on the drogue

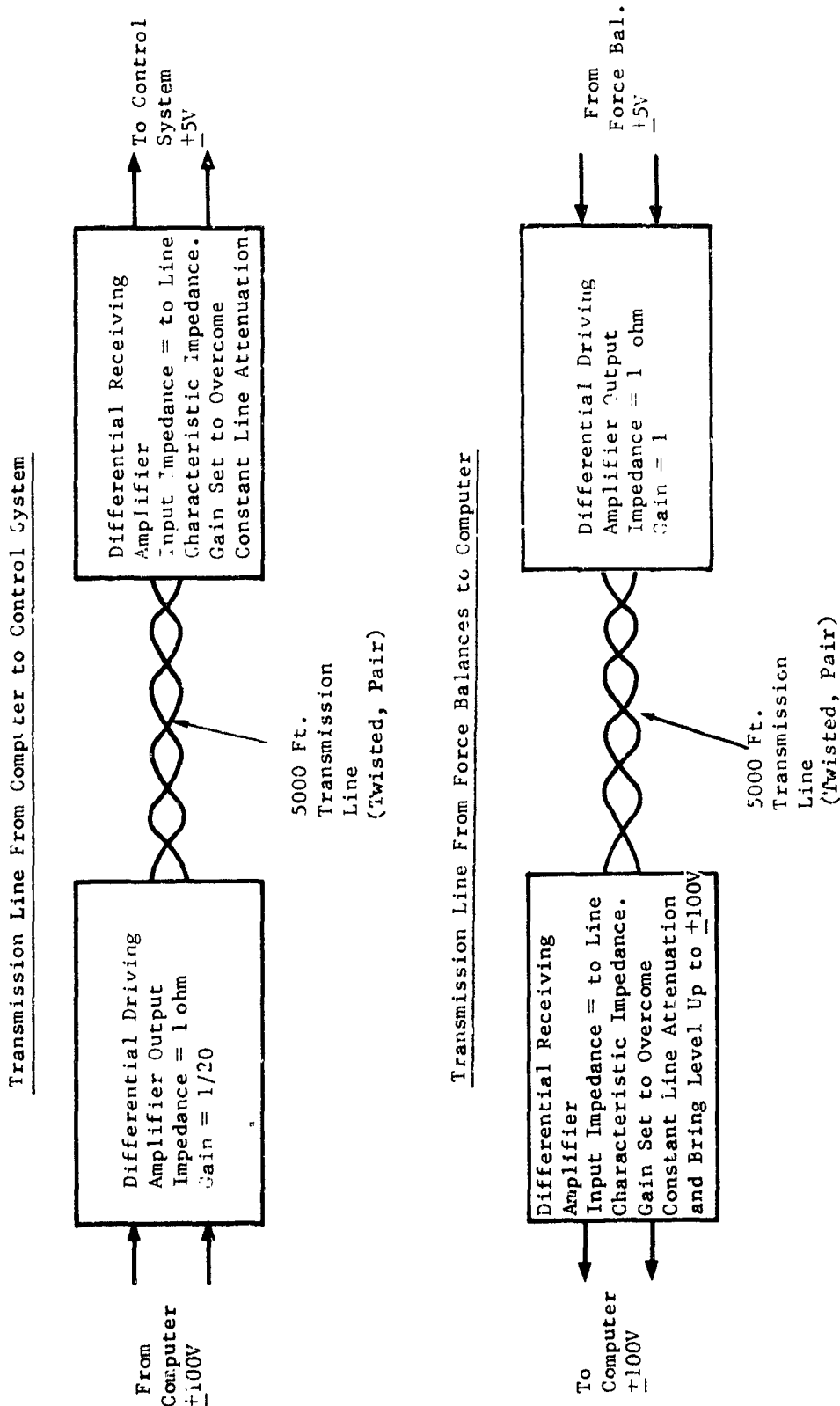


FIGURE 3-22 TYPICAL TRANSMISSION LINE

NORTHROP SPACE LABORATORIES

and some point on the probe, which will be called points of interest. The motions of the two points of interest are then resolved into motions, both angular and translational, relative to simulator space.

The simulator servos are essentially velocity servos requiring correctional displacement signals to eliminate displacement errors due to velocity errors encountered during acceleration; therefore, both rate and displacement signals are generated. The computer returns 12 signals to the transmission equipment.

In addition to this work, the computer must provide for graphic outputs indicating not only the commanded motion of the simulator equipment, but also any auxiliary information which will be required. Furthermore, all initial conditions of position and angular and translational rates are established in the computer. It appears desirable to have automatic cut-offs built into the computer circuitry to stop the computation (and the simulator) under certain conditions, as when forces become too large. The wiring diagrams include such provisions.

The analog computer will supply the graphic results of each run. No customer requirement has been set for these, but the logical minimal requirement would include the recording of inputs and outputs, requiring 24 channels. If the motion of the center of gravity of each vehicle in fixed space were also required, another 24 channels would be necessary. In addition, there are the angular and translational rates of the c.g.'s along rigid vehicle axes, requiring another twelve channels. Thus, from 24 to 60 channels of recording will be needed, depending on the ultimate requirements of the customer.

One problem that arises is the starting transient. When computation is started, the acceleration of the simulator probe and drogue will cause forces and moments to appear on the balances. The simple solution

NORTHROP SPACE LABORATORIES

to this problem was to provide for computation of the torque and force impulses required to produce the required motion and adjust the initial conditions accordingly.

The concept of proposed computer setup is to use analog elements to solve the basic dynamic problems and produce the required outputs. Digital computing elements will be used to calculate constant coefficient settings and initial conditions. Logic elements will be used primarily for control purposes, although there are points in the computation process and in coefficient and initial condition setting where they may be utilized for sign changing. The general plan is to devise the elements such that the inertial properties, c.g. locations, and initial conditions as required are each entered once by the operator and all the coefficients are set accordingly by automatic process. Figure 3-23 shows the block diagram of the analog computer portion of the simulator.

Appropriate equipment for noise-free conversion of the dc analog outputs to transmission line signals, and for conversion of the transmission line signals from the simulator to noise-free dc voltages for the computer will be required, along with appropriate cabling and junctions for 24 signals. Such equipment is envisioned as having dc voltage levels commensurate with the use of available solid-state converters, except for the voltage level adjusting. This vacuum tube equipment is located in the transmission line termination rack where the 10 volt signals from the line are raised to 100 volt level.

Computer Equations

The problem discussed here carries the equations of motion and the study of vehicle dynamics to a new height of complexity. Previous studies (Reference 7, 8, 9, 10) have not been so sophisticated.

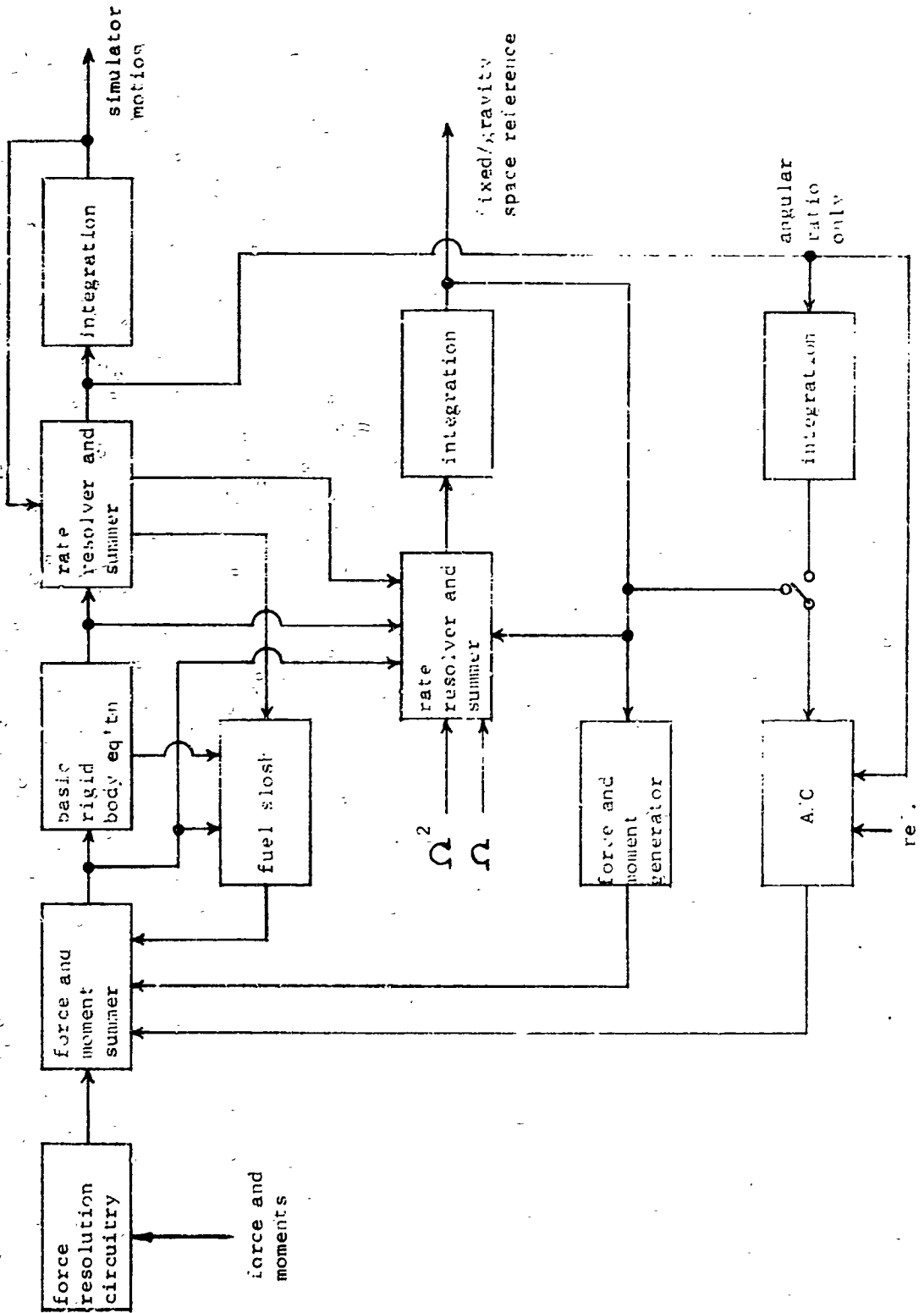


FIGURE 3-23 DOCKING SIMULATION COMPUTER BLOCK DIAGRAM

NORTHROP SPACE LABORATORIES

The mathematical development of the basic equations of motion required for simulation is contained in Appendices G through L. The effort was to reduce as much as possible the amount of computing equipment required for solving the basic simulation problem. Information in addition to that required for operation of the simulator will then require additional equipment if "on-line" results are desired.

Fundamental to a clear understanding of the equations is the axis system used. The axis system used is discussed in Reference 11, 12 and 13. Simulator axes are oriented in the same general direction as the vehicle axes so that if the vehicles are not displaced in any angle, or in any direction except x, the three x axes would fall on a single line. Simulator axes are illustrated in Figure 3-24 as well as the angular translational displacements.

For each vehicle, there is an angular (Euler) rotation with respect to an arbitrary reference space which assists in understanding the development. Referring to Figure 3-25, the vehicle is presumed to rotate first through the angle ψ then through the angle θ , then through the angle ϕ . The relationships are the same in Figure 3-24 except that the simulator x-axis remains parallel to the probe vehicle x-axis so that θ_p and ψ_p are zero, and rolls such that ϕ_d is zero.

For convenience, the vehicle axes are presumed to pass through the center of gravity. However, the axes of simulator interest are such that they are parallel to the vehicle axes, but with the x-axes passing along the centerline of the probe or drogue, as the case may be. The latter are parallel to and the x-axis coincides with, the design axes. The arrangement is illustrated generally in Figure 3-26. The terms x, y, and z on the diagram appear as coefficients in the equations of motion, but given center of gravity (that is, c.g.) data are in terms of x_{cg} , y_{cg} , and z_{cg} .

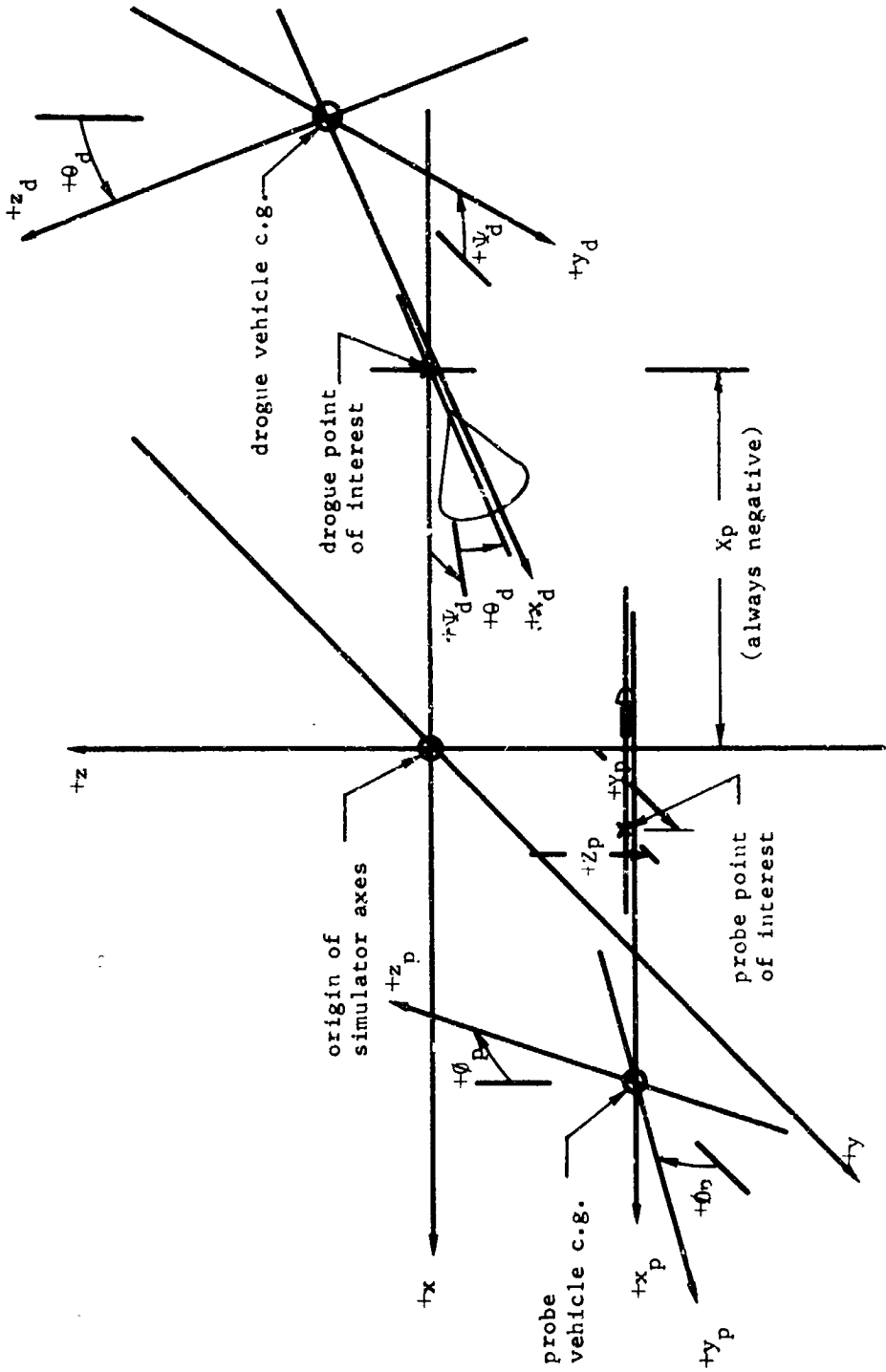


FIGURE 3-24 SIMULATOR AXES AND ALIGNMENTS

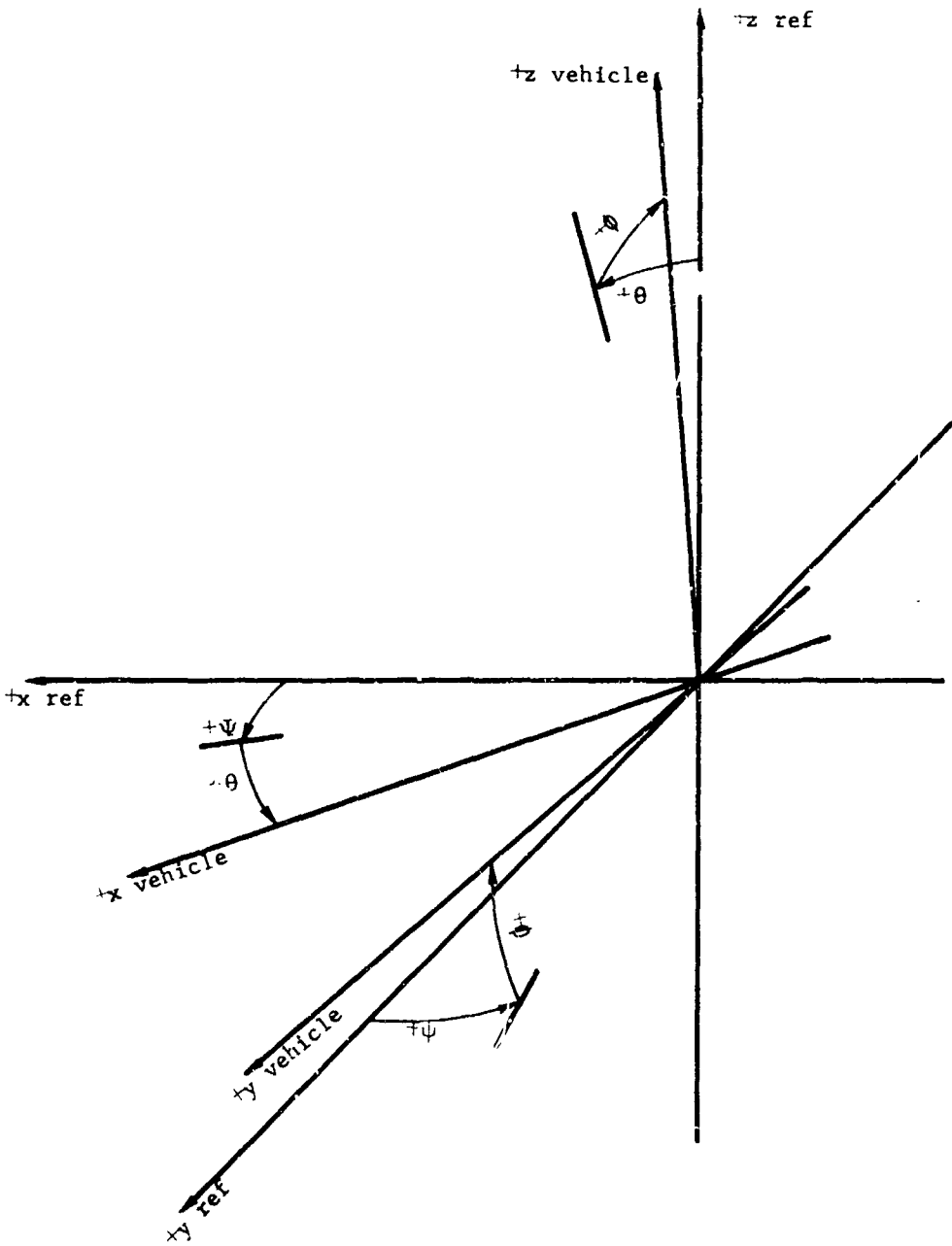


FIGURE 3-25 EULER ANGLE NOMENCLATURE

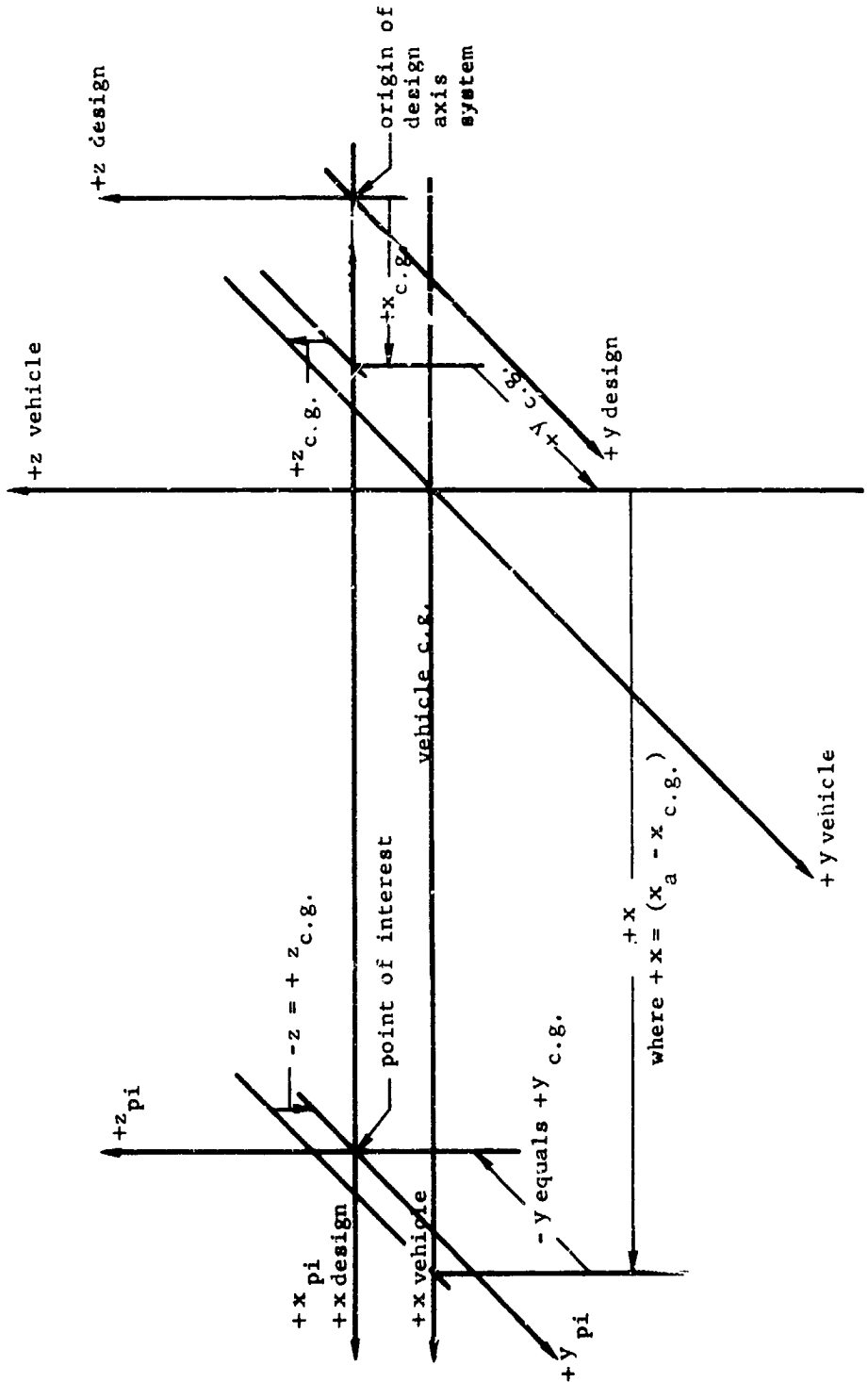


FIGURE 3-26 AXIS NOMENCLATURE

NORTHROP SPACE LABORATORIES

As in all simulations (Reference 14 and 10), the basic problem of the analog computer is to calculate the effects of force and moment inputs to each vehicle on the vehicle motion and to transform vehicle motion into simulator motion. The fundamental solution is for rigid bodies. This solution is then modified to incorporate other effects.

In setting up the computer solution equations, the rigid body case was developed first (Appendix G). Then fuel slosh (Appendix H) and structural flexure (Appendix I) were treated as added effects to be summed into the rigid body solution with minimum modification of the basic development.

The decision to reduce a twelve degree of freedom for two bodies to six relative degrees of freedom to reduce complexity and cost of simulation equipment also reduces the complexity of equipment required for the basic solution for rigid bodies. Rather than reducing the motions of each vehicle to an inertially fixed reference space, a non-inertial reference corresponding to the actual simulator was chosen. This space mathematically pitches and yaws with the probe vehicle and rolls with the drogue vehicle. Thus the simulator probe does not pitch and yaw, and the simulator drogue does not roll. The origin of this reference space remains in the y-z plane containing the probe point of interest, so the simulator probe does not translate in the x direction. The x-axis of the reference space passes through the drogue vehicle point of interest, so that the simulator drogue does not translate in y and z.

While the direct relationship with the simulator space developed in Appendix G simplifies the computations associated with simulation, and this increases the reliability and response of the computer in the vital loop, it also contains the information required to develop the motions of each vehicle with respect to an inertially fixed reference. This is conceived as an auxiliary calculation which may be performed through processes indicated in Appendix G.

NORTHROP SPACE LABORATORIES

The forces and moments obtained from the simulator balances to excite the vehicles may be modified by internal effects. One such is fuel sloshing. Although the presumption is made that fuel slosh may be represented by a point mass suspended in the tank by a spring and damper (Appendix H), this is only a crude representation. In a space vehicle, globules of fuel will be floating loose in the tank, and will collect in one concentrated mass only during certain intervals of time. However, the assumption allows a convenient analysis which is arranged to modify the forces and moments to the rigid, non-sloshing vehicle by simple addition.

Structural flexure introduces deflections of the points of interest in y and z from the rigid axes and angular deflections about all axes. In Appendix I the problem is treated by finding the deflection rate in each mode and summing them to produce total deflection rates. Due to the fact that mode data are uncoupled, these rates are with respect to the rigid axes.

The axes of interest are deflected in this case, however, and the motions must be transformed to the deflected axes. Only in this manner will the drogue cone and the probe tip be properly positioned in the simulator. Appendix I uses small-angle theory to simplify the calculations. Again, inclusion of this effect is done in such a way that the basic computation set-up will be modified only minimally. The prime effect is to add equipment.

Forces and moments will be presented to the computer in the form of the basic strain gauge readings. There is a calibration for each force (there are 12) and the calibration may be non-linear. The readings are then brought to zero by opposing dc voltages and combined to produce the final forces and moments. Preliminary resolution will produce forces and moments at the point of interest so that force and moment resolution will be independent of variations in c.g. location.

NORTHROP SPACE LABORATORIES

Two items of force and moment that are not generated by the simulator are the forces and moments due to controls and gravity. Although the vehicle attitude control transfer functions have not been made available, it has been presumed that each axis will be commanded by an on-off system with the usual dead-band and a minimum on-time. These devices are readily simulated by logic and analog hybrid circuits.

The forces and moments due to gravity are treated briefly in Appendix J. The results to be obtained by their inclusion are of dubious value. The only items of significance are due to gravity gradient effects which affect the differential translation of the two vehicles and their rotations. These small motions require determining the position and attitude orientation of each vehicle in a rotating axis system with its x-z plane coplanar with the nominal orbit. A large number of resolvers and multipliers are needed, and the maximum voltage level at which the signals appear in the computer are around 7 microvolts in translational acceleration and 150 microvolts in rotational acceleration. The abbreviated discussion in Appendix J is included as a basis of mechanization, but it would appear to be of insufficient and questionable value to carry the burden of the extra mechanization.

Appendix K contains a discussion of the computer simulation of the probe-drogue interaction. The development is complete for three-dimensional simulation, but the complexity is sufficient to make simplification desirable. Such a mechanization is desirable for checking out the computer set-up, and the equations are developed in detail for this purpose. Much of the complexity is lost by considering the coplanar motions in either the x-y or x-z planes. The development in the appendix is for the x-y plane. Simplifications result from the coplanar approach partly through the fact that simple logic circuits can replace complex arrays of multipliers and amplifiers.

The analog computer program with wiring diagrams is presented in Appendix L.

Typical Program Results

Figure 3-27 shows the results of a sample run made on Northrop's AD256 computer (See Figure 3-28). The run was started with the probe tip 2 feet in the x direction from the cone apex (channel 1) and one foot above it (channel 2). Neither vehicle was rotating (channel 6), and there was no initial angle. Closing velocity (all in x direction) was 1 ft/second (channel 4). The start of the run is indicated when the curve of x distance in channel 1 suddenly slopes toward zero.

Not quite .9 seconds later, the sudden change in velocity in the x direction (channel 4) and z direction (channel 5) and the sharp rise in the z (channel 7) and x (channel 8) forces on the drogue vehicle signal the start of contact. The roughness in channels 7 and 8 is due to some amplifier noise. At the same time, a sharp rise in pitch rate to .036 rad/sec occurs (channel 6). This just about accounts for the .675 ft/sec change in vertical velocity (channel 5).

The recordings are made of simulator motions, so that the motions are actually combinations of the motions of two vehicles.

The variation in vertical velocity and pitch rate between "bumps" are due to vehicle rotations about the x and z axes due to c.g. misalignment and to product of inertia effects. The maximum pitch angle experienced in this run was .054 radians (channel 3). In none of the runs made was small angle theory exceeded.

It is interesting that the probe bumped the same side of the drogue three times and never rattled from side to side. The final bump was interrupted by the automatic run termination. At that point, the probe tip was retracted about 3.5 inches.

A slight drift is apparent in the vertical velocity and pitch rate channels (5 and 6). The elements from which the forces and moments are derived come through multipliers which tend to have some zero offset. Also, minor imbalances in amplifiers may be critical. The problem

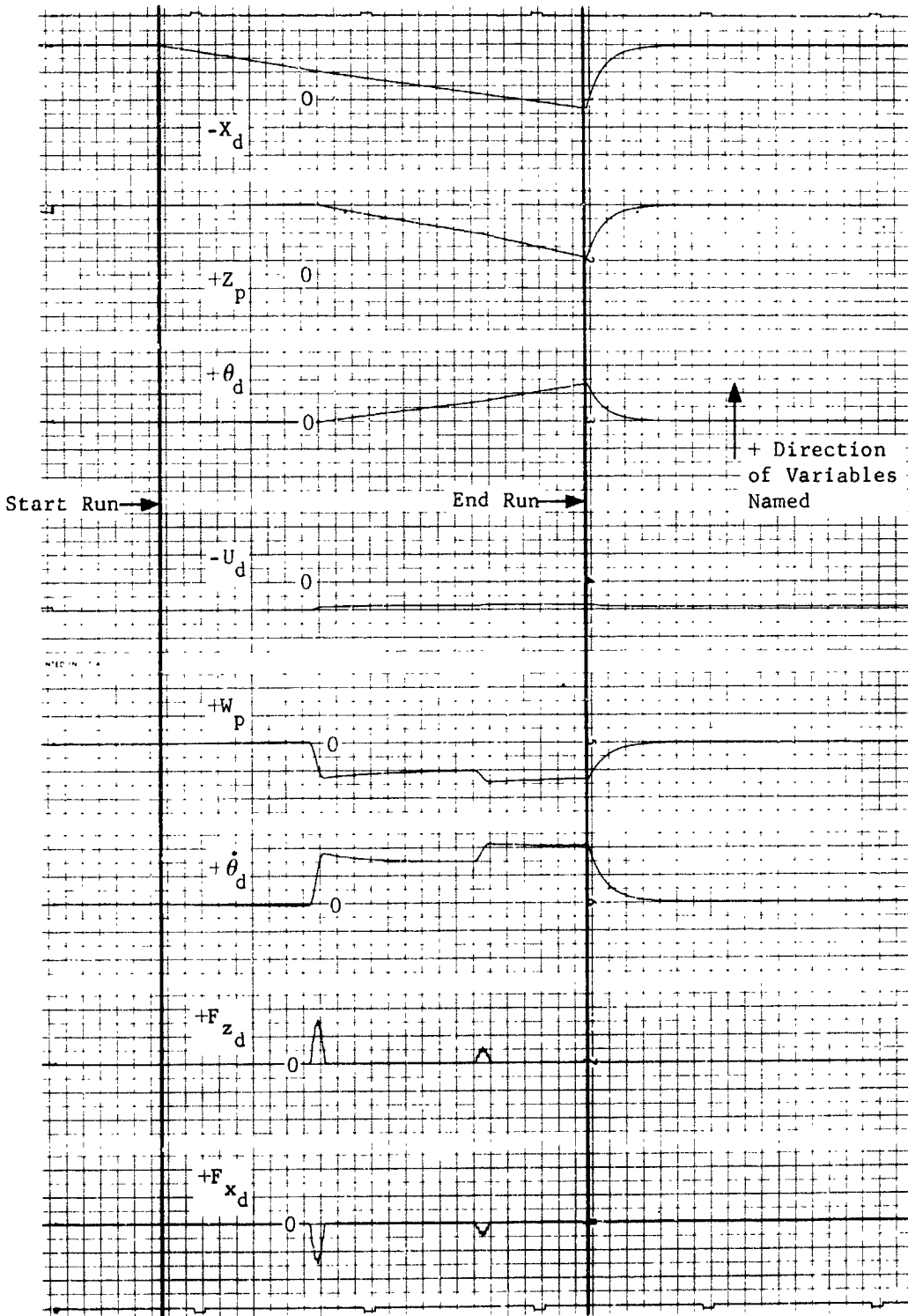
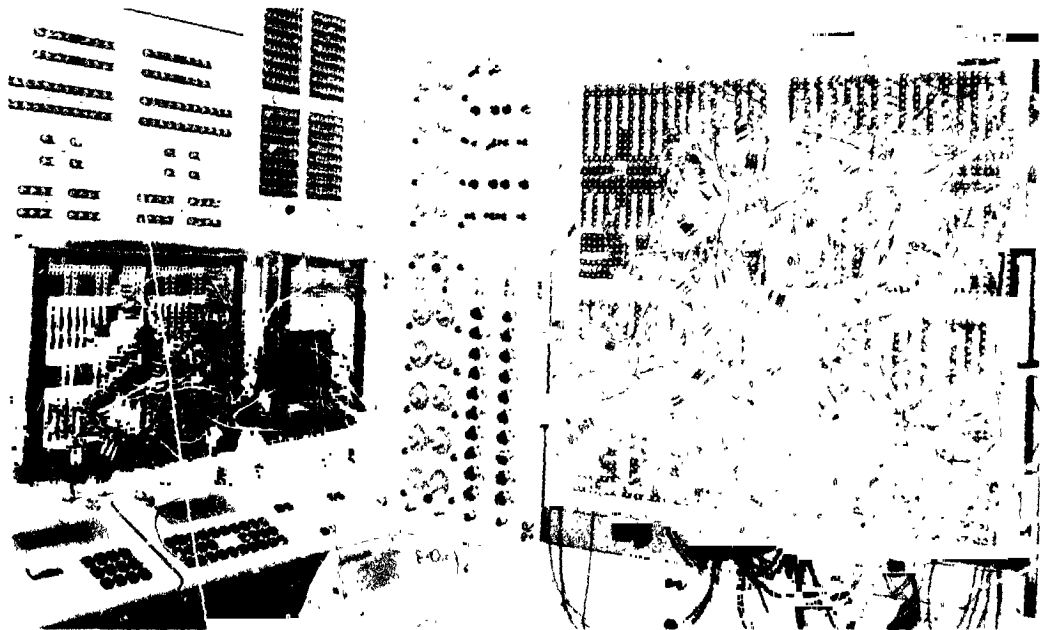


FIGURE 3-27 TYPICAL COMPUTER RUN SHOWING OUTPUTS TO SIMULATOR SERVO SYSTEM

NORTHROP SPACE LABORATORIES



Operators Shown at AD-256 Console and Plug Board During Investigation of Transients Resulting from Simulated Docking Impact.



Plug Board and Control Panels of AD-256 Computer. Board is wired for Simulation of Docking Impact to Confirm Continuity of the equations of Motion for Transient Response.

FIGURE 3-28 NORTHROP AD-256 ANALOG COMPUTER

NORTHROP SPACE LABORATORIES

would not exist on the simulator as the terms would not come through multipliers and the sources would be very carefully zeroed: This problem might arise in checkout, however.

3.4 Chamber Interfaces

This section discusses those factors relating to the interfacing of the simulator with the space simulation chamber. Discussions on vibration isolation, chamber penetration, installation and removal and safety are provided.

VIBRATION ISOLATION

In accelerating the large masses within the simulator, high reactive forces from the hydraulic actuators are imposed on the simulator structure. These forces are then transmitted to the structure on which the simulator is mounted. It is imperative that these forces are not transmitted to the chamber structure, particularly at the natural frequencies of this structure, or catastrophic damage to the chamber could occur.

To prevent these large forces from reaching the chamber structure, a vibration isolator system will be utilized. The design of this system is largely governed by the structural impedance characteristics of the chamber which have not been evaluated in detail by MSC at this time. However, conclusions pertaining to the required system have been made based on the simulator forces which are applied.

The forces resulting from translational motions within the simulator govern the design of the isolator system since the rotational reactions will be significantly lower. These translational forces are plotted as a function of frequency in Figure 3-29. As seen from these curves, the magnitude of the forces decreases rapidly with decreasing frequency. Therefore, it appears advantageous to choose an isolator frequency as low as possible in order to secure maximum attenuation of the larger forces which occur at higher frequencies.

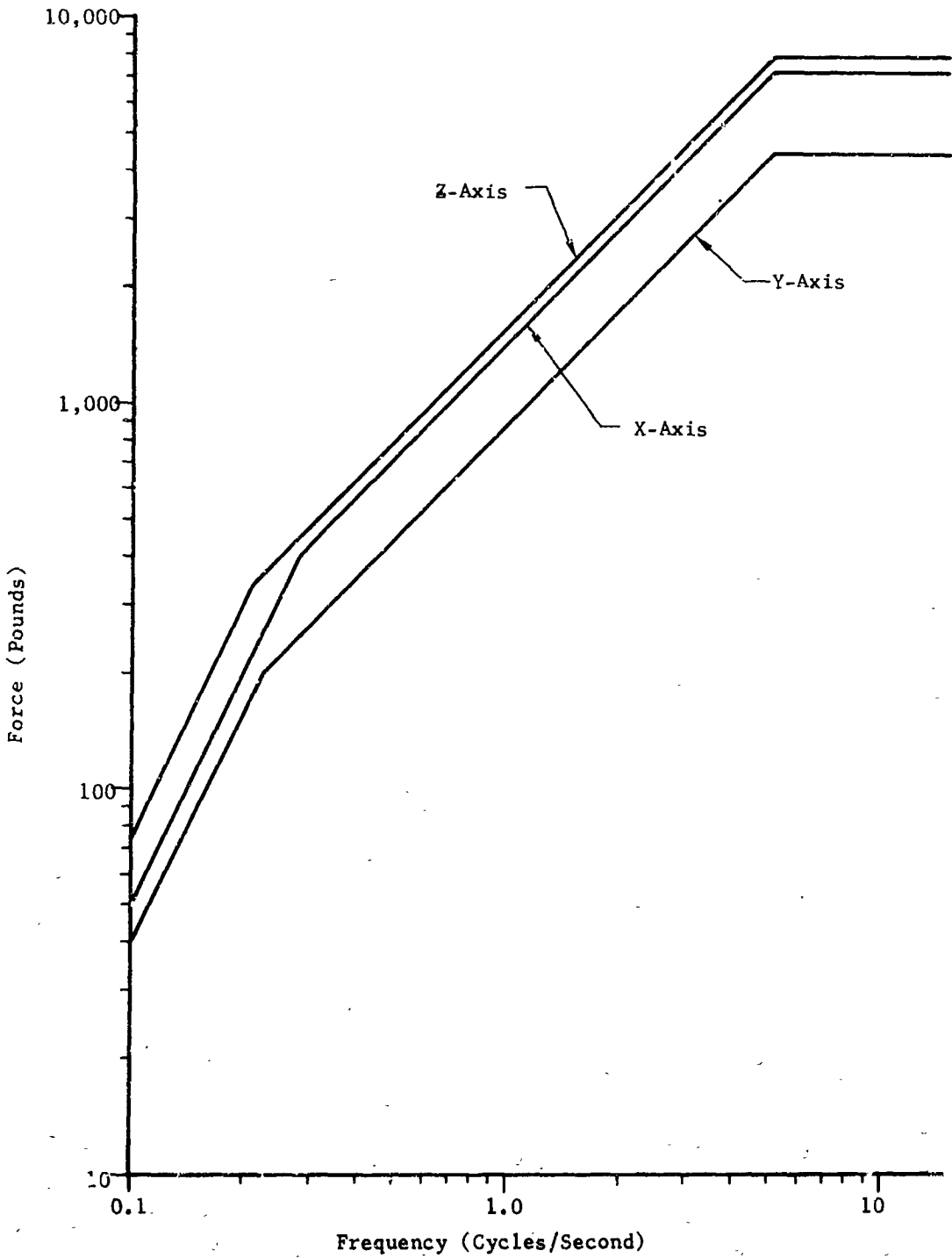


FIGURE 3-29 TRANSLATIONAL FORCES PRODUCED IN SIMULATOR

NORTHROP SPACE LABORATORIES

The attenuation obtained with various isolation frequencies is shown in Figure 3-30. These curves have been plotted assuming a damping ratio of 0.17. (Adequate dampers will be included in the isolation system design). Extremely low isolation frequencies will attenuate the applied forces to a negligible level; however, the development of such a low frequency system would pose design problems well beyond the state of the art in conventional isolator design. For example, a conventional spring isolator would require over eighty feet of static deflection to achieve a 0.1 cps system. Alternatively, the one or two-cps systems are relatively simple design problems. The final choice of the isolation system must be based on the structural impedance characteristics of the chamber. When these characteristics are fully known, trade-offs will be made to achieve an optimum design.

In addition to the forces transmitted to the chamber structure, the amplitude of the motion of the simulator and seismic mass mounted on the isolators is a major consideration in the design of the isolation system. It is desirable to keep the amplitude as low as possible for the following reasons:

- 1) To reduce flexibility requirements for hydraulic lines and electrical cables going to the simulator, and
- 2) To reduce the accelerations of the simulator structure which otherwise could require extensive correction for extraneous force balance outputs.

For any given isolator natural frequency the amplitude of motion is inversely proportional to the weight of the isolated mass. Therefore, to achieve these lower amplitudes, the simulator will be mounted on a large seismic mass which in turn will be mounted through the isolation system to the lunar plane. This seismic mass, while being as large as possible (on the order of 50,000 pounds), still maintains the total load on the lunar plane within its design limits. It consists of a carbon steel block of sufficient area to support the simulator and has a thickness (about 8 inches) which results in the desired mass.

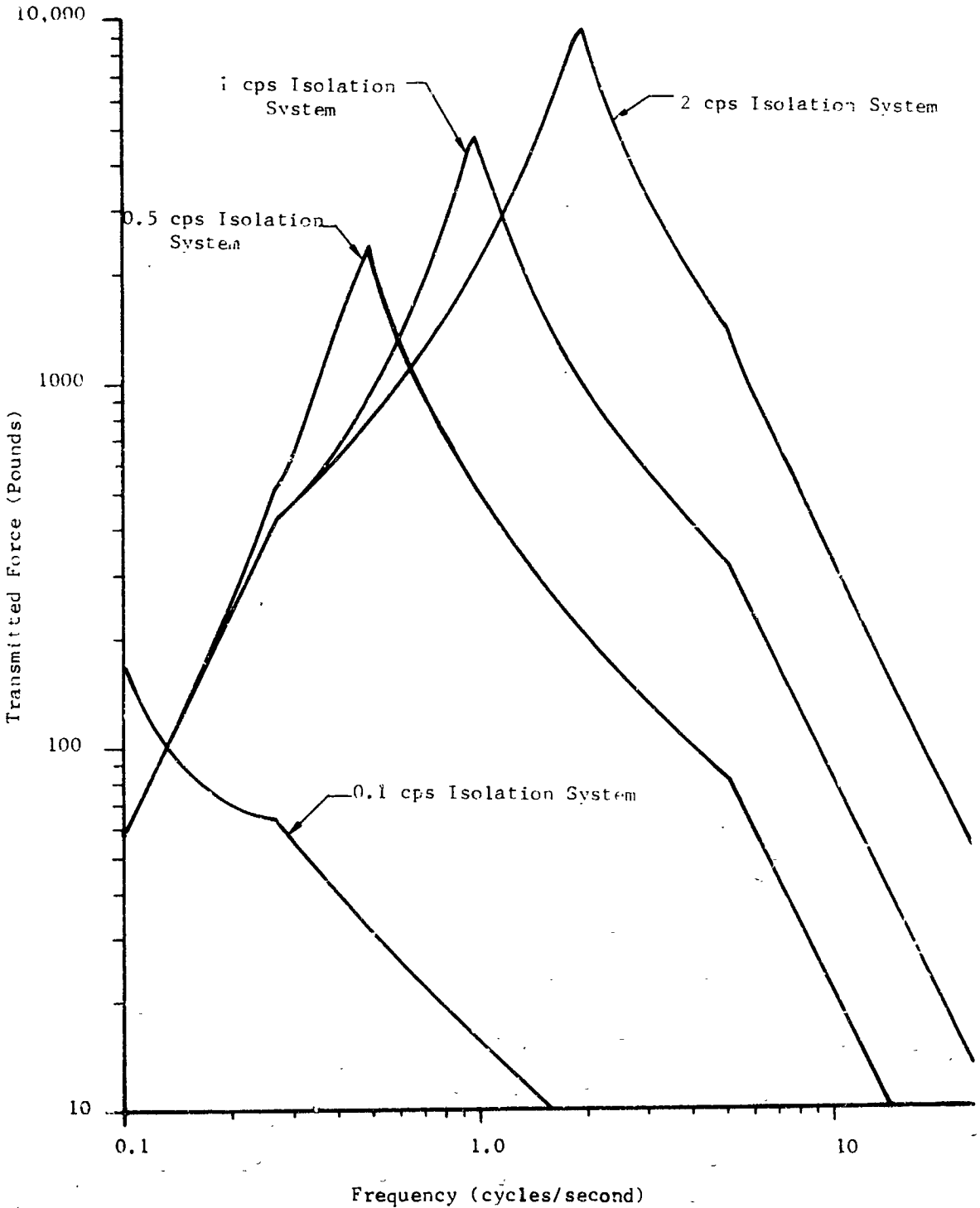


FIGURE 3-30 FORCE TRANSMITTED TO LUNAR PLANE THROUGH ISOLATION SYSTEM (Z-Axis Forces Assuming Infinite Impedance for Lunar Plane)

NORTHROP SPACE LABORATORIES

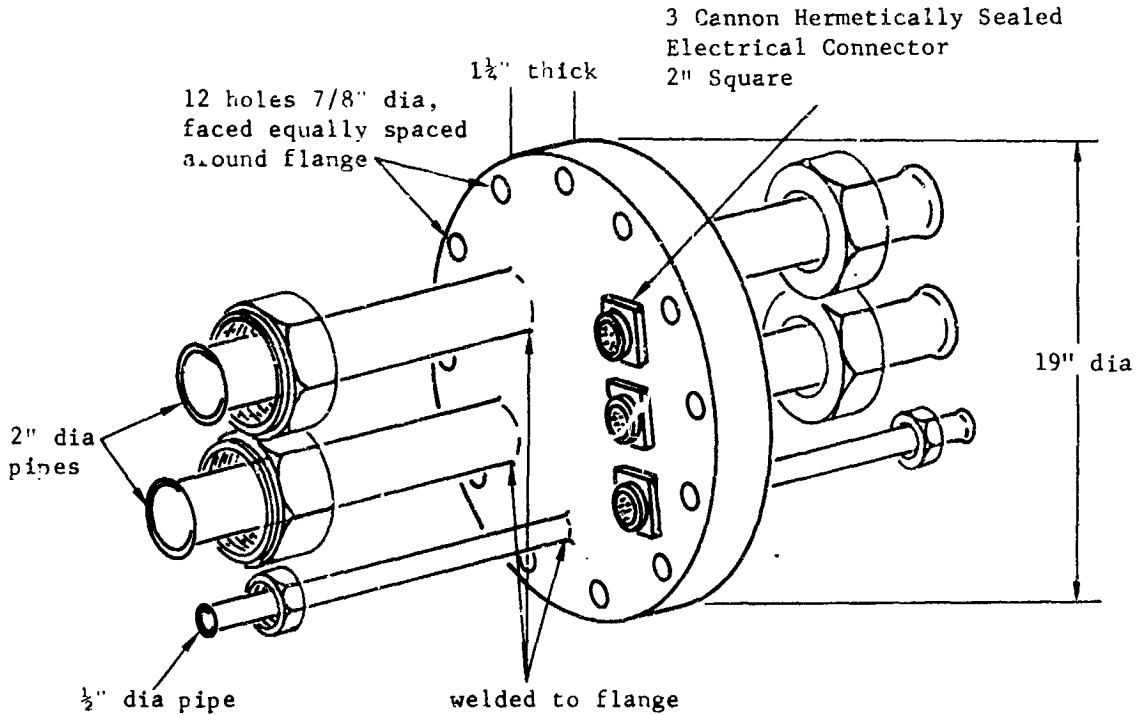
The use of the seismic mass, in addition to reducing amplitudes of simulator motion, yields another major advantage in isolating the simulator from the lunar plane. Due to the weight ratio of the mass and the simulator structure, the center of gravity of the simulator-seismic mass combination is moved downward to a point near the plane of the isolators. This results in a very stable isolation system which would be difficult to achieve if the simulator alone was isolated without the seismic block. Cross-coupling between the translational motion and rotary modes of oscillation on the isolators will be virtually eliminated.

Attachment fittings on the seismic mass will allow for thermal expansion differences between the carbon steel block and the stainless steel mounting structure.

CHAMBER PENETRATION

All chamber penetrating lines, both electrical and hydraulic will pass through a single stainless steel flange which seals the chamber port. The supply, return, and drain hydraulic lines will connect to steel couplings welded into the removable flange. This allows for ease in installing and in disconnecting lines both inside and outside the chamber. This permits rapid removal of the flange for reinstalling the solid port seal for other testing. All hydraulic lines inside the chamber will be stainless type, with flexible couplings minimized. Electrical lines will penetrate through multiple pin plugs sealed into the feed-through flange. This design is illustrated on the installation drawing and by Figure 3-31. The total leakage into the chamber for all penetrations (3 electrical and 3 hydraulic) should be less than 10^{-6} torr liters per second and will be verified by test with a helium leak detector. The electrical cabling inside the chamber will utilize insulating materials which do not contribute any large outgassing loads, either because of composition or due to multilayers which constitute large virtual leaks.

[Flange bolts to outside of
chamber port VS104]



All pipe ends flared (both ends)
for "B" nut AN connector

Pipes and connectors
within a 12 dia.

FIGURE 3-31 CHAMBER PORT PENETRATION FLANGE

NORTHROP SPACE LABORATORIES

INSTALLATION AND REMOVAL

The simulator structure is designed to require a minimum amount of time for installation and removal. The seismic mass is provided with lift points and is installed as a unit with the vibration isolators. The isolators are bolted to the radial beams of the lunar plane support. The simulator mechanism is then lowered into the chamber as a complete assembly and attached to the seismic mass. Initial installation of the isolators to the lunar plane beams will require drilling and tapping; these operations will be conducted under strict precautions to minimize contamination of the chamber.

All penetrations of the chamber are made through Port VS-104. The hydraulic lines and electrical cabling are routed through the umbilical tunnel in the pedestal and through an opening in the seismic mass to the simulator mechanisms. A hydraulic manifold block with manual valves is used at the simulator so that only three corrections are required: 1) supply pressure, 2) system return, and 3) scavenging return. The electrical leads are three continuous cables from the simulator to the connectors in the port flange.

SAFETY

General

As with any potentially dangerous device, either to personnel or facilities, safety must be designed into the system. Mechanical and electronic systems must be designed with sufficient safety factors to provide high reliability.

Due to the high structural rigidity required for the simulator, it is obvious that the resulting stress levels are exceeding low, giving large factors of safety for the simulator structure. The complete hydraulic system will be pressure tested to two times the operating pressure as a proof test.

Lock-out pins are provided on all actuation mechanisms so that mechanisms may be fixed while the simulator is being installed or removed

NORTHROP SPACE LABORATORIES

from the chamber. These lock-out devices will resist the full driving force of the actuators permitting these devices to be used as safeties against accidental pressurization of the system.

To prevent loss of control which might be experienced due to electrical power failure, a system of parallel nickel-cadmium battery supplies is utilized. These batteries are automatically charged when the system is functioning properly.

The control console was designed using proven human factors engineering methods to obtain safe and efficient manual or automatic control.

Cleanliness

All items placed in the chamber will be cleaned and degreased prior to installation. The interior hydraulic system will be previously leak-checked to assure no accumulation of oil will occur in the chamber. Where hydraulic piston rods are exposed for proper operation, those rods are kept cool by radiation shielding positioned to reduce migration of vapors. Prior to removal, all chamber hydraulic lines will be purged of oil by suction. Removable gravity head pans will be utilized to collect inadvertently discharged oil. The system is designed to close off pressure and oil flow in a fail-safe manner to prevent contamination of the chamber. Points used on surfaces to achieve thermal control and which are exposed to the chamber vacuum should be cured epoxies. All operations which create dust or other litter within the space chamber will be avoided. These factors are discussed in more detail in Appendix C.

Explosion

The oil selected for use in the simulator hydraulic system has a very low vapor pressure and reduces oil migration by evaporation.

The very low vapor pressure of the selected hydraulic oil is maintained through the removal of unwanted gases and contaminants by imposing

a vacuum on the low pressure side of the hydraulic system. For this purpose, a separate vacuum system is included in the ancillary equipment

Operational procedures will include techniques for minimizing pressure unbalances between the hydraulic system low pressure side and the ambient pressure external to the servo system. By this accomplishment, no hazard of explosion due to oil vapor will exist, even in an oxygen-rich atmosphere. The vapor pressure of this oil is too low to establish an explosive mixture under any conditions. Should any oil vapors mix with the diffusion pump oil, no hazard will exist because of the very small quantities which can be encountered and because the selective refraction occurring in the pump will purge the higher vapor pressure constituents on through the system. Should any oil originally emanating from the hydraulic system eventually collect in the mechanical vacuum pumps, there would still be no explosion hazard because of its low vapor pressure. Further, it should cause no impairment in pump performance. These factors are discussed in more detail in Appendix C, E, and F.

Fail-Safe Loop Closure

The electronic circuits and their components of the servo control system are designed for a maximum of reliability. However, in the unlikely event of a component failure during a test, a stable loop closure is still retained. If the loop failure results in a loss or diminished control of the mechanism which produces excess forces on the probe or drogue assemblies, the axial servo is immediately withdrawn to eliminate contact. Excessive forces are sensed by an automatic monitoring of the force balance outputs by "go, no-go" provision voltage comparators. The comparator is fail-safe: component failure, or loss of power will always result in a no-go condition. The voltage comparator activates the final safe manifold which supplies hydraulic pressure to the servo valve. The lack of an electrical command signal initiates

NORTHROP SPACE LABORATORIES

operation of the manifold driving the actuator to its fully retarded position. The operation of the manifold is completely independent of command to the servo valve or servo valve failure. In fail-safe operation, the manifold isolates the servo valve output and assumes direct command of the actuator.

3.5 Specifications, Ancillary Equipment and Requirements

The following preliminary specifications for the ancillary elements and requirements of the Docking Simulator System have been developed, as complete as possible at the present stage of hardware design. As the design of the elements of the system are completed these preliminary specifications shall be modified into final specifications.

Spcn 100 Basic Mounting Structure

Spcn 200 Seismic Mass

Spcn 300 Chamber Penetration Seal

Spcn 400 Actuator Oil Conditioning Unit

Spcn 500 Vacuum System

Spcn 600 Control Console

Spcn 700 Transmission Line

Spcn 800 Transmission Line Terminal Racks

Spcn 900 Electrical Requirements

Spcn 1000 Spares

Spcn 1200 Shipping

Spcn 1300 Operations and Maintenance Manual

**NORTHROP SPACE LABORATORIES
PRELIMINARY SPECIFICATION**

APOLLO DOCKING SIMULATOR SYSTEM

SPEC. NO.	DESCRIPTION AND REQUIREMENTS																						
100	<p><u>BASIC MOUNTING STRUCTURE</u></p> <p>This preliminary specification describes the Basic Mounting Structure which holds the Docking Simulator System and instrumentation devices during test runs. The components specified below comprise the complete structure.</p> <p style="text-align: center;">SPECIFICATIONS</p> <p><u>Structural Framework</u></p> <table style="width: 100%; border-collapse: collapse;"> <tr> <td style="width: 50%;">Material</td> <td>Stainless steel tubing</td> </tr> <tr> <td>Size</td> <td>6" O.D. x 1/2 wall</td> </tr> <tr> <td>Construction</td> <td>Welded</td> </tr> <tr> <td>Conformation</td> <td>Per Figure</td> </tr> </table> <p><u>Probe and Drogue Adapters</u></p> <table style="width: 100%; border-collapse: collapse;"> <tr> <td style="width: 50%;">Material</td> <td>Stainless steel, 300-series</td> </tr> <tr> <td>Construction</td> <td>Welded</td> </tr> <tr> <td>Probe adapter, conformation mating</td> <td>Per Figure 3-8 To Apollo Command Module seal ring (GFE) and to force balance.</td> </tr> <tr> <td>Drogue adapter, conformation mating</td> <td>Per Figure 3-9 To LEM tunnel (GFE) and force balance.</td> </tr> </table> <p><u>Force Measurement Balances</u></p> <table style="width: 100%; border-collapse: collapse;"> <tr> <td style="width: 50%;">Type</td> <td>6-component internal strain gage balance, floating frame.</td> </tr> <tr> <td>Sensing components</td> <td>2-normal force and pitching moment. 2-side force and yawing moment. Dual axial force and rolling moment.</td> </tr> <tr> <td>Performance accuracy</td> <td>All points from any series of loadings of a single element produce data within ± 0.25 (one-quarter) percent of maximum load or ± 0.5 (one-half) percent of applied load when compared with the best straight line fit. This accuracy is inclusive of all scatter, hysteresis, and non-linearity for both plus and minus loads.</td> </tr> </table>	Material	Stainless steel tubing	Size	6" O.D. x 1/2 wall	Construction	Welded	Conformation	Per Figure	Material	Stainless steel, 300-series	Construction	Welded	Probe adapter, conformation mating	Per Figure 3-8 To Apollo Command Module seal ring (GFE) and to force balance.	Drogue adapter, conformation mating	Per Figure 3-9 To LEM tunnel (GFE) and force balance.	Type	6-component internal strain gage balance, floating frame.	Sensing components	2-normal force and pitching moment. 2-side force and yawing moment. Dual axial force and rolling moment.	Performance accuracy	All points from any series of loadings of a single element produce data within ± 0.25 (one-quarter) percent of maximum load or ± 0.5 (one-half) percent of applied load when compared with the best straight line fit. This accuracy is inclusive of all scatter, hysteresis, and non-linearity for both plus and minus loads.
Material	Stainless steel tubing																						
Size	6" O.D. x 1/2 wall																						
Construction	Welded																						
Conformation	Per Figure																						
Material	Stainless steel, 300-series																						
Construction	Welded																						
Probe adapter, conformation mating	Per Figure 3-8 To Apollo Command Module seal ring (GFE) and to force balance.																						
Drogue adapter, conformation mating	Per Figure 3-9 To LEM tunnel (GFE) and force balance.																						
Type	6-component internal strain gage balance, floating frame.																						
Sensing components	2-normal force and pitching moment. 2-side force and yawing moment. Dual axial force and rolling moment.																						
Performance accuracy	All points from any series of loadings of a single element produce data within ± 0.25 (one-quarter) percent of maximum load or ± 0.5 (one-half) percent of applied load when compared with the best straight line fit. This accuracy is inclusive of all scatter, hysteresis, and non-linearity for both plus and minus loads.																						

**NORTHROP SPACE LABORATORIES
PRELIMINARY SPECIFICATION**

APOLLO DOCKING SIMULATOR SYSTEM

SPEC. NO.	DESCRIPTION AND REQUIREMENTS	
100	Gage characteristics	<p>Bridge resistance is 120 ohms for normal and side force elements.</p> <p>The basic bridge resistance of the folling moment and chord force elements is 120 ohms. However, these components each operate with two full bridges wired in parallel. Thus the resistance is 60 ohms.</p> <p>Operating voltage of each element is 6 volts. Lower voltage is recommended for balances 0.75 inches diameter or less.</p>
	<u>Hydraulic Servo Valves</u>	
	Valve type	1 stage voice coil/permanent magnet
	Material	Stainless steel, 300-series
	Natural frequency	Above 600 cps
	Flow rate	40 gallons per minute at 1500 psi
	Operating pressure	3000 psi
	Coil power	40 watts peak
	<u>FEEDBACK SENSING DEVICES</u>	
	POSITION POTENTIOMETERS	
	Function	Linear
	Resistance	1.5K ohms
	Resistance per turn	150 ohms
	Temperature coefficient of resistance wire	20 ppm per °C
	Resolution	Infinite
	Linearity independent	0.005%
	Turns	10 turns
	Noise	50 ohms max ENR per MIL-R-12934B
	Power rating	1 watt
	Torque starting	1 oz inch max
	Torque running	0.6 oz inch max
	Stop strength	100 oz inch
	Service life	5 x 10 ⁵ revolutions
	Operating speed	500 rpm max

**NORTHROP SPACE LABORATORIES
PRELIMINARY SPECIFICATION**

APOLLO DOCKING SIMULATOR SYSTEM

SPEC. NO.	DESCRIPTION AND REQUIREMENTS	
100	<u>Hydraulic Flexible Lines</u>	
	Material	Stainless steel, series 300
	Construction	Helical corrugated core reinforced with wire braid.
	Fittings	MS standard attached by inert gas shielded-arc welding.
	Maximum working pressure	3,500 psi
	Maximum test pressure	7,000 psi
	<u>Electrical Wiring</u>	
	Lengths	Minimum consistent with good design practice.
	Specification	MIL-W-15878C
	Type (feedback signals)	Twisted, shielded pairs
	<u>Shock Absorbers</u>	
	Material	Stainless steel
	Bore	4 inches
	Stroke	4 inches
	Mating	To Docking Simulator System

**NORTHROP SPACE LABORATORIES
PRELIMINARY SPECIFICATION**

APOLLO DOCKING SIMULATOR SYSTEM

SPEC. NO.	DESCRIPTION AND REQUIREMENTS												
200	<p><u>SEISMIC MASS</u></p> <p>This preliminary specification described a seismic mass to be used to hold a basic mounting structure for the Docking Simulator System during test.</p> <p style="text-align: center;">SPECIFICATIONS</p> <table style="width: 100%; border-collapse: collapse;"> <tr> <td style="width: 50%;"><u>Dimensions, Thickness</u></td> <td style="width: 50%;">8 inches</td> </tr> <tr> <td style="padding-left: 40px;">Width</td> <td>15 feet</td> </tr> <tr> <td style="padding-left: 40px;">Length</td> <td>10 feet</td> </tr> <tr> <td><u>Material</u></td> <td>Low carbon steel (single piece)</td> </tr> <tr> <td><u>Finish</u></td> <td>Completely sandblasted, painted with Catalac epoxy paint</td> </tr> <tr> <td><u>Attachments</u></td> <td>Moving rings, shock absorber attach fittings, and support skids as required per print (Figures 3-7).</td> </tr> </table>	<u>Dimensions, Thickness</u>	8 inches	Width	15 feet	Length	10 feet	<u>Material</u>	Low carbon steel (single piece)	<u>Finish</u>	Completely sandblasted, painted with Catalac epoxy paint	<u>Attachments</u>	Moving rings, shock absorber attach fittings, and support skids as required per print (Figures 3-7).
<u>Dimensions, Thickness</u>	8 inches												
Width	15 feet												
Length	10 feet												
<u>Material</u>	Low carbon steel (single piece)												
<u>Finish</u>	Completely sandblasted, painted with Catalac epoxy paint												
<u>Attachments</u>	Moving rings, shock absorber attach fittings, and support skids as required per print (Figures 3-7).												

**NORTHROP SPACE LABORATORIES
PRELIMINARY SPECIFICATION**

APOLLO DOCKING SIMULATOR SYSTEM

SPEC. NO.	DESCRIPTION AND REQUIREMENTS												
300	<p><u>CHAMBER PENETRATION SEAL</u></p> <p>This preliminary specification describes a seal to be installed at the Chamber B wall to carry hydraulic oil and instrumentation to the Docking Simulator System.</p> <p style="text-align: center;">SPECIFICATIONS</p> <p><u>Flange Installation</u></p> <table style="width: 100%; border: none;"> <tr> <td style="padding-left: 20px;">Maximum leakage</td> <td style="padding-left: 100px;">1 x 10⁻⁶ torr liters/second</td> </tr> <tr> <td style="padding-left: 20px;">Seal materials</td> <td style="padding-left: 100px;">Elastomer</td> </tr> </table> <p><u>Electrical Lines</u></p> <table style="width: 100%; border: none;"> <tr> <td style="padding-left: 20px;">Number</td> <td style="padding-left: 100px;">3</td> </tr> <tr> <td style="padding-left: 20px;">Receptacles</td> <td style="padding-left: 100px;">Hermetically sealed with O-ring mount</td> </tr> </table> <p><u>Hydraulic Lines</u></p> <table style="width: 100%; border: none;"> <tr> <td style="padding-left: 20px;">Number</td> <td style="padding-left: 100px;">3 (System pressure, system return and scavenger return)</td> </tr> <tr> <td style="padding-left: 20px;">Material</td> <td style="padding-left: 100px;">Stainless steel</td> </tr> </table> <p>Reference: Figure 3-31, Chamber Port Penetration Flange</p>	Maximum leakage	1 x 10 ⁻⁶ torr liters/second	Seal materials	Elastomer	Number	3	Receptacles	Hermetically sealed with O-ring mount	Number	3 (System pressure, system return and scavenger return)	Material	Stainless steel
Maximum leakage	1 x 10 ⁻⁶ torr liters/second												
Seal materials	Elastomer												
Number	3												
Receptacles	Hermetically sealed with O-ring mount												
Number	3 (System pressure, system return and scavenger return)												
Material	Stainless steel												

**NORTHROP SPACE LABORATORIES
PRELIMINARY SPECIFICATION**

APOLLO DOCKING SIMULATOR SYSTEM

SPEC.
NO.

DESCRIPTION AND REQUIREMENTS

400

ACTUATOR OIL CONDITIONING UNIT

This preliminary specification describes an actuator oil conditioning unit used to condition and circulate hydraulic oil through the Docking Simulator System installed in the test chamber during test or quiescent runs. The unit shall be located adjacent to the test chamber.

SPECIFICATIONS

Oil pressure	3000 psiG
Oil temperature regulation	50 ± 10°F
Heater	30 KW
Heat exchanger	100 HP
Rate of flow	80 gallons/minute
Input to system	2-inch socket weld flange
System return	3-inch threaded pipe
Controls	Local and remote from control console
Operating power	440 volts, 60 cps, 3-phase at 500 amperes
Electrical motor	150 horsepower
Full flow filters	
Outlet	Nominal - 5 microns
Low pressure	Nominal - 20 microns
Supercharging pump	70 PSIG, 80 gallons/minute

**NORTHROP SPACE LABORATORIES
PRELIMINARY SPECIFICATION**

APOLLO DOCKING SIMULATOR SYSTEM

SPEC.
NO.

DESCRIPTION AND REQUIREMENTS

500

VACUUM SYSTEM

The vacuum system supplies balance pressure, within selected portions of the hydraulic system, equivalent to that simulated within the Chamber B test space to operate the hydraulic oil scavenge return from the servo valves.

SPECIFICATIONS

Vacuum capability	1 micron
Operating cycle	10 minutes to reach 1 micron, and maintain for test run
Main valve leak rate	1×10^{-4} torr liter/seconds maximum
Controls and instrumentation	1) Remote and local control 2) Remote and local monitors 3) Fail-safe and shutdown 4) Interlocking on-off control with Actuator Oil Condition- ing Unit
Operating power	115 volts, 60 cps

**NORTHROP SPACE LABORATORIES
PRELIMINARY SPECIFICATION**

APOLLO DOCKING SIMULATOR SYSTEM

SPEC. NO.	DESCRIPTION AND REQUIREMENTS																										
600	<p><u>CONTROL CONSOLE</u></p> <p>This preliminary specification describes the control console used to program, control and monitor Docking Simulator System test and status.</p> <p style="text-align: center;">SPECIFICATION</p> <p><u>Hydraulic Servo Controller</u></p> <p>Hydraulic Servo Controller is a servo power amplifier assembly having all functions necessary to close and equalize a high performance electro-hydraulic control loop.</p> <p>Output</p> <table style="width: 100%; border: none;"> <tr> <td style="padding-left: 20px;">Power</td> <td>100W max</td> </tr> <tr> <td style="padding-left: 20px;">Voltage</td> <td>±20 volts</td> </tr> <tr> <td style="padding-left: 20px;">Current</td> <td>±6 amperes</td> </tr> </table> <p>Input</p> <p>Response</p> <p>Drift</p> <p>Noise</p> <p>Inputs</p> <p>Controls</p> <p><u>Feedback Sensing Devices</u></p> <p><u>Velocity (Rate) Sensor</u></p> <table style="width: 100%; border: none;"> <tr> <td style="padding-left: 20px;">Excitation</td> <td>115 volts, 400 cps, 0.160 ampere</td> </tr> <tr> <td style="padding-left: 20px;">Output</td> <td>2 volts at 1000 rpm</td> </tr> <tr> <td style="padding-left: 20px;">Linearity</td> <td>0.02% 0 to 36 rpm</td> </tr> <tr> <td style="padding-left: 20px;">Rotor Moment of Inertia</td> <td>31 gm/cm²</td> </tr> <tr> <td style="padding-left: 20px;">Ambient Temperature</td> <td>-25° to +75°C</td> </tr> </table> <p><u>Pressure Transducer</u></p> <table style="width: 100%; border: none;"> <tr> <td style="padding-left: 20px;">Excitation</td> <td>10v dc or ac rms, 0-20kc</td> </tr> <tr> <td style="padding-left: 20px;">Input Resistance</td> <td>330 ohms minimum</td> </tr> <tr> <td style="padding-left: 20px;">Output</td> <td>350 ± 3.5 ohms</td> </tr> <tr> <td style="padding-left: 20px;">Sensitivity</td> <td>±40 millivolts at +20 -10% open circuit</td> </tr> <tr> <td style="padding-left: 20px;">Resolution</td> <td>Infinite</td> </tr> </table>	Power	100W max	Voltage	±20 volts	Current	±6 amperes	Excitation	115 volts, 400 cps, 0.160 ampere	Output	2 volts at 1000 rpm	Linearity	0.02% 0 to 36 rpm	Rotor Moment of Inertia	31 gm/cm ²	Ambient Temperature	-25° to +75°C	Excitation	10v dc or ac rms, 0-20kc	Input Resistance	330 ohms minimum	Output	350 ± 3.5 ohms	Sensitivity	±40 millivolts at +20 -10% open circuit	Resolution	Infinite
Power	100W max																										
Voltage	±20 volts																										
Current	±6 amperes																										
Excitation	115 volts, 400 cps, 0.160 ampere																										
Output	2 volts at 1000 rpm																										
Linearity	0.02% 0 to 36 rpm																										
Rotor Moment of Inertia	31 gm/cm ²																										
Ambient Temperature	-25° to +75°C																										
Excitation	10v dc or ac rms, 0-20kc																										
Input Resistance	330 ohms minimum																										
Output	350 ± 3.5 ohms																										
Sensitivity	±40 millivolts at +20 -10% open circuit																										
Resolution	Infinite																										

**NORTHROP SPACE LABORATORIES
PRELIMINARY SPECIFICATION**

APOLLO DOCKING SIMULATOR SYSTEM

SPEC. NO.	DESCRIPTION AND REQUIREMENTS	
600	<p>Full Range Output</p> <p>Operable Temperature Range</p> <p>Combined Nonlinearity and Hysterisis</p>	<p>80 millivolts (nominal)</p> <p>-65°F to +275°F</p> <p>0.5% maximum at full range independently determined for positive and negative pressure.</p>
	<p><u>Signal Conditioning Circuits</u></p> <p>The Signal Conditioning Circuits apply input signals from the transmission line to the servo control system and conditions signals between the strain gauge amplifiers and the transmission line.</p>	
	<p><u>Control Console Conditioning Amplifiers</u></p>	
	Type	Wideband differential dc (solid state)
	Number Required	12 (one per channel)
	Input Range	±5 volts from computer
	Output Range	±5 volts to Transmission Line
	Drift Rate	Less than +1 microvolt referred to the input and ±0.005 percent of full scale, over 40 hours of operation
	Noise Level	Less than 2 microvolts rms referred to the input and 250 microvolts referred to the output from 0.05 cps to 10 kc
	Output Impedance	Less than 1 ohm
	Common Mode Rejection	160 db at dc, 120 db to 120 cps
	Power Requirements	115 volts, 400 cps, 14 watts
	<p><u>Control Console Input Conditioning Amplifiers</u></p>	
	Type	Wideband differential dc (solid state)
	Number	12 (1 per channel)
	Input Range	±5 volts from transmission line
	Output Range	±5 volts to servo controller
	Common Mode Rejection	Maximum error less than ±20 mv
	Power Requirements	+15 volts 24 ma

**NORTHROP SPACE LABORATORIES
PRELIMINARY SPECIFICATION**

APOLLO DOCKING SIMULATOR SYSTEM

SPEC.
NO.

DESCRIPTION AND REQUIREMENTS

600

Control Console Input Conditioning Amplifier Power Supply

Operating Power	115 volts 400 cps
Output	+15 and -15 volts at 0-300ma
Stability	Preset to $\pm 0.01\%$ at 25°C
Regulation	Within 250 microvolts over 115 volts $\pm 10\%$
Noise and Ripple	Less than 250 microvolts p-p
Temperature Range	-25°C to 85°C

Electronic Safety System

The Electronic Safety System comprises fail-safe and interlock manifolds for servo valves and sensors to prevent operation under unsafe conditions.

Voltage Comparator

Accuracy	1 millivolt maximum, 0.3 millivolt typical
Repeatability	50 microvolts
Response Time	20 milliseconds
Input Voltage Range	± 50 volts dc
Maximum Difference Voltage	± 10 volts dc
Operating Power	115 volts at 400 cps

Fail-Safe Interlock Manifold

Modes of Operation	1) Fail in last position 2) Fail to one end 3) Float
Control	Local or remote
Operating Pressure	To 3000 psi
Flow Rate	To 60 gpm
Temperature Range	-60°F to 180°F
Operating Power	28 volts dc

Force Measurement System

Force Measurement System comprises an oscillator, amplifier, and demodulator combination used for excitation of the Force Measurement Balance Transducers and to amplify the output of the transducers to the transmission line input amplifiers.

NORTHROP SPACE LABORATORIES

PRELIMINARY SPECIFICATION

APOLLO DOCKING SIMULATOR SYSTEM

SPEC. NO.	DESCRIPTION AND REQUIREMENTS	
600	<u>Transducer Output Amplifier</u>	
	Type	Carrier amplifier (with a bridge balancing unit and phase sensitive demodulation)
	Number	12 (1 per channel)
	Frequency Response	Uniform within $\pm 2\%$ from 0 to 600 cps
	Sensitivity	1 millivolt rms input (unattenuated) produces full scale output; 1 volt rms input fully attenuated produces full scale output.
	Input Attenuator Required Controls	1 to 100 in 20 steps bridge. Zero-center meter for initial balance, and percentage of full scale output; transducer and cabling resistive and reactive balancing out controls; attenuator selector; smooth initial balance control adjustment at maximum sensitivity.
	Oscillator - Power Supply	
	Input	115 volts 400 cps
	Carrier Oscillator Output	3kc at 10 volts (nominal)
	<u>Control and Monitoring Displays</u>	
	Controls	<ol style="list-style-type: none"> 1) Controls and interlocks to transfer manual control of individual system operator for checkout and maintenance. 2) Emergency stop (see Electronic Safety System). 3) Master stop for normal shut down.
	Monitoring Displays	<ol style="list-style-type: none"> 1) Appropriate meter indicators for parameter. 2) Operational status 3) Test environment 4) Closed circuit television (GFE)

**NORTHROP SPACE LABORATORIES
PRELIMINARY SPECIFICATION**

APOLLO DOCKING SIMULATOR SYSTEM

SPEC. NO.	DESCRIPTION AND REQUIREMENTS
600	<p><u>Voice Communication System</u></p> <p>Modes of Operation Individual station, conference, hot-mike hands off.</p> <p>Ambient Acoustical Levels for 100% Sentence Intelligibility 120 db</p> <p>Compatibilities To existing SESL voice communication and PA systems, RF, digital, sound alert, commercial telephone systems.</p> <p>Area of Coverage Control control panel to remote areas approximately 1 mile away.</p> <p>Power Requirements 28v dc central power supply, automatic battery supply for emergency.</p> <p>Stations Required Control Console - 2 Computer - 3 Actuator Oil Conducting Unit - 1 Vacuum Pumping Unit - 1 Chamber B Operator Station - 1 Test Program Director Station - 1</p> <p>Reference: Figure 3-20, Control Console</p>

**NORTHROP SPACE LABORATORIES
PRELIMINARY SPECIFICATION**

APOLLO DOCKING SIMULATOR SYSTEM

SPEC.
NO.

DESCRIPTION AND REQUIREMENTS

700

TRANSMISSION LINE

This preliminary specification describes a Transmission Line connecting the control console and the computer. The Transmission Line consists of two cables, one cable carrying signals from the computer to the control console. The second carries force balance signals from the control console to the computer. The following specifications apply to each cable.

SPECIFICATIONS

Number of pairs	24
Wire type	Shielded twisted pairs, 20 gauge
Connectors	To MIL-C-5015 at each end

**NORTHROP SPACE LABORATORIES
PRELIMINARY SPECIFICATION**

APOLLO DOCKING SIMULATOR SYSTEM

SPEC. NO.	DESCRIPTION AND REQUIREMENTS																																
800	<p><u>TRANSMISSION LINE TERMINATION RACK</u></p> <p>This preliminary specification describes a Transmission Line Termination Rack located in the vicinity of the computer. The Termination Rack contains amplifiers (and one power supply) used to condition signals between the Control Console and the computer.</p> <p style="text-align: center;">SPECIFICATIONS</p> <p><u>Computer Output Signal Amplifiers</u></p> <table style="width: 100%; border-collapse: collapse;"> <tr> <td style="width: 30%;">Type</td> <td>Wideband differential dc (solid state)</td> </tr> <tr> <td>Number required</td> <td>12 (1 per channel)</td> </tr> <tr> <td>Input range</td> <td>± 100 volts from computer</td> </tr> <tr> <td>Output range</td> <td>± 5 volts to Transmission Line</td> </tr> <tr> <td>Drift rate</td> <td>Less than ± 1 microvolt referred to the input and ± 0.005 percent of full scale, over 40 hours of operation.</td> </tr> <tr> <td>Noise Level</td> <td>Less than 2 microvolts rms from 0.05 cps to 10 kc.</td> </tr> <tr> <td>Output impedance</td> <td>Less than 1 ohm</td> </tr> <tr> <td>Common mode rejection</td> <td>160 db at dc, 120 db to 120 cps</td> </tr> <tr> <td>Power requirements</td> <td>115 volts, 400 cps, 14 watts</td> </tr> </table> <p><u>Computer Input Conditioning Amplifiers</u></p> <table style="width: 100%; border-collapse: collapse;"> <tr> <td style="width: 30%;">Type</td> <td>Wideband, differential dc (vacuum tube)</td> </tr> <tr> <td>Number required</td> <td>12 per channel</td> </tr> <tr> <td>Input range</td> <td>± 5 volts from Transmission Line</td> </tr> <tr> <td>Output range</td> <td>± 100 volts to computer</td> </tr> <tr> <td>Gain</td> <td>20</td> </tr> <tr> <td>Noise</td> <td>Less than 20 microvolts</td> </tr> <tr> <td>Power requirements</td> <td>+300 and -300 volts at 11 ma and 6.3 volts ac at 920 ma</td> </tr> </table>	Type	Wideband differential dc (solid state)	Number required	12 (1 per channel)	Input range	± 100 volts from computer	Output range	± 5 volts to Transmission Line	Drift rate	Less than ± 1 microvolt referred to the input and ± 0.005 percent of full scale, over 40 hours of operation.	Noise Level	Less than 2 microvolts rms from 0.05 cps to 10 kc.	Output impedance	Less than 1 ohm	Common mode rejection	160 db at dc, 120 db to 120 cps	Power requirements	115 volts, 400 cps, 14 watts	Type	Wideband, differential dc (vacuum tube)	Number required	12 per channel	Input range	± 5 volts from Transmission Line	Output range	± 100 volts to computer	Gain	20	Noise	Less than 20 microvolts	Power requirements	+300 and -300 volts at 11 ma and 6.3 volts ac at 920 ma
Type	Wideband differential dc (solid state)																																
Number required	12 (1 per channel)																																
Input range	± 100 volts from computer																																
Output range	± 5 volts to Transmission Line																																
Drift rate	Less than ± 1 microvolt referred to the input and ± 0.005 percent of full scale, over 40 hours of operation.																																
Noise Level	Less than 2 microvolts rms from 0.05 cps to 10 kc.																																
Output impedance	Less than 1 ohm																																
Common mode rejection	160 db at dc, 120 db to 120 cps																																
Power requirements	115 volts, 400 cps, 14 watts																																
Type	Wideband, differential dc (vacuum tube)																																
Number required	12 per channel																																
Input range	± 5 volts from Transmission Line																																
Output range	± 100 volts to computer																																
Gain	20																																
Noise	Less than 20 microvolts																																
Power requirements	+300 and -300 volts at 11 ma and 6.3 volts ac at 920 ma																																

NORTHROP SPACE LABORATORIES
PRELIMINARY SPECIFICATION

APOLLO DOCKING SIMULATOR SYSTEM

SPEC.
NO.

DESCRIPTION AND REQUIREMENTS

800

Computer Input Signal Amplifier Power Supply

Input	115 volts, 400 cps
Output	+300 and -300 volts at 300 ma
Stability	0.003% at 115 to 125 volts
Hum and Noise	<u>+100 millivolts dc (0.03%)</u>

**NORTHROP SPACE LABORATORIES
PRELIMINARY SPECIFICATION**

APOLLO DOCKING SIMULATOR SYSTEM

SPEC.
NO.

DESCRIPTION AND REQUIREMENTS

900 ELECTRICAL POWER REQUIREMENTS

This preliminary specification establishes the electrical power requirements for testing the Docking Simulator System test program.

SPECIFICATIONS

Power	115 volts, 400 cps, 3-phase at 30 amperes
Distribution	Control console, 20 amperes Transmission Line Termination Rack, 10 amperes
Power	440 volts, 60 cps. 3-phase at 500 amperes
Distribution	At the Actuating Oil Condi- tioning Unit
Restrictions	No 60-cps power at control console
Power Wiring	To Electrical Code of National Board of Fire Under- writers
	12 gauge minimum power wiring 14 gauge minimum control wiring

NORTHROP SPACE LABORATORIES
PRELIMINARY SPECIFICATION

APOLLO DOCKING SIMULATOR SYSTEM

SPEC. NO.	DESCRIPTION AND REQUIREMENTS
1000	<p><u>SPARES</u></p> <p>This preliminary specification establishes the philosophy of spares provisioning for the Docking Simulator System. It shall be a design goal to achieve maximum reliability to reduce requirements for spares. After further analysis indicates the need for spares, long-lead items will be identified for procurement within the prescribed time.</p> <p>Present analysis indicates that the following items may be required as spares.</p> <ul style="list-style-type: none">1 complete hydraulic servo controller plug in unit (common to all systems)1 servo valve (common to all systems)2 amplifiers; transmission line driver amplifier and transmission line receiver amplifier

**NORTHROP SPACE LABORATORIES
PRELIMINARY SPECIFICATION**

APOLLO DOCKING SIMULATOR SYSTEM

SPEC. NO.	DESCRIPTION AND REQUIREMENTS						
1200	<p><u>SHIPPING</u></p> <p>This preliminary specification established shipping requirements for the Docking Simulator System and ancillary equipment to NASA/MSC. All components have been designed for easy disassembly and handling and reassembly.</p> <p style="text-align: center;">SPECIFICATIONS</p> <table style="width: 100%; border: none;"> <tr> <td style="width: 50%; vertical-align: top;"> Docking Simulator System and Basic Mounting Structure </td> <td style="width: 50%; vertical-align: top;"> Dimensions 9 x 14 x 10 feet Weight 10 tons Suitable for standard truck or railroad flatcar </td> </tr> <tr> <td style="vertical-align: top;"> Seismic mass </td> <td style="vertical-align: top;"> Local procurement in Houston, Texas </td> </tr> <tr> <td style="vertical-align: top;"> Chamber Penetration Seal Actuator Oil Conditioning Unit Vacuum System Control Console Transmission Line Transmission Line Termination Rack </td> <td style="vertical-align: top;"> Suitable for conventional truck or railroad shipment </td> </tr> </table>	Docking Simulator System and Basic Mounting Structure	Dimensions 9 x 14 x 10 feet Weight 10 tons Suitable for standard truck or railroad flatcar	Seismic mass	Local procurement in Houston, Texas	Chamber Penetration Seal Actuator Oil Conditioning Unit Vacuum System Control Console Transmission Line Transmission Line Termination Rack	Suitable for conventional truck or railroad shipment
Docking Simulator System and Basic Mounting Structure	Dimensions 9 x 14 x 10 feet Weight 10 tons Suitable for standard truck or railroad flatcar						
Seismic mass	Local procurement in Houston, Texas						
Chamber Penetration Seal Actuator Oil Conditioning Unit Vacuum System Control Console Transmission Line Transmission Line Termination Rack	Suitable for conventional truck or railroad shipment						

**NORTHROP SPACE LABORATORIES
PRELIMINARY SPECIFICATION**

APOLLO DOCKING SIMULATOR SYSTEM

SPEC.
NO.

DESCRIPTION AND REQUIREMENTS

1300

OPERATIONS AND MAINTENANCE MANUAL

This preliminary specification establishes the requirement for an Operation and Maintenance Manual for the Docking Simulator System and ancillary equipment.

CONTENTS

Component identification	Drawing, specification or manufacturer's model number as applicable
Operation	All components
Installation	All components
Maintenance	All components
Adjustment	All components
Calibration	All components
Equipment layout	All components
Block diagrams	All components

SECTION 4.0

CONCLUSIONS

**SECTION 4.0
CONCLUSIONS**

As a result of the performance of this study and the conceptual development necessary for evolving the design, several conclusions have been reached. These include the following:

1. The study clearly indicated that the concept is feasible and that the resultant design is sound and practical to construct. All requested specifications were met or exceeded. The device can be easily installed and removed from the chamber. The testing can be safely conducted without damage to the chamber. Thermal and vacuum operation conditions have been included in the design concept. Chamber penetration through the port will not adversely affect chamber operation.
2. The proposed configuration can easily be converted to a more general purpose simulator because of the large motion and solar radiation area available, and due to the flexible performance capability.
3. The analytic approach to the servo loop closure indicates that the specified performance can be met or exceeded.
4. A unique approach in developing the rigid body equations resulted in a computer program which requires the minimum number of analog computer components to solve the equations of motion; however, MSC must order more analog computer components than presently planned to accommodate inclusion of the modal response.

NORTHROP SPACE LABORATORIES

of the vehicles and the reference of vehicle motion with respect to fixed space and the inclusion of differential gravitation effects.

5. The accuracy of the docking test will not be adversely affected by the resonant characteristics of the simulator.
6. Chamber B can be modified structurally to allow its use for the tests.
7. Structural dynamics analysis performed by digital computer confirmed that the simulator structural stiffness is satisfactory, and therefore, servo compensation will not be required.
8. The transmission line problem lends itself to conventional solutions.
9. Oil selection has been made and will meet all requirements.
10. Ancillary equipment requirements can be satisfied by standard equipment or by current engineering state of the art.

SECTION 5.0

RECOMMENDATIONS

SECTION 5.0

RECOMMENDATIONS

Recommendations to the Manned Spacecraft Center are provided here to facilitate the fabrication and assembly of the docking simulator system and to enhance complete achievement of all program objectives.

1. Provide for remote release of the probe latches following a test run so that a man is not required to enter the chamber.
2. The resonant frequencies of Chamber B should be increased by methods such as employment of cross bracing of the legs or other stiffening of the structure.
3. Conduct impedance vibration tests on Chamber B to substantiate the dynamic analysis.
4. Lease the transmission line system from Southwestern Bell Telephone. This would very possibly result in a lower total cost for the program, and should be investigated locally.
5. In order to insure against avoidable schedule slippages, the four tests recommended in Northrop's unsolicited proposal should be undertaken immediately.
6. Consider at this time other NASA programs and applications for the subject simulator (which can be modified by minor design changes) to produce a research and development test tool rather than a special purpose simulator.
7. Pursue the possibility of powering the analog computer with 400 cps A.C. rather than 60 cps A.C. to minimize simulator noise problems.

NORTHROP SPACE LABORATORIES

7. Review last year's RFI and EMI tests of the transmission line tunnel and possibly re-run tests at this time to determine current conditions and all interface requirements if line leasing is not utilized.
8. Provide the following configuration data at the earliest possible date:
 - a. LEM and C/SM elastic mode and fuel slosh data.
 - b. Product of inertia data.
 - c. Parameters for earth-orbit flight condition.
9. Procure additional amplifiers, multipliers, resolvers, and potentiometers for the analog computer to satisfy the programming of the required equations.
10. Include requirements for preparation of a comprehensive operations and maintenance manual which can be effectively utilized by operating personnel.
11. Include provision for the continuation of the analog computer program optimization upon availability of all pertinent elastic mode, fuel slosh, and attitude control data.

SECTION 6.0

APPENDICES

APPENDIX A

ELASTIC STRUCTURAL DYNAMICS DEVELOPMENT

The approach used in this preliminary dynamics analysis was to form a mathematical model of the system under consideration, set up the dynamic equations of motion for the model, and to determine the resonant frequencies from these equations. These equations, with the addition of damping terms, are applicable in the more advanced stages of design for determining the entire frequency response of the structure. In forming the mathematical model, the principal masses of interest are considered as rigid bodies acted upon by linear springs. The simulator frame in all cases is considered to be infinitely rigid.

The equations of motion are derived by determining the kinetic energy, T , of the system, the potential energy, V , and writing the Lagrangian,

$$L = T - V, \quad (1)$$

The equations of motion are then obtained by the familiar relationship,

$$\frac{d}{dt} \left(\frac{\partial L}{\partial \dot{q}} \right) - \frac{\partial L}{\partial q} = 0, \quad (2)$$

where q denotes any one of the generalized coordinates of the system, and \dot{q} denotes the derivative of the coordinate in respect to time.

From these equations, a mass matrix, M , and a spring matrix, K , are formed from which the resonant frequencies are obtained by the following equation:

$$\left[K \right]^{-1} \left[M \right] \left\{ X \right\} = \frac{1}{\omega^2} \left\{ X \right\} \quad (3)$$

After substituting the proper mass and spring constant values in the matrix equation, a computer is used to solve the equation for the resonant frequencies, ω .

PROBE STRUCTURE, VERTICAL AND PITCH VIBRATION

Figure A-1 illustrates the mathematical model of probe structure for vertical and pitch motion.

Kinetic Energy

$$T = \frac{1}{2} \left\{ M_1 \dot{X}_1^2 + M_2 \dot{X}_2^2 + M_3 \dot{X}_3^2 + I_1 \dot{\theta}_1^2 + I_2 \dot{\theta}_2^2 + I_3 \dot{\theta}_3^2 \right\} \quad (4)$$

Potential Energy

$$V = \frac{1}{2} \left\{ K_1 d_1^2 (\theta_2 - \theta_1)^2 + K_2 (X_3 + b_2 \theta_3 - X_2 + a_2 \theta_2)^2 + K_{T2} (\theta_3 - \theta_2)^2 + K_{T3} \theta_3^2 \right\} \quad (5)$$

Since four coordinates, in addition to the forcing function coordinate, X_0 , are sufficient to completely describe motion in this system, we eliminate X_1 and X_3 from the energy equations by the following relationships:

$$X_1 = X_2 + b_1 \theta_2 + a_1 \theta_1 \quad (6)$$

$$X_3 = X_0 + (a_3 - d_3) \theta_3 \quad (7)$$

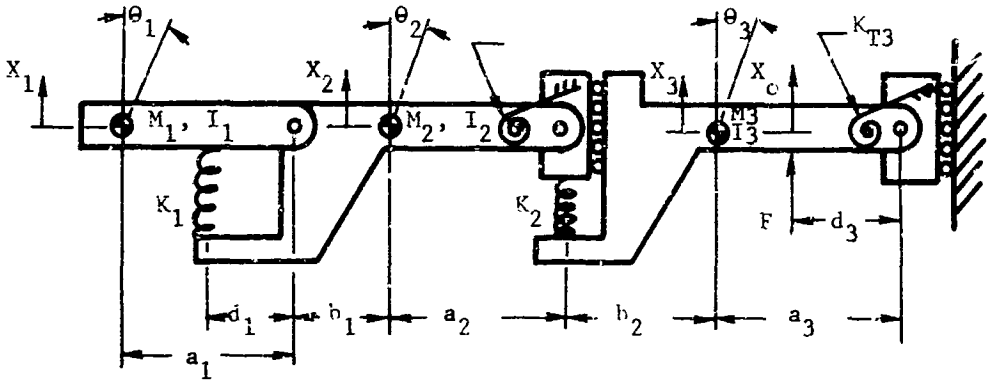
Rewriting the equations for kinetic and potential energy

$$T = \frac{1}{2} \left\{ M_1 (\dot{X}_2 + b_1 \dot{\theta}_2 + a_1 \dot{\theta}_1)^2 + M_2 \dot{X}_2^2 + M_3 \left[\dot{X}_0 + (a_3 - d_3) \dot{\theta}_3 \right]^2 + I_1 \dot{\theta}_1^2 + I_2 \dot{\theta}_2^2 + I_3 \dot{\theta}_3^2 \right\} \quad (8)$$

$$V = \frac{1}{2} \left\{ K_1 d_1^2 (\theta_1 - \theta_2)^2 + K_2 \left[X_2 - X_0 - (a_3 - d_3 + b_2) \theta_3 - a_2 \theta_2 \right]^2 + K_{T2} (\theta_2 - \theta_3)^2 + K_{T3} \theta_3^2 \right\} \quad (9)$$

The Lagrangian then becomes

$$L = \frac{1}{2} \left\{ M_1 (\dot{X}_2 + b_1 \dot{\theta}_2 + a_1 \dot{\theta}_1)^2 + M_2 \dot{X}_2^2 + M_3 \left[\dot{X}_0 + (a_3 - d_3) \dot{\theta}_3 \right]^2 + I_1 \dot{\theta}_1^2 + I_2 \dot{\theta}_2^2 + I_3 \dot{\theta}_3^2 - K_1 d_1^2 (\theta_1 - \theta_2)^2 - K_2 \left[X_2 - X_0 - (a_3 - d_3 + b_2) \theta_3 - a_2 \theta_2 \right]^2 - K_{T2} (\theta_3 - \theta_2)^2 - K_{T3} \theta_3^2 \right\} \quad (10)$$



M_1 = Drogue and drogue support mass

M_2 = Lateral carriage mass

M_3 = Vertical carriage mass

I_1 = Drogue and drogue support mass moment of inertia about its c.g.

I_2 = Lateral carriage mass moment of inertia about its c.g.

I_3 = Vertical carriage mass moment of inertia about its c.g.

K_1 = Lateral spring constant of force balance

K_2 = Vertical spring constant of lateral carriage support bars

K_{T2} = Torsional spring constant of lateral carriage support bars

K_{T3} = Torsional spring constant of vertical carriage support bars

F = Applied vertical actuator force

FIGURE A-1 MATHEMATICAL MODEL OF PROBE STRUCTURE

NORTHROP SPACE LABORATORIES

The equations of motion can now be written using the relationship given in equation (2):

$$M_2 \ddot{X}_2 + M_1 (\ddot{X}_2 + b_1 \ddot{\theta}_2 + a_1 \ddot{\theta}_1) + K_2 [X_2 - X_0 - (a_3 - d_3 + b_2) \theta_3 - a_2 \theta_2] = 0 \quad (11)$$

$$I_1 \ddot{\theta}_1 + M_1 a_1 (\ddot{X}_2 + b_1 \ddot{\theta}_2 + a_1 \ddot{\theta}_1) + K_1 d_1^2 (\theta_1 - \theta_2) = 0 \quad (12)$$

$$I_2 \ddot{\theta}_2 + M_1 b_1 (\ddot{X}_2 + b_1 \ddot{\theta}_2 + a_1 \ddot{\theta}_1) - K_1 d_1^2 (\theta_1 - \theta_2) - K_2 a_2 [X_2 - X_0 - (a_3 - d_3 + b_2) \theta_3 - a_2 \theta_2] + K_{T2} (\theta_2 - \theta_3) = 0 \quad (13)$$

$$I_3 \ddot{\theta}_3 + M_3 (a_3 - d_3) [\ddot{X}_2 + (a_3 - d_3) \ddot{\theta}_1] - K_2 (a_3 - d_3 + b_2) [X_2 - X_0 - (a_3 - d_3 + b_2) \theta_3 - a_2 \theta_2] - K_{T2} (\theta_2 - \theta_3) + K_{T3} \theta_3 = 0 \quad (14)$$

These equations can be written in matrix form

$$[M] \{\ddot{X}\} + [K] \{X\} = \{F\}$$

where $[M]$ is a square matrix of the coefficients for \ddot{X}_2 , $\ddot{\theta}_1$, $\ddot{\theta}_2$ and $\ddot{\theta}_3$.

$[K]$ is a square matrix of the coefficients for X_2 , θ_1 , θ_2 and θ_3 .

$\{\ddot{X}\}$ is a column matrix $\{\ddot{X}_2, \ddot{\theta}_1, \ddot{\theta}_2, \ddot{\theta}_3\}$

$\{X\}$ is a column matrix $\{X_2, \theta_1, \theta_2, \theta_3\}$

$\{F\}$ is a column matrix consisting of all terms containing X_0 and \ddot{X}_0 including the coefficients transposed to the right side of the equation. (Forcing function matrix)

$$[M] = \begin{bmatrix} M_1 + M_2 & M_1 a_1 & M_1 b_1 & 0 \\ M_1 a_1 & I_1 + M_1 a_1^2 & M_1 a_1 b_1 & 0 \\ M_1 b_1 & M_1 a_1 b_1 & I_2 + M_1 b_1^2 & 0 \\ 0 & 0 & 0 & I_3 + M_3 (a_3 - d_3)^2 \end{bmatrix}$$

NORTHROP SPACE LABORATORIES

$$[M] = \begin{bmatrix} M_1 + M_2 & M_1 a_1 & M_1 b_1 & 0 \\ M_1 a_1 & I_1 + M_1 a_1^2 & M_1 a_1 b_1 & 0 \\ M_1 b_1 & M_1 a_1 b_1 & I_2 + M_1 b_1^2 & 0 \\ 0 & 0 & 0 & I_3 + M_3 (a_3 - d_3)^2 \end{bmatrix}$$

$$[K] = \begin{bmatrix} K_2 & 0 & -K_2 a_2 & -K_2 (a_3 - d_3 + b_2) \\ 0 & K_1 d_1^2 & -K_1 d_1^2 & 0 \\ -K_2 a_2 & -K_1 d_1^2 & K_1 d_1^2 + K_2 a_2^2 + K_{T2} & K_2 a_2 (a_3 - d_3 + b_2) \\ K_2 (a_3 - d_3 + b_2) & 0 & K_2 a_2 (a_3 - d_3 + b_2) & -K_{T2} \\ & & & K_2 (a_3 - d_3 + b_2)^2 \\ & & & + K_{T2} + K_{T3} \end{bmatrix}$$

$$F = \begin{cases} K_2 X_0 \\ 0 \\ -K_2 a_2 X_0 \\ -M_3 (a_3 - d_3) \ddot{X}_0 - K_2 (a_3 - d_3 + b_2) X_0 \end{cases}$$

For computation of resonant frequencies only the M and K matrices are required. The physical constants are simply substituted in these matrices and a standard Northrop Computer Program is used to solve equation (3) for the resonant frequencies and mode shapes. Computer sheets showing the results for this problem are shown in Figure A-2.

APOLLO DOCKING SIMULATOR /PRCBE NATURAL FREQUENCIES /VERTICAL

SPRING MATRIX (K)

1	0.63699999E 07	0.	0.23599999E 08	-0.22300000E 08
2	0.	0.12780000E 09	-0.12730000E 09	0.
3	0.23599999E 08	-0.12780000E 09	0.2749999E 10	-0.31426000E 10
4	-0.22300000E 08	0.	-0.31426000E 10	0.76799999E 10

INPLT MASS MATRIX (M)

RCW	CCL	DATA	CCL	DATA	CCL	DATA	CCL	DATA
1	1	0.22759999E 04	2	0.10089999E 05	3	-0.36300000E C4	4	C.
2	1	0.10089999E 05	2	0.33300000E 06	3	-0.78705999E 05	4	0.
3	1	-0.36300000E 04	2	-0.78705999E 05	3	0.38699999E 06	4	0.
4	1	0.	2	0.	3	0.	4	C.32443000E 06

MATRIX OF EIGENVECTORS

1	0.52675896E 00	0.05995999E 01	0.09999999E 01	0.09999999E 01
2	0.09995999E 01	-0.38495896E-01	-0.88226196E-02	0.68528900E-01
3	0.49752420E-01	-0.30016015E-01	0.14193306E-00	0.43958520E-00
4	0.22229027E-01	-0.10716818E-01	0.76469658E-01	-0.57752533E 00

MODE	EIGENVALUE	F(I)
1	0.27535824E-02	0.59619678E 02
2	0.33826107E-03	0.17007813E 03
3	0.20859517E-03	0.21661401E 03
4	0.35552272E-04	0.52439038E 03

FIGURE A-2 IBM PROGRAM RESONANT FREQUENCIES RESULTS

APPENDIX B

SERVO CONTROL SYSTEM DEVELOPMENT

1.1 SERVO SYSTEM BLOCK DIAGRAM

The generalized block diagram for the Z-axis control system is shown in Figure B-1, which shows all three feedback control loops. For ease in analysis, the blocks have been assigned numbers from 1 through 7.

The analysis starts by deriving the mathematical expression for the hydromechanical system¹⁵, blocks 3 and 4.

The following parameters all referred to the actuator piston, are involved.

- q = total flow rate from the valve into the actuator ports - in^3/sec .
- q_o = flow rate which results in actuator motion - in^3/sec .
- q_c = flow rate which results in compression of fluid - in^3/sec .
- q_l = flow rate which leaks past piston - in^3/sec .
- B = damping of actuator and load.
- L = coefficient of piston leakage - $\frac{\text{in}^3/\text{sec}}{\text{lb}/\text{in}^2}$
- C_p = flow coefficient of valve with respect to pressure - $\frac{\text{in}^3/\text{sec}}{\text{lb}/\text{in}^2}$
- C_e = flow coefficient of valve with respect to coil voltage - $\frac{\text{in}^3/\text{sec}}{\text{volt}}$
- $\dot{\delta}$ = relative velocity between actuator and piston - inches/sec.
- A = effective piston area - in^2 .

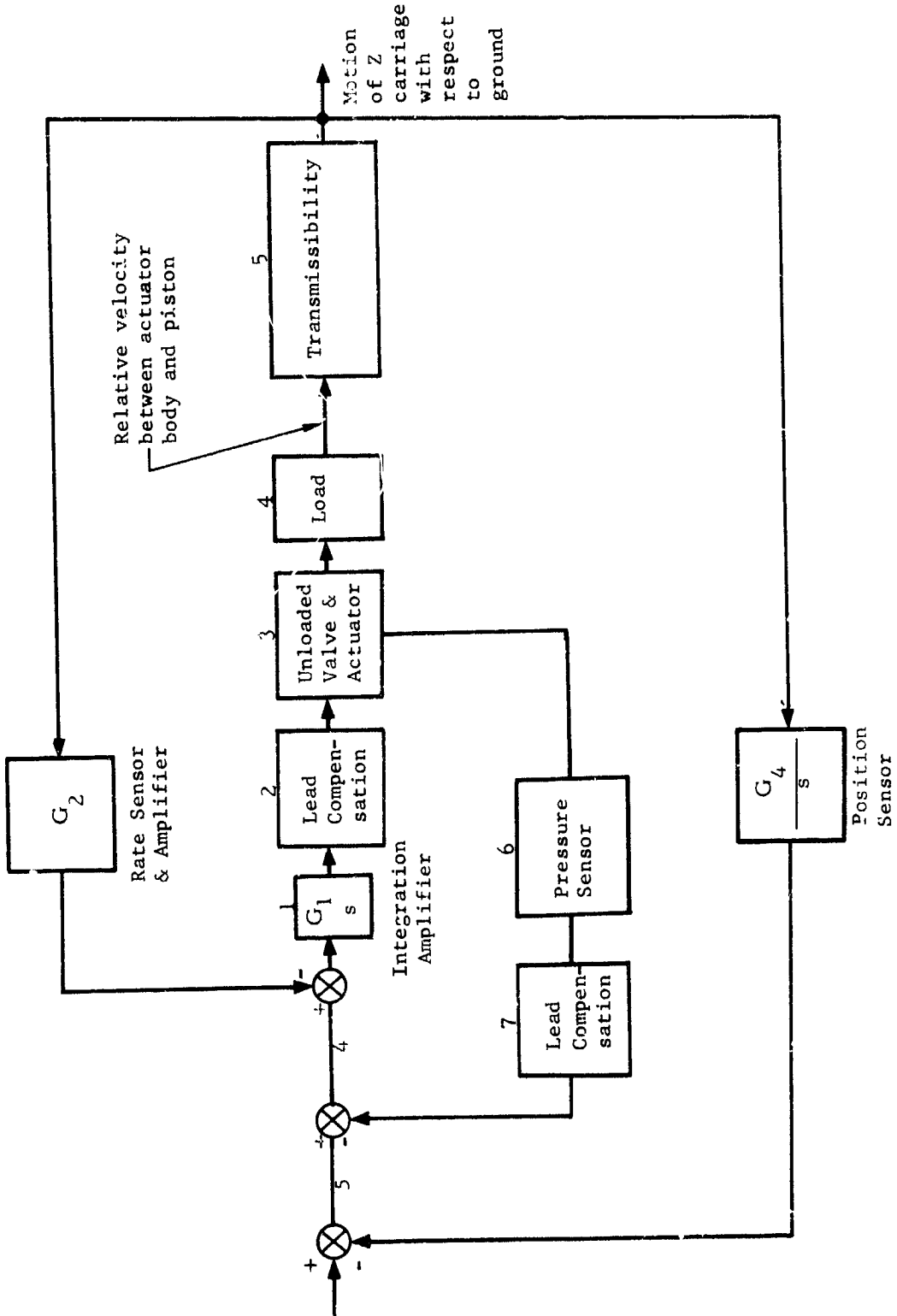


FIGURE B-1 GENERALIZED BLOCK DIAGRAM FOR THE Z- AXIS SERVO

NORTHROP SPACE LABORATORIES

P_L = load induced pressure lb/in²

M = mass of load in/sec²

τ_v = valve time constant - sec.

K_o = hydraulic spring rate lb/in

F = load induced force on piston - lb

e_c = valve coil voltage - volts

$\mathcal{L}\{\}$ = Laplace transform

S = Laplace operator

The basic equation involved may be expressed as:

$$q = q_o + q_c + q_1 \quad (1)$$

Further:

$$q = \frac{C_e e_c}{\tau_v s + 1} - C_p P_L \quad (2)$$

$$q_o = A s \delta = \mathcal{L}\left\{A \frac{d\delta}{dt}\right\} \quad (3)$$

$$q_c = \frac{A s P_L A}{K_o} = \mathcal{L}\left\{\frac{A^2}{K_o} \frac{d P_L}{dt}\right\} \quad (4)$$

$$q_1 = L P_L \quad (5)$$

Combining these relationships:

$$\frac{C_e e_c}{\tau_v s + 1} = A \delta + \left[\frac{A^2}{K_o} s + (C_p + L) \right] P_L \quad (6)$$

The load dynamics may be expressed as: $Y_L = \frac{F}{\delta} = \frac{P_L A}{\delta} \quad (7)$

NORTHROP SPACE LABORATORIES

Equations 6 and 7 may be combined to yield:

$$\frac{C_e e_{\epsilon}}{\tau_v s + 1} = A \dot{\delta} + \frac{A^2}{K_o} s + (C_p + L) \frac{\dot{\delta} Y_L}{A} \quad (8)$$

Rearranging the above will give:

$$\frac{\dot{\delta}}{e_{\epsilon}} = \frac{C_e / A}{\left(\tau_v s + 1 \right) \left[1 + \left[\frac{s}{K_o} + \frac{(C_p + L)}{A^2} \right] Y_L \right]} \quad (9)$$

Equation 9 may be represented by the following block diagram, Figure B-2. The problem now becomes one of the admittance, Y_L , of the load in Block 4. As stated in paragraph 3.3, the Z carriage may be represented by a single spring mass system. The spring K will be that of the piston rod. A mechanical model for the Z carriage is shown in Figure B-3.

From the model in Figure B-3, the admittance may be derived

$$Y_L = \frac{F}{\dot{\delta}} = \frac{SMK + BK}{s^2 M + Bs + K} \quad (10)$$

The transmissibility of Block 5 may also be found:

$$\frac{V_o}{\dot{\delta}} = \frac{K}{s^2 M + Bs + K} \quad (11)$$

The generalized block diagram of Figure B-1 may now be redrawn to show the specific form of the transfer functions involved, Figure B-4.

With the aid of block diagram algebra, the point at which the force is obtained for the pressure feedback may be moved to the output velocity (V_o) by adding in series a block which contains the transfer function:

$$Y_L \left(\frac{s^2 M + Bs + K}{K} \right) \quad (12)$$

The generalized block diagram of Figure B-4 may now be redrawn and combined with the use of equations 10, 11, and 12. See Figure B-5.

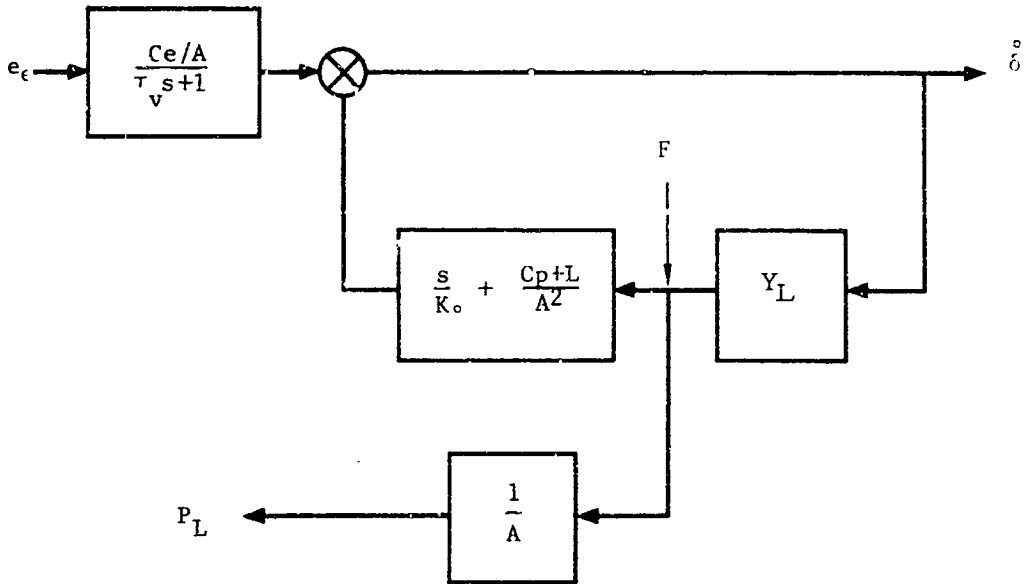


FIGURE B-2 DIAGRAM OF EQUATION 9

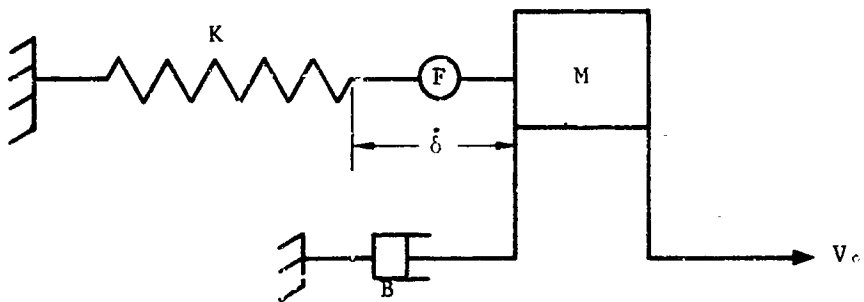


FIGURE B-3 MECHANICAL MODEL FOR THE Z CARRIAGE

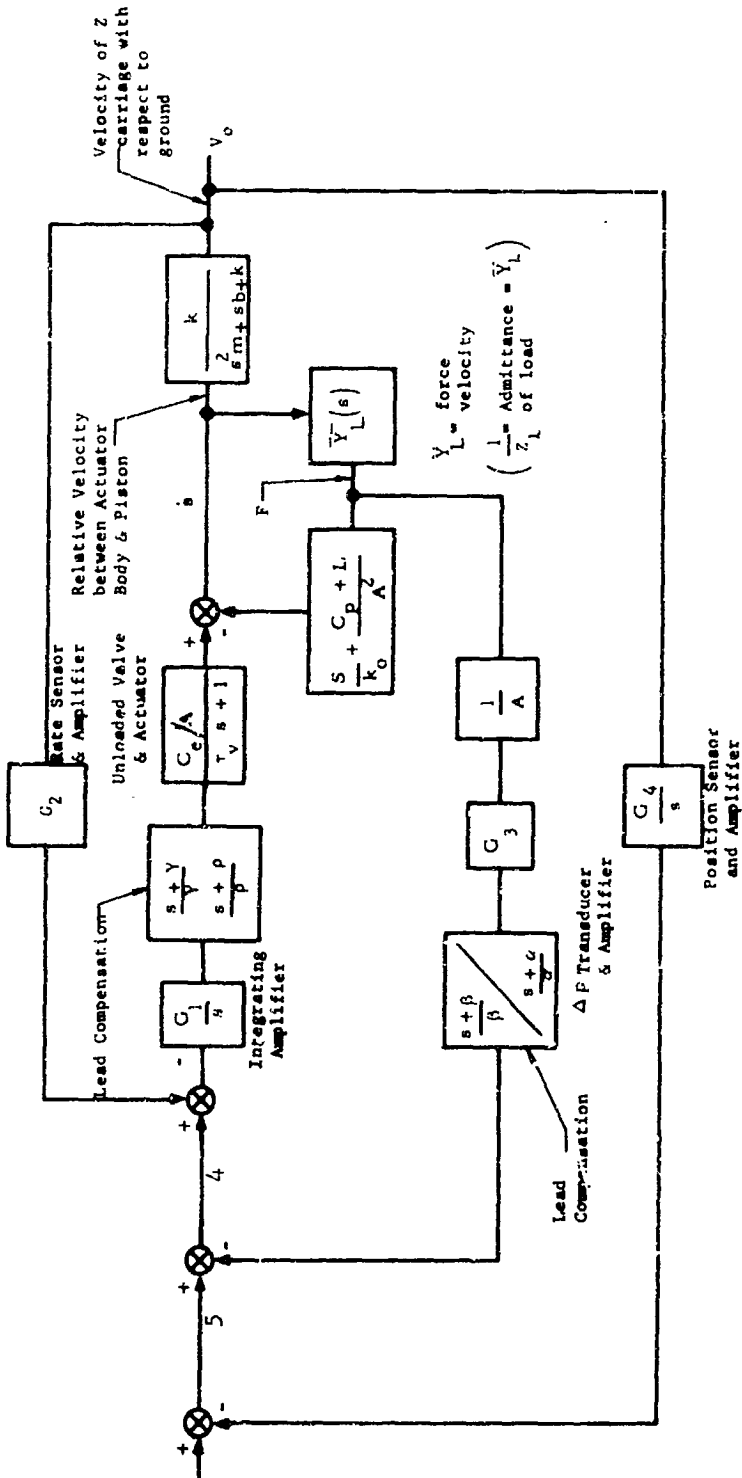


FIGURE B-4 GENERAL BLOCK DIAGRAM

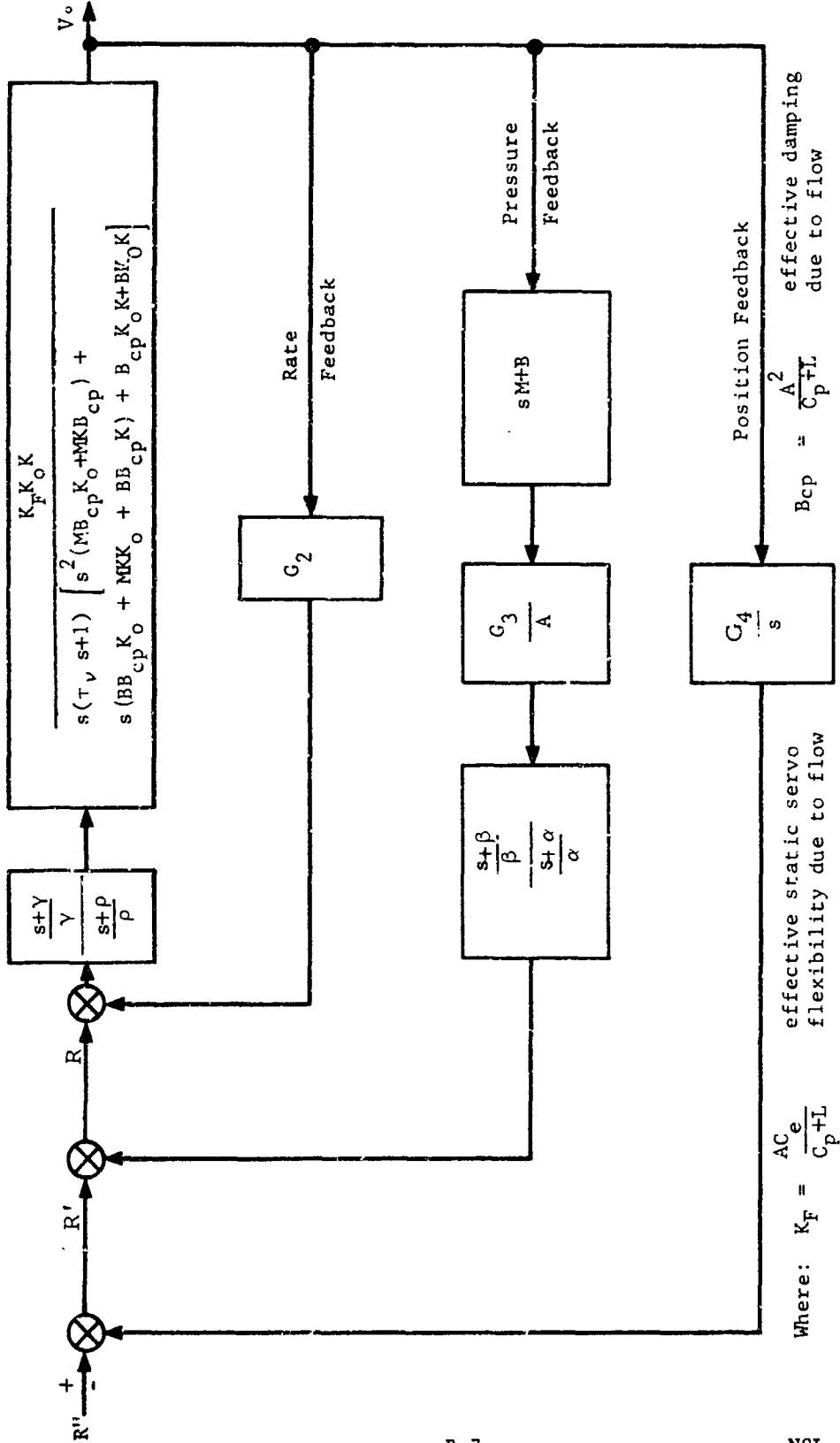


FIGURE B-5 GENERALIZED COMBINED BLOCK DIAGRAM

NORTHROP SPACE LABORATORIES

The problem now becomes one of assigning reasonably accurate values to all the system parameters. The most elusive are c_p and c_e , which are non-linear except over a small operating range.

Figure B-6 and B-7 show typical operating characteristics of flow control valves¹⁶. An examination of these characteristics reveals the inherent non-linear behavior of a hydraulic servo valve. In selecting valve and actuator sizes for the mechanization of the Z-axis servo, a performance envelope has been specified which limits P_L , the load induced pressure, so that it does not exceed $\frac{1}{2} p_s$, where p_s is the system operating pressure. Further, the valve has been selected such that the maximum required flow rate is available with only $\frac{1}{2} P_s$ across the valve. These linearizing restrictions on the operating range required of the valve are shown on Figure B-6 and B-7. The values of C_e and C_p are defined as follows:

$$C_e = \left(\frac{\partial Q}{\partial e} \right)_{P_L = \text{constant}} \quad (13)$$

and

$$C_p = \left(\frac{\partial Q}{\partial P_L} \right)_{e = \text{constant}} \quad (14)$$

where C_e is the valve flow coefficient with respect to input voltage

C_p is the valve flow coefficient with respect to load pressure

Q is the flow rate through the cylinder parts (in³/sec)

P_L is the load induced pressure

e is the valve coil voltage

For the analysis then, values of these valve coefficients are measured at the operating points indicated. The rated valve flow requirements, specified in Table 3-4, are 64 in³/sec at $P_L = \frac{1}{2} P_s$ for each Z axis servo.

- P_L = load induced pressure (psi)
- P_s = supply pressure (psi)
- e = valve coil voltage
- Q = flow rate (in³/sec.)

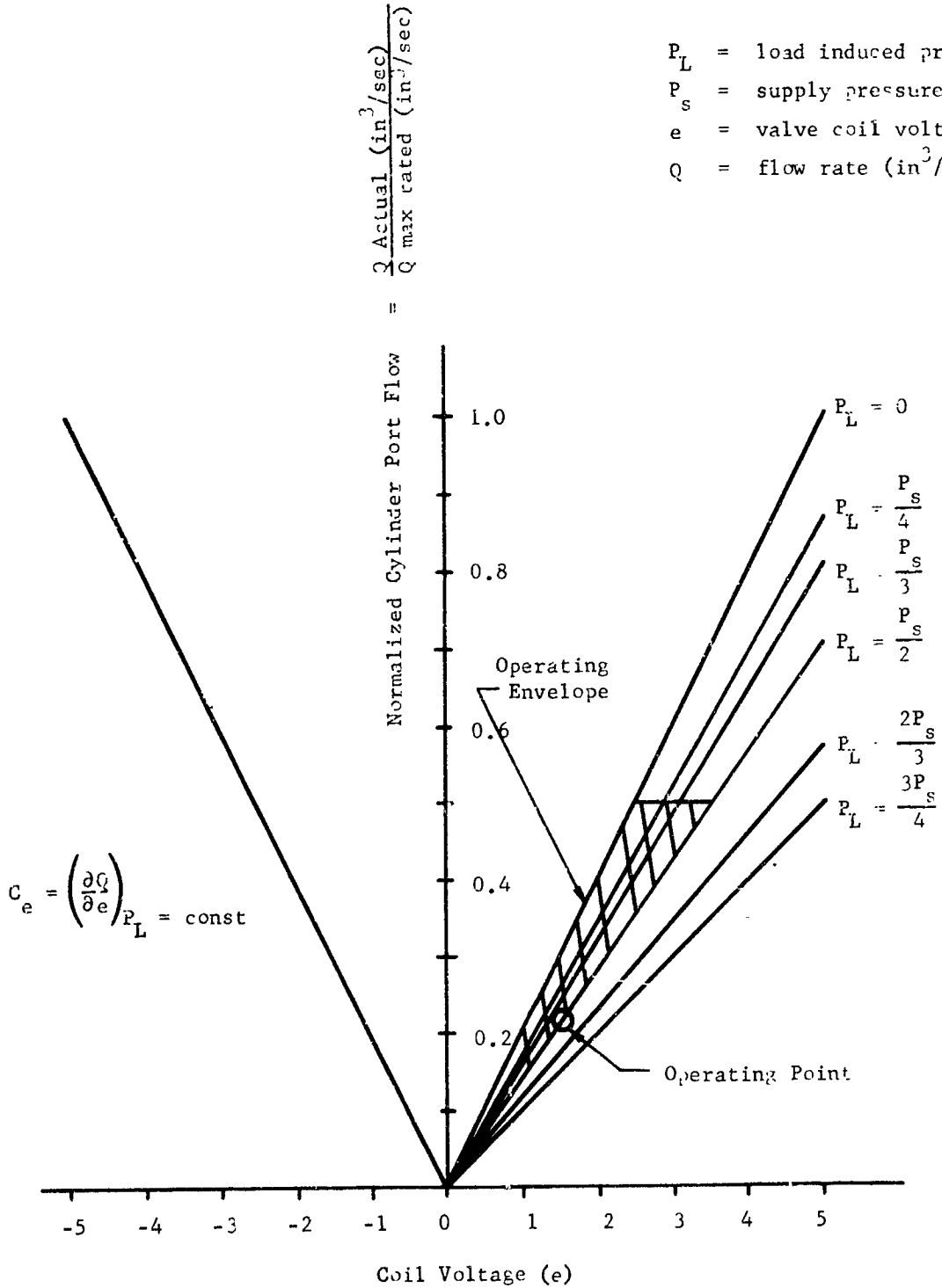


FIGURE B-6 TYPICAL CHARACTERISTICS OF FLOW CONTROL VALVES

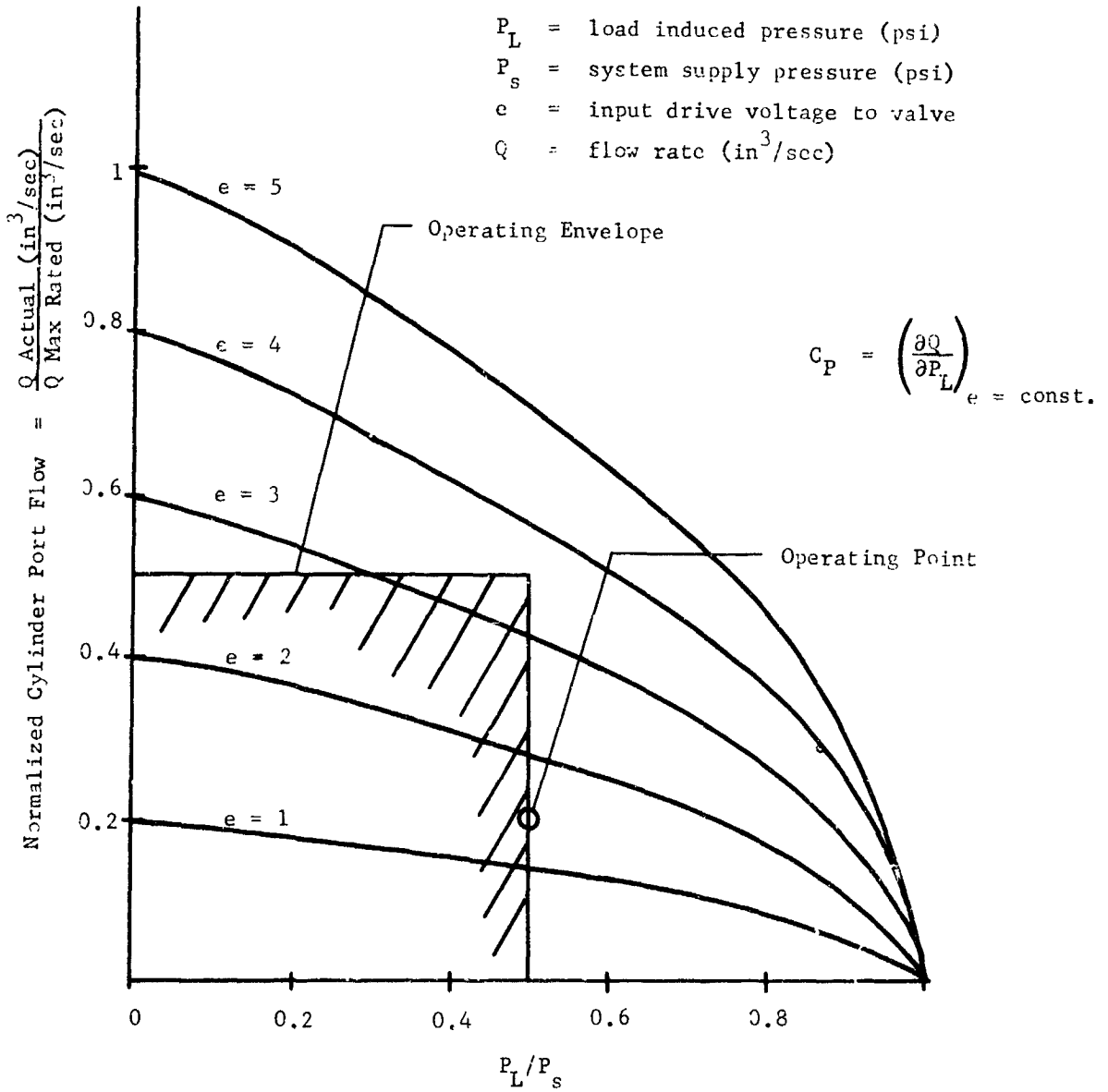


FIGURE B-7 TYPICAL CHARACTERISTICS OF FLOW CONTROL VALVES

At these requirements,

$$C_a = 12.8 \text{ in}^3/\text{sec/volt}$$

$$C_p = 4.98 \times 10^{-3} \text{ in}^3/\text{sec/psi}$$

The remaining Z servo parameters, some of which have been determined in the body of the report, are shown below. It should be noted that some of the parameters are affected by the fact that the Z-axis servo is mechanized with dual actuators.

$$M = 5.21 \frac{\text{lb-sec}^2}{\text{in}} \quad (\frac{1}{2} \text{ Z carriage mass})$$

$$K = 5.3 \times 10^6 \text{ lbs/in (2" steel rod 27" total length)}$$

$$B = 20.8 \text{ lb/in/sec. (for assumed damping ratio of 0.002)}$$

$$A = 2.68 \text{ in}^2 \quad (\text{volumetric displacement})$$

$$K_o = 7.95 \times 10^4 \text{ lb/in (hydraulic spring rate)}$$

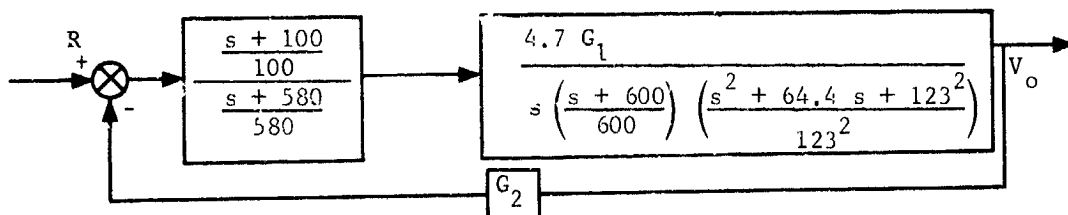
$$\tau_v = 0.0016 \text{ sec.}$$

$$L = 1.04 \times 10^{-3} \text{ in}^3/\text{sec/psi computed for a piston with 0.0017 in clearance and hydraulic fluid (skydrol) at 100°F.}$$

The block diagram of figure B-5 may be redrawn with the above system parameters inserted, Figure B-8.

1.2 SERVO SYSTEM LOOP CLOSURE

The control system as shown in Figure B-8 is analyzed by the root-locus method¹⁷. The procedure will be to close each feedback loop one at a time until the entire system can be represented by a single transfer function. Rate loop closure is shown below.



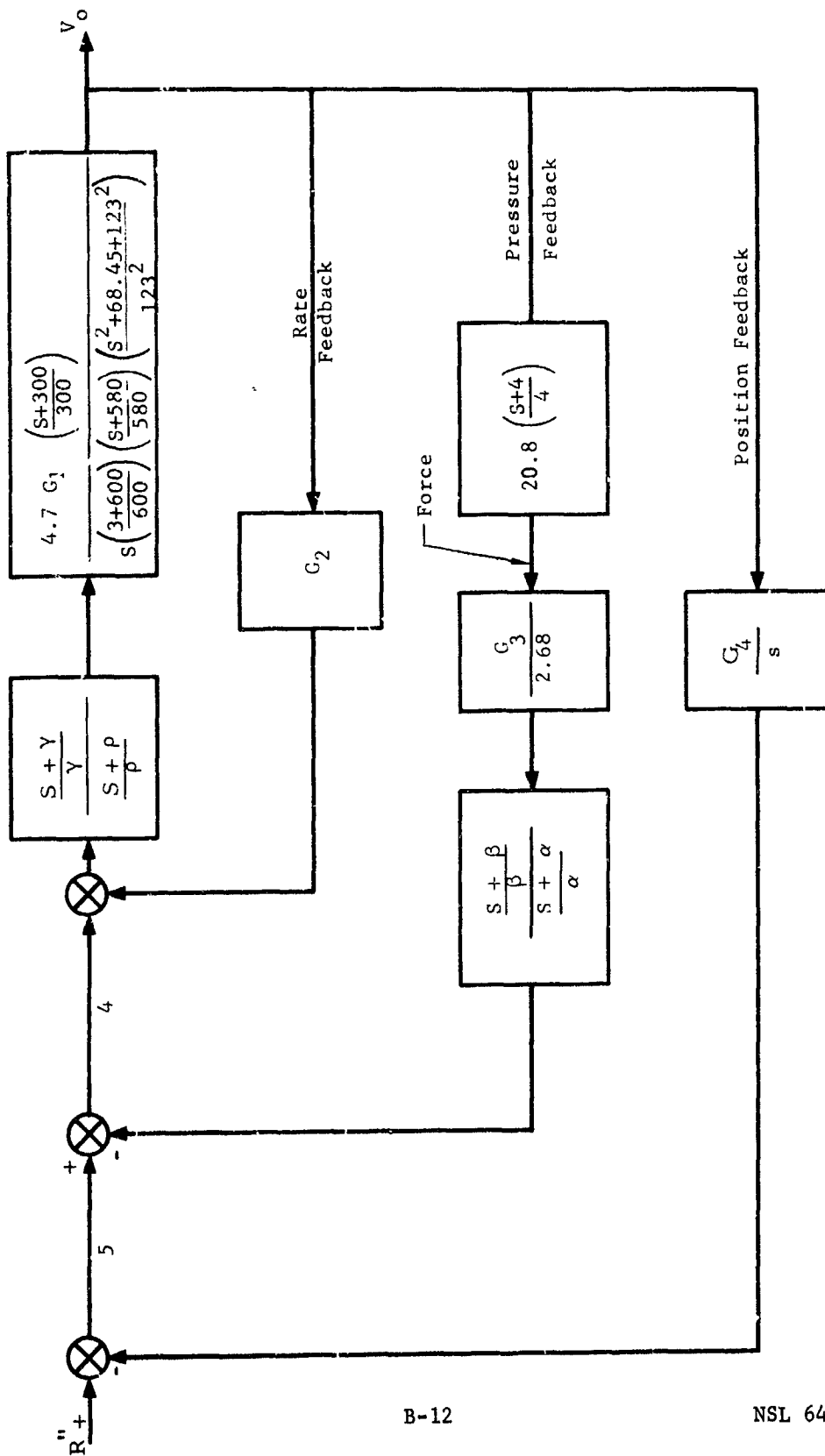


FIGURE B-8 BLOCK DIAGRAM WITH SYSTEM PARAMETER

NORTHROP SPACE LABORATORIES

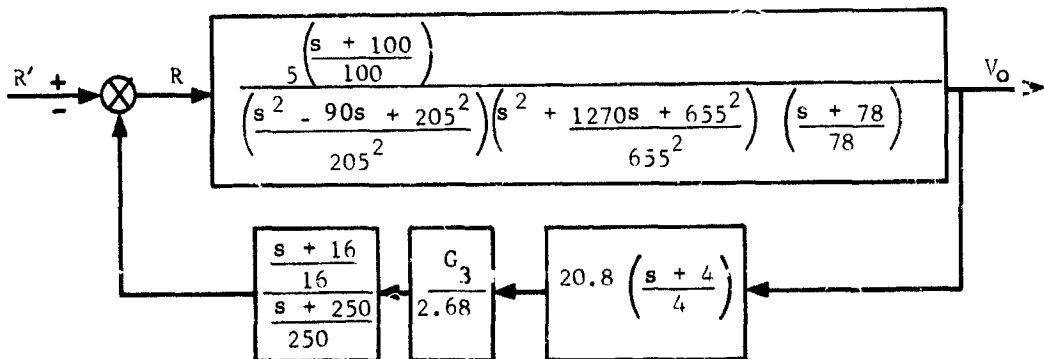
The lead shown in the first block of the open loop transfer function is picked to increase the natural frequency of the system. The close loop transfer function for the rate loop is:

$$\frac{V_o}{R} = \frac{4.7 G \left(\frac{s + 100}{100} \right)}{s \left(\frac{s + 600}{600} \right) \left(\frac{s + 580}{580} \right) \left(\frac{s^2 + 64.4 s + 123^2}{123^2} \right) + 4.7 G_1 G_2 \left(\frac{s + 100}{100} \right)} \quad (15)$$

A root-locus plot of V_o/R is shown in Figure B-9. The gain is picked such that the natural frequency of the dominant roots are raised to 200 radians/sec. Picking a gain of 0.2 volt/in.sec. for G_2 the value of G_1 becomes 287 volt/volt. The closed loop transfer function may now be written in factored form.

$$\frac{V_o}{R} = \frac{5 \left(\frac{s + 100}{100} \right)}{\left(\frac{s^2 - 90s + 205^2}{205^2} \right) \left(\frac{s^2 + 1270s + 655^2}{655^2} \right) \left(\frac{s + 78}{78} \right)} \quad (16)$$

To bring the locus back into the left-half s plane, a pressure feedback loop is closed. The forward loop transfer function is the closed loop transfer function of V_o/R .



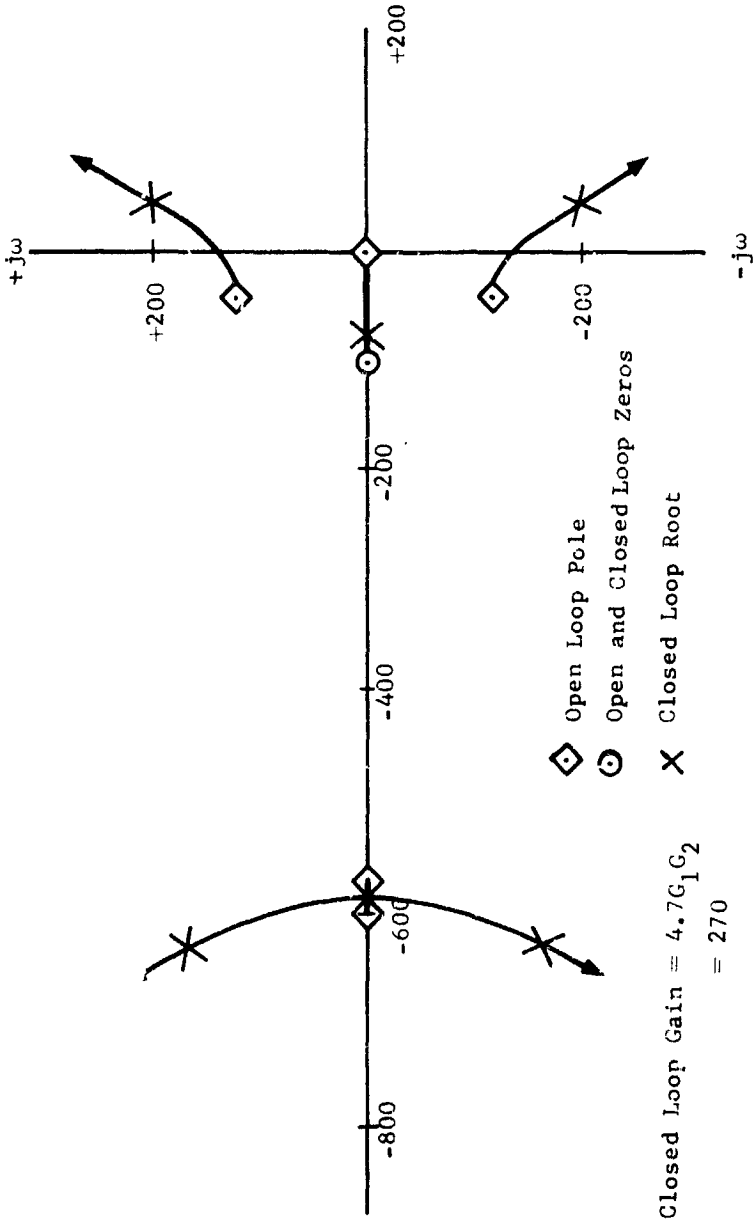


FIGURE B-9 RATE LOOP ROOT-LOCUS

NORTHROP SPACE LABORATORIES

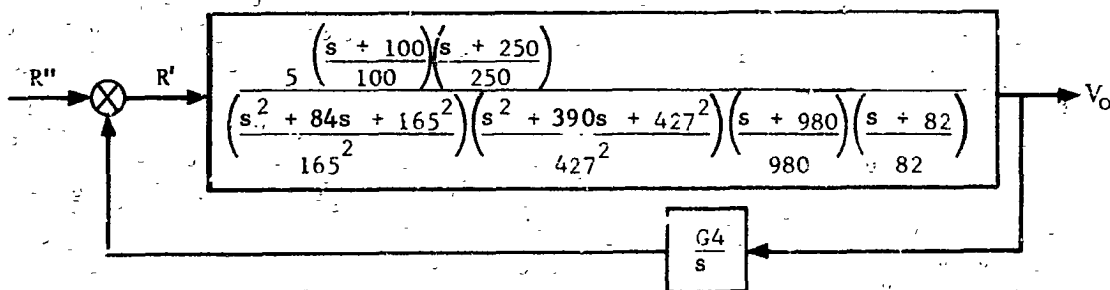
The lead compensation shown in the feedback loop is picked to draw the locus into the left-hand of the complex s plane. The closed loop transfer function for the pressure loop is:

$$\frac{V_o}{R'} = \frac{5 \left(\frac{s + 100}{100} \right) \left(\frac{s + 250}{250} \right)}{\left(\frac{s^2 - 90s + 205^2}{205^2} \right) \left(\frac{s^2 + 1270s + 655^2}{655^2} \right) \left(\frac{s + 78}{78} \right) \left(\frac{s + 250}{250} \right) + \frac{5 G_3 (20.8)}{2.68} \left(\frac{s + 16}{16} \right) \left(\frac{s + 4}{4} \right) \left(\frac{s + 100}{100} \right)} \quad (17)$$

A root-locus plot of V_o/R' is shown in Figure B-10. The gain is picked at 2.44×10^{-3} such that maximum damping may be realized. At this gain G_3 becomes 6.3×10^{-5} volts/psi. The factored form of V_o/R' may now be written

$$\frac{V_o}{R'} = \frac{5 \left(\frac{s + 100}{100} \right) \left(\frac{s + 250}{250} \right)}{\left(\frac{s^2 + 84s + 165^2}{165^2} \right) \left(\frac{s^2 + 390s + 427^2}{427^2} \right) \left(\frac{s + 980}{980} \right) \left(\frac{s + 82}{82} \right)} \quad (18)$$

To give complex stiffness to the system and a method of setting position, a position loop is closed. The open loop transfer function of V_o/R'' is the closed loop transfer function of V_o/R .



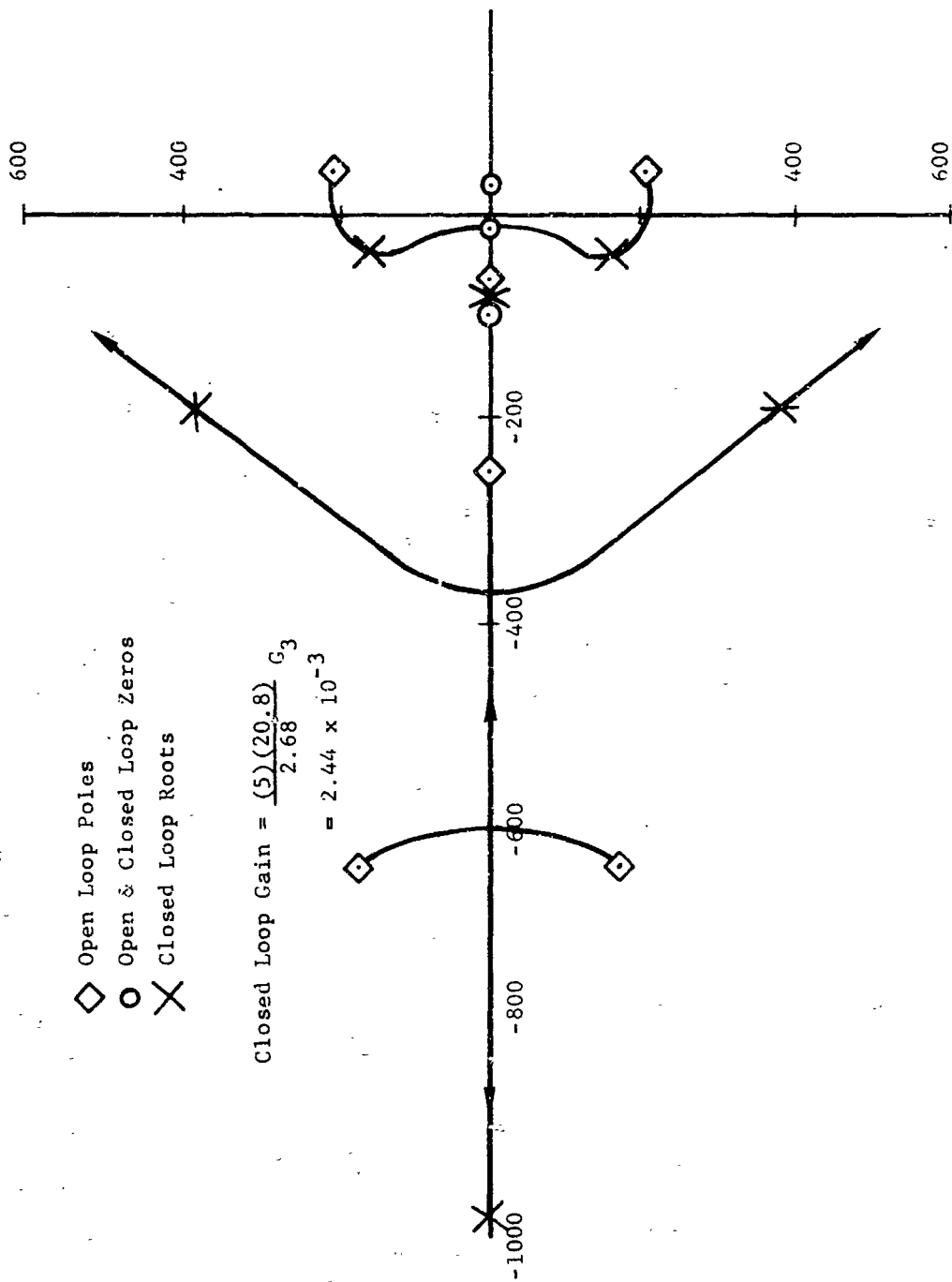


FIGURE B-10 PRESSURE LOOP
ROOT - LOCUS

NORTHROP SPACE LABORATORIES

The closed loop transfer function of V_o/R'' is

$$\frac{V_o}{R''} = \frac{5s \left(\frac{s+100}{100} \right) \left(\frac{s+250}{250} \right)}{\left(\frac{s^2 + 84s + 165^2}{165^2} \right) \left(s^2 + \frac{390s + 427^2}{427^2} \right) \left(\frac{s+980}{980} \right) \left(\frac{s+82}{82} \right) + 5 G_4} \quad (19)$$

$$\frac{\left(\frac{s+100}{100} \right) \left(\frac{s+250}{250} \right)}{\left(\frac{s+100}{100} \right) \left(\frac{s+250}{250} \right)}$$

The root-locus plot of V_o/R'' is shown in Figure B-11. A low gain of 17.5 is picked such that the complex dominant roots do not move far from their original position. At this gain G_4 becomes 3.5 volt/in.

The factored form of V_o/R'' is:

$$\frac{V_o}{R''} = \frac{0.27S \left(\frac{s+100}{100} \right) \left(\frac{s+250}{250} \right)}{\left(\frac{s^2 + 64s + 160^2}{160^2} \right) \left(\frac{s^2 + 420s + 440^2}{440^2} \right) \left(\frac{s+980}{980} \right) \left(\frac{s+18}{18} \right) \left(\frac{s+78}{78} \right)} \quad (20)$$

To keep the system, a velocity servo in which the second order complex poles dominate and yet has complex stiffness at the load, open loop compensation will be used to remove the unwanted zero at S and pole at $\left(\frac{s+18}{18} \right)$.

This compensation will be of the form $(18) \left(\frac{s+18}{s} \right)$

With this compensation the total system may be represented by a single transfer function:

$$\frac{V_o}{V_i} = \frac{5 \left(\frac{s+100}{100} \right) \left(\frac{s+250}{250} \right)}{\left(\frac{s^2 + 64s + 160^2}{160^2} \right) \left(\frac{s^2 + 420s + 440^2}{440^2} \right) \left(\frac{s+980}{980} \right) \left(\frac{s+78}{78} \right)} \quad (21)$$

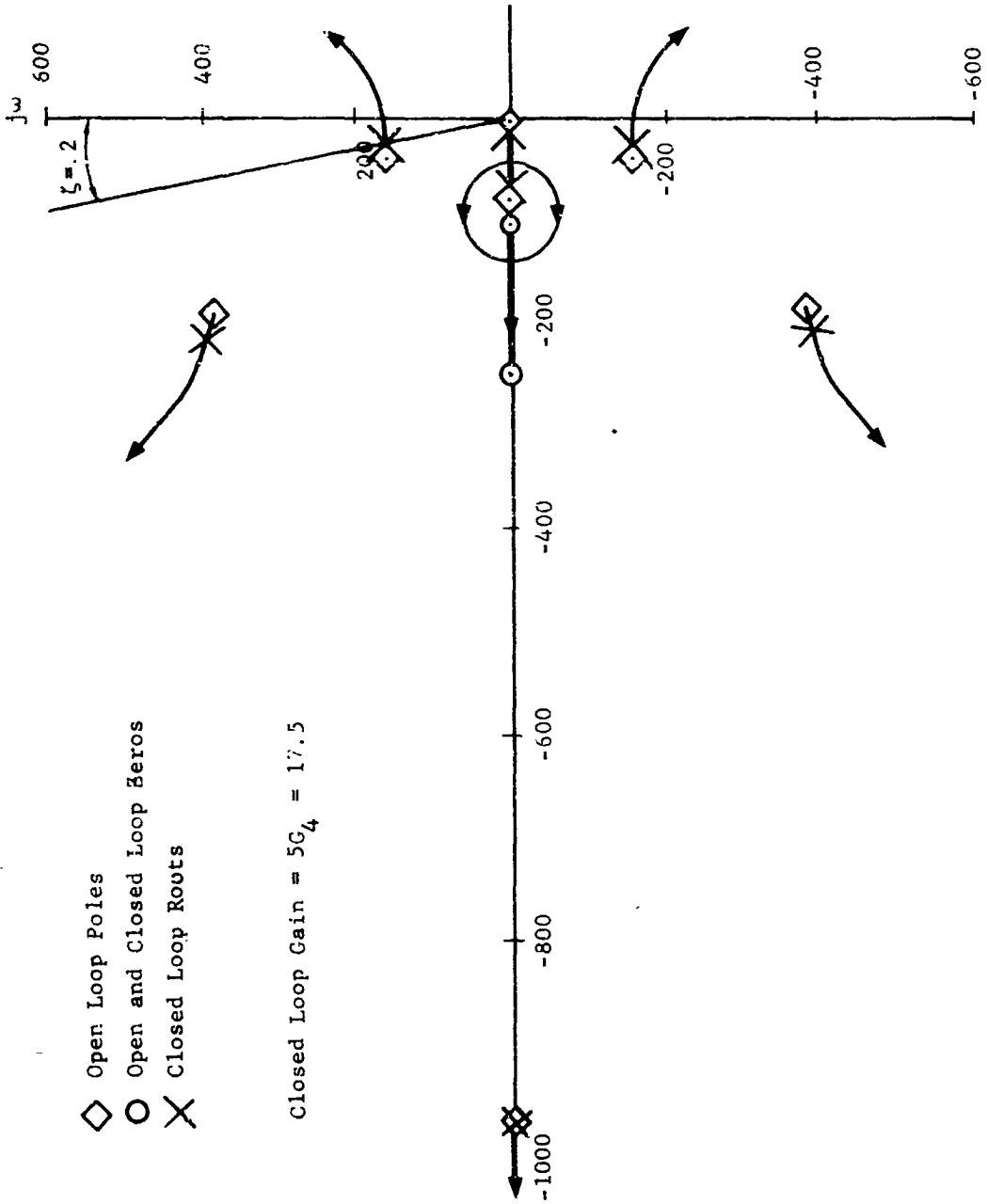


FIGURE B-11 POSITION LOOP ROOT LOCUS

1.3 CONTROL STIFFNESS

To determine the complex control stiffness, the transfer function relating a force on the load to a displacement of the load will be found. From Figure B-8 the force in the pressure feedback loop is related to R'' by:

$$\frac{G_3}{2.68} \left(\frac{\frac{s + \beta}{\beta}}{\frac{s + \alpha}{\alpha}} \right) \quad (22)$$

Values for G_3 , α , and β were determined in the servo loop closure. The transfer function between the output velocity and the force may now be written in the following form:

$$\frac{V_o}{F} = 2.34 \times 10^{-5} \left(\frac{\frac{s + 16}{16}}{\frac{s + 250}{250}} \right) \frac{V_o}{R''} \quad (23)$$

Substituting equation 20 into equation 23

$$\frac{V_o}{F} = \frac{6.3 \times 10^{-6} s \left(\frac{s + 16}{16} \right) \left(\frac{s + 100}{100} \right)}{\left(\frac{s^2 + 64s + 160^2}{160^2} \right) \left(\frac{s^2 + 420s + 440^2}{440^2} \right) \left(\frac{s + 980}{980} \right) \left(\frac{s + 18}{18} \right) \left(\frac{s + 78}{78} \right)} \quad (24)$$

Integrating Equation 24 yields the desired transfer function:

$$\frac{X_o}{F} = 6.3 \times 10^{-6} \frac{\left(\frac{s + 16}{16} \right) \left(\frac{s + 100}{100} \right)}{\left(\frac{s^2 + 64s + 160^2}{160^2} \right) \left(\frac{s^2 + 420s + 440^2}{440^2} \right) \left(\frac{s + 980}{980} \right) \left(\frac{s + 18}{18} \right) \left(\frac{s + 78}{78} \right)} \quad (25)$$

1.4 NOISE SENSITIVITY

Any noise introduced by feedback transducers or line pickup can be represented in a block diagram by an additional input which is summed with the transducer output. By referring to Figure 3-13, any

NORTHROP SPACE LABORATORIES

noise (N_p) applied at the output of the position transducer will be related to the system output V_o as shown below:

$$\frac{V_o}{N_p} = \frac{V_o}{R''} \cdot \frac{R''}{N_p} \quad (26)$$

$$\frac{R''}{N_p} = 4.7 \quad (27)$$

where 4.7 is the gain between the transducer and R'' .

From equations 26 and 27,

$$\frac{V_o}{N_p} = (0.27)(4.7) \frac{\left(\frac{s+100}{100}\right)\left(\frac{s+250}{250}\right)}{\left(\frac{s^2+64s+160^2}{160^2}\right)\left(\frac{s^2+420s+440^2}{440^2}\right)\left(\frac{s+980}{980}\right)\left(\frac{s+18}{18}\right)\left(\frac{s+78}{78}\right)} \quad (28)$$

If all the noise, N_p , introduced into the system is greater than 18 radians/sec (2.86 cps) equation 28 becomes

$$\frac{V_o}{N_p} = \frac{(5)(4.7)\left(\frac{s+100}{100}\right)\left(\frac{s+250}{250}\right)}{\left(\frac{s^2+64s+160^2}{160^2}\right)\left(\frac{s^2+420s+440^2}{440^2}\right)\left(\frac{s+980}{980}\right)\left(\frac{s+78}{78}\right)} \quad (29)$$

Equation 29 is of the same form as equation 21, the transfer function of the total system.

A Bode plot of V_o/V_{V_1} is shown in Figure 3-17. From this figure it may be seen that V_o/N_p is down 11 db at 60 cps and attenuating at a rate of 100 db/decade. Zero db corresponds to 25.5 in/sec/volt.

The same procedure is used to evaluate the effect of noise applied at the output of the demodulator in the rate loop (N_r) and the noise applied at the output of the pressure transducer ($N_{\Delta P}$).

NORTHROP SPACE LABORATORIES

A tabulation of the results for noise injected into critical points in the servo is shown in Table B-1.

1.5 STEADY STATE VELOCITY ERRORS

For the servo system of this report the output velocity of the Z carriage is V_o . The desired output velocity is 5 times the input command since the velocity feedback gain is 0.2. The error E between the desired velocity and the actual velocity is:

$$E = 5 v_{V_i} - V_o \tag{30}$$

$$= v_{V_i} \left(5 - \frac{V_o}{v_{V_i}} \right) \tag{31}$$

$\frac{V_o}{v_{V_i}}$ is the system transfer function of equation 21. If the servo

is commanded with the unit step in velocity, $v_{V_i} = \frac{1}{s}$ the error becomes

$$E = \frac{1}{s} \left[5 - \frac{5 \left(\frac{s+100}{100} \right) \left(\frac{s+250}{250} \right)}{\left(\frac{s^2 + 64s + 160^2}{160^2} \right) \left(\frac{s^2 + 420s + 440^2}{440^2} \right)} \cdot \frac{\left(\frac{s+980}{980} \right) \left(\frac{s+78}{78} \right)}{\left(\frac{s+980}{980} \right) \left(\frac{s+78}{78} \right)} \right] \tag{33}$$

from the final value theorem¹⁸

$$(e_{ss}) = \lim_{s \rightarrow 0} s E \tag{34}$$

$$(e_{ss})_{step} = \lim_{s \rightarrow 0} s \left[5 - \frac{5 \left(\frac{s+100}{100} \right) \left(\frac{s+250}{250} \right)}{\left(\frac{s^2 + 64s + 160^2}{160^2} \right) \left(\frac{s^2 + 420s + 440^2}{440^2} \right)} \cdot \frac{\left(\frac{s+980}{980} \right) \left(\frac{s+78}{78} \right)}{\left(\frac{s+980}{980} \right) \left(\frac{s+78}{78} \right)} \right] \tag{35}$$

TABLE B-1 NOISE SENSIVITY ABOVE 60 cps.

Transfer Function	Gain at zero db and zero frequency $\frac{\text{in/sec}}{\text{volt}}$	Log Magnitude at 60 cps (db)	Rate of Change of Log Magnitude at 60 cps db/decade
$\frac{V_o}{N_p}$	23.5	-11	100
$\frac{V_o}{N_R}$	78	-11	100
$\frac{V_o}{N_p}$	5	+22	100

$$(e_{ss})_{\text{step}} = 0 \quad (36)$$

This means that the output velocity will follow the input command with zero steady state error.

If the servo is commanded with a unit acceleration input

$$v_{i} = \frac{1}{s^2} \quad (37)$$

equation 31 becomes:

$$E = \frac{1}{s^2} \left[5 - \frac{5 \left(\frac{s+100}{100} \right) \left(\frac{s+250}{250} \right)}{\left(\frac{s^2 + 645s + 160^2}{160^2} \right) \left(\frac{s^2 + 420s + 440^2}{440^2} \right) \left(\frac{s + 980}{980} \right) \left(\frac{s + 78}{78} \right)} \right] \quad (38)$$

and the steady state value from equation 34 becomes:

$$(e_{ss})_{\text{ramp}} = 0.0225 \frac{\text{in/sec.}}{\text{in/sec.}^2} \quad (39)$$

APPENDIX C

**OPERATIONAL CONDITIONS AFFECTING
HYDRAULIC FLUID SELECTION**

The total behavior of the hydraulic fluid will depend on operational conditions prevailing in the servo system and in the space chamber. Principal operational factors which affect the fluid include the following:

SERVO SYSTEM

1. Temperature - Near ambient of 70^oF, regulated to a nominal $\pm 10^{\circ}$ F.
2. Pressure - 1500 - 3000 psi.
3. Frequency Response - Zero to 60 cps; influences bulk modulus and viscosity requirements.
4. Duty Cycles - Each on-test cycle up to 3 minutes; 24 hour dwell with either of actuator rods under hydraulic pressure and chamber vacuum.
5. Checkout - Precheck-out of system in air, then checkout inside chamber.
6. Lubricity - Hydrodynamic lubrication of actuator pistons, pumps, and valves.
7. Gas Entrapment and Foaming - Require minimal entrained air, nitrogen, and water vapor.

NORTHROP SPACE LABORATORIES

8. Clearances - Nominal .003 inch clearance for actuator rod.
9. Cleanliness - Pre-use filtration of fluid and system cleanup.
Use of low micro rating filters to protect valves and pump.
10. Seals - Fluid used with compatible materials.
11. Leakage - Suction return of fluid from actuator rod surfaces;
control of manufacturing and maintenance procedures:
close fits, smooth and passive surface finishes.
12. Safety - Fluid inert to oxygen gas from 5 psia oxygen
pressurized chamber.
13. Materials - Metal alloys to be 300 series stainless steels
and passive.

SPACE CHAMBER

1. Temperature - Hydraulic Fluid on actuator rods in approximate
ambient range of +70^oF to -100^oF; (may have net
heat transfer out of fluid to chamber); cryopanel
as low as -250^oF.
2. Vacuum - 10⁻⁵ torr level or less; pump capacity 250,000
liters per second; non-condensable outgassing
load minimized to order of 0.25 torr liter/second.
3. Tests - Solar radiation simulation tests with UV collimated
beam on specimens (fluid not in path of UV light).
4. Safety - Emergency repressurization by flooding with
oxygen to 5 psia.

APPENDIX D

BULK MODULUS DEFINITIONS AND FACTORS INVOLVED

1. BULK MODULUS

1.1 General Bulk modulus, or reciprocal of the compressibility hydraulic fluid is one of the critical design parameters affecting the performance of hydraulic servomechanisms.

1.2 ASTM Definitions⁹ These have been standardized as follows:

1.2.1 Secant Bulk Modulus (also "mean or average" bulk modulus) is defined as the total change in fluid pressure divided by the total change in fluid volume per unit initial volume under pressure.

1.2.1.1 Secant Isothermal Bulk Modulus ("Static" process) is

$$B_T = \left[\frac{\Delta P}{\Delta V/v_1} \right]_T \quad (1)$$

1.2.1.2 Secant Isentropic Bulk Modulus "dynamic", constant entropy is

$$B_S = \left[\frac{\Delta P}{\Delta V/v_1} \right]_S \quad (2)$$

1.2.2 Tangent Bulk Modulus is defined as the product of fluid volume under compression and the partial derivative of fluid pressure with respect to volume.

1.2.2.1 Isothermal Tangent Bulk Modulus (for a specified quiescent pressure and temperature) is

$$B_T = V \left[\frac{\partial P}{\partial V} \right]_T \quad (3)$$

1.2.2.2 Isentropic Tangent Bulk Modulus (also "adiabatic" bulk modulus, at constant entropy) is

$$B_S = V \left[\frac{\partial P}{\partial V} \right]_S \quad (4)$$

The adiabatic bulk modulus provides instantaneous values for dynamic or transient conditions. Sonic bulk modulus is an isentropic dynamic bulk modulus that is defined as the product of the mass fluid density and the squared value of the speed of sound. The expression is: $B_S = \rho V^2$ or ω / gV^2 . When calculating the volumetric relationship of pumps or actuators, the average bulk modulus may be used if temperature is essentially constant.

Where pressure variations are small at the given pressure, i.e., in a servo valve circuit application the isothermal tangent bulk modulus may be used.

1.2.4 Relationships ^{20,21}

The isothermal and adiabatic bulk modulus are related through the expression $B_S/B_T = \gamma$ where $\gamma = C_P/C_V$ the ratio of specific heats. For most liquids γ ranges from 1.1 to 1.5.

1.2.5 Measurements ²⁰ Two types of measurements account for modulus values: pressure-volume-temperature (P-V-T) and ultrasonic velocity measurements. P-V-T is used mostly under isothermal

conditions, giving B_T , whereas the ultrasonic velocity methods yields the bulk modulus directly.

1.3 Effect of Pressure and Temperature on Bulk Modulus

The effect of pressure and temperature on isothermal secant and tangent bulk modulus values of silicone, siloxane, silane, ester, polyphenyl ether and hydrocarbon fluids has been reported in modulus curves²². The temperature data shows a progressive increase in modulus with a decrease in temperature with the rate of increase greater at the lower temperatures. (Thus, for MLO 59-692, psi (phenoxy phenoxy) benzene, B_T (isothermal) values are 415,000, 320,000, and 250,000 psi at 100°F, 200°F, and 300°F, respectively).

Pressure

The effect of pressure increase is an increase in the bulk modulus value. In the pressure range of 1000 psi to 3000 psi the increase in modulus is frequently of the order to 10,000 to 20,000 psi.

1.4 Effect of Entrained Gas on Bulk Modulus^{23,5}

Entrainment of air or nitrogen or other gases can have an adverse effect on the bulk modulus of the hydraulic fluid. A suspension of air could be produced by agitation of fluid in contact with air, by a leak in the suction line to a pump, or by the reduction of pressure in a fluid containing air in solution. At pressures less than 1500 psi, the pressure of suspended air has a marked influence upon the elasticity of the fluid. (The mass of air dissolved per unit volume of the fluid increases linearly with pressure.) For standard hydraulic fluids, the percentage volume of dissolved air lies between 5 and 12 percent, but the main effect on modulus is from the free air volume. Foaming is caused by the entrained gas in the form of bubbles attempting to leave the liquid and may occur when the pressure is reduced as the gas in solution will then leave the liquid and be entrained or suspended in the fluid.

NORTHROP SPACE LABORATORIES

Minimization of the effects of air entrainment or foaming is best accomplished by choice of a low-foaming fluid and by preventive methods, such as, by reducing extent of gas contact with the fluid, by providing a reservoir adequate to facilitate gas-liquid separation, or by use of an airless reservoir and by keeping return lines well below liquid levels.

APPENDIX E

**CLASSES OF HYDRAULIC FLUIDS
AND THEIR CHARACTERISTICS**

1.0 CLASSES OF HYDRAULIC FLUIDS

1.1 Chemical Classes of fluids for hydraulic uses:

Esters: phosphates, silicates, dibasic acid type, disiloxanes.

Ethers: polyphenyl ethers

Hydrocarbons: super-refined (deep - dewaxed)

Silicones: silicones, fluorosilicones

1.2 Classes with Limitations

1.2.1 Silicates: Poor stability to hydrolysis (forming gels or silica), high vapor pressure, and low bulk modulus, moderate fire resistance.

1.2.2 Dibasic acid esters: Susceptible to hydrolysis, high vapor pressure, poor fire resistance.

1.2.3 Disiloxanes: Bulk modulus in range of 250,000 - 300,000 psi, auto-ignition temperature and flash point lower than for phosphates.

1.2.4 Polyphenyl ethers: Viscosity extremely high for a high modulus and low vapor pressure compound.

1.2.5 Super-refined Hydrocarbons: Poor fire resistance, bulk modulus (iso-thermal secant) less than 250,000 psi, cost near \$100/gallon. (Example: Oronite HTHF 6294).

1.2.6 Silicones: Low bulk modulus of order of 150,000 psi, vapor pressure slightly high. (Example: Versilube F-50. General Electric).

1.2.7 Fluorosilicones: Low bulk modulus, high vapor pressure.

2.0 FLUID PERFORMANCE AND FLUID PERMANENCE

Performance and permanence characteristics relative to the operational conditions for the overall servo and space chamber system will guide the hydraulic fluid selection. A property check list follows here. Also see Appendix F, Comparison Chart For Specific Properties of Fluids for Selection).

2.1 Governing Properties Check List Fluid Performance

1. Modulus
2. Viscosity: Temperature, pressure effects
3. Fire Resistance
4. Foaming
5. Lubricity
6. Corrosion Resistance

Fluid Permanence

1. Shear Stability
2. Chemical Stability: hydrolytic, oxidation, thermal, corrosion
3. Volatility: vapor pressure, evaporation rate in chamber
4. Service Life: low maintenance (low aeration, low evaporation, conventional contamination control)

3.0 PHOSPATE ESTERS Chemistry and Fire Resistance²⁴

- 3.1 Chemistry - Phosphate esters find uses in the hydraulic-fluid and lubricant fields as either undiluted phosphate esters (e.g., Cellulubes), or as phosphate ester base fluids to which chlorinated hydrocarbon diluents may be added. Structurally, they may be triaryl phosphate esters (Cellulube 90 is the latter type). The undiluted esters have inherent properties of excellent lubricity, fire-resistance, and fluid stability, and hence do not normally require additives to enhance them.

NORTHROP SPACE LABORATORIES

3.2 Fire-Resistance - Fire resistant hydraulic fluids combine resistance to ignition and flame propagation with required hydraulic characteristics. An outstanding characteristic of the phosphate esters is their ability to resist ignition. Although phosphate esters have flash points as high as 500°F, and would be mis-named as "non-inflammable," these flash points are not generally considered to be a true measure of fire resistance, but are more a measure of volatility and thermal stability. The fire points are from 200-300°F above the flash point and this property is again a measure of thermal instability. The spontaneous or autogenous ignition temperature which may range to 1200°F is considered a better measure of the flammability characteristics of the phosphate esters.⁸ Specifications which define fire resistance tests in terms of fluid performance are AMS-3150B and MIL-F-7100. Such tests as "High Pressure Spray Test," "Low Pressure Spray Test", and "Hot Manifold Test" are designed to simulate conditions resulting from a broken line spraying hydraulic fluid into a source of ignition, such as a flame or a hot surface. Phosphate esters which excel in such tests may be considered to possess significant fire-resistance characteristics and are of practical value in many hazardous applications.

Phosphate esters of very low pressure (e.g., Cellulubes and some Pydrauls) show autoignition in air or oxygen atmospheres only at elevated temperature. It is not expected that vacuum pump operations will exhibit detonation phenomena in the presence of this fluid class. For example, one phosphate ester, Pydraul 150 (whose vapor pressure is appreciably higher than Pydraul 60 or Cellulube 90) is used in gears of LOX pumps located in oxygen-rich atmospheres at missile-fueling sites.²⁵

4.0 VISCOSITY CHARACTERISTICS ^{5,26}

4.1 General

Viscosity characteristics of the hydraulic fluid should meet the desired hydrodynamic lubricity necessary for smooth wear-free operation and provide uniform performance over the (limited) temperature of operation and not be subjected to critical changes due to friction. Viscosity over changing conditions of temperature and pressure and flow should be within the limits required for pump lubricity and operation of servo controls and valves. The hydraulic line external to the chamber will be provided with a heat exchange system so as to regulate the fluid in the slightly warm hydraulic loop to $\pm 10^{\circ}\text{F}$. During down time in the space chamber, the temperature of the fluid on exposed actuator rods is expected to be 70°F or less. Therefore, the fluid should possess viscosity-temperature properties compatible with these considerations.

4.2 Viscosity-Temperature Relationships

Viscosity-temperature values in the range of expected operation are presented for several candidate phosphate esters. Values given are for atmospheric pressure. Viscosity values will increase at higher pressures (See 4.2.3).

4.2.1 Characteristics for Pump Lubricity

Assume operation at temperatures where the viscosity is less than 70 SUS, Saybolt viscosity. (Note: The values in the table indicate maximum temperature for a value < 70 SUS).

NORTHROP SPACE LABORATORIES

<u>Fluid</u>	<u>Temperature for SUS = 70</u>	<u>Temperature for SUS = 60</u>	<u>Temperature For SUS = 40</u>
Cellulube 90	117°F	122°F	190°F
Cellulube 150	136°F	148°F	7200°F
Pydraul 60	90°F	100°F	140°F

The values indicate approximate maximum temperature limits to meet a desired viscosity. Actual values will be higher under pressure loading (See 4.2.3).

4.2.2 Characteristics for Servo Response

A lower viscosity is generally preferred in the servo system, especially in view of the high frequency response and operation within a vacuum chamber at low temperature. Although an ultimate limit of 200 centistokes might be accommodated by the equipment, the viscosity-temperature values of the phosphate esters appear to be in a suitable range, extending to below 70°F.

Kinematic Viscosity at Temperature

<u>Fluid</u>	<u>100°F</u>	<u>70°F</u>	<u>50°F</u>
Cellulube 90	19.2 cs	--	99.8
Cellulube 125	32.1 cs	--	260.4
Pydraul 60	11.7 cs	30 cs	/20

4.2.3 Viscosity - Pressure Relationships⁵

For Cellulube phosphate esters, the absolute viscosity in centipoise has been plotted as a semi-log function of pressure.²⁷ Isothermal curves for fluid temperatures of 100, 150, and 200°F demonstrate an increasing film strength (viscosity) with increasing pressure. Data for Cellulube 220 indicates an approximate viscosity increase of 20-40% at the 15-50 cps level when increasing the pressure from 0 to 1500 psi.

4.2.4 Other Viscosity Effects

1. Foaming. High viscosity fluids are more apt to foam since air bubbles take more time to disengage. Higher temperatures lower the viscosity, and favor more rapid foam collapse. The viscosity effect on foaming is not critical with most phosphate fluids because of inherent low or nonfoaming characteristics.

2. Leakage. Lower leakage through a clearance gaps and from seals and exposed surfaces will be favored by higher viscosity. One potential source of leakage is from actuator rod surfaces located inside the vacuum chamber. The temperature effect due to the relatively cool chamber surroundings will favorably reduce the viscosity of the hydraulic fluid on actuator rods.

APPENDIX F

COMPARISON CHART, SPECIFIC PROPERTIES OF FLUIDS FOR SELECTION

Properties	Hydraulic 60	Cellulube 90	Cellulube 15J	Cellulube 220	OS-124	HTHF 7277B	HTHF 70	MIL-H-5606
Bulk Modulus (1000-5000 psi, 80°F) psi	328,000 Adiabatic	350,000 Isothermal Tangent	350,000 Isothermal Tangent	551,000 Isothermal Tangent	400,000 Isothermal Tangent	275,000 Adiabatic	245,000 Adiabatic	240,000(80°F) Adiabatic
Viscosity, Saybolt, SUS	43 (140°) 58 64 85	49 64 96	52.5 85 151	69.5 112 223	--	--	--	--
Kinematic, cs	740 (40°) -- 11.7 30.0 182 (40°)	450 11.2 19.2 99.8	1190 16.8 32.1 260.4	2280 22.7 48 200 500	--	72.8	24.4	14.2
Fire Resistance	--	680	690	700	660	--	--	--
Fire Point, °F	450	480	490	500	550	420	430	225
Flash Point, CUC, °F	1100	1200	1200	1180	1135	735	735	475
Autogenous Ignition Temp., °F	1300	1390	1380	1370	--	--	--	--
Hot Manifold Test (MIL-F-7100)°F	1200	1500	1500	1500	--	--	--	--
Molten Metal Ignition Test, °F	Self-extinguish Slight increase	Self-extinguish Decrease	Self-extinguish Decrease	Self-extinguish Decrease	Self-extinguish Decrease	--	--	--
High Pressure Spray Test (AMS 3150B)								
Low Pressure Spray Test (AMS 3150E)								
Flame Intensity								
Boiling Point, 760 mm. Hg., °F	690	756	766	770	982	--	--	--
Yield Strength, mm. Hg. 50°F (Extrapolated) $\times 10^{-5}$ (70°)	5×10^{-7}	0.58	0.48	5×10^{-8}	--	--	5×10^{-6}	High
Water Solubility, wt. %	0.50			0.61	--	--	--	--
Density at 60°F, gm/cc	1.090(77°)	1.210	1.175	1.165	--	0.890	0.953	0.860
Foam Tendency (ASTM D286-30)	Low	25	25	25	--	70	Nil	45(200°F)
5 minutes aeration at 75°F, ml. max	Pass	Pass	Pass	Pass	--	--	--	--
Hydrolytic Stability Test (MIL-R-19457)	Excellent	Excellent	Excellent	Excellent	--	--	Excellent	Fair
Shear Stability Pump Test 1000 psi	Good	Good	Good	Good	--	--	--	Fair
Chemical Stability (Oxidation, thermal)								
In operating range								
Corrosion to Metals in System	None	None	None	None	None	None	None	None
Compatible Elastomers	Butyl silicone	Butyl silicone	Butyl silicone	Butyl silicone	None	None	None	Buna-N

APPENDIX G

SIMULATION OF TWO RIGID BODIES

All studies of a rigid vehicle motion necessarily involve the motion of some point on the vehicle with respect to inertial space (reference 35, 36). If the velocity of the center of gravity (that is c.g.) of the vehicle is $\vec{\mu}$ and the point whose motion is to be measured is located at distance $\vec{\xi}$ from the c.g., the velocity \vec{v} of the point with respect to inertial space will be:

$$\vec{v} = \vec{\mu} + \dot{\vec{\xi}} + \vec{\omega} \times \vec{\xi} \quad (1)$$

where $\vec{\omega}$ is the rate of rotation of the vehicle axes. The values of $\dot{\vec{\xi}}$ are obtained from:

$$\dot{\vec{\xi}} = \dot{\vec{\xi}}_0 + \int_0^t \ddot{\vec{\xi}} dt \quad (2)$$

$$\ddot{\vec{\xi}} = \int_0^t \ddot{\ddot{\xi}} dt \quad (3)$$

$$\ddot{\ddot{\xi}} = \sum \ddot{\ddot{\xi}}_i \quad (4)$$

where $\ddot{\ddot{\xi}}_i$ is the acceleration in $\ddot{\xi}$ due to mode i . For completely rigid bodies, $\dot{\vec{\xi}}$ and $\ddot{\vec{\xi}}$ are zero, and $\ddot{\xi}$ equals $\ddot{\xi}_0$.

The net unopposed force acting on the vehicle causes an acceleration of the center of gravity such that:

$$\vec{F} = m (\ddot{\vec{\mu}} + \vec{\omega} \times \dot{\vec{\mu}}) \quad (5)$$

$$\ddot{\vec{\mu}} = \frac{\vec{F}}{m} - \vec{\omega} \times \dot{\vec{\mu}} \quad (6)$$

$$\dot{\vec{\mu}} = \dot{\vec{\mu}}_0 + \int_0^t \ddot{\vec{\mu}} dt \quad (7)$$

NORTHROP SPACE LABORATORIES

A moment acting on a vehicle creates a rate of change in the moment of momentum:

$$d\vec{M} = d\vec{h} + \vec{\omega} \times d\vec{h} \quad (8)$$

where:

$$d\vec{h} = \vec{r} \times (\vec{\omega} \times \vec{r}) dm = [\eta^2 \vec{\omega} - (\vec{\omega} \cdot \vec{r}) \vec{r}] dm \quad (9)$$

thus,

$$\begin{aligned} M &= \int \{ \eta^2 \vec{\omega} - (\vec{\omega} \cdot \vec{r}) \vec{r} + \eta^2 (\vec{\omega} \times \vec{r}) - (\vec{\omega} \cdot \vec{r})(\vec{\omega} \times \vec{r}) \} dm \\ &= \int [\eta^2 \vec{\omega} - (\vec{\omega} \cdot \vec{r}) \vec{r} - (\vec{\omega} \cdot \vec{r})(\vec{\omega} \times \vec{r})] dm \end{aligned} \quad (10)$$

These equations may be expanded to Cartesian form and must be mechanized for each vehicle. For either vehicle, the expanded forms are:

$$u_c = u_o + \int_0^t \left(\frac{F_x}{m} - \omega_y \omega + \omega_z v \right) dt \quad (11)$$

$$v_c = v_o + \int_0^t \left(\frac{F_y}{m} - \omega_z u + \omega_x w \right) dt \quad (12)$$

$$w_c = w_o + \int_0^t \left(\frac{F_z}{m} - \omega_x v + \omega_y u \right) dt \quad (13)$$

$$u = u_c + \omega_y Z - \omega_z Y \quad (14)$$

$$v = v_c + \omega_z X - \omega_x Z \quad (15)$$

$$w = w_c + \omega_x Y - \omega_y X \quad (16)$$

$$\begin{aligned} \dot{\omega}_x &= \frac{M_x}{I_{xx}} + \frac{I_{xz}}{I_{xx}} \dot{\omega}_z + \frac{I_{xy}}{I_{xx}} \dot{\omega}_y + \frac{I_{xz}}{I_{xx}} \omega_x \omega_y - \frac{I_{xy}}{I_{xx}} \omega_x \omega_z \\ &+ \frac{I_{yz}}{I_{xx}} (\omega_y^2 - \omega_z^2) + \frac{I_{yy} - I_{zz}}{I_{xx}} \omega_y \omega_z \end{aligned} \quad (17)$$

$$\begin{aligned} \dot{\omega}_y = & \frac{M_y}{I_{yy}} + \frac{I_{xy}}{I_{yy}} \dot{\omega}_x + \frac{I_{yz}}{I_{yy}} \dot{\omega}_z + \frac{I_{xy}}{I_{yy}} \omega_y \omega_z - \frac{I_{yz}}{I_{yy}} \omega_x \omega_y \\ & + \frac{I_{xz}}{I_{yy}} (\omega_z^2 - \omega_x^2) + \frac{I_{zz} - I_{xx}}{I_{yy}} \omega_x \omega_z \end{aligned} \quad (18)$$

$$\begin{aligned} \dot{\omega}_z = & \frac{M_z}{I_{zz}} + \frac{I_{xz}}{I_{zz}} \dot{\omega}_x + \frac{I_{yz}}{I_{zz}} \dot{\omega}_y + \frac{I_{yz}}{I_{zz}} \omega_x \omega_y - \frac{I_{xz}}{I_{zz}} \omega_y \omega_z \\ & + \frac{I_{xy}}{I_{zz}} (\omega_x^2 - \omega_y^2) + \frac{I_{xx} - I_{yy}}{I_{zz}} \omega_x \omega_y \end{aligned} \quad (19)$$

$$\omega_x = \omega_{x_0} + \int_0^t \dot{\omega}_x dt \quad (20)$$

$$\omega_y = \omega_{y_0} + \int_0^t \dot{\omega}_y dt \quad (21)$$

$$\omega_z = \omega_{z_0} + \int_0^t \dot{\omega}_z dt \quad (22)$$

The development of the actual attitude orientation is based on the assumption that the vehicle starts with its axes coincident with those of the reference axes. It first rotates about its z-axis (yaw) through the angle ψ . Next, it pitches about its y-axis through the angle θ . Last, it rolls through the angle ϕ about its x-axis. The positive sense of all rotations is according to the right-hand rule.

Thus far, the motions have been developed such that the rate vectors exist in a system of axes fixed in reference space and instantaneously coincident with the vehicle in question. If reference space is inertial, the rates of change of ψ , θ , and ϕ may be written:

NORTHROP SPACE LABORATORIES

$$\dot{\theta} = \omega_y \cos \phi - \omega_z \sin \phi \quad (22)$$

$$\dot{\psi} = (\omega_y \sin \phi + \omega_z \cos \phi) / \cos \theta \quad (24)$$

$$\dot{\phi} = \omega_x + \dot{\psi} \sin \theta \quad (25)$$

$$\theta = \theta_0 + \int_0^t \dot{\theta} dt \quad (26)$$

$$\psi = \psi_c + \int_0^t \dot{\psi} dt \quad (27)$$

$$\phi = \phi_0 + \int_0^t \dot{\phi} dt \quad (28)$$

A vector ξ_i , where i denotes an axis (1 for x, 2 for y, 3 for z), in vehicle space transforms to the vector η_j in reference space through the formula:

$$\eta_j = \sum_{i=1}^3 f_{j,i} \xi_i \quad (29)$$

where

$$f_{1,1} = \cos \theta \cos \psi \quad (30)$$

$$f_{1,2} = \sin \phi \sin \theta \cos \psi - \cos \phi \sin \psi \quad (31)$$

$$f_{1,3} = \cos \phi \sin \theta \cos \psi + \sin \phi \sin \psi \quad (32)$$

$$f_{2,1} = \cos \theta \sin \psi \quad (33)$$

$$f_{2,2} = \sin \phi \sin \theta \sin \psi + \cos \phi \cos \psi \quad (34)$$

$$f_{2,3} = \cos \phi \sin \theta \sin \psi - \sin \phi \cos \psi \quad (35)$$

$$f_{3,1} = -\sin \theta \quad (36)$$

$$f_{3,2} = \sin \phi \cos \theta \quad (37)$$

$$f_{3,3} = \cos \phi \cos \theta \quad (38)$$

NORTHROP SPACE LABORATORIES

The reverse transformation is obtained through the equation:

$$\xi_i = \sum_{j=1}^3 f_{j,i} \eta_j \quad (39)$$

In the problem at hand, the simulator concept is that of reducing the twelve degrees of freedom of the two vehicles to six degrees divided as follows:

1. The simulator probe will translate in the y and z directions and will rotate in roll.
2. The simulator drogue will translate in x and rotate in yaw and pitch.

By this concept, the probe x axis will maintain a fixed attitude orientation with respect to the simulator. We conceive, therefore, of simulator reference axes from which the probe does not develop any yaw or pitch and the drogue does not roll. These reference axes are moving with respect to inertial space, and the rotation rates about inertial axes instantaneously coincident with the reference axes are developed as follows:

Denoting the motion of the drogue by the subscripted and that of the reference axes by the subscript r,

$$\omega_{i1} = \omega_{i_d} - \sum_{j=1}^3 f_{j,i} \omega_{j_r} \quad (40)$$

Since θ_d equals zero,

$$\dot{\theta}_d = \omega_{21} = \omega_{y_d} + \omega_{x_r} \sin \psi_d - \omega_{y_r} \cos \psi_d \quad (41)$$

$$\begin{aligned} \psi_d &= \omega_{31} \cos \theta_d = (\omega_{z_d} - \omega_{x_r} \sin \theta_d \cos \psi_d - \omega_{y_r} \sin \theta_d \sin \psi_d \\ &\quad - \omega_{z_r} \cos \theta_d) / \cos \theta_d \\ &= [\omega_{z_d} - (\omega_{x_r} \cos \psi_d + \omega_{y_r} \sin \psi_d) \sin \theta_d] / \cos \theta_d - \omega_{z_r} \quad (42) \end{aligned}$$

$$\begin{aligned} \dot{\theta}_d = 0 &= \omega_{l_1} + \dot{\psi}_d \sin \theta_d = \omega_{x_d} - \omega_{x_r} \cos \theta_d \cos \psi_d - \omega_{y_r} \cos \theta_d \sin \psi_d \\ &\quad + \omega_{z_r} \sin \theta_d + \dot{\psi}_d \sin \theta_d \\ &= \omega_{x_d} + [\omega_{z_d} \sin \theta_d - \omega_{x_r} \cos \theta_d - \omega_{y_r} \sin \psi_d] / \cos \theta_d \end{aligned} \quad (43)$$

The terms ω_{x_r} and ω_{y_r} may be determined from the probe motion:

$$\dot{\theta}_r = \dot{\theta}_p = \omega_{y_r} = \omega_{y_p} \cos \theta_p - \omega_{z_p} \sin \theta_p \quad (44)$$

$$\dot{\psi}_r = \dot{\psi}_p = \omega_{z_r} = \omega_{y_p} \sin \theta_p + \omega_{z_p} \cos \theta_p \quad (45)$$

where, since there is no motion of the probe in θ and with respect to the reference axes, $\dot{\theta}_p$, $\dot{\psi}_p$, $\dot{\theta}_r$ and $\dot{\psi}_r$ are expressed with respect to inertial space. On this basis, equation (43) indicates that

$$\omega_{x_r} = \left[\omega_{x_d} \cos \theta_d + \omega_{z_d} \sin \theta_d - \omega_{y_r} \sin \psi_d \right] / \cos \psi_d \quad (46)$$

thus,

$$\dot{\theta}_d = \omega_{y_d} + \left[(\omega_{x_d} \cos \theta_d + \omega_{z_d} \sin \theta_d) \sin \psi_d - \omega_{y_r} \right] / \cos \psi_d \quad (47)$$

$$\dot{\psi}_d = \omega_{z_d} \cos \theta_d - \omega_{x_d} \sin \theta_d - \omega_{z_r} \quad (48)$$

$$\dot{\theta}_p = \omega_{x_p} - \omega_{x_r} \quad (49)$$

Since the probe does not move in x and the drogue does not move in y and z, it is convenient to select a reference axis system such that the x axis passes through the center of rotation of the drogue and the y-z plane coincides with the probe y-z plane. In this case, using U, V and W to denote translational velocities, and X, Y and Z to denote position,

NORTHROP SPACE LABORATORIES

$$U_d = u_d \cos \theta_d \cos \psi_d - v_d \sin \psi_d + w_d \sin \theta_d \cos \psi_d - u_p + \omega_{y_r} Z_p - \omega_{z_r} Y_p \quad (50)$$

$$V_p = v_p \cos \theta_p - w_p \sin \theta_p - u_d \cos \theta_d \sin \psi_d - v_d \cos \psi_d - w_d \sin \theta_d \sin \psi_d + \omega_{z_r} X_d + \omega_{x_r} Z_p \quad (51)$$

$$W_p = v_p \sin \theta_p + w_p \cos \theta_p + u_d \sin \theta_d - w_d \cos \theta_d - \omega_{x_r} Y_p - \omega_{y_r} X_d \quad (52)$$

$$X_d = X_{d_0} + \int_0^t U_d dt \quad (53)$$

$$Y_p = Y_{p_0} + \int_0^t V_p dt \quad (54)$$

$$Z_p = Z_{p_0} + \int_0^t W_p dt \quad (55)$$

$$\theta_d = \theta_{d_0} + \int_0^t \dot{\theta}_d dt \quad (56)$$

$$\psi_d = \psi_{d_0} + \int_0^t \dot{\psi}_d dt \quad (57)$$

$$\phi_p = \phi_{p_0} + \int_0^t \dot{\phi}_p dt \quad (58)$$

Equations (11) through (22) must be mechanized for each vehicle and the appropriate initial conditions supplied. The u_0 , v_0 and w_0 values are the velocities of the c.g. at the start of the run. The x , y and z values are the coordinates of the point on the real vehicle at which simulator measurements are made, based on an axis system with its origin at the c.g. and with the x - axis parallel to the axis of the probe or drogue, whichever vehicle is being considered. If the attitude of the vehicle with respect to fixed space is desired, equations (23) through (28) may be mechanized as an auxiliary calcu-

lation. If the motion of the c.g. in inertial space is desired, u_o , v_o and w_o may be substituted in the expanded form of (29) to yield the velocity components with respect to the inertial axes, where the angles come from (26) through (28) and the f transforms come from (30) through (38).

For simulation, equations (44) through (58) supply all the answers and are convenient for the use of rate-commanded servos.

At this point, the forces required for equations (11) through (13) and the moments for equations (17) through (19) have not been developed. In the simulator, strain gages supply the forces and moments at a point which will, in general, not be at the origin of mensuration. The forces may be used directly, but the moments about the c.g. will be

$$M_x = M_{x_o} + y_f F_z - z_f F_y \quad (59)$$

$$M_y = M_{y_o} + z_f F_x - x_f F_z \quad (60)$$

$$M_z = M_{z_o} + x_f F_y - y_f F_x \quad (61)$$

where x_f , y_f and z_f are the coordinates (c.g. as origin) of the point at which the forces and moments are applied and the subscript (o) denotes moments applied and measured directly.

APPENDIX H

FUEL SLOSHING

Fuel sloshing will be represented by presuming a point mass of sloshing fuel suspended by a spring-damper. The mass is presumed to have no rotational inertia.

Taking the vehicle mass as m , the fuel sloshing mass as m_s , and the location of the sloshing mass as $\vec{\eta}$, referred to the c.g., we can break into two parts:

$$\vec{\eta} = \vec{\xi}_0 + \vec{\xi} \quad (1)$$

where $\vec{\xi}_0$ is the neutral location and $\vec{\xi}$ the deviation. Differentiating,

$$\dot{\vec{\eta}} = \dot{\vec{\xi}} + \vec{\omega} \times \vec{\eta} \quad (2)$$

and the velocity of the sloshing mass with respect to inertial space is

$$\vec{v} = \dot{\vec{\mu}} + \dot{\vec{\eta}} = \dot{\vec{\mu}} + \dot{\vec{\xi}} + \vec{\omega} \times \vec{\eta} \quad (3)$$

The acceleration is

$$\begin{aligned} \ddot{\vec{v}} = \ddot{\vec{\mu}} + \vec{\omega} \times \dot{\vec{\mu}} + \dot{\vec{\omega}} \times \vec{\eta} + \dot{\vec{\xi}} + 2(\vec{\omega} \times \dot{\vec{\xi}}) \\ + (\vec{\omega} \cdot \vec{\eta})\vec{\omega} - \omega^2 \vec{\eta} \end{aligned} \quad (4)$$

The force required to produce this motion is

$$\vec{F}_s = m_s \ddot{\vec{v}} \quad (5)$$

It is produced by the elastic and damping restraints and is related to the displacement by

$$\vec{F}_s = f(\vec{\xi}, \dot{\vec{\xi}}) \quad (6)$$

NORTHROP SPACE LABORATORIES

This force may be divided into two parts:

$$\vec{F}_s = \vec{F}_{s_1} + \vec{F}_{s_2} \quad (7)$$

$$\vec{F}_{s_1} = m_s \left\{ \vec{\mu} + \vec{\omega} \times \vec{\mu} + \vec{\omega} \times \vec{\xi}_0 + (\vec{\omega} \cdot \vec{\xi}_0) \vec{\omega} - \omega^2 \vec{\xi}_0 \right\} \quad (8)$$

$$\vec{F}_{s_2} = m_s \left\{ \vec{\omega} \times \vec{\xi} + \vec{\xi} + 2(\vec{\omega} \times \vec{\xi}) + (\vec{\omega} \cdot \vec{\xi}_0) \vec{\omega} - \omega^2 \vec{\xi} \right\} \quad (9)$$

\vec{F}_{s_1} is seen to be associated with the motion of the vehicle without sloshing.

Similarly, the moments may be developed as

$$\vec{M}_s = \vec{\eta} \times \vec{F}_s = \vec{M}_{s_1} + \vec{M}_{s_2} \quad (10)$$

$$\vec{M}_{s_1} = \vec{\xi}_0 \times \vec{F}_{s_1} \quad (11)$$

$$\vec{M}_{s_2} = \vec{\xi}_0 \times \vec{F}_{s_2} + \vec{\xi} \times \vec{F}_s \quad (12)$$

Again, \vec{M}_{s_1} is obviously associated with the motion of the vehicle without sloshing (i.e., with the fuel rigidly restrained).

Actually, the force of equation (6) and the moment of equation (10) may be considered as being applied to a vehicle of mass

$$m_v = m - m_s \quad (13)$$

whose c.g. is δ units away from the c.g. of m in the direction opposite to $\vec{\xi}$. If an external force \vec{F} and moment \vec{M} are applied at the c.g. of m , the force and moment at the c.g. of m_v to produce similar motion will be

$$\vec{F}' = \vec{F} - \vec{F}_s \quad (14)$$

$$\vec{M}' = \vec{M} - \vec{M}_s + \delta \times \vec{F} - \delta \times \vec{F}_s \quad (15)$$

NORTHROP SPACE LABORATORIES

Since

$$\vec{\mu} + \vec{\omega} \times \vec{\mu} = \vec{\alpha} + \vec{\omega} \times \alpha + \dot{\vec{\omega}} \times \delta + (\vec{\omega} \cdot \delta) \vec{\omega} - \omega^2 \delta \quad (16)$$

where $\vec{\alpha}$ is the velocity of the c.g. of m_v ,

$$\vec{F}' = m_v \{ \vec{\mu} + \vec{\omega} \times \vec{\mu} - \vec{\omega} \times \delta - (\vec{\omega} \cdot \delta) \vec{\omega} + \omega^2 \delta \} \quad (17)$$

$$\begin{aligned} \vec{F} = \vec{F}' + \vec{F}_s = m (\vec{\mu} + \vec{\omega} \times \vec{\mu}) + m_s \{ \vec{\xi} + \dot{\vec{\omega}} \times \vec{\xi} \\ + 2 (\vec{\omega} \times \vec{\xi}) + (\vec{\omega} \cdot \xi) \vec{\omega} - \omega^2 \vec{\xi} \} \end{aligned} \quad (18)$$

where

$$\vec{\delta} = \frac{m_s}{m_v} \vec{\xi}_0 \quad (19)$$

Now,

$$\begin{aligned} \vec{\xi} = \frac{F_s}{m_s} - (\vec{\mu} + \vec{\omega} \times \mu) - [\dot{\vec{\omega}} \times \vec{\xi}_0 + (\vec{\omega} \cdot \xi) \vec{\omega} \\ - \omega^2 \vec{\xi}_0] - [\dot{\vec{\omega}} \times \vec{\xi} + 2 (\vec{\omega} \times \xi) + (\vec{\omega} \cdot \xi) \vec{\omega} - \omega^2 \xi] \end{aligned} \quad (20)$$

Substituting (18),

$$\begin{aligned} \vec{\xi} = \frac{m \vec{F}_s}{m_v m_s} - \frac{\vec{F}}{m_v} - \frac{m}{m_v} [\dot{\vec{\omega}} \times \vec{\xi}_0 + (\vec{\omega} \cdot \xi_0) \vec{\omega} - \omega^2 \vec{\xi}_0] \\ - \dot{\vec{\omega}} \times \vec{\xi} - 2 (\vec{\omega} \times \vec{\xi}) - (\vec{\omega} \cdot \xi) \vec{\omega} + \omega^2 \vec{\xi} \end{aligned} \quad (21)$$

$$\vec{\xi} = (\vec{\xi})_0 + \int_0^t \dot{\vec{\xi}} dt \quad (22)$$

$$\xi = (\xi)_0 + \int_0^t \dot{\xi} dt \quad (23)$$

NORTHROP SPACE LABORATORIES

The subscript \circ denotes initial conditions.

Inspecting equations (10) and (15),

$$\vec{M}' = \vec{M} - (\vec{\delta} + \vec{\eta}) \times \vec{F}_s + \delta \vec{x} \times \vec{F} \quad (24)$$

Now, for the complete vehicle, about the vehicle c.g.,

$$\vec{M} = \int \dot{\omega} \sigma^2 dm - \int (\dot{\omega} \cdot \vec{\sigma}) \vec{\sigma} dm + \int (\omega \cdot \vec{\sigma}) (\vec{\sigma} \times \vec{\omega}) dm \quad (25)$$

and

$$\int \vec{\sigma} dm = 0 \quad (26)$$

The complete vehicle, without sloshing, would react according to

$$\begin{aligned} \vec{M}' &= \int (\vec{\sigma} + \vec{\delta}) \cdot (\vec{\sigma} + \vec{\delta}) dm - \int [(\vec{\omega} \cdot (\vec{\sigma} + \vec{\delta})) (\vec{\sigma} + \vec{\delta}) dm \\ &\quad + \int [(\vec{\omega} \cdot (\vec{\sigma} + \vec{\delta})) ((\vec{\sigma} + \vec{\delta}) \times \vec{\omega})] dm \\ &= \dot{\omega} [\int \sigma^2 dm + \delta^2 m] - [\int (\dot{\omega} \cdot \vec{\sigma}) \vec{\sigma} dm + (\dot{\omega} \cdot \vec{\delta}) \delta m] \\ &\quad + [\int (\vec{\omega} \cdot \vec{\sigma}) (\vec{\sigma} \times \vec{\omega}) dm + (\vec{\omega} \cdot \vec{\delta}) (\vec{\delta} \times \vec{\omega}) m] \end{aligned} \quad (27)$$

Since the sloshing mass effect, even in the non-sloshing case, is included in \vec{F}_s and \vec{M}_s , the term $[(\vec{\delta} + \vec{\xi}_0) \times \vec{F}_{s1}]$ should be subtracted to produce the actual response to \vec{M}' . An alternative means of expressing the reaction is

$$\begin{aligned} \dot{\omega} \int \sigma^2 dm - \int (\dot{\omega} \cdot \vec{\sigma}) \vec{\sigma} dm + \int (\vec{\omega} \cdot \vec{\sigma}) (\vec{\sigma} \times \vec{\omega}) dm = \\ \vec{M}' - [\delta^2 \vec{\omega} - (\vec{\omega} \cdot \vec{\delta}) \vec{\delta} + (\vec{\omega} \cdot \vec{\delta}) (\vec{\delta} \times \vec{\omega})] m \quad (28) \\ - \vec{\xi} \times \vec{F}_{s1} - (\vec{\delta} + \vec{\eta}) \times \vec{F}_{s2} + \delta \times \vec{F} \end{aligned}$$

Denoting the left side by \vec{R} and substituting (9) and (18),

$$\vec{R} = \vec{M} - \vec{I} - \vec{\xi} \times \vec{F}_{s1} - \vec{\eta} \times \vec{F}_{s2} + \delta \times m (\vec{\mu} - \vec{\omega} \times \vec{\mu}) \quad (29)$$

where

$$\vec{I} = m [\delta^2 \vec{\omega} - (\vec{\omega} \cdot \vec{\delta}) \vec{\delta} \times (\vec{\omega} \cdot \vec{\delta}) (\vec{\delta} \times \vec{\omega})] \quad (30)$$

NORTHROP SPACE LABORATORIES

Alternatively,

$$\vec{R} = \vec{M} - \vec{I} \cdot \vec{\xi} \times \vec{F}_s - \vec{\xi}_0 \times \vec{F}_{s_2} + \delta \times m(\vec{\omega} \times \vec{\omega} \times \vec{\mu}) \quad (31)$$

\vec{R} is, of course, equivalent to the moment for the non-sloshing case.

To modify the computing set-up for the inclusion of sloshing it is desirable to keep sloshing separate. The three slosh-forcing equations (6) are set up. For linear spring and damper the form is

$$\vec{F}_s = -A\vec{\xi} - B\dot{\vec{\xi}} \quad (32)$$

then

$$\vec{F}_{s_2} = \vec{F}_s - q\vec{F} - qm[\vec{\omega} \times \vec{\xi}_0 + (\vec{\omega} \cdot \vec{\xi}_0)\vec{\omega} - \omega^2 \vec{\xi}_0] + q\vec{F}_{s_2} \quad (33)$$

where

$$q = \frac{m_s}{m} \quad (34)$$

and F is the force developed in the simulator. Previously, the force F was the forcing input to the c.g. motion equation. Replacing F in this function with

$$\vec{F}_1 = \vec{F} - \vec{F}_{s_2} \quad (35)$$

Since $\vec{\xi}_0$ is fixed by the location of the centroid of the tank with respect to the c.g. of m , the term

$$\vec{X} = m[\vec{\omega} \times \vec{\xi}_0 + (\vec{\omega} \cdot \vec{\xi}_0)\vec{\omega} - \omega^2 \vec{\xi}_0] \quad (36)$$

may be calculated separately and then summed with F and F_{s_2} prior to multiplying the sum by the term η .

Now,

$$\vec{\xi} = \frac{F_{s_2}}{m_s} - \vec{\omega} \times \vec{\xi} - 2(\vec{\omega} \times \vec{\xi}) - (\vec{\omega} \cdot \vec{\xi})\vec{\omega} + \omega^2 \vec{\xi} \quad (37)$$

and $\vec{\xi}$ and $\dot{\vec{\xi}}$ may be calculated from (22) and (23)

NORTHROP SPACE LABORATORIES

The \vec{M} of the non-sloshing case is now replaced by the \vec{R} of (29), which is now rewritten

$$\vec{R} = \vec{M} - q^2 \vec{I}_1 - \vec{\xi}_0 \times \vec{F}_{s_2} - \vec{\xi} \times \vec{F}_s + q(\vec{\xi}_0 \times \vec{F}) \quad (38)$$

where

$$\vec{I}_1 = m \left[\xi_0^2 \vec{\omega} - (\vec{\omega} \cdot \vec{\xi}_0) \vec{\xi}_0 + (\vec{\omega} \cdot \vec{\xi}_0) (\vec{\xi}_0 \times \vec{a}) \right] \quad (39)$$

APPENDIX I

ELASTIC CORRECTIONS TO EQUATIONS OF MOTION

Structural bending is represented by several modes of vibration, there being a shape for the amplitude curve represented by the shape parameter (references 37, 38, 39, 40, 41). The motion of the point i due to mode j is obtained from

$$\ddot{\eta}_{i,k} + \alpha_k \dot{\eta}_{i,k} + \beta_k \eta_{i,k} = \frac{F_{i,k}}{m_{i,k}} \quad (1)$$

where the α , β and $m_{i,k}$ values are supplied externally to this discussion. The deflection, ξ , is obtained from

$$\xi_{i,k} = \phi_{i,k} \eta_{i,k} \quad (2)$$

and

$$\xi = \sum_k \phi_{i,k} \eta_{i,k} \quad (3)$$

The angle, δ , due to this deflection may be obtained from

$$\delta_{i,k} = \phi'_{i,k} \eta_{i,k} \quad (4)$$

$$\delta = \sum_k \phi'_{i,k} \eta_{i,k} \quad (5)$$

ϕ' and ϕ are developed along with α , β and m .

For the purposes of vehicle motion analysis the terms $\vec{\xi}_k$ and $\vec{\delta}_k$ are developed in the following manner:

$$\vec{\xi}_k + \alpha_k \dot{\vec{\xi}}_k + \beta_k \vec{\xi}_k = -\gamma_{k1} \vec{F} - \gamma_{k2} \vec{M} \quad (6)$$

$$\vec{\xi}_k = \int_0^t \ddot{\xi}_k dt \quad (7)$$

$$\dot{\xi}_k = \int_0^t \ddot{\xi}_k dt \quad (8)$$

γ_k is a constant developed along with α_k and β_k .

$$\vec{\delta}_k = \lambda_k \left(i \times \dot{\xi}_k \right) \quad (9)$$

where the unit vector i is in x direction.

$$\vec{\xi}_f = \sum_k \vec{\xi}_k \quad (10)$$

$$\vec{\delta}_k = \sum_k \vec{\delta}_k \quad (11)$$

where all motions are relative to the rigid axis system of the vehicle. In the case of torsion, the $\vec{\delta}_f$ is developed directly from an equation having the same form as (6) except that δ_k is substituted for ξ_k and there is no force term. There is also no deflection.

Equation (1) of Appendix G gives the velocity of a point referred to inertial axes. Modifying this equation,

$$\vec{v} = \vec{u} + \dot{\xi}_f + \omega \times \xi + \omega \times \xi_f \quad (12)$$

where ξ is a constant. Since ξ_f only appears in y and z this is not as large a change as might be expected.

Assuming that angles developed due to structural deflection remain small,

$$\theta_f = \omega y_f \quad (13)$$

$$\psi_f = \omega z_f \quad (14)$$

$$\phi_f = \omega x_f \quad (15)$$

where

NORTHROP SPACE LABORATORIES

$$\vec{\delta}_f = \vec{i} w_{x_f} + \vec{j} w_{y_f} + \vec{k} w_{z_f} \quad (16)$$

and all non-linear terms are neglected.

The desired axes are rigidly fixed to a point on the probe or drogue and rotate as the material around this point rotates. The axes are, generally, rotated through the angles θ_f , ϕ_f and ψ_f with respect to the rigid vehicle axes. However, presuming small deflections,

$$\vec{V}_{i_1} = \vec{V}_i + \Delta\vec{V} \quad (17)$$

where \vec{V}_{i_1} will be used to replace \vec{V}_i for the rigid vehicle.

$$U_{i_1} = U_c + W_{yz} - W_{zy} + W_{yz_f} - W_{zy_f} \quad (18)$$

$$V_{i_1} = V_c + W_{zx} - W_{xz} - W_{xz_f} + \dot{y}_f \quad (19)$$

$$W_{i_1} = W_c + \dot{z}_f + W_{xy} - W_{yx} + W_{xy_f} \quad (20)$$

$$U_i = U_{i_1} + V_{i_1} \psi_f - W_{i_1} \theta_f \quad (21)$$

$$v_i = v_{i_1} + W_{i_1} \phi_f - U_{i_1} \psi_f \quad (22)$$

$$W_i = W_{i_1} + U_{i_1} \theta_f - v_{i_1} \phi_f \quad (23)$$

Similarly,

$$W_{xi_1} = W_x + W_{x_f} \quad (24)$$

$$W_{yi_1} = W_y + W_{y_f} \quad (25)$$

$$W_{zi_1} = W_z + W_{z_f} \quad (26)$$

$$W_{xi_1} = W_{xi_1} + W_{yi_1} \psi_f - W_{zi_1} \theta_f \quad (27)$$

$$W_{yi_1} = W_{yi_1} + W_{zi_1} \phi_f - W_{xi_1} \psi_f \quad (28)$$

$$W_{zi_1} = W_{zi_1} + W_{xi_1} \theta_f - W_{yi_1} \phi_f \quad (29)$$

The W_{xi_1} , W_{yi_1} and W_{zi_1} values given involve small additions to the W_x , W_y and W_z values of Appendix G, and substitute for them.

NORTHROP SPACE LABORATORIES

Similarly, the u_i , v_i and w_i values given here substitute for the u_i , v_i and w_i values of Appendix G. The U_e , V_e and W_e values of (18) through (20) are the u_c , v_c and w_c terms of Appendix G. With these changes, no further changes need be made.

APPENDIX J

EFFECTS OF GRAVITY ON EQUATION OF MOTION

The primary effect of the gravitational field for this problem is the differential acceleration on the two vehicles, and on the various elements of each vehicle. The first effect causes one vehicle to translate with respect to the other, and the second causes rotation. Since the effect is small, the assumption that the vehicles are in very nearly a circular orbit is reasonable for determining the effect.

Because the vital motions are those of one vehicle relative to the other, it is convenient to use the drogue as a base. The drogue vehicle is given an initial orientation with respect to the response axis system in terms of the Euler angles ψ , θ , and ϕ . Separately, the simulator initial angles, ψ_d , θ_d and ϕ_p have been established. From these two sets of angles, the Euler angles for the probe vehicle with respect to gravity reference space may be established. Then the constant

$$\Omega^2 = \frac{GM}{R^3}$$

is established, where

G = Newton's gravitational constant

M = planetary mass

R = distance of drogue c.g. from center
of planet

NORTHROP SPACE LABORATORIES

For orbits close to the earth Ω^2 will be about 1.5×10^{-6} per second².

For drogue vehicle c.g. starts at the origin of the rotating system thus formed and any velocity imparted to its c.g. will cause it to move. The probe vehicle c.g. starts off the origin. The position of the drogue is determined first by the formula

$$\vec{\eta} = \int_0^t \vec{\eta} dt \quad (2)$$

$$\vec{\eta} = \vec{\mu} - (\vec{k} \Omega) \times \vec{\eta} \quad (3)$$

where $\vec{\mu}$ is obtained by axis transformation from the c.g. velocity of the drogue. The position of the probe is determined first by establishing its position in drogue space (origin at drogue c.g.), transforming this position to gravity space, then adding to the drogue position. For each vehicle, then, the acceleration due to gravity is

$$\vec{a} = -\Omega^2 \left[z \vec{i} x + \vec{j} y + \vec{k} z \right] \quad (4)$$

The separation of the two c.g.'s is in the order of 40 to 50 ft. At the end of five minutes, one vehicle will move about 6.5 ft. under the influence of differential gravity.

The acceleration is then transformed back to vehicle axes and summed into the acceleration produced by other forces.

To perform the transformation, the angles are needed. For each vehicle

$$\dot{\theta} = \omega_y \cos \theta - \omega_z \sin \theta \quad (5)$$

$$\dot{\psi} = (\omega_y \sin \theta + \omega_z \cos \theta) / \cos \theta - \Omega \quad (6)$$

$$\dot{\phi} = \omega_x + \dot{\psi} \sin \theta \quad (7)$$

$$\theta = \theta_0 + \int_0^t \dot{\theta} dt \quad (8)$$

$$\psi = \psi_0 + \int_0^t \dot{\psi} dt \quad (9)$$

$$\phi = \phi_0 + \int_0^t \dot{\phi} dt \quad (10)$$

NORTHROP SPACE LABORATORIES

Each vehicle is also acted upon by the moments,

$$M_x = -\Omega^2 \left\{ f_{11} (f_{13} I_{xy} - f_{12} I_{xz}) + f_{13} f_{12} (I_{zz} - I_{yy}) + (f_{13}^2 - f_{12}^2) I_{yz} \right\} \quad (11)$$

$$M_y = -\Omega^2 \left\{ f_{12} (f_{11} I_{yz} - f_{13} I_{xy}) + f_{11} f_{13} (I_{xx} - I_{zz}) + (f_{11}^2 - f_{13}^2) I_{xz} \right\} \quad (12)$$

$$M_z = -\Omega^2 \left\{ f_{13} (f_{12} I_{xz} - f_{11} I_{yz}) + f_{11} f_{12} (I_{yy} - I_{xx}) + (f_{12}^2 - f_{11}^2) I_{xy} \right\} \quad (13)$$

which act along vehicle axes, the f terms being determined as in Appendix C for the angles as determined above. Near the Earth, the maximum angular acceleration will be 1.5×10^{-6} rad/sec².

APPENDIX K

PROBE-DROGUE RELATIONSHIP

For checkout purposes, it was necessary to substitute for the simulator probe and drogue with the analogue computer. The method of doing this is to assume a probe consisting of a spherical tip on a shank which has length but no other dimension.

The center of the probe tip is located at

$$X_{t_p} = X_{t_0} = X_t \quad (1)$$

from the point of interest on the probe vehicle. The probe consists of a spring damper arrangement which is non-linear.

$$\ddot{X}_t = A (F_{x_{p1}} - F_{x_p}) \quad (2)$$

$$F_{x_p} = f (X_t, \dot{X}_t) \quad (3)$$

$$\dot{X}_t = \int_0^t \ddot{X}_t dt \quad (4)$$

$$X_t = \int_0^t \dot{X}_t dt \quad (5)$$

In addition, the probe tip deflects:

$$Y_{t_p} = BF_{y_p} \quad (6)$$

$$Y_{t_p} = BF_{z_p} \quad (7)$$

NORTHROP SPACE LABORATORIES

However, some simplification results from circular similarity and we may write

$$X_{t_{p1}} = X_t \quad (8)$$

$$Y_{t_{p1}} = BF_{y_p} \quad (9)$$

$$Z_{t_p} = BF_{z_p} \quad (10)$$

$$F_{y_{p1}} = F_{y_p} \cos \theta_p - F_{z_p} \sin \theta_p \quad (11)$$

$$F_{z_p} = F_{z_p} \cos \theta_p = F_{y_p} \sin \theta_p \quad (12)$$

On the drogue, the apex of the cone is at a distance X_a from the point of interest. The distance of the center of the probe tip from the apex is, then,

$$\begin{aligned} x_1 &= - (X_d - x_{t_{p1}}) \cos \theta_d \cos \psi_d + X_a + (Z_p + z_{t_p}) \sin \theta_d \\ &= (Y_p + y_{t_{p1}}) \cos \theta_d \sin \psi_d \end{aligned} \quad (13)$$

$$y_1 = (X_d - x_{t_p}) \sin \theta_d + (Y_p + y_{t_{p1}}) \cos \psi_d \quad (14)$$

$$\begin{aligned} z_1 &= - (X_d - x_{t_{p1}}) \sin \theta_d \cos \psi_d + (Y_p + y_{t_{p1}}) \sin \theta_d \sin \psi_d \\ &\quad + (Z_p + z_{t_p}) \cos \theta_d \end{aligned} \quad (15)$$

Let

$$r_1 = \sqrt{y_1^2 + z_1^2} \quad (16)$$

NORTHROP SPACE LABORATORIES

and

$$r_c = \frac{r_1 - kx_1}{\sqrt{1 + k^2}} + r_t \quad (17)$$

$$x_c = \frac{x_1 + kr_1}{\sqrt{1 + k^2}} \quad (18)$$

$$\dot{x}_c = \frac{dx_c}{dt} \quad (19)$$

$$\dot{\phi}_c = \frac{y_1 \dot{z}_1 - z_1 \dot{y}_1}{y_1^2 + z_1^2} \quad (20)$$

$$V_\phi = r_m \dot{\phi}_c \quad (\text{neglecting effect of } \dot{\phi}_p) \quad (21)$$

$$V_s = \sqrt{V_\phi^2 + x_c^2} \quad (22)$$

$$F_n = 0 \text{ for } r_c = 0 \quad (23)$$

$$Cr_c \text{ for } r_c = 0 \quad (C \text{ very large}) \quad (24)$$

$$\Gamma_s = \mu F_n \quad (25)$$

$$F_c = r_s \frac{\dot{x}_c}{V_s} \quad (26)$$

$$F_\phi = F_s \frac{V_\phi}{V_s} \quad (27)$$

$$F_{x_d} = \frac{F_c - F_{mk}}{\sqrt{1 + k^2}} \quad (28)$$

$$F_r = \frac{F_n + kF_c}{\sqrt{1 + k^2}} \quad (29)$$

$$F_{y_d} = \frac{y_1 \Gamma_r - z_1 F_\phi}{r_1} \quad (30)$$

NORTHROP SPACE LABORATORIES

$$F_{z_d} = \frac{z_1 F_{x_1} + y_1 F_{y_1}}{1} \quad (31)$$

$$x_m = x_1 + x_a + \frac{kr_t}{\sqrt{1+k^2}} \quad (32)$$

$$r_m = r_1 + \frac{r_t}{\sqrt{1+k^2}} \quad (33)$$

$$y_m = r_m \frac{y_1}{r_1} = y_1 + \frac{r_t}{r_1} \frac{y_1}{\sqrt{1+k^2}} = y_1 \left(1 + \frac{r_t/r_1}{\sqrt{1+k^2}}\right) \quad (34)$$

$$z_m = r_m \frac{z_1}{r_1} = z_1 + \frac{r_t}{r_1} \frac{z_1}{\sqrt{1+k^2}} = z_1 \left(1 + \frac{r_t/r_1}{\sqrt{1+k^2}}\right) \quad (35)$$

$$M_{x_d} = y_m F_{z_d} - z_m F_{y_d} = \left(r_1 \frac{r_t}{\sqrt{1+k^2}}\right) F_{y_1} \quad (36)$$

$$M_{y_d} = z_m F_{x_d} - x_m F_{z_d} \quad (37)$$

$$M_{z_d} = x_m F_{y_d} - y_m F_{x_d} \quad (38)$$

The terms F_{x_d} , F_{y_d} , F_{z_d} , M_{x_d} , M_{y_d} , and M_{z_d} are the forces and moments applied to the drogue vehicle at the point of interest.

They are thus substituted directly for the forces and moments to be supplied by the simulator.

For the probe vehicle, the values of F_{x_d} , F_{y_d} , and F_{z_d} are reversed in sign and transformed by the equations.

$$F_{x_p} = -F_{x_d} \cos \theta_d \cos \psi_d + F_{y_d} \sin \psi_d - F_{z_d} \sin \theta_d \cos \psi_d \quad (39)$$

$$F_{y_p} = -F_{x_d} \cos \theta_d \sin \psi_d - F_{y_d} \cos \psi_d - F_{z_d} \sin \theta_d \sin \psi_d \quad (40)$$

$$F_{z_p} = F_{x_d} \sin \theta_d - F_{z_d} \cos \theta_d \quad (41)$$

Then, F_{x_p} may be developed from (3) using equations (1), (2), (4) and (5).

NORTHROP SPACE LABORATORIES

$$F_{y_p} = F_{y_{p_1}} \cos \theta_p + F_{z_{p_1}} \sin \theta_p \quad (42)$$

$$F_{z_p} = F_{z_{p_1}} \cos \theta_p - F_{y_{p_1}} \sin \theta_p \quad (43)$$

There is a small moment on the tip of the probe:

$$M_{x_{p_4}} = -F_{\theta} r_t \quad (44)$$

$$M_{y_{p_4}} = -F_c r_t \quad (45)$$

from which

$$M_{x_{p_3}} = M_{x_{p_4}} \sqrt{1+k^2} \quad (46)$$

$$M_{y_{p_3}} = M_{y_{p_4}} \quad (47)$$

$$M_{y_{p_3}} = M_{y_{p_3}} \quad (47)$$

$$M_{x_{p_2}} = M_{x_{p_3}} \quad (48)$$

$$M_{y_{p_2}} = -M_{y_{p_3}} \frac{z_1}{r_1} + M_{z_{p_3}} \frac{y_1}{r_1} \quad (49)$$

$$M_{z_{p_2}} = M_{y_{p_3}} \frac{y_1}{r_1} - M_{z_{p_3}} \frac{z_1}{r_1} \quad (50)$$

$$M_{x_{p_1}} = M_{x_{p_2}} \cos \theta_d \cos \psi_d - M_{y_{p_2}} \sin \psi_d + M_{z_{p_2}} \sin \theta_2 \cos \psi_d + y_t F_{z_{p_1}} - z_t F_{y_{p_1}} \quad (51)$$

NORTHROP SPACE LABORATORIES

$$M_{y_{p_1}} = M_{x_{p_2}} \cos \theta_d \sin \psi_d + M_{y_{p_2}} \cos \psi_d + M_{z_{p_2}} \sin \theta_d \sin \psi_d + z_{t_{p_1}} F_{x_p} - x_{t_p} F_{z_{p_1}} \quad (52)$$

$$M_{z_{p_1}} = -M_{x_{p_2}} \sin \theta_d + M_{z_{p_1}} \cos \theta_d + x_{t_p} F_{y_{p_1}} - y_{t_{p_1}} F_{x_p} \quad (53)$$

$$M_{x_p} = M_{x_{p_1}} \quad (54)$$

$$M_{y_p} = M_{y_{p_1}} \cos \theta_p + M_{z_{p_1}} \sin \theta_p \quad (55)$$

$$M_{z_p} = M_{z_{p_1}} \cos \theta_p - M_{y_{p_1}} \sin \theta_p \quad (56)$$

The terms F_{x_p} , F_{y_p} , F_{z_p} , M_{x_p} , M_{y_p} and M_{z_p} are directly applicable to the point of interest on the probe.

These expressions may be mechanized and used for checkout of the computer setup. However, the large requirement for multipliers may create equipment problems. An approach to avoid excessive complication is to presume that the angles ψ_d , θ_d , and θ_p are small. By making ψ_d and θ_p negligible, the terms containing sines of these angles are eliminated and r_1 becomes $|z_1|$. This permits the use of switching to replace resolving action in many areas. Also, terms involving multiplication may be linearized ($\cos \theta_d \approx 1$), thus eliminating more multipliers. The final mechanization at Northrop involved 8 multipliers, some of those not really needed. If the desire is to check to x-y plane instead of x-z, the mechanization is substantially the same, but using y_1 instead of z_1 .

APPENDIX L

ANALOG COMPUTER PROGRAM

WIRING NETWORKS AND DIAGRAMS

Figure L-1 shows the symbols used in the analog computer circuit diagrams.

Figures L-2 through L-10 show the analog computer schematic for the solution of the basic rigid-body problem. The force and moment amplifiers are buffers between the simulator force balance output resolver circuit (not shown) and the computer proper. They may be used as summers when additional forces and moments (e.g., due to controls, gravity, fuel slosh) must be considered.

As developed in these diagrams, the computer will act simply as a substitute for the vehicles, the main outputs being the motions directly applicable to the simulator. Although the information required to develop individual vehicle motion with respect to fixed space is available, the circuitry for making the necessary computations is not shown.

This portion of the computer utilizes 58 electronic multipliers, 6 electronic resolves, 170 amplifiers (18 as integrators) and 96 servoset potentiometers. It includes every term in the rigid-body equations of motion, and has been checked out on the Northrop Corporation AD 256 Analog computer. Development of the motion with respect to fixed space of each vehicle will require 54 additional electronic multipliers, 12 additional electronic resolves, 114 amplifiers (12 as

NORTHROP SPACE LABORATORIES

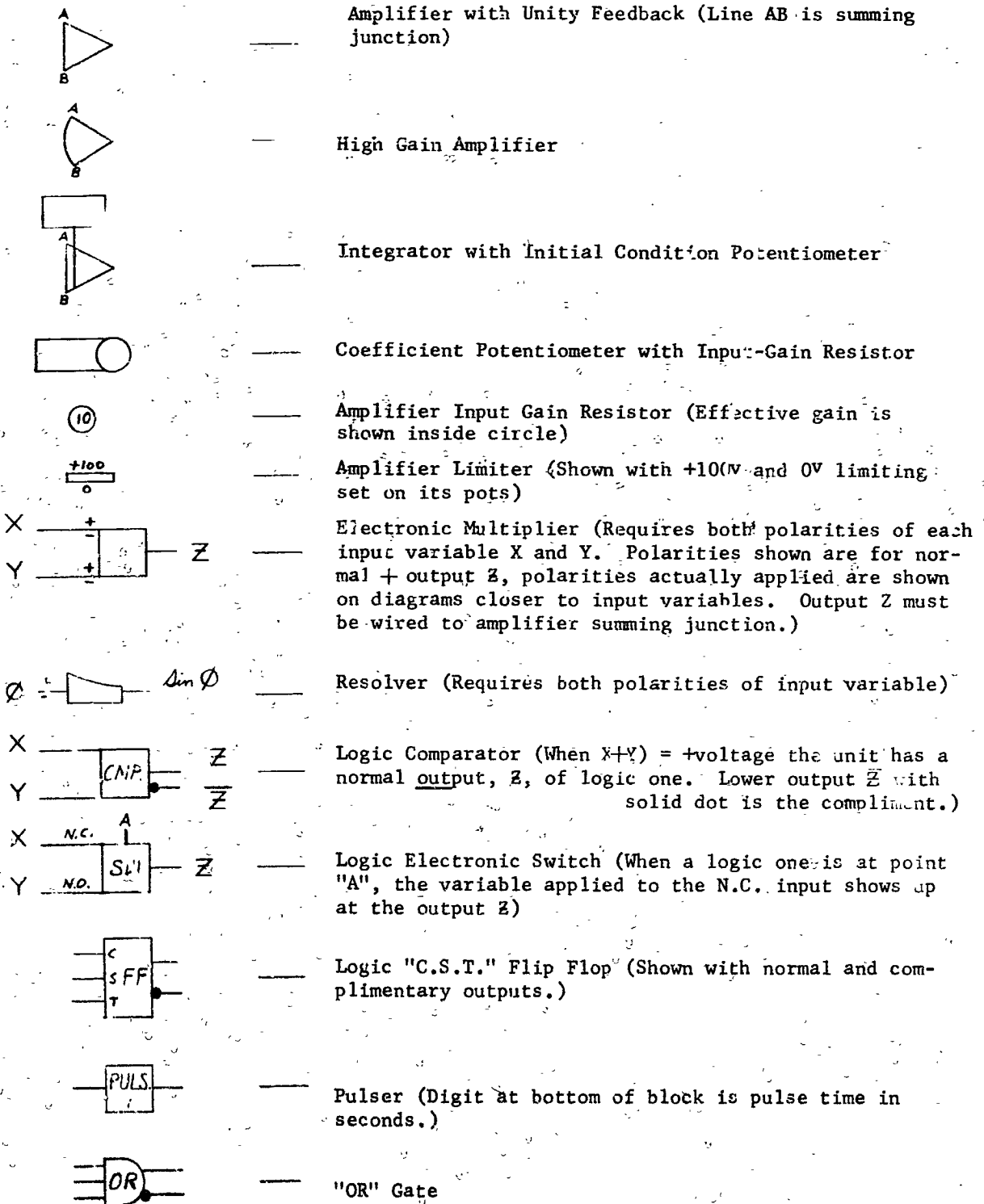


FIGURE L-1 KEY TO ANALOG SYMBOLS

NORTHROP SPACE LABORATORIES

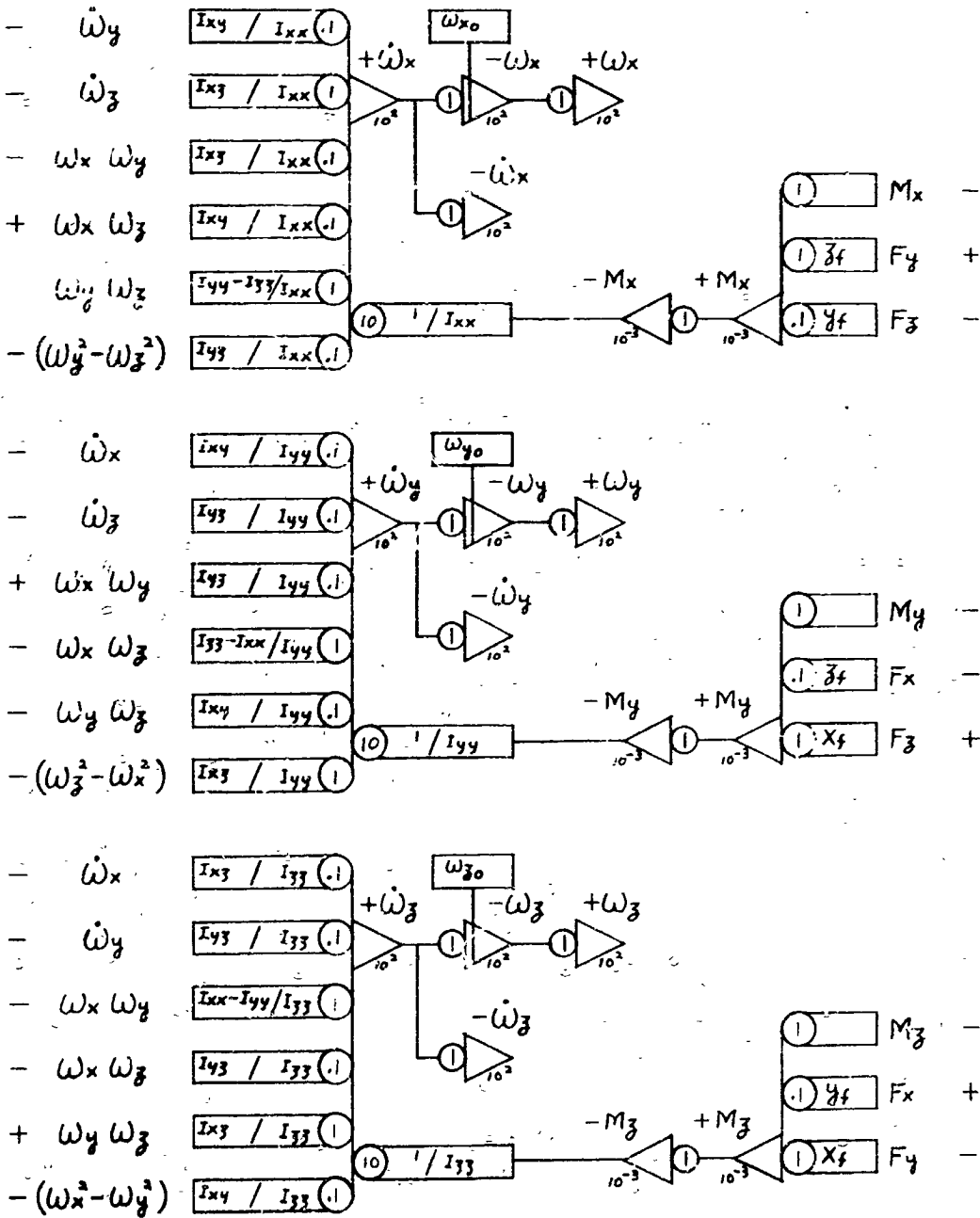


FIGURE L-2 PROBE VEHICLE MOTION - ROTATIONAL MOTION
(All Identities On This Sheet Are To Be Subscript P)

NORTHROP SPACE LABORATORIES

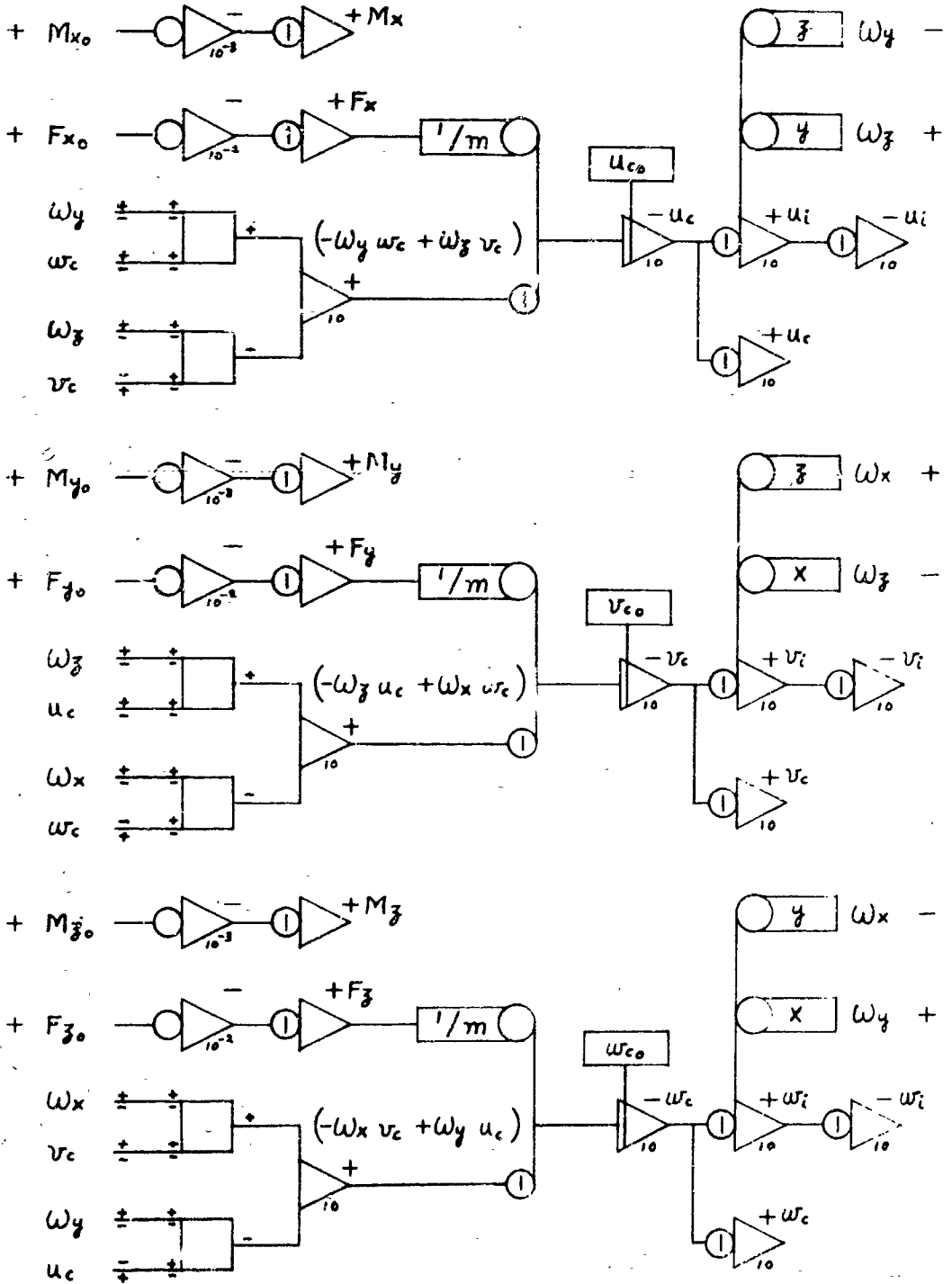


FIGURE L-3 - PROBE VEHICLE MOTION - TRANSLATIONAL MOTION

(All Identities On This Sheet Are To Be Subscript P)

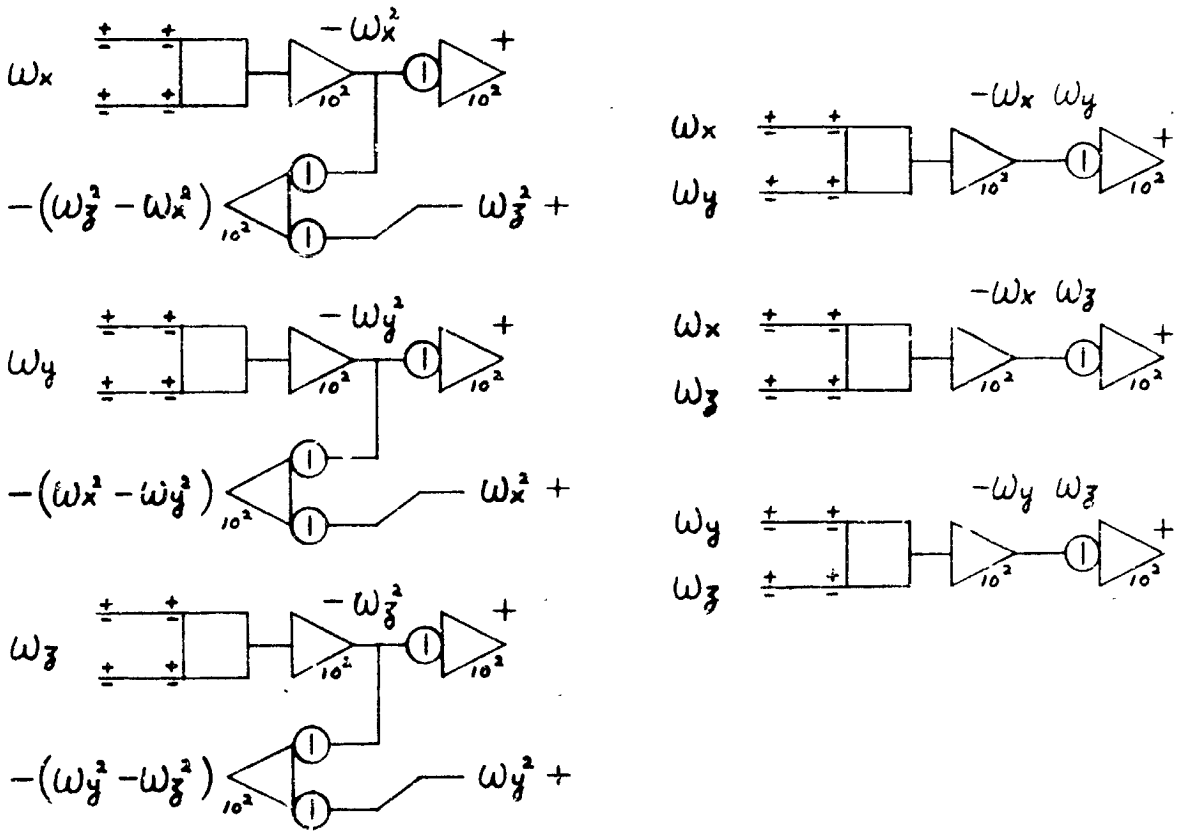


FIGURE L-4 PROBE VEHICLE MOTION - ROTATIONAL RATE PRODUCTS
 (All Identities On This Sheet Are To Be Subscript P)

NORTHROP SPACE LABORATORIES

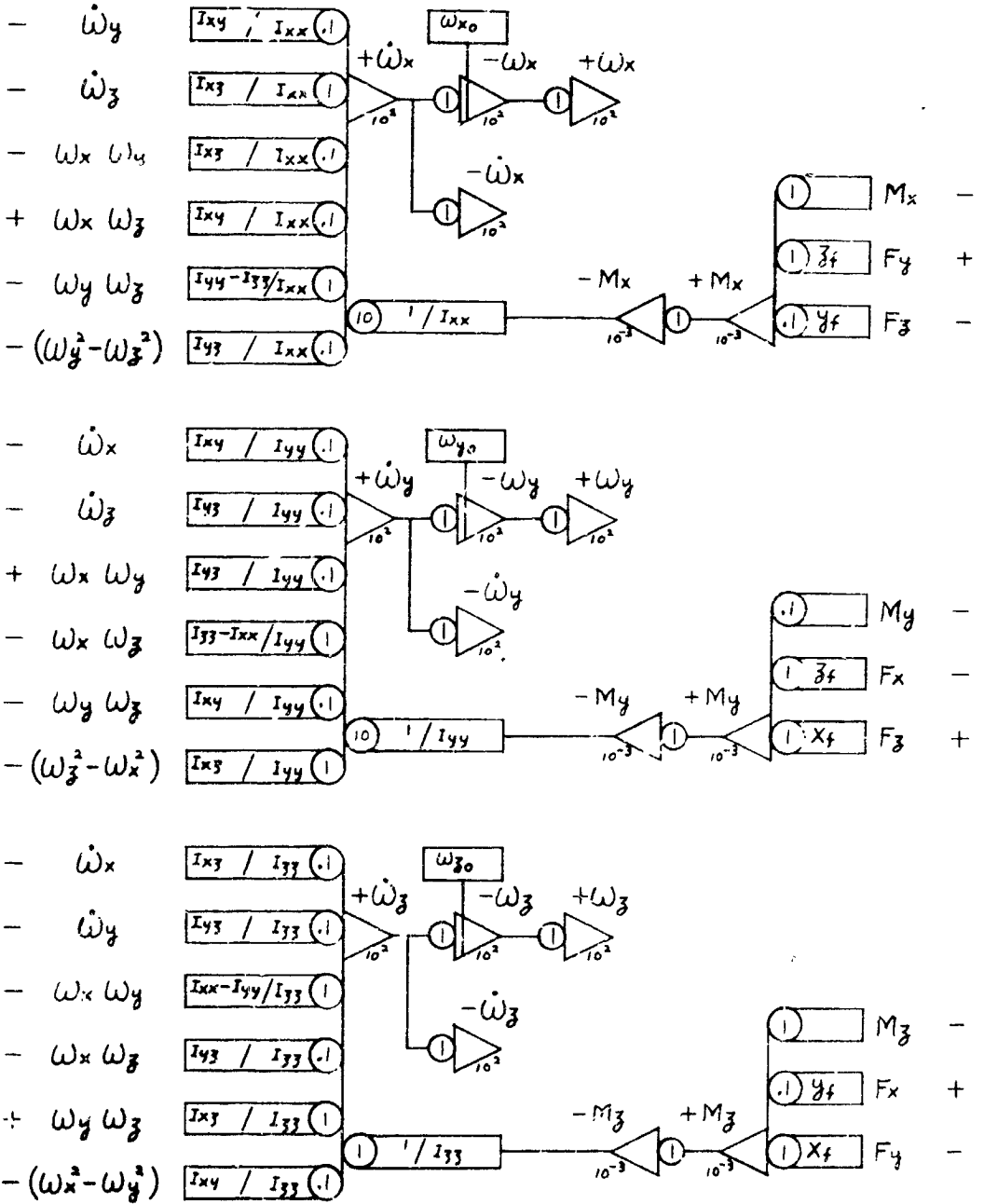


FIGURE L-5 DROGUE VEHICLE MOTION - ROTATIONAL MOTION
(All Identities On This Sheet Are To Be Subscript d)

NORTHROP SPACE LABORATORIES

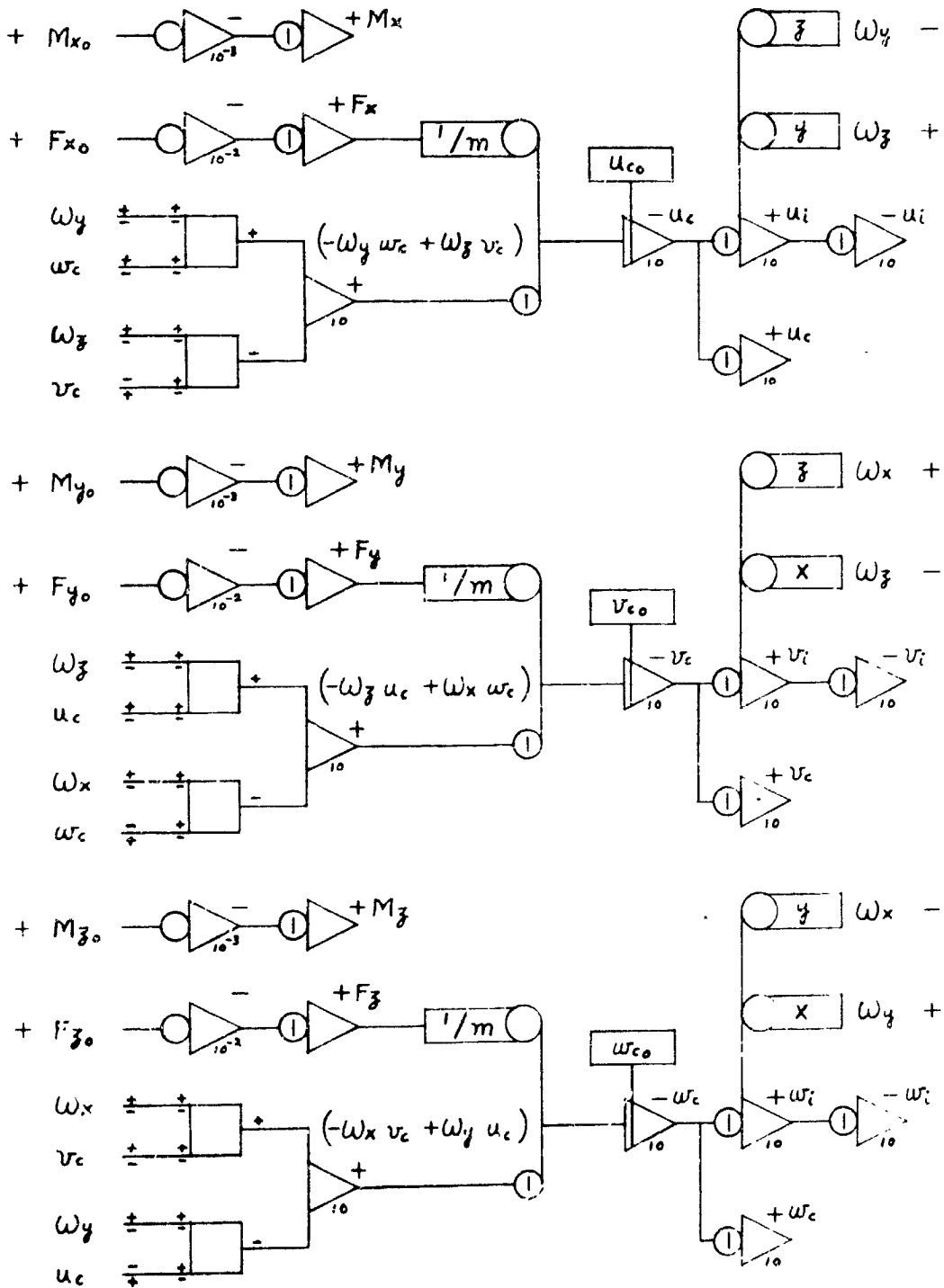


FIGURE L-6 DROGUE VEHICLE MOTION - TRANSLATIONAL MOTION
(All Identities On This Sheet Are To Be Subscript d)

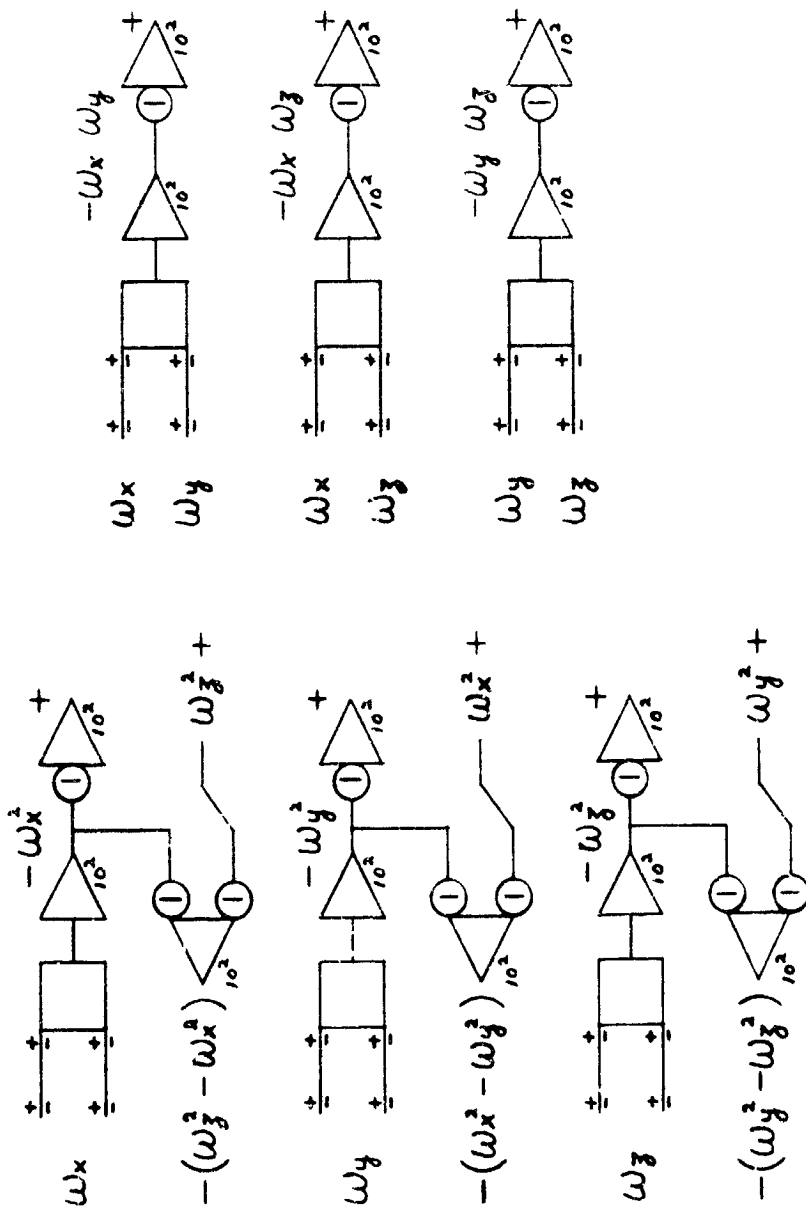


FIGURE L-7 DROGUE VEHICLE MOTION - ROTATIONAL RATE PRODUCTS
(All Identifications On This Sheet
Are To Be Subscript d)

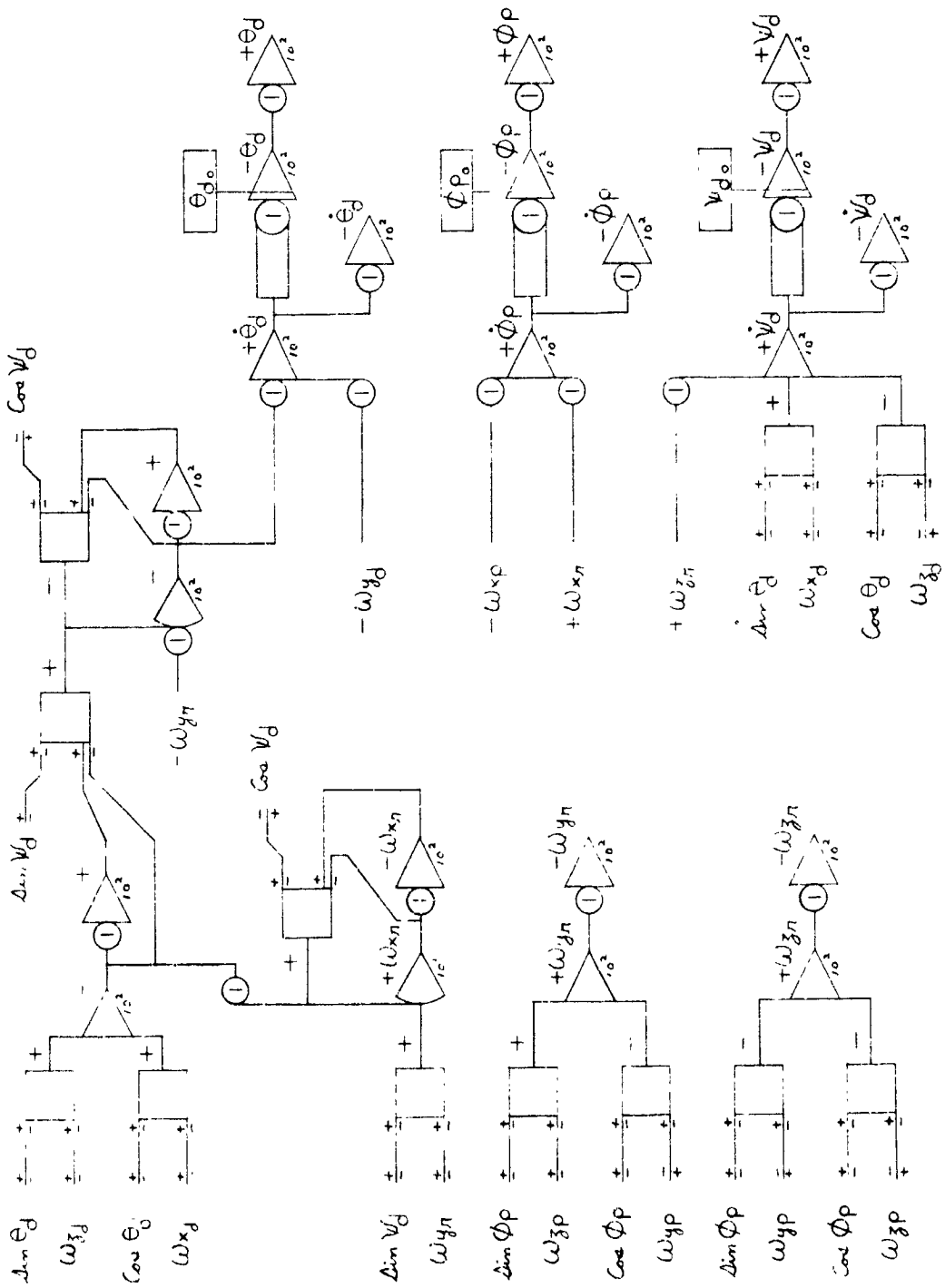


FIGURE L-8 SIMULATOR MOTION - ANGLE DEVELOPMENT

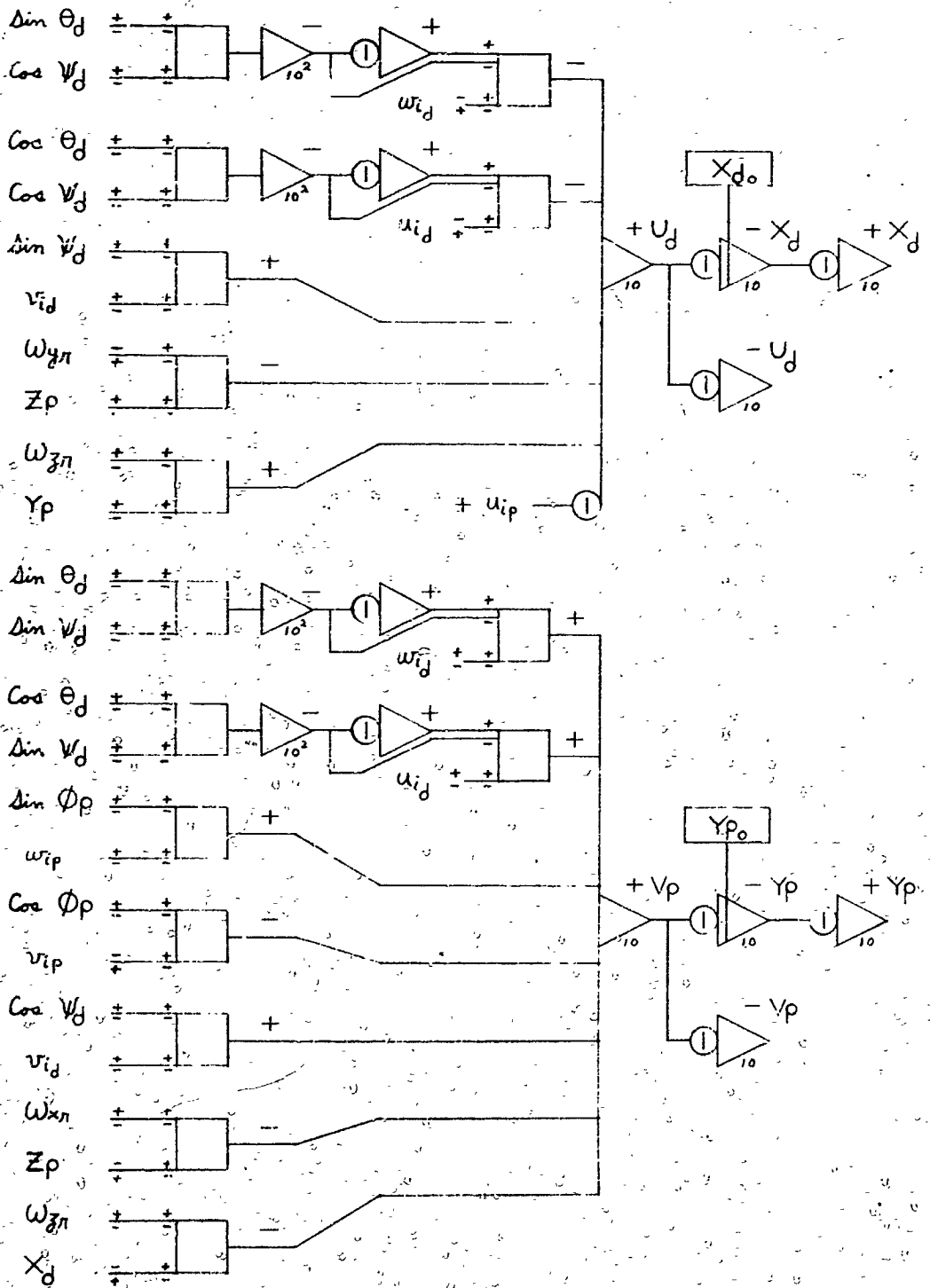


FIGURE L-9 SIMULATOR MOTION - TRANSLATIONAL MOTION

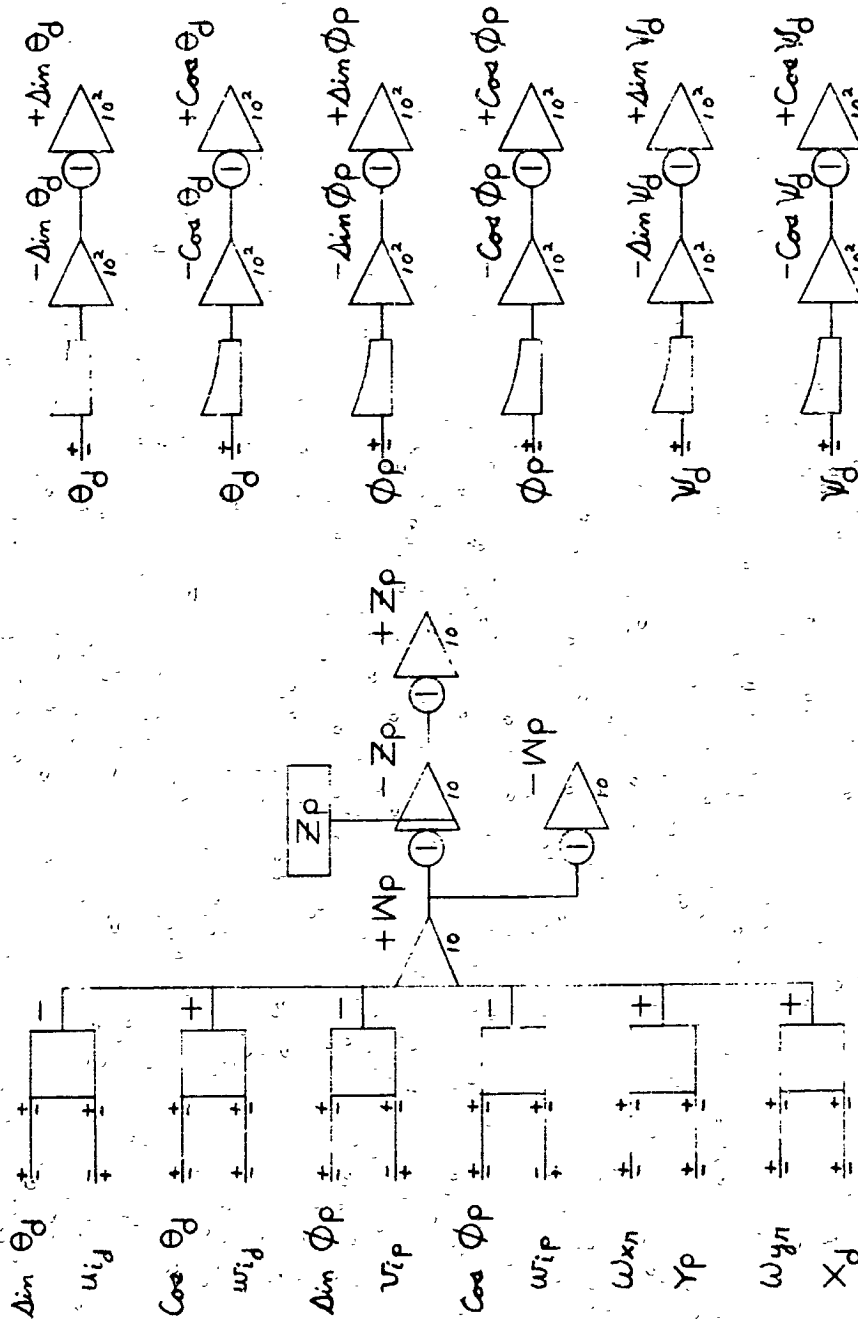


FIGURE L-10 SIMULATOR MOTION - VEHICLE RESOLUTIONS

NORTHROP SPACE LABORATORIES

integrators) and twelve additional servo-set potentiometers.

Figure L-11 shows a single-channel attitude control using on-off control to produce moments and unbalanced forces. The on-time minimum is continuously variable from the minimum computer response time to 0.1 second. Since no attitude control information has been received, this diagram is included as representative. If this represents the vehicle control systems, then 12 operational amplifiers (one as an integrator), 2 electronic switches, 3 comparators, 3 "or" gates, 2 flip-flops limiter and 5 potentiometers will be needed for each control channel, of which there are six.

The inclusion of fuel sloshing in the computer schematic is not shown, but will add about 12 electronic multipliers, 18 operational amplifiers and 20 potentiometers per tank. Conceivably, some of the multipliers might be dropped on the basis that the contribution will be below the level of inaccuracy introduced by the basic assumption of the fuel acting as a spring-supported point mass. Fuel sloshing may occur in 0, 2, or 4 tanks for the two vehicles.

Structural flexure may be included rather simply, although the schematics are not shown here. The requirement is for 3 operational amplifiers (2 integrators) and 5 potentiometers per mode. Because deflections are summed together before further operations are performed, the rest of the equipment required is per vehicle. This totals 44 amplifiers (5 integrators) and 16 multipliers. Three types of flexure may be handled: symmetric, anti-symmetric, and torsional. Assuming 9 modes per type, the total requirement for handling two vehicles will be 250 amplifiers (118 as integrators) 270 potentiometers and 32 multipliers.

The gravity influence is also not shown, but approximate requirements may be inferred from the information in Appendix J. To generate the angles (2 vehicles) will require 12 multipliers and 16 amplifiers, assuming that only roll needs be considered to $\pm 180^\circ$ and

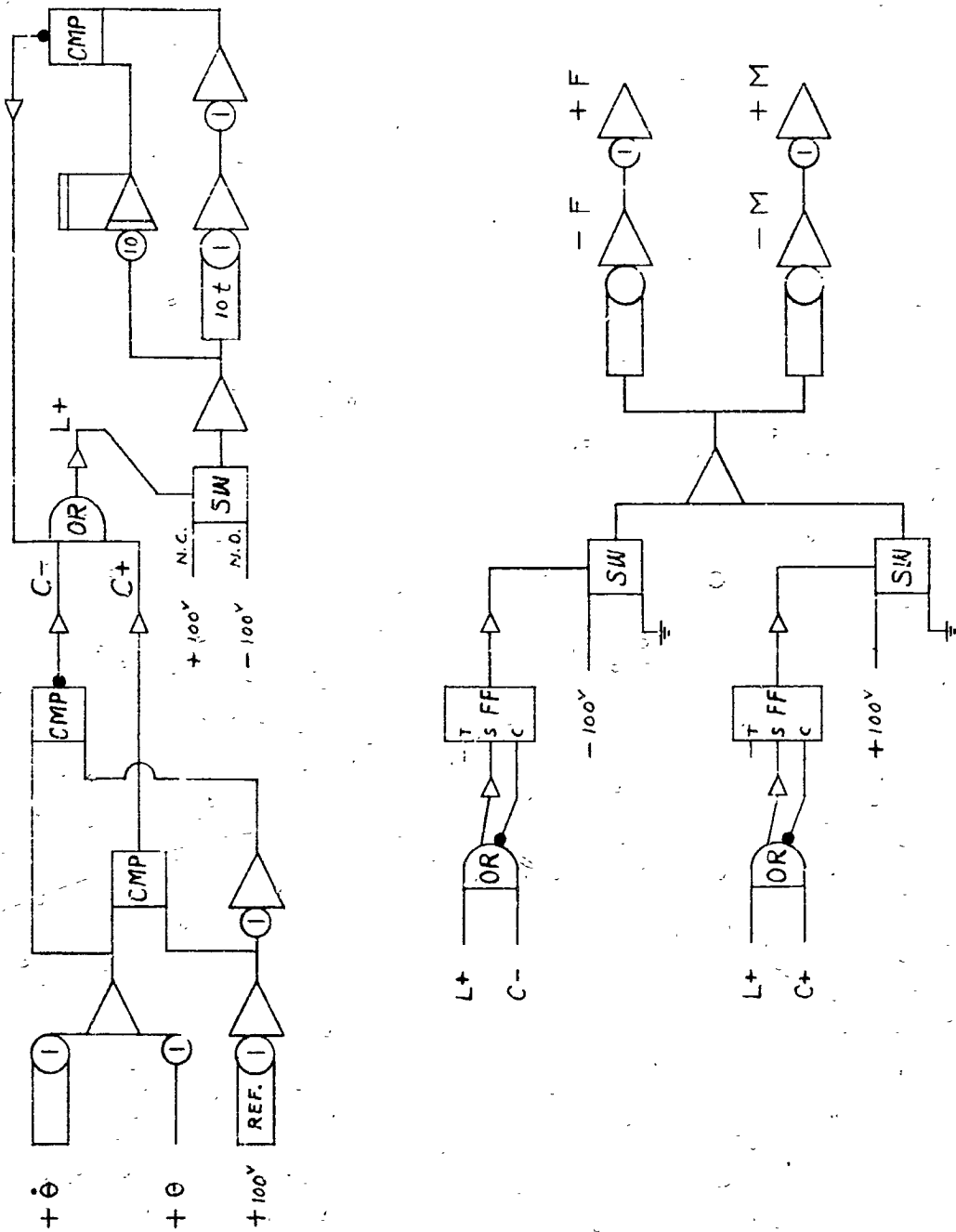


FIGURE L-11 ATTITUDE CONTROL

NORTHROP SPACE LABORATORIES

that ψ and θ are neutral at 90° increments from the gravity axes. The axis transformation coefficients require 24 multipliers and 48 amplifiers. Resolution of drogue vehicle velocities and computation of its distance from the gravity axis origin require 9 multipliers, 9 amplifiers (3 integrators) and 6 potentiometers. Resolution of probe vehicle c.g. position is done in a different manner to preserve accuracy of the intervehicle distances and requires 21 multipliers, 21 amplifiers and 3 potentiometers. Generation of the six components of acceleration (three per vehicle) requires 12 amplifiers and 6 potentiometers. Transformation of these accelerations back to vehicle axes requires 18 multipliers and an amplifier. Generation of the moments requires 12 multipliers, 30 amplifiers and 12 potentiometers. Thus, a total of 96 multipliers, 160 amplifiers (6 as integrators) 12 resolvers and 27 potentiometers is required. The only realistic method of getting the small voltages through is to generate the accelerations and moments at high voltage levels and then reduce them just prior to summing into the motion integrators.

Figures L-12 and L-13 show the probe-drogue interaction mechanization used to check out the Northrop set-up of the basic equations of motion. This simplified coplaner solution was intended only to indicate the nature of the collision and did not attempt to duplicate exactly the action of the real equipment. The circuit requires 8 multipliers, 40 amplifiers (3 integrators) 18 potentiometers, 2 limiters, 3 comparators, 2 electronic switches, 2 single-show multivibrators and 1 flip-flop. This includes a cut-off circuit (Figure L-14) which returns the computer to initial condition when the probe tip enters the apex of the drogue cone. This circuit may be used in the simulator for safety cut-off either returning the computer to "hold" or initial condition.

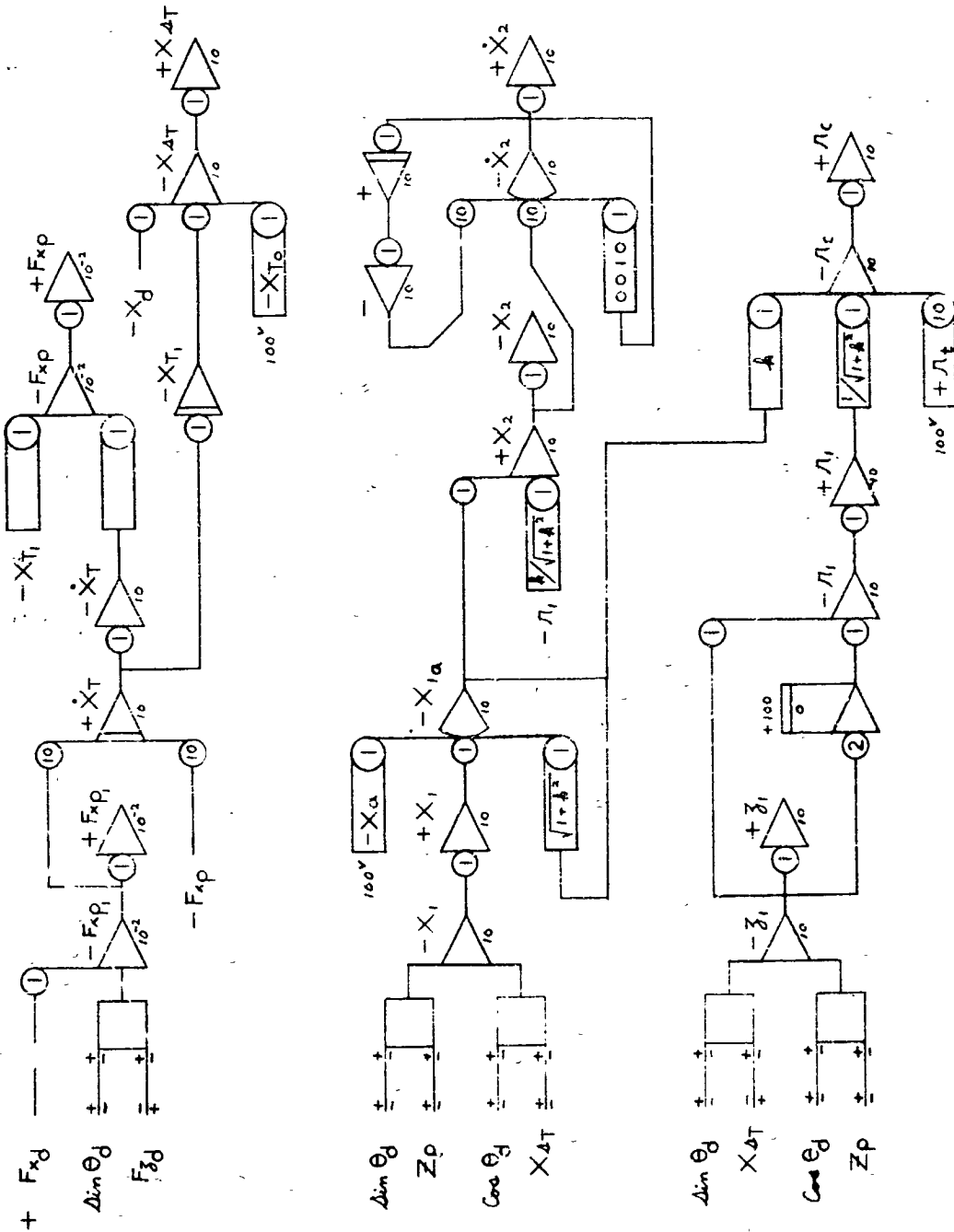


FIGURE L-12 PROBE-DROGUE INTERACTION - POSITION RELATIONSHIP

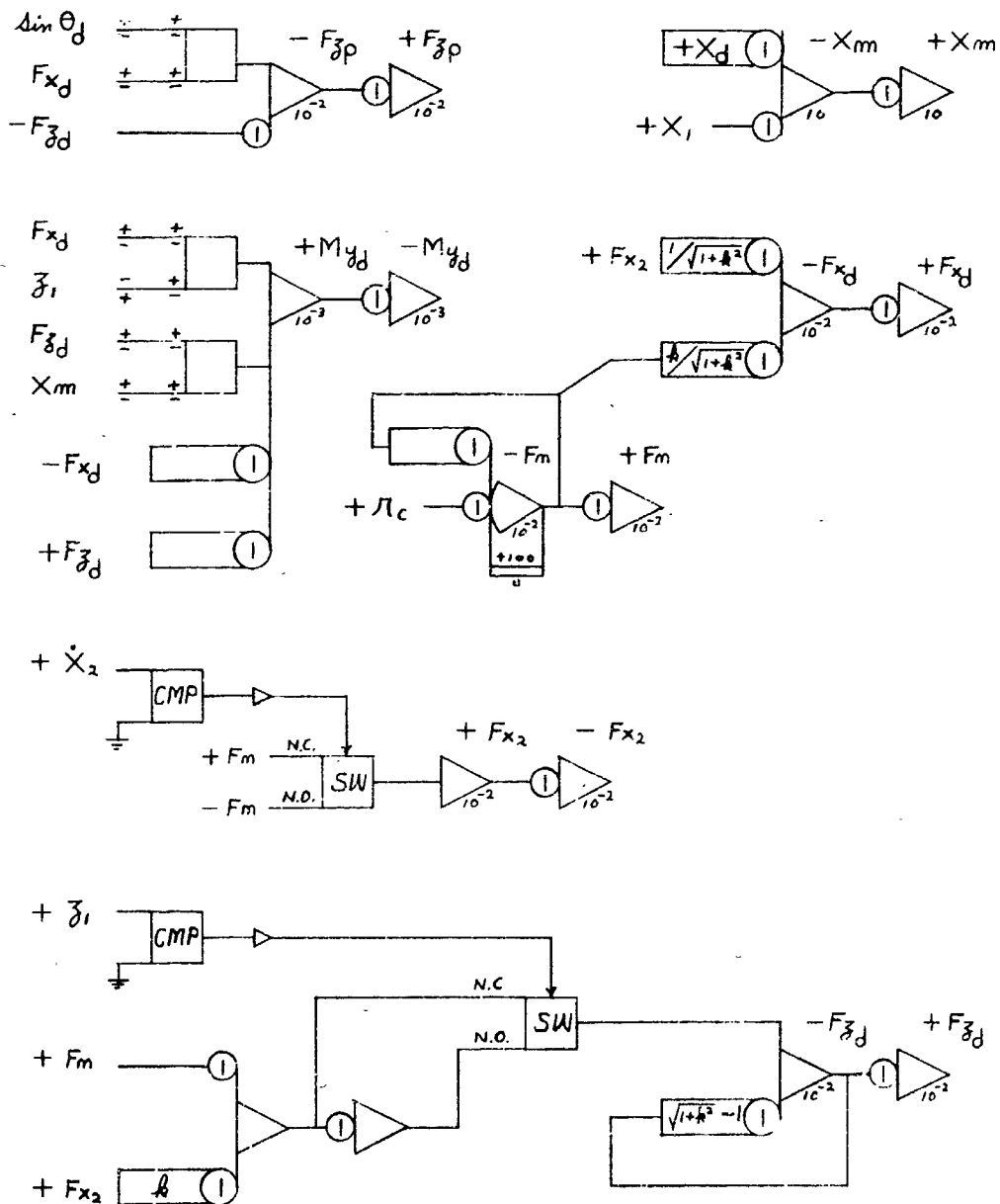


FIGURE L-13 PROBE-DROGUE INTERACTION - FORCE AND MOMENTS

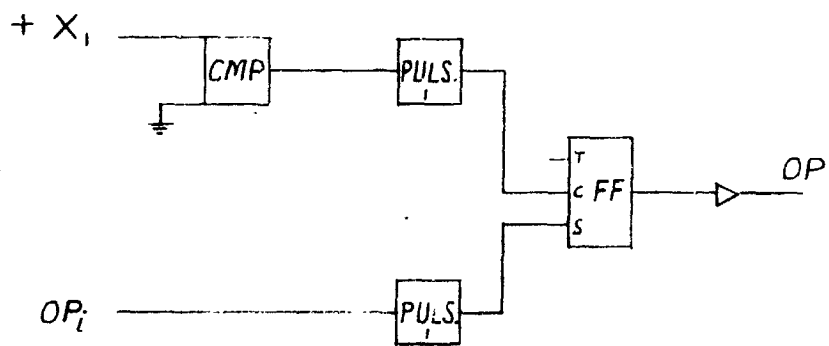


FIGURE L-14 COMPUTER OPERATION CONTROL

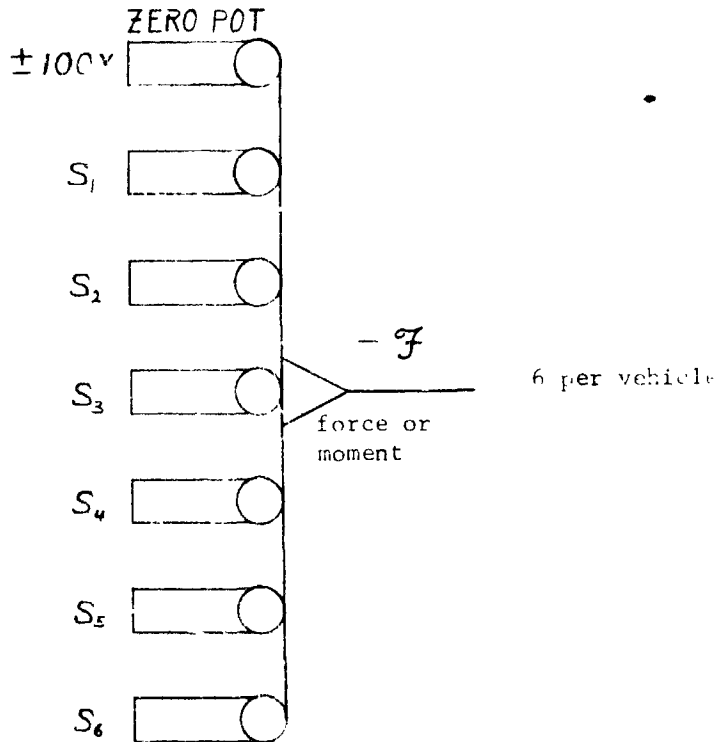
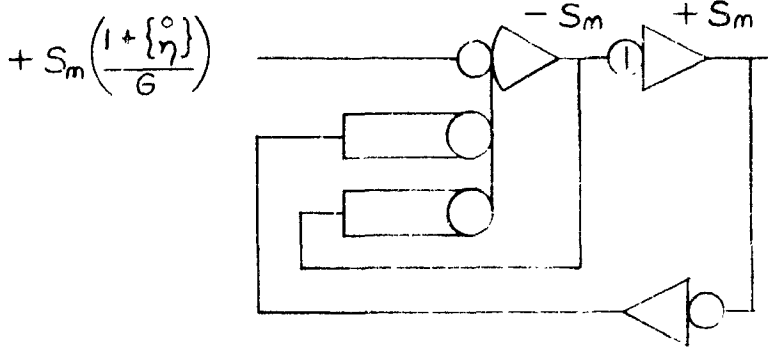
NORTHROP SPACE LABORATORIES

Table L-1 summarizes the estimates of computer requirements. The first 7 items constitute parts of the program, the rest various combinations of these. At the end of the table is a listing from the computer specification from MSC (Reference 42) showing items available without additional purchases. It should be noted that the provision for obtaining orientation with respect to fixed space is the most demanding and that a reduction in the number of flexure modes greatly relieves the strain on numbers of integrators.

Six items of information are obtained from each force and moment balance and transmitted to the computer. Calibration curves must be entered for each signal, but the shape of the curve will be restricted by choice of strain gauges to two slopes maximum. The calibration-corrected signal is then combined with the other five signals linearly to produce the three forces and three moments acting on the vehicle. To arrange for this in a general manner, the input is fed through the calibration section consisting of 3 amplifiers, 2 potentiometers and a limiter. This arrangement provides the entire correction required. There are six channels per vehicle making a total of 36 amplifiers, 24 potentiometers and twelve limiters. Where the corrections are linear, 1 potentiometer, 1 amplifier and 1 limiter may be dropped. The six signals are then combined and a zeroing signal added to give the output signal for summing into the computer. One amplifier and 7 potentiometers per channel are required for this operation, adding a total of 12 amplifiers and 84 potentiometers. Thus, for a general solution, 48 amplifiers, 12 limiters and 108 potentiometers are required. However, 12 of those amplifiers may be taken as already accounted for in the basic computer set-up so that the amount to be added is 24-36 amplifiers, 0-12 limiters and, by proper adjusting of gains, 72-96 potentiometers. The circuitry for individual calibration and resolution channels are shown in Figure L-15.

TABLE L-1 SUMMARY OF ESTIMATED COMPUTER REQUIREMENTS

	Products										Flip		
	Resolvers	Amplifiers	Integrators	Attenuators	Limiters	Compartators	Switches	Flop	OR	Gatcs	Pulses		
1. Basic	58	6	156	18	96	0	0	0	0	0	0	0	0
2. Slosh (per tank)	12	0	15	3	20	0	0	0	0	0	0	0	0
3. Flexure (Requirement Adjust. Per Vehicle Modes)	0	0	1	2	5	0	0	0	0	0	0	0	0
	16	0	39	5	0	0	0	0	0	0	0	0	0
	32	0	132	118	270	0	0	0	0	0	0	0	0
4. Attitude Control	0	0	66	6	30	0	18	12	12	12	18	0	0
5. Fixed Space	54	12	102	12	12	0	0	0	0	0	0	0	0
6. Gravity Addition To Fixed Space	-2	0	52	-6	15	0	0	0	0	0	0	0	0
7. Interaction	8	0	37	3	18	2	3	2	1	0	0	2	0
8. (1) + (5)	112	18	258	30	108	0	0	0	0	0	0	0	0
9. (8) + (2)	136	18	288	36	148	0	0	0	0	0	0	0	0
10. (9) + (3)													
27 Modes/Vehicles	166	18	420	154	418	0	0	0	0	0	0	0	0
11. (10) - (5)	144	6	308	142	406	0	0	0	0	0	0	0	0
12. (1) + (3)	90	6	288	136	366	0	0	0	0	0	0	0	0
13. (1) + (3) 12 Modes/Vehicles	90	6	219	71	216	0	0	0	0	0	0	0	0
14. (13) + (4)	90	6	285	77	246	0	18	12	12	18	0	0	0
15. (14) + (2)	114	6	315	83	286	0	18	12	12	18	0	0	0
2 Tanks	154	18	310	24	123	0	0	0	0	0	0	0	0
16. (8) + (6)													
17. Deluxe - 4 Tank Slosh													
27 Modes/Vehicles Gravity A/C	234	18	568	160	463	0	18	12	12	18	0	0	0
18. (14) + (2)	138	6	345	89	326	0	18	12	12	18	0	0	0
4 tanks													
SPEC	120	12	430	120	360	20/10	40	60	60	200	0	0	0



NOTE: If gains G are adjusted properly, at least one of these S_n potentiometers will be unnecessary. Others may possibly be zero.

FIGURE L-15 FORCE AND MOMENT RESOLUTION

SECTION 7.0

REFERENCES

SECTION 7.0

REFERENCES

1. Northrop Corporation, Engineering Test Summary 10993, Dynamic Flight Simulator, August 1963.
2. Courant, R., and Hubert, D., Methods of Mathematical Physics, Volume I, Interscience, New York, 1953.
3. Scanlan, R.H., and Rosenbua, R., Aircraft Vibration and Flutter, MacMillan, New York, 1951.
4. "Electrohydraulic Servomechanisms," Author, Allen C. Morse (1963) McGraw-Hill Book Co., New York, New York.
5. "Design of Hydraulic Control Systems," Authors, E.E. Lewis and H. Stern (1962), McGraw-Hill Book Co., New York, New York.
6. Electronic Designers' Handbook: McGraw-Hill, written by Robert W. Landee, Donovan C. Dav's, and Albert P. Albrecht.
7. "Orbital Assembly Simulator," by Astro Sciences Group, Northrop Corporation/Norair Division, ASG-TM-61-82, dated November 1961.
8. "Methodology for Evaluating and Validating Mechanical Rendezvous Subsystems." Technical Documentary Report RTD-TDR-63-4292, February 1964.
9. "Orbital Docking Dynamics." J. W. Ward and H. M. Williams American Rocket Society; Guidance, Control and Navigation Conference, August 1961.
10. "The Design and Evaluation Tests of a Full Scale Prototype Docking Mechanism," by L. J. Maltby, Menasco Manufacturing Company.

NORTHROP SPACE LABORATORIES

11. "Recommended Coordinate System for Use in Describing Docking Dynamics," received from MSC, 12 November 1964.
12. "Coordinate System for Describing Docking Dynamics," received from MSC, 7 December 1964.
13. "LEM/S IV B Vehicle Axes," received from MSC, 8 December 1964.
14. "Study of Requirements for the Simulation of Rendezvous and Docking of Space Vehicles." Technical Documentary Report No. AMRL-TDR-63-100, October 1963.
15. The Hydraulic System: BUAER Report AE-61-4 IV, written by Servo-mechanisms Section, Northrop Corporation, for the Bureau of Aeronautics, Navy Department.
16. Fluid Power Control: Technology Press of M.I.T. and John Wiley and Sons, written by Blackburn, Reethoff, and Shearer.
17. Control System Synthesis: McGraw-Hill, written by John G. Truxal.
18. Servo-mechanisms Practice: McGraw-Hill, written by Ahrendt and Savant.
19. 1955 Book of ASTM Standard, Tentative Definitions of Terms Relating to Methods of Mechanical Testing (E6-54T).
20. ASTM Bulletin January 1959, pp. 51-57, by R. L. Peeler and J. Green, "Measurement of Bulk Modulus of Hydraulic Fluids."
21. Aerospace Fluid Component Designers' Handbook, Vol. I. RPL-TDR-64-25, (May 1964), Space Technology Laboratories, Redondo Beach, Calif.
22. ASD-TOR-63-359, July 1963, "Isothermal Secant and Tangent Bulk Modulus of Selected Hydraulic-Type Fluids to 750°F and 10,000 psig.
23. Fluid Contamination Project, Report No. 1, by A. G. Comer, College of Engineering, Oklahoma State University (Aug. 1959). Contract No. AF 34(601)5470 with Oklahoma City Air Materiel Area.

NORTHROP SPACE LABORATORIES

24. "Synthetic Lubricants," Editors, R. C. Gunderson and A. W. Hart (1962), Reinhold Publishing Corp., New York, New York.
25. Pydraul, Selector, Fire Resistant Hydraulic Fluid, Monsanto Chemical Company, St. Louis, Missouri.
26. "New Developments in Synthetic Liquid Lubricants," E. E. Klaus, Machine Design, July 4, 1963, pp. 126-132.
27. Cellulube Safety Series Product Bulletin S-49-1 (1961), Fire Resistant Hydraulic Fluids and Synthetic Lubricants, Celanese Chemical Co., New York 36, New York.
28. "Effect of Pressure on Viscosity," E. M. Barber, Lubrication Engineering, November 1964.
29. "Considerations on the Evaporation of Materials in Vacuum," W. A. Rich (MSFC), Chemical Engineering Progress, No. 40, Vol. 59 (1963) pp. 103-117.
30. OS-124, High Temperature Functional Fluid and Lubricant, Technical Data Sheet, Feb. 1, 1960, Monsanto Chemical Co., St. Louis, Missouri.
31. Oronite Functional Fluids (June 1, 1964), California Chemical Co., Oronite Division, San Francisco, California.
32. Super Refined Hydraulic Oils, Lubetest D-237-E (1964), Humble Oil and Refining Co., Houston, Texas.
33. Versilube Silicone Lubricants, Technical Data Book S-10A, General Electric Co., Silicone Products Department, Waterford, New York.
34. Dow Corning 560 Fluid, Bulletin 05-001 (1962), Dow Corning Corporation, Midland, Michigan.
35. "Dynamics of the Airframe," BUAER Report AE-61-4II by Servo-Mechanisms Section and Aerodynamics Section of Northrop Corporation/Norair Division, dated September 1952.

NORTHROP SPACE LABORATORIES

36. "Introduction to Space Dynamics," by Thomson, John Wiley and Sons, Inc., 1961.
37. "Stabilizing Flexible Vehicles," *Astronautics and Aeronautics*, August 1964, pps. 38-44.
38. "Aeroelasticity," Bisplinghoff, Ashley and Holfman, Addison-Wesley Publishers, 1955.
39. "Introduction to the Study of Aircraft Vibration and Flutter," Scalan and Rosenbaum, MacMillan Publishers, 1960.
40. "Topics on Flexible Airplane Dynamics - Part IV Coupling of the Rigid and Elastic Degrees of Freedom of an Airframe-Autopilot System," ASD-TDR-63-334, Part IV, July 1963, prepared by Systems Technology, Inc.
41. "Analytical Study of Approximate Longitudinal Transfer Functions for a Flexible Airframe," ASD-TDR-62-279, June 1962, prepared by Systems Technology, Inc.
42. "Specifications for MSC Hybrid Computer Installation," received from MSC, November 1964.
43. "Postimpact Dynamics During the Docking of a Logistic Vehicle to a Space Station," Bruce B. Rennie, Boeing Aero-Space Division, Seattle, Washington.

NORTHROP SPACE LABORATORIES

Reference Drawings

<u>Title</u>	<u>Drawing Number</u>
Chamber B Schem. Elev., Top Plan & Flange Detail - Structural	S-32-9
Chamber B Sect. Plans @ Elevs. 11'3" & 0'0" - Structural	S-32-10
Chamber B Sect. Plan Below El. 0'0" & Details - Structural	S-32-11
Chambers A & B Nozzle & Flange Tubular Details - Structural	S-32-15
Chamber B Loading Diagrams - Structural	S-32-17
Chamber B Penetration Location Develop, Plans & Elev. - Mechanical	M-32-3
Lunar Plane Deck Plate Details - Sheet 2 - Structural	S-32-61
Gen. Arrange. Chamber B Plans & Section- Mechanical	M-32-16
Lunar Plane Piping Chamber B - Plans, Sects., Details - Mechanical	M-32-112
Chamber B Fixed Lunar Plane Details - Structural	S-32-2
NB 64-167 Proposal for An Analytical Study of An Advanced Dynamic Simulator	July 1964

NORTHROP SPACE LABORATORIES

Reference Drawings

		<u>Dated</u>
	Docking Test Facility Concept NASA - MSC	10-3-64
	North American Aviation - Kinematics Layout	
V16-956072	North American Aviation - Probe Capture Latch	9-25-64
	North American Aviation - Initial Seal Latch	8-7-64
	North American Aviation - Docking Configuration Location	8-11-64
V16-956063	North American Aviation	8-26-64
	North American Aviation - Layout LEM Docking Ring Blk II	3-11-64
MH01-05127-116	North American Aviation - Sh. 1, 2, & 3 LEM - Drogue Interface	9-16-64
MH01-05128-116	North American Aviation - C/M - LEM - Structural Interfaces	9-29-64
	North American Aviation - Multi-Shock Strut & Probe	5-27-64
	North American Aviation - Probe Assembly - Docking System (Layout)	8-12-64